



Epidemiology and evolution of fungal foliar pathogens in the face of changes in crop fertilization : application of evolutionary-ecological theory to crop epidemiology

Pierre-Antoine Précigout

► To cite this version:

Pierre-Antoine Précigout. Epidemiology and evolution of fungal foliar pathogens in the face of changes in crop fertilization : application of evolutionary-ecological theory to crop epidemiology. Other [q-bio.OT]. Université Sorbonne Paris Cité, 2018. English. NNT: 2018USPCC108 . tel-02333571

HAL Id: tel-02333571

<https://theses.hal.science/tel-02333571>

Submitted on 25 Oct 2019

HAL is a multi-disciplinary open access archive for the deposit and dissemination of scientific research documents, whether they are published or not. The documents may come from teaching and research institutions in France or abroad, or from public or private research centers.

L'archive ouverte pluridisciplinaire **HAL**, est destinée au dépôt et à la diffusion de documents scientifiques de niveau recherche, publiés ou non, émanant des établissements d'enseignement et de recherche français ou étrangers, des laboratoires publics ou privés.

Thèse de doctorat

de l'Université Sorbonne Paris Cité
Préparée à l'Université Paris Diderot

Ecole doctorale Frontières du Vivant (ED 474)

UMR 1402 INRA-AgroParisTech ; Écologie fonctionnelle et écotoxicologie des agroécosystèmes

UMR 8197 CNRS-ENS-INSERM ; Institut de Biologie de l'Ecole Normale Supérieure

Epidemiology and evolution of fungal foliar pathogens in the face of changes in crop fertilization

Application of evolutionary-ecological theory to crop epidemiology

Par Pierre-Antoine Précigout

Thèse de doctorat en Biologie

Dirigée par Corinne Robert et David Claessen

Présentée et soutenue publiquement à Paris le 22 Janvier 2018

Président du jury : Dajoz Isabelle, Professeur à l'Université Paris 7

Rapporteur : van den Bosch Frank, directeur de recherche au Rothamsted Research Centre

Rapporteur : Lion Sébastien, chargé de recherche au CNRS (CEFE) de Montpellier

Examinateur : Lescourret Françoise, directrice de recherche au centre INRA d'Avignon

Directeur de thèse : Claessen David, maître de conférence à l'Institut de Biologie de l'ENS à Paris

Co-directrice de thèse : Robert Corinne, chargée de recherche au centre INRA de Versailles-Grignon



Titre : Epidémiologie et évolution des pathogènes fongiques foliaires face à des changements de fertilisation des cultures - Application de la théorie de l'écologie évolutive à l'épidémiologie des cultures.

Résumé : La recherche d'une agriculture durable et respectueuse de l'environnement passe par une réduction de l'usage d'intrants de synthèse. L'agroécologie cherche à utiliser les interactions entre les organismes de l'agroécosystème pour optimiser son fonctionnement, comme la régulation naturelle des bioagresseurs. C'est dans cette optique que s'inscrit ce travail de thèse qui étudie l'effet de la fertilisation des cultures sur les épidémies de pathogènes foliaires fongiques des cultures. De plus, nous étudions l'évolution des pathogènes face aux différents effets de la fertilisation sur le pathosystème. Cela questionne la durabilité des pratiques culturales qui participent à la régulation des épidémies.

Pour répondre à ces questions, nous avons adopté une démarche de modélisation qui permet de simuler indépendamment les différents effets de la fertilisation sur le pathosystème. Le point de départ et l'originalité de notre démarche a été de considérer le système hôte-pathogène comme un système ressource-consommateur et d'y appliquer des concepts de l'écologie évolutive pour répondre à ces questions agronomiques. Dans les deux modèles construits durant cette thèse, la fertilisation influence directement la quantité de ressources disponible pour le pathogène. Nous nous y concentrons sur un trait d'histoire de vie du pathogène, la période de latence (durée séparant l'infection du début de la sporulation), qui correspond à la durée minimale d'un cycle infectieux et qui, conditionne la stratégie d'allocation des ressources du pathogène. La latence détermine en effet la quantité de ressource qui sera allouée à la croissance du mycélium (donc sa taille à maturité) et celle qui sera ensuite allouée à la sporulation (en relation avec sa taille). Les modèles développés permettent d'étudier les réponses épidémiologique et évolutive des pathogènes foliaires fongiques à la fertilisation des cultures, avec comme référence le système Blé d'hiver/Rouille brune. Nous avons considéré différentes échelles dans ce travail : depuis la lésion où le pathogène se nourrit directement sur son hôte, jusqu'à la parcelle où se développent les épidémies et au paysage où les flux de spores entre les parcelles sont source d'extension des épidémies dans l'agroécosystème. Un premier modèle, à l'intersection des modèles épidémiologiques "SEIR" et des modèles de populations structurées, couvre les échelles de la lésion à celles de l'épidémie et de la parcelle. Le second modèle, à l'intersection des modèles SEIR et des modèles spatiaux d'épidémiologie du paysage, couvre les échelles de la parcelle au paysage agricole. Nous étudions les dynamiques épidémiologiques et évolutives, en comparant des concepts de fitness empiriques et d'invasion.

Nous montrons que la fertilisation des cultures, en déterminant la dynamique des ressources disponibles pour les pathogènes, impacte fortement les épidémies. Nos modèles prédisent que la latence des pathogènes évolue en réponse à des compromis écologiques variés, d'une part pour optimiser l'allocation des ressources au niveau des feuilles, mais également pour gagner la course face à la croissance du couvert. La fertilisation, en changeant les concentrations de métabolites foliaires et les dynamiques de croissance du couvert, impacte donc épidémies et réponses évolutives de la latence des pathogènes. A l'échelle du paysage, l'introduction de pratiques variées de fertilisation dans un paysage préalablement homogène pourrait permettre de réduire les épidémies. Cependant, notre modèle prédit une durée limitée de cet effet du fait de l'évolution et de la diversification des pathogènes dans un paysage hétérogène. Ce travail ouvre la voie à des travaux sur l'effet et la durabilité des pratiques pour réguler les épidémies dans l'agroécosystème. Enfin, nous montrons par un travail de mété-analyse qu'il existe une relation forte entre type trophique et latence du pathogène, suggérant que les différents types de pathogènes répondront différemment à des scénarios de réduction de fertilisation.

Mots clefs : agroécologie ; modélisation ; épidémiologie ; écophysiologie ; écologie évolutive ; fertilisation des cultures ; champignons pathogènes ; latence ; rouille du blé ; mété-analyse

Title: Epidemiology and evolution of fungal foliar pathogens in the face of changes in crop fertilization – Application of evolutionary-ecological theory to crop epidemiology.

Abstract: The quest for a sustainable agriculture requires a reduction in the use of synthetic inputs. In this perspective, agroecology seeks to use interactions between organisms in the agroecosystem to replace inputs by ecosystem services, such as the natural regulation of pests and diseases. In this context, this thesis studies the effect of crop fertilization on epidemics of crop fungal foliar pathogens. We also take into account the evolution of these pathogens in response to fertilization. This allows us to study the sustainability of agricultural practices that contribute to the regulation of epidemics.

To answer these questions, we adopted a modelling approach that independently simulates the different effects of fertilization on the pathosystem. The starting point and originality of our approach was to consider the pathosystem as a consumer-resource system and to use concepts of evolutionary ecology to answer the abovementioned agronomic questions. In the two models developed in this thesis, fertilization directly determines the quantity of resources available for the pathogen. We focus on one of the pathogen's life history traits, the latent period (time period between infection and the onset of sporulating lesions), which corresponds to the minimum duration of an infectious cycle and constrains the pathogen's resource allocation strategy. The latent period determines the amount of resource that will be allocated to either growth of mycelium (and therefore to pathogen size at maturity) or to sporulation (proportional to the pathogen's size). The models we developed make it possible to study the epidemiological and evolutionary responses of fungal foliar pathogens to crop fertilization. We parameterized our models according to our biological knowledge of the wheat-rust pathosystem. Our modelling work encompasses different spatial and temporal scales: from the lesion where the pathogen feeds directly on its host, to the field and the landscape where the spores that flow between fields are the source of epidemics in the agroecosystem. The first model, at the intersection of the "SEIR" epidemiological models and structured population models, covers the scales of a lesion, the crop canopy and the field. The second model, at the intersection of SEIR and spatial landscape epidemiology models, covers the scales of the field and the agricultural landscape. We study epidemiological and evolutionary dynamics of pathogen populations by comparing empirical and invasion fitness concepts.

We show that crop fertilization, by determining the dynamics of available resources for pathogens, has a strong impact on foliar fungal epidemics. Our models predict that pathogen latent period evolves in response to various ecological trade-offs; on the one hand to optimize resources allocation at the leaf scale, on the other hand to win the race against canopy growth. By changing the leaf metabolite content and the rate of canopy growth, fertilization therefore impacts both epidemics and evolutionary responses of pathogen latent period. At the landscape scale, the introduction of various fertilization practices in a previously homogeneous landscape could help to partially regulate epidemics. However, our model predicts that the beneficial effects of heterogeneity will vanish due to the evolution and diversification of pathogens in heterogeneous landscapes. This work sets the stage for further work on the effect and sustainability of agricultural practices on the regulation of crop epidemics in agroecosystems. Finally, by performing a meta-analysis, we bring out a strong relation between pathogen trophic type and latent period, suggesting that different trophic types of pathogens will respond differently to decreasing fertilization levels.

Keywords: agroecology ; modelling ; epidemiology ; ecophysiology ; evolutionary ecology ; crop fertilization ; plant pathogenic fungi ; latent period ; brown rust ; meta-analysis

A ma mère

A Daphné et Noémie

A Marine, Anthony, Héloïse, Antonin et Morgane

Remerciements

Tout d'abord je tiens à remercier très chaleureusement Corinne Robert et David Claessen d'avoir accepté de codiriger ma thèse. Leur disponibilité, leur gentillesse, leur énergie, leur imagination et leur rigueur scientifique ont fait de ces (presque) quatre années des moments inoubliables. La complémentarité de leurs points de vue et de leurs approches est l'essence de l'originalité de ce travail. Je n'aurais pu imaginer meilleurs directeurs de thèse.

Un grand merci à Christophe Gigot pour son aide, ses nombreux conseils techniques, ses nombreuses anecdotes et sa si sympathique compagnie. J'espère que ce « quatuor agroécologie » que nous constituons continuera, pour au moins quelques temps encore, de travailler ensemble.

Je tiens à remercier tout particulièrement David Makowski pour son accompagnement et sa précieuse collaboration dans notre travail de méta-analyse.

Un grand merci également aux stagiaires que j'ai eu le plaisir de co-encadrer et qui m'ont beaucoup aidé dans l'avancement de mon travail de thèse : Morgane Maillard et Matthieu Gélin dans le développement du modèle « EBT », Xue-Fan Xu dans celui du modèle « paysage » et Maureen Beaudor dans notre étude sur la diversité des champignons pathogènes des plantes.

Je suis très reconnaissant envers Frank van den Bosch et Sébastien Lion pour l'intérêt qu'ils ont porté à mon travail et le temps qu'ils ont consacré à son évaluation. Je remercie également Isabelle Dajoz et Françoise Lescourret d'avoir accepté de participer à mon jury de thèse. Je tiens à remercier chaleureusement Minus van Baalen et Sébastien Barrot pour leur accompagnement tout au long de ces trois ans et demi en tant que membres de mon Comité de Thèse. Je tiens à les remercier pour leur disponibilité, leur écoute et leurs judicieux conseils. Merci également à Bruno Andrieu, mon parrain dans le programme Agreenium, pour les discussions enrichissantes que nous avons eu durant la thèse.

Je tiens également à remercier tous mes collègues d'EcoSys, de l'IBENS et du CERES pour leur bonne humeur, leur aide et leurs idées ou tout simplement les bons moments passés avec eux, et tout particulièrement Boris Sauteret, Célian Colon, Clara Champagne, Julia

Clause, Emeline Comby et Jonathan Rault pour nos nombreuses discussions passionnées, leur aide précieuse et leurs conseils.

Je souhaite également remercier chaleureusement mes collègues de l'Université Paris 7, qui m'ont accueilli comme moniteur dans leur unité d'enseignement. Auprès d'eux et avec eux, j'ai pu découvrir et apprécier l'enseignement universitaire des Sciences du Vivant. Merci tout particulièrement à Vincent Chassany, Anouck Diet, Céline Sorin et Patricia Genet pour leurs conseils pédagogiques.

Je tiens enfin à remercier mes camarades sportifs du club Ping Paris 14, sans le sourire et la bonne humeur de qui la fin de la thèse eut été ô combien moins agréable.

REMERCIEMENTS	5
INTRODUCTION.....	11
Contexte du travail : nécessité de diminuer les intrants en agriculture	11
Un travail au cœur de l'agroécologie	19
Objectifs, méthodes	22
Plan de la thèse	26
Synthèse bibliographique et choix de thèse.....	28
Principales caractéristiques de l'objet d'étude	28
Les céréales (exemple du blé d'hiver)	28
Les maladies foliaires fongiques polycycliques (exemple de la rouille du blé).	29
Effet de la fertilisation sur les épidémies fongiques	33
Une bibliographie contrastée	33
De multiples effets de la fertilisation azotée sur les plantes.....	34
De la plante fertilisée aux épidémies	36
Références	41
CHAPTER 1: MODELLING PHYSIOLOGICALLY STRUCTURED CROP EPIDEMICS AND THE PATHOGEN'S LIFE HISTORY PROBLEM.....	49
ABSTRACT	49
INTRODUCTION	50
MATERIALS AND METHODS	54
Model overview	54
Within-patch dynamics (lesion model)	57
Canopy-level dynamics.....	60
Year-to-year dynamics	63
Practical implementation and parameterization	63
Uninfected canopy dynamics	64
Infected canopy dynamics.....	66
Parameterization.....	70
Analysis methods	70
RESULTS	72
Within-patch dynamics	72
Canopy-level model simulations	75
Canopy level dynamics	76
Age at infection (a_i) and epidemics.....	82
Optimal latent period for canopy-level (epidemic) spores production.....	83
The effect of latent period on epidemics	83
DISCUSSION	86
REFERENCES	91

CHAPTER 2: CROP FERTILISATION IMPACTS EPIDEMICS AND OPTIMAL LATENT PERIOD OF BIOTROPHIC FUNGAL PATHOGENS	94
ABSTRACT	94
INTRODUCTION	95
MATERIALS AND METHODS.....	99
Pathosystem biology	99
Model overview	100
Patch submodel.....	101
Canopy-level model.....	103
Pathogen fitness and optimal latent period.....	104
Effects of fertilization	105
Analysis methods and simulations	106
RESULTS	108
Effect of resource level at the patch scale	108
Effect of fertilization at the canopy level	110
Effect of fertilization on optimal latent period	113
DISCUSSION	117
Effect of fertilization on optimal latent period and consequences.....	117
Data and optimal latent period.....	119
Spore production under varied fertilization levels.....	120
Modelling choices and hypothesis	121
CONCLUSION.....	124
APPENDIX: comparison of two maturation rules	125
REFERENCES	128
CHAPTER 3: FERTILIZATION-TRIGGERED EVOLUTIONARY CHANGES IN THE LATENT PERIOD OF LEAF FUNGAL PATHOGENS AT THE SCALE OF A CROP FIELD.	133
ABSTRACT	133
INTRODUCTION	134
MATERIALS AND METHODS.....	137
Theoretical framework.....	137
Empirical fitness measures.....	138
Invasion fitness.....	138
Analysis methods and simulations	140
RESULTS	141
DISCUSSION	146
A third empirical fitness measure	147
Conjecturing about pathogen latent period evolution in the field	149
Evolutionary ecology: optimization or invasion analysis?.....	150
CONCLUSIONS AND PERSPECTIVES	152

REFERENCES	153
CHAPTER 4: INFLUENCE OF CROP FERTILIZATION STRATEGIES AT THE LANDSCAPE-SCALE ON EPIDEMIOLOGY AND EVOLUTION OF LEAF FUNGAL PATHOGENS..... 156	
ABSTRACT	156
INTRODUCTION	157
MATERIALS AND METHODS.....	160
Within-patch dynamics of canopy functioning and pathogen development.....	160
Between-field pathogen dispersal and multi-annual dynamics.....	165
Analysis methods and simulations	168
Invasion analysis.....	172
RESULTS	176
Epidemics at the scale of an isolated field	176
Epidemics in a homogeneous landscape.....	180
Landscape heterogeneity and epidemics.....	181
Landscape heterogeneity and crop loss	186
Evolutionary responses of pathogens to fertilization	187
DISCUSSION	198
Spatial fertilization heterogeneity is beneficial through maladaptation	198
The need to take into account pathogen adaptation	201
Pathogen adaptation to landscape fertilization heterogeneity	202
CONCLUSION.....	205
SUPPLEMENTARY MATERIALS	206
REFERENCES	210
CHAPTER 5: DOES LATENT PERIOD OF LEAF FUNGAL PATHOGENS REFLECTS THEIR HOST TROPHIC TYPE? A META-ANALYSIS..... 214	
ABSTRACT	214
INTRODUCTION	215
MATERIALS AND METHODS.....	219
Data	219
Studies included in the meta-analysis	219
Response variable.....	219
Explanatory variables	221
Statistical methods.....	226
First look into the data	226
Statistical model	226
RESULTS	228
Data presentation	228
Statistical analysis	230
Incubation versus latent period	232

DISCUSSION	238
Defining the latent periods	238
Incubation and latent periods.....	240
Adaptation or constraints ?.....	242
REFERENCES	244
DISCUSSION	255
Questions, démarche et originalités du travail de these	255
1) Une démarche pluridisciplinaire	255
2) Difficultés et choix.....	257
3) Principales simplifications et perspectives de modélisation.....	258
Effet « climat x fertilisation »	258
Effet « fertilisation x niveau de résistance de l'hôte »	259
Latence, type trophique et fertilisation.....	260
La fertilisation des cultures impacte les épidémies foliaires fongiques.....	261
Evolution des pathogènes face à des changements de fertilisation des cultures	264
1) Fitness, latence optimale et compromis	264
2) Fertilisation et évolution de la latence.....	266
2.1) Direction de l'évolution	266
2.2) Coexistence et maladaptation.....	268
3) Prise en compte de la virulence dans le modèle.....	268
4) La latence, seule adaptation des pathogènes à la fertilisation ?	269
Des pratiques de fertilisation comme levier pour limiter les épidémies ?.....	271
Conclusion.....	272
References	272
ANNEXES 1 : ENGLISH VERSION OF SECTION “INTRODUCTION”	278
APPENDIX 2: ENGLISH VERSION OF SECTION “DISCUSSION”	285

Introduction

Dans cette partie introductive, je m’emploierai à replacer ce travail de thèse dans les contextes socio-économique et scientifique actuels, à en énoncer l’objectif, à en présenter le plan et à argumenter les choix (tant théoriques que méthodologiques), en relation avec l’état actuel des savoirs.

Contexte du travail : nécessité de diminuer les intrants en agriculture

Il serait abusif de considérer que les sévères épidémies de champignons pathogènes foliaires qui ont ravagé les cultures d’Europe occidentale entre 1845 et 1848 sont le déclencheur du Printemps des Peuples. Il est néanmoins certain que la coïncidence d’épidémies de Rouille jaune du seigle (*Puccinia striiformis f. sp. secalis*) exacerbées par un climat favorable et de l’arrivée dans une Europe aux résistances variétales encore balbutiantes du Mildiou de la pomme de terre (*Phytophthora infestans*) a contribué à exacerber le mal-être des populations humaines (surtout rurales) alors déjà rongées par le paupérisme (Zadoks, 2008). Conséquences de pertes de rendement considérables dues à ces champignons pathogènes, disettes, famines (comme la Grande Famine d’Irlande) et leur cortège de maladies (choléra, dysenterie, typhus) ont leur part de responsabilité, dans une proportion aujourd’hui encore difficile à estimer, dans les grands changements politiques du milieu du XIX-ième siècle, illustrant l’importance qu’ont pu avoir par le passé les épidémies de champignons pathogènes des cultures tant sur le plan économique que politique et social. Si aujourd’hui les dommages que causent ces pathogènes sont plus limités par nos méthodes de protection des plantes, leur incidence est loin d’être devenue négligeable. En effet, les pertes de rendement occasionnées par certains pathogènes peuvent être sévères. Ainsi, sur la culture de blé d’hiver, les années de fortes épidémies, les pertes de rendement peuvent s’élèver jusqu’à 50 % pour *Puccinia triticina* et *Puccinia striiformis* (principales rouilles sur blé) (Oerke et Dehne 1997 ; Roelfs et coll. 1992) et pour *Zymoseptoria tritici*, l’agent de la

septoriose du blé (Eyal et coll. 1987 ; Berraies et coll. 2014 ; Fones et Gurr 2015) ; comme en témoignent d'ailleurs les pertes de rendement de blé considérables de la récente année 2016. De même, sur le riz, les pertes peuvent atteindre 50% pour *Magnaporthe oryzae* l'agent de la pyriculariose du riz (Khush et Jena 2009, Chuwa et coll. 2015).

Avec l'usage grandissant de l'utilisation des fongicides au cours du XX-ième siècle, l'Europe n'a plus connu de disettes et un certains nombre de pathogènes ont perdu en incidence (comme par exemple l'Ergot du seigle, *Claviceps purpurea*). Néanmoins, certains champignons pathogènes ont continuellement occasionné et occasionnent toujours des pertes de rendement significatives. A titre d'exemple, les pertes de rendement liées aux pathogènes des cultures aux Etats-Unis étaient de 32% sur la période 1942-1950 et de 37% sur la période 1984-1990 (Altieri et coll. 2015). Plus généralement, il est admis que la perte totale de rendements en céréales due aux pathogènes, adventices et autres ravageurs est en moyenne de 40% à l'échelle mondiale (Oerke et Dehne 1997, Bruce 2010, De Schutter 2010), alors même qu'une augmentation de la production de 40 à 70% serait nécessaire pour répondre à la croissance démographique de la population humaine d'ici 2050 (rapport de la FAO 2006, 2012). Ainsi les problèmes de perte de récoltes liées aux bioagresseurs sont encore notamment importants.

Les transformations de l'agriculture au cours de la seconde moitié du vingtième siècle (connues sous le nom de « révolution verte ») ont permis de compenser (au moins en partie) la croissance démographique consécutive à la seconde guerre mondiale. Une agriculture reposant sur les technologies de l'après-guerre a en effet permis de doubler la production annuelle mondiale de nourriture en trente-cinq ans (*FAO technical background document on Green Revolution (1996)*¹, Tilman, 1999, Evenson 2003, FAOSTAT 2014). Elle a également fait reculer la malnutrition dans certaines régions du monde, permis d'atteindre l'autosuffisance alimentaire dans d'autres et placé la France dans les premiers rangs des puissances agricoles mondiales. L'idée de base était (1) de réduire le plus possible les facteurs limitant la production agricole : fertilité des sols, carences en nutriments, adventices, maladies et ravageurs en utilisant des intrants de synthèse issus de l'industrie du pétrole, et d'y associer (2) une productivité accrue avec la sélection variétale ainsi que (3) une capacité croissante à récolter et à cultiver via la mécanisation des pratiques agricoles. Des facteurs limitant la

¹ <http://www.fao.org/docrep/003/w2612e/w2612e06a.htm>

croissance des plantes, potentiellement, seul le climat restait non manipulable. La révolution verte a permis en France une constante augmentation de la production céréalière et de ses rendements entre les années 1950 et les années 1990 (Figure 1). Cependant, depuis les années 1990, on observe une stagnation des rendements des céréales. De plus, cette stagnation est observée sur plusieurs cultures, et dans des endroits variés du globe (Ray et coll. 2012, Zhang et coll. 2014). La cause n'est pas tranchée entre une conséquence du changement climatique ou bien l'essoufflement et la limite d'un système de production intensive (Brisson et coll. 2010).

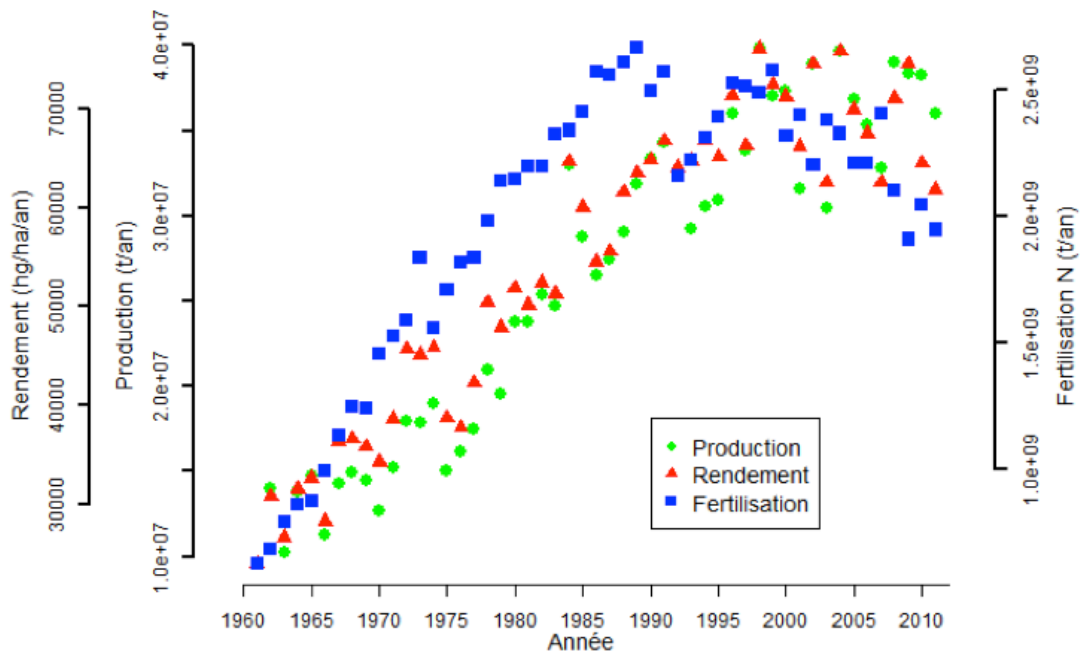


Figure 1: L'utilisation de fertilisants a largement contribué à l'augmentation des rendements lors de la « révolution verte ». Data issues de FAOSTAT (2014).

La stagnation des rendements n'est pas la seule préoccupation liée à cette agriculture qualifiée d'intensive. L'ensemble des pratiques qui lui sont associées a eu (et a toujours) pour conséquence une dramatique réduction de biodiversité et une forte pollution environnementale. Les vastes surfaces cultivées n'abritent qu'un petit nombre d'espèces, pour la plupart domestiquées (Tilman (1999) rapporte que 598 millions d'hectares, soit environ dix fois la surface du territoire français métropolitain, sont plantés de quatre céréales, maïs, riz, blé et orge). Celles-ci forment de vastes peuplements monospécifiques de quelques clones appartenant à un spectre variétal réduit, conduisant à une relative homogénéité génétique des cultures sur de vastes espaces. La diversité a diminué non seulement du point de vue des

espèces cultivées, mais également de leur diversité intra-spécifique (Figure 2). La faible richesse spécifique permet peu d'interactions biotiques au sein des écosystèmes agricoles « simplifiés » et cela s'accompagne d'une simplification des paysages agricoles (Tilman, 1999, Wilson et Tisdell, 2001). La diversité diminue ainsi également chez les espèces (végétales et animales) des populations naturelles (non cultivées) de l'agroécosystème.

Figure 2 : réduction de la diversité intra-spécifique (nombre de variétés) pour dix espèces cultivées au cours du XX-ième siècle. D'après une étude conduite en 1983 par la « Rural Advancement Foundation International ». <http://ngm.nationalgeographic.com/2011/07/food-ark/food-variety-graphic>

Pour le contrôle des maladies, l'agriculture intensive montre également de nombreuses limites. En effet, au-delà de la valeur intrinsèque de la biodiversité perdue, l'abondance d'hôtes génétiquement et phénotypiquement homogènes sur de vastes surfaces crée des conditions favorables au développement d'épidémies de champignons pathogènes des cultures. De plus la perte de diversité des populations naturelles diminue également les

possibilités de régulations des pathogènes. Ainsi en simplifiant fortement la diversité cultivée, l'agriculture intensive favorise l'explosion de certaines maladies. Contrôler les maladies est donc d'autant plus important pour éviter leur explosion dans un milieu homogène. Actuellement, les deux principales méthodes de contrôle sont l'utilisation des variétés résistantes et les traitements pesticides (Plantagenest et coll. 2007 ; Berry et coll. 2008 ; Edwards-Jones 2008). Or, il est maintenant admis que l'épandage de pesticides est nocif à la fois pour l'Homme et pour son environnement (Tilman et al 2001 ; Wilson et Tisdell, 2001 ; Pimentel et coll 2005). De plus, ces méthodes ne sont pas durables car elles sont rapidement contournées par les pathogènes qui s'y adaptent. Ainsi, l'efficacité des principales familles de fongicides utilisées au champs diminue au fur et à mesure que se répandent des souches de pathogènes résistantes à ces composés (Figure 3, Gullino et coll. 2000 ; Urech et coll. 1997 ; Hewitt 1998 ; Ma et Michailides 2005 ; Brent et Holloman 2007 ; Deising et coll. 2008 ; Sierotzki et Scalliet 2013 ; Hayes et coll. 2016). Un cas extrême est celui des strobilurines utilisées pour traiter le blé, et dont la durée d'efficacité a été de 2 années seulement ! Ainsi pathogènes, scientifiques, sélectionneurs et ingénieurs des firmes phytosanitaires se sont-ils lancés dans une course aux armements, qui voit se succéder sans relâche la découverte de nouvelles molécules actives et l'apparition de souches qui y sont résistantes.

Figure 3 : illustration de la course aux armements entre pesticides et pathogènes. La figure montre l'apparition entre 1970 et 2010 de résistances aux principaux produits de contrôle du champignon pathogène foliaire *Zymoseptoria tritici*, agent de la septoriose du blé. D'après Leroux et Walker (2009).

Les pesticides ne sont pas les seuls intrants dont l'utilisation est devenue problématique. En effet, Tilman (1999) calcule que l'augmentation de 35% de la production de nourriture à l'échelle globale entre 1960 et 2000 s'est accompagnée d'une multiplication par un facteur 3.5 et 6.9 des taux de fertilisation phosphorée et azotée respectivement. Il estime donc que, par simple, extrapolation linéaire, un nouveau doublement de la production impliquerait une multiplication par trois des taux actuels de fertilisation, ce qui semble irréaliste.

Azote et phosphore sont deux des principaux éléments chimiques limitants dans les écosystèmes, naturels comme cultivés. Si le phosphore n'est que modérément emporté hors des terres cultivées par érosion des sols liée aux précipitations météoriques, l'azote est quant à lui un élément beaucoup plus mobile. La matière organique ou les déchets animaux sont transformés en ammoniac par ammonification fongique ou bactérienne. L'ammoniac, NH_3 , qu'il soit répandu directement comme fertilisant ou issu de la minéralisation de matière organique, est hautement volatile. Par nitrification, les bactéries du sol peuvent le transformer en nitrites NO_2^- puis en nitrates NO_3^- (autre forme de l'azote couramment utilisée comme fertilisant), composés très solubles et facilement emportés dans les eaux de ruissellement jusque dans les nappes phréatiques où ils posent un risque de pollution, ou directement dans les cours d'eau. Enfin, les nitrates peuvent être transformés par dénitrification bactérienne en oxyde nitreux, N_2O , un puissant gaz à effet de serre. Les composés azotés gazeux ainsi émis sont en partie redéposés par les précipitations météoriques dans des écosystèmes non directement fertilisés par l'Homme. Une nouvelle augmentation de l'usage de fertilisants azotés et phosphorés va donc encore accentuer l'eutrophisation des eaux douces et des mers entraînant une forte réduction de la biodiversité aquatique, accroître les pullulations d'espèces nitrophiles témoignant de profonds changements dans la structure des réseaux trophiques, augmenter le niveau d'eutrophisation des sols des écosystèmes « naturels » et conduire à davantage d'émissions de gaz à effet de serre (Tilman, 1999, Loeuille et coll. 2013). Certains de ces phénomènes sont déjà largement observables. Le lessivage des sols par les précipitations météoriques entraîne une pollution aux nitrates des eaux de surface dans les principales régions agricoles françaises (Figure 4) ainsi que des phénomènes de marées vertes dans les zones côtières (Beman et coll. 2005, Howarth et coll., 2006) avec déjà des conséquences sur les réseaux trophiques de ces écosystèmes (Chen et coll. 2004, Laursen et Møller, 2014). En milieu terrestre, la fertilisation en azote des sols par les dépôts atmosphériques conduit à une acidification des sols et à de profondes transformations des

cortèges spécifiques associés (Fenn et coll., 2003 ; De Schrijver 2007 ; Stevens et coll. 2010, Dirnböck et coll., 2014).

Notons enfin que la fabrication de fongicides comme de fertilisants de synthèse est dépendante de l'utilisation de pétrole, ressource finie et non-renouvelable, dont le coût ne pourra qu'augmenter dans le futur.

Une certaine volonté politique de réduire l'utilisation d'intrants de synthèse dans les pratiques agricoles s'est manifestée en France et en Europe durant les vingt dernières années, notamment via la promulgation de réglementations poussant à la réduction de l'usage des pesticides. La nécessité de cette réduction était, par exemple, une des conclusions majeures du Grenelle de l'Environnement de 2007. A sa suite fut lancé en 2008 le premier plan Ecophyto, qui visait à réduire l'utilisation de pesticides en France via une meilleure formation des agriculteurs à une utilisation responsable de ces produits et via l'encouragement au recours à des méthodes de protection alternatives. Mais, en 2015, l'observation d'une augmentation de l'utilisation des produits phytopharmaceutiques sur la période 2010-2014 (note de suivi 2015 des tendances du recours aux produits phytopharmaceutiques de 2009 à 2014, ministère de l'agriculture²) signe l'échec de ce premier plan. Un nouveau plan est alors lancé (Ecophyto 2) visant une réduction de l'usage des pesticides de 25% d'ici 2020 et de 50% d'ici 2025, à la fois par l'encouragement au recours à des techniques alternatives et par des leviers économiques. Pendant ce temps, la loi n° 2014-1170³ d'avenir pour l'agriculture, l'alimentation et la forêt est votée, qui, allant dans le même sens que les paquets rapidement présentés ci-dessus, encourage en plus à l'usage de techniques innovantes issues de l'agroécologie à l'initiative des territoires.

Une volonté semblable est visible pour un autre type d'intrants : les fertilisants. Même s'il n'existe en France aucun plan d'action nationale équivalant aux plans Ecophyto, ni de texte de loi spécifique, c'est du côté de Bruxelles que sont venues des directives visant à la limiter les émissions de polluants gazeux d'origine agricole (Directive 1999/30/CE du Conseil de l'UE, DIRECTIVE 2008/50/CE du parlement et du conseil, Directive (EU) 2016/2284).

² http://www.senat.fr/espace_presse/actualites/201403/le_projet_de_loi_davenir_pour_lagriculture_lalimentation_et_la_foret.html

³ <https://www.actu-environnement.com/media/pdf/news-25554-note-suivi-ecphyto.pdf>

Figure 4: Pourcentage par département de la population desservie par une eau conforme vis-à-vis des concentrations en nitrates. D'après la Notice : La qualité de l'eau du robinet en France (données 2012). http://www.eaufrance.fr/IMG/pdf/eaurobinet_qualite_2012_201410.pdf

Pour conclure, l'ensemble de ces éléments demande une transition vers une agriculture moins dépendante des intrants de synthèse, aussi bien les pesticides que les fertilisants. Il est nécessaire de développer des agricultures plus durables, moins dépendantes des énergies fossiles, plus respectueuses de la biodiversité et conciliant performance économique et environnementale. Des travaux de recherche sont nécessaires afin de construire cette transition. C'est dans ce contexte que s'inscrit mon travail de thèse. Il porte sur les possibilités de régulation des épidémies de champignons pathogènes foliaires des grandes cultures via des changements de pratiques agricoles, plus particulièrement via des scénarios de réduction de la fertilisation des cultures, ainsi que sur la durabilité de ces pratiques en prenant en compte l'évolution des pathogènes face à ces changements de pratiques.

Un travail au cœur de l'agroécologie

Face à une demande de réduction de l'utilisation des produits phytosanitaires, plusieurs pistes, complémentaires, s'ouvrent à nous. Une voie, plutôt inscrite dans la continuité, est d'optimiser les méthodes de contrôle actuelles, dans une optique d'agriculture de précision par exemple. Ainsi, en terme de lutte contre les pathogènes, de nouvelles méthodes ont récemment été expérimentées, faisant appel à l'utilisation d'éliciteurs tels que des lipopeptides (Brotman et coll. 2009, Esmaeel et coll. 2016) ou des ulvanes (Stadnik et Freitas, 2014), d'agents de biocontrôle tels que des champignons endophytes (Comby et coll. 2017) ou à des outils génétiques tels que l'ARN interférence (Koch et coll. 2016) ou la technique CRISPR-Cas (Collinge, 2016), visant sinon à remplacer l'usage de pesticides, au moins à le réduire. Mais ces prothèses technologiques d'une agriculture de précision seront-elles suffisantes pour nous maintenir en tête dans la course aux armements évolutifs qui nous oppose aux champignons pathogènes dans la compétition pour l'accès aux ressources agricoles ? Pouvons-nous, à travers nos pratiques culturelles, imaginer des systèmes de production qui soient résilients à la fois aux épidémies et aux capacités d'adaptation des pathogènes ?

Une autre piste proposée pour réduire l'utilisation de produits phytosanitaires est l'agroécologie. Le vocable « agroécologie » recouvre en fait au moins trois réalités dont certaines sont au cœur de ce travail de thèse (Wezel et coll. 2009). L'agroécologie est à la fois :

- (1) Un mouvement social, ou plus exactement une constellation de mouvements sociaux prenant leurs origines dans différents pays.
Il peut s'agir de revendications partant du monde agricole et visant à atteindre sécurité alimentaire, souveraineté alimentaire et autonomie agricole comme de volontés politiques plus ou moins institutionnelles. Cet aspect n'est pas pris en compte dans notre travail.

- (2) Un ensemble de pratiques agricoles qui visent à diminuer l'utilisation des intrants de synthèse avec une utilisation de pratiques qui permettent par

exemple de mieux réguler les ravageurs des cultures tout en augmentant la qualité des sols (voir par exemple Altieri 1994).

On peut citer comme exemples de techniques le travail du sol, les cultures en mélange, ou encore la rotation des cultures, toutes susceptibles de limiter le développement des bioagresseurs. López-Ráez et coll. (2012) rapportent par exemple que la fertilisation phosphorée modérée d'une culture de sorgho réduit significativement le degré de parasitisme de la culture par des *Striga ssp.* (Orobanchacées parasites racinaires) en regard d'une culture non fertilisée au phosphate. L'ajout de phosphate stimule en effet la production de strigolactones par les racines des plantes, favorisant leur mycorhization, qui à son tour diminue de taux de parasitisme racinaire (López-Ráez et coll. 2012). L'utilisation de la biodiversité cultivée est également à la base de ces pratiques. Sapoukhina et coll. (2013) montrent par exemple que l'utilisation refléchie d'un mélange de variétés de blé diversement résistantes à la maladie peut permettre de réduire de (au plus) 30% la sévérité d'épidémies de rouille. De plus, la présence de cette biodiversité ne favoriserait pas seulement la régulation des bioagresseurs mais également la résilience de l'agroécosystème dans son ensemble face à des événements perturbateurs, comme des événements climatiques extrêmes par exemple (Altieri et coll. 2015). Enfin, la gestion du paysage agricole (son architecture, sa diversité), est également un levier mis en avant par l'agroécologie pour atteindre des propriétés d'autorégulation des agroécosystèmes. Par exemple, on peut utiliser la structure du paysage pour diminuer les flux de spores des pathogènes entre les parcelles et diminuer ainsi la pression parasitaire (Garett et Mundt, 1999).

Ce travail de thèse, en s'intéressant à la régulation des épidémies via des pratiques de fertilisation, s'intègre dans ce type de raisonnement. Il peut potentiellement être une brique pour la construction de nouveaux modes d'agriculture plus respectueux de l'environnement. En effet, en utilisant la fertilisation pour mieux réguler les épidémies, on gère d'une part la pollution liée aux fertilisants eux-mêmes, et d'autre part celles liées aux fongicides dont l'utilisation diminuerait également. De plus, nous considérons les deux échelles que sont la parcelle et le paysage pour simuler les différents effets de la fertilisation azotée sur le pathosystème.

- (3) Au niveau scientifique, l'agroécologie se base sur l'hypothèse que l'on peut utiliser/valoriser les interactions biotiques qui existent au sein de l'agroécosystème pour optimiser son fonctionnement.
- A l'extrême l'idée est de copier la nature, ou du moins des processus clé de régulation à l'œuvre dans les écosystèmes naturels (Ford et McGuire, 2015). C'est pourquoi la discipline de l'agroécologie a pour ambition d'utiliser des concepts de l'écologie pour répondre à des questions d'agronomie. C'est tout à fait la démarche de mon travail de thèse qui utilise des concepts et des outils de l'écologie comme la théorie de traits d'histoire de vie et la dynamique adaptative pour appréhender un sujet agronomique (les épidémies des cultures).

Objectifs, méthodes

L’objectif de mon travail est de quantifier l’effet de la fertilisation sur les épidémies des cultures et l’évolution des pathogènes. L’objectif plus appliqué associé est de déterminer s’il est théoriquement possible d’utiliser la fertilisation comme levier pour réguler les épidémies des cultures. Ce travail repose sur l’hypothèse que la fertilisation des cultures, en déterminant la croissance et le développement des plantes, impacte les interactions entre plantes et champignons pathogènes et est donc un potentiel levier d’action pour contrôler les épidémies dans les agroécosystèmes.

Pour répondre à cette question, notre objectif est de simuler l’impact de fertilisations variées sur les épidémies mais également les réponses évolutives des pathogènes à des changements de régimes de fertilisation. Combiner un certain degré de réalisme biologique, en tenant compte (1) des interactions entre le pathogène et son hôte et (2) de l’évolution du système dans un environnement (fertilisation) changeant doit nous permettre de tester comment de traduiront certains effets de la fertilisation sur le pathosystème et, en cas de réduction des épidémies, si les améliorations constatées seront « durables ». Notre idée est donc d’utiliser la fertilisation pour faire émerger des propriétés d’autorégulation des agroécosystèmes via les interactions entre les organismes, plus précisément des propriétés de réduction de l’incidence des maladies foliaires fongiques via l’étude des réponses épidémiologique et évolutive des pathosystèmes.

Nombre d’études antérieures à cette thèse ont permis de déterminer sur quels traits des plantes l’effet de la fertilisation se manifeste. Un certain nombre de ces traits sont connus pour avoir un effet sur le pathogène, effet qui entraînera une rétroaction sur la plante. Tous les effets de la fertilisation sur la plante sont hautement dynamiques et impliquent des phénomènes allant d’échelles spatiales très fines (échanges de nutriments à l’échelle d’une lésion) à celle plus large du couvert végétal (dont la taille peut par exemple jouer sur la dispersion du pathogène) et jusqu’à celle du paysage au niveau duquel l’hétérogénéité des pratiques pourrait limiter l’étendue des épidémies. De même, les échelles de temps concernées s’étalent d’événements ponctuels de dispersion, à la durée d’un cycle infectieux (plusieurs jours) et à des échelles longues pour l’évolution des populations de pathogènes (qui nécessitera plusieurs années de culture). Face à la multiplicité des interactions nous pensons que la modélisation est un outil intéressant pour mieux comprendre les effets de la fertilisation

sur les épidémies et simuler les différentes échelles d'espace et de temps en jeux. C'est donc une approche de modélisation qui a été choisie pour ce travail, avec la considération de plusieurs échelles spatiales et temporelles. Deux principaux modèles, permettant d'étudier le lien entre fertilisation, épidémies et évolution des pathogènes ont été développés au cours de ma thèse. Le premier simule les épidémies à l'échelle de la parcelle et couvre les échelles allant de la lésion au couvert végétal ; le second modèle simule les épidémies à l'échelle du paysage, couvrant cette fois les échelles allant de la parcelle au paysage. Il existe un lien fort entre ces deux modèles : dans le second (échelle du paysage), l'implémentation de l'échelle de la parcelle correspond à un métamodèle utilisant les principaux résultats issus du premier.

Parmi la grande diversité des modèles existants, cinq grands types de modèles ont été source d'inspiration pour notre travail. (1) Les « functional-structural plant models » (FSPMs) sont des modèles qui cherchent à représenter la dynamique spatio-temporelle du développement des plantes en 3D (Godin et Sinoquet 2005, Vos et coll. 2009, Sievänen et coll. 2014). Ils ont été assez récemment couplés à des modèles d'épidémies afin de comprendre comment l'architecture des couverts impacte le développement des épidémies (Robert et coll. 2008, Calonnec et coll. 2008, Baccar et coll. 2011, Garin et coll. 2014, Robert et al. 2017). Les résultats acquis en particulier sur le blé et ses maladies foliaires fongiques nous ont permis d'identifier les effets clés de l'architecture des blés sur les épidémies et de sélectionner les mécanismes à intégrer dans notre propre travail de modélisation. Il s'agit en particulier du rythme de développement de la plante qui détermine la course entre le couvert et son pathogène mais également de la localisation et de la sénescence des feuilles (Robert et al. 2017) qui influencent la dispersion des spores dans le couvert et la compétition pour les métabolites foliaires respectivement. Nous y puisons une certaine dose de réalisme biologique et une dimension fonctionnelle qui nous permet de modéliser l'hôte dans notre pathosystème comme bien davantage qu'un simple substrat à coloniser. (2) Les « physiologically structured population models » (PSPMs) sont des modèles d'écologie des populations offrant un puissant cadre théorique pour décrire la dynamique de populations structurées en classes d'individus caractérisées par des valeurs de traits tels que l'âge ou la taille (De Roos et coll. 1992, De Roos 1997, Claessen et coll. 2000). L'utilisation d'un tel cadre théorique nous permet de coupler les dynamiques développementales de la plante et du pathogène en termes de leur « *life history* » et de décrire de façon rigoureuse la colonisation du couvert végétal par ce dernier ainsi que le déroulement des épidémies. Par rapport aux modèles FSPM décrits ci-dessus, ces modèles sont moins détaillés. Ils prennent en compte les rétroactions entre la

plante et son pathogène et permettent des simulations sur plusieurs années de culture. Ils sont à la base du premier modèle développé dans la thèse. (3) Les modèles de type « susceptible-exposed-infectious-removed » (SEIR) sont classiques en épidémiologie et souvent utilisés pour décrire la dynamique temporelle de maladies, pour prédire leur survenue ou pour modéliser l'efficacité de vaccins (Gilchrist et coll. 2006, Li and Muldowney 1995, D'Onofrio 2002). Leur simplicité et leur maniabilité mathématique opèrent néanmoins souvent aux dépends du réalisme biologique de l'interaction hôte/pathogène. Nous conservons de ces modèles compartimentés le type de description de l'épidémie en classes d'hôtes, dont nous avons produit une version structurée (type PSPM) pour décrire les épidémies à l'échelle d'une parcelle ainsi qu'une version spatiale (épidémiologie du paysage) pour décrire les épidémies à l'échelle du paysage. (4) Pour modéliser la dynamique évolutive, nous nous appuyons sur deux approches : le principe d'optimisation issue de l'écologie évolutive classique (Stearns 1992, Roff 2002) et la théorie de la dynamique adaptative (Metz et al 1992, Geritz et al 1998). Nous appliquons et comparons les deux approches aux différentes échelles spatiales pour prédire comment les pathogènes vont évoluer face à des changements de fertilisation. (5) Les modèles spatialement explicites d'épidémiologie du paysage sont encore peu nombreux mais offrent un cadre pour étudier l'effet de la dispersion des pathogènes ou de l'hétérogénéité spatiale sur les épidémies (Park et coll. 2001, Skelsey et coll. 2010, Jones et coll. 2011, Papaïx et coll. 2014, 2015). Beaucoup considèrent le paysage comme une mosaïque de champs ayant chacun leurs particularités, l'ensemble fonctionnant, une fois l'épidémie initiée, comme une méta-population de pathogènes. Nous avons construit un modèle de ce type pour étudier l'effet de la fertilisation sur les épidémies à l'échelle du paysage.

Notre étude a pour objectif d'être générique, mais les modèles ont été en particulier paramétrés sur le système blé-rouille brune (*Puccinia triticina*, ex *P. recondita f. sp. tritici*).

Une des fondations de ce travail est de considérer le système hôte-pathogène comme un système consommateur-ressource. Cet angle d'approche est fondamental pour faire le lien entre les concepts de l'écologie et la question agronomique posée. La fertilisation détermine la quantité de ressources qui sera disponible pour le pathogène. Ce dernier doit donc mettre en place une stratégie d'exploitation optimale des ressources, stratégie qui varie probablement avec les niveaux et surtout la dynamique de mise en place de cette ressource. Dans notre cas, la quantité de ressources que représente l'hôte est finie, dans le temps au niveau foliaire du

fait de la sénescence naturelle des feuilles de blé, comme dans l'espace du fait de la quantité finie de blé. La théorie écologique évolutive des traits d'histoire de vie prédit alors que le consommateur (ici le pathogène) fait face à un dilemme dans l'allocation de ses ressources pour les différentes grandes fonctions de son organisme : croissance, défense, maintenance et reproduction (Stearns 1992, Roff 2002). Il est clair que tous les traits relatifs à toutes ces fonctions ne peuvent pas être optimisés en même temps. Des compromis existent donc entre ces traits, qui contraignent l'évolution des pathogènes en réponse, par exemple, à des variations dans l'accessibilité aux ressources (baisse de fertilisation, ...). L'un de ces traits a particulièrement retenu notre attention : la période de latence. La latence peut être conçue alternativement comme la durée de croissance somatique (« juvénile ») du pathogène avant reproduction (déterminant alors sa taille, donc lié à la croissance), comme la durée minimale d'un cycle infectieux (temps séparant l'infection de nouveaux tissus de l'émission de nouvelles particules infectieuses, donc lié à la reproduction) ou encore comme une mesure de l'efficacité d'une souche de pathogène à coloniser son hôte (« *aggressiveness* » des phytopathologistes). Sous l'hypothèse que la capacité du pathogène à se reproduire (taux de sporulation) est proportionnelle à sa taille (donc à sa période de latence), le pathogène pourra soit se reproduire plus rapidement mais moins efficacement, soit grandir le plus possible avant de se reproduire, au risque d'avoir épuisé ses ressources lorsqu'arrive le moment de la reproduction. En théorie des traits d'histoire de vie, cela correspond à une question d'évolution de la maturation (Cohen 1976, Stearns 1989, Kozlowski 1992, Engen et Saether 1994) : comme croissance et reproduction ne peuvent être maximisées en même temps, le pathogène va vraisemblablement adopter une stratégie intermédiaire, que nous appellerons « latence optimale ». La question initiale sur le lien entre fertilisation, développement épidémique et évolution se traduit maintenant de façon plus pratique par l'étude du lien entre fertilisation et latence, que l'on retrouvera tout au long de cette thèse.

Plan de la thèse

La thèse comprend cinq chapitres qui présentent les travaux réalisés et se termine par une discussion générale des résultats. Cette partie de l'introduction a pour objectif de décrire rapidement chacun des chapitres et leurs objectifs ainsi que de montrer la logique de leur énchaînement.

Dans le Chapitre 1, je présente un modèle de réponse des épidémies polycycliques de champignons pathogènes foliaires à la fertilisation à l'échelle de la parcelle (couvert végétal). Les échelles considérées vont de la lésion à la parcelle. A l'intersection des modèles épidémiologiques et PSP, le nôtre correspond à un modèle SEIR où les compartiments bénéficient d'une double structuration, en terme d'âge du tissu et d'âge de l'infection. Il permet d'étudier les interactions et les rétroactions entre plante et pathogène ainsi que d'explorer la question de la latence optimale aux échelles de la lésion et de la parcelle. L'objectif de ce chapitre est en particulier de présenter le modèle qui sera utilisé dans les chapitres 2 et 3 de la thèse.

Le Chapitre 2 est centré sur l'effet de la fertilisation sur les épidémies et la latence optimale à l'échelle de la parcelle. Il utilise le modèle présenté dans le chapitre 1 associé à des effets variés de la fertilisation. Nous proposons deux mesures de valeur sélective pour le pathogène et nous évaluons comment elles sont maximisées par une latence optimale et cela dans différents effets de la fertilisation sur la plante. Ce chapitre traite donc des effets de la fertilisation sur les épidémies et c'est un premier pas vers de possibles réponses évolutives.

Le Chapitre 3 est centré sur l'évolution des pathogènes face à la fertilisation des cultures. Il confronte les réponses évolutives contrastées montrées dans le Chapitre 2 et établies sur la base de mesures de valeur sélective du pathogène « ad hoc » avec celle, théoriquement plus rigoureuse, établie en utilisant les outils de la dynamique adaptative.

Le Chapitre 4 présente l'étude de l'effet de la fertilisation à l'échelle du paysage et en particulier l'effet de l'hétérogénéité spatiale en terme de fertilisation sur les épidémies et l'évolution du pathogène. Le paysage y est représenté comme une mosaïque de parcelles diversement (ou non) fertilisées. A l'intérieur d'une parcelle, ce modèle utilise directement le

compromis latence/sporulation établi dans les chapitres précédents de la thèse. Dans le chapitre nous présentons le modèle et les simulations associées. Ce chapitre est donc centré sur le changement d'échelle spatiale et les résultats à l'échelle du paysage.

Le Chapitre 5 présente, en guise d'ouverture, une méta-analyse portant sur la relation entre les types trophiques et la durée de latence des pathogènes. Notre hypothèse était que si la quantité/dynamique des ressources est fondamentale dans l'optimisation de la durée de latence, alors le type trophique pourrait également influencer les durées optimales de latence. C'est ce que nous testons dans ce dernier chapitre de la thèse.

La dernière partie de la thèse est une discussion plus générale des résultats, associée à des propositions de perspectives.

Synthèse bibliographique et choix de thèse

Avant de passer à la présentation des deux modèles proprement dits, la fin de cette introduction sera consacrée à éclairer nos choix de modélisation à la lumière d'un état de l'art relatif à la biologie du pathosystème, à sa réponse à la fertilisation aux différentes échelles (organe, parcelle, paysage) et à la théorie écologique qui sera utilisée dans l'ensemble du manuscrit.

Dans cette partie, on présente certains aspects de la biblio sur la sujet de thèse et les choix faits en s'appuyant dessus.

Principales caractéristiques de l'objet d'étude

Bien que notre objectif soit de développer un cadre théorique assez générique, un certain nombre de choix de modélisation (en particulier de paramétrage) ont dû être faits suite au choix de l'objet d'étude que sont les maladies fongiques foliaires sur céréales. Dans la suite, nous détaillons certaines des particularités de ce pathosystème qui ont guidé nos choix de modélisation.

Les céréales (exemple du blé d'hiver)

Le blé est une plante à croissance semi-déterminée. Le maître brin, dans des conditions favorables, développe entre 11 et 13 feuilles à phyllotaxie alterne. Chacune émerge en une centaine de degrés-jours (unité de temps-thermique utilisée pour décrire le développement des plantes et, parfois, de leurs pathogènes). Cette durée, assez conservée entre cultivars (Evers et coll. 2007), est appelée phyllochron. L'émergence des feuilles est donc successive et non-chevauchante. Les 6 ou 7 feuilles basales forment une pseudo-rosette. Les feuilles apicales présentent des entre-nœuds plus allongés du fait du phénomène d'elongation qui intervient pendant la montaison à 600-800 degrés-jours de développement post-semis. Chez les poacées sauvages, cette elongation rapide de la tige permet de situer l'inflorescence momentanément au dessus du couvert prairial ce qui facilite la pollinisation anémophile. L'émergence de

toutes les feuilles et l'élongation de la tige nécessitent donc quelques 1300 à 1500 degrés-jours. Ce délai varie selon les variétés et les conditions environnementales. Lorsque les conditions nutritives sont favorables, des talles (rameaux latéraux semblables au maître brin) se forment successivement à partir de chacun des nœuds basaux. Le talle du nœud n commence à se développer lorsque la feuille $n+4$ émerge. Seuls les nœuds des feuilles de rosette développent des talles.

Les maladies foliaires fongiques polycycliques (exemple de la rouille du blé).

Comme nombre de champignons pathogènes foliaires, la rouille du blé, ou rouille brune (*Puccinia triticina*, ex *P. recondita f. sp. tritici*) se caractérise par le développement d'épidémies polycycliques. Il s'agit d'épidémies au cours desquelles le pathogène complète plusieurs cycles infectieux. Comme le pathogène produit lors de chaque cycle une grande quantité de spores, toutes susceptibles de coloniser de nouvelles surfaces foliaires, la dynamique des épidémies polycycliques est exponentielle. La plupart des champignons pathogènes polycycliques alternent également entre une forme sexuée (téléomorphe) et une forme asexuée (anamorphe). La Rouille brune ne fait pas exception à cette règle : il s'agit d'une rouille macrocyclique hétéroïcée, i.e. qu'elle produit cinq types de propagules au cours de son cycle de vie (trois stades asexués et deux stades sexués) et infecte au moins deux hôtes d'espèces différentes. D'un point de vue épidémiologique, nous ne nous intéresserons ici qu'au type de spores responsable des plus gros dégâts au cours des épidémies, les urédospores. Ce sont les spores asexuées produites au cours des cycles printaniers et estivaux que le pathogène effectue sur le seul de ses hôtes cultivés, le blé.

Il est classique de séparer les champignons pathogènes en trois groupes écologiques caractérisés par leur type trophique (Mendgen and Hahn 2002, Divon et Fluhr 2007, Horbach et coll., 2011). Les biotrophes, tels que les rouilles (Pucciniales), les charbons (Ustilaginales), les mildious poudreux (Erysiphales), les cloques (Taphriniales) ou les ergots (Clavicipitacées pathogènes), exploitent leur hôte sans endommager le tissu infecté. L'exploitation se fait souvent au moyen de structures d'absorption comme des haustoria. A l'opposé, les nécrotrophes comme les agents des alternarioSES (*Alternaria spp*), des fusarioSES (*Fusarium spp*, *Microdochium spp*), les pourritures nobLES (*Botrytis spp*) ou des pathogènes tels que *Scerotinia spp*, *Cochliobolus spp*, ou *Ascochyta spp*, tuent presque immédiatement leur tissu

hôte après infection. Ils ne sont capables d'exploiter leur hôte qu'en induisant une nécrose active des tissus. La stratégie hémibiotrophe, que l'on rencontre chez les agents des septoriose (*Zymoseptoria tritici*, *Parastagonospora nodorum*), des pyriculariose (*Magnaporthe oryzae*, ...), des cercosporiose (*Cercospora spp*), ou encore chez les tavelures (*Venturia spp*), apparaît de prime abord comme un intermédiaire entre biotrophie et nécrotrophie. Ces pathogènes sont biotropes durant leur période de latence (parfois même présentant des haustoria comme le Mildiou de la pomme de terre *Phytophthora infestans*) mais doivent nécessairement tuer le tissu hôte pour sporuler.

Le cycle infectieux des rouilles débute par la germination d'une urédospore sur la surface de la feuille de blé. L'apex du tube germinatif qui émerge de la spore se différencie en appressorium, cellule à la paroi épaisse et mélanisée à l'intérieur de laquelle s'accumule une forte pression de turgescence. Cette pression permet au champignon de forcer son chemin à travers l'ostiole d'un stomate fermé. Une fois dans la chambre sous-stomatique, le champignon différencie une vésicule sous-stomatique qui se prolonge en hyphes intercellulaires, au contact de l'apoplasm. Au contact de la paroi pectocellulosique des cellules du mésophylle, le mycélium se différencie en cellule mère haustoriale, qui traverse la paroi et différencie au contact du plasmalemme de la cellule végétale un diverticule cellulaire appelé haustorium. L'haustorium est une structure trophique qui, entourée d'une matrice extra-cellulaire spécialisée assurant à la fois l'évitement du système immunitaire de la plante et l'absorption de nutriments, permet au pathogène d'exploiter son hôte sans causer de dommage au tissu infecté (caractéristique principale du mode de vie « biotrophe » des rouilles). A partir du point d'infection, le champignon progresse de façon centrifuge dans les tissus, créant une lésion qui s'élargit avec le temps. Au cœur de la lésion, le mycélium se développe. Après une période d'environ 180 degrés-jours appelée période de latence, la croissance mycélienne au cœur de la lésion est remplacée par la production de structures reproductrices (urédies) contenant les urédospores, dont la dispersion anémophile assure la colonisation du couvert. Dans nos modèles, nous résumerons le cycle infectieux de la rouille de la façon suivante (Figure 5) : à une période juvénile uniquement consacrée à la croissance du mycélium (latence) succède une période uniquement dédiée à la reproduction. Cette stratégie en tout ou rien est qualifiée de stratégie « bang bang ». Nous ferons l'hypothèse dans nos modèles que le pathogène adopte une telle stratégie.

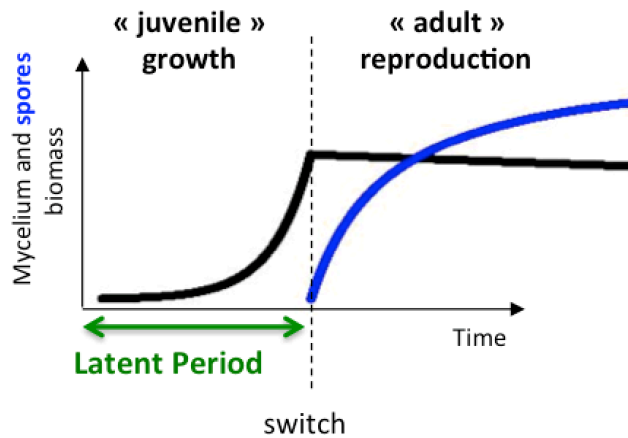


Figure 5 : simplification du cycle infectieux de la rouille du blé telle qu'utilisée dans nos modèles.

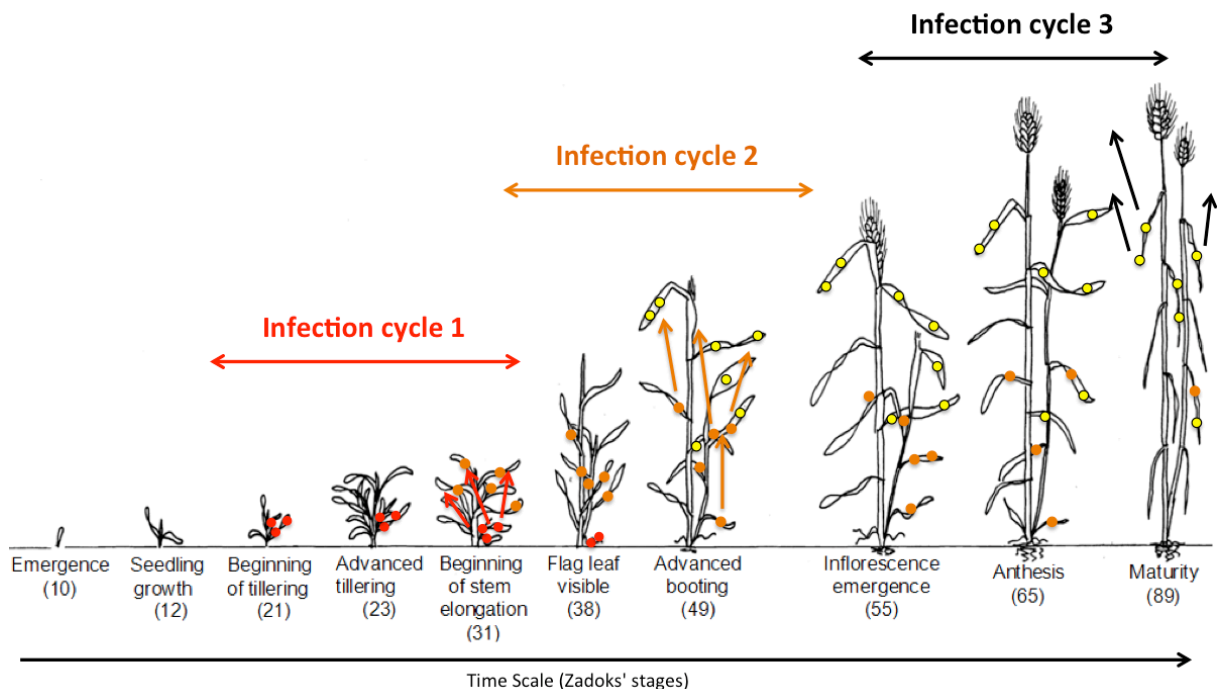


Figure 6 : schéma simplifié du déroulement d'épidémies polycycliques de Rouille du blé

Au cours d'une épidémie polycyclique, plusieurs cycles infectieux vont ainsi se succéder (Figure 6). L'épidémie est initiée par l'arrivée dans la parcelle d'un inoculum apporté de l'extérieur par le vent, souvent vers la fin avril ou début mai à la latitude de Paris (soit 1 000 à 1 300 degrés jours après semis, en fonction des conditions climatiques locales ; El Jarroudi et coll., 2014, Duvivier et coll., 2016). L'infection a lieu sur les feuilles de rosette. D'abord latentes, ces lésions finissent par émettre des spores qui, emportées par le vent, vont coloniser les feuilles qui ont eu le temps d'émerger pendant la latence du pathogène. Ainsi, le pathogène « grimpe » dans le couvert en suivant la croissance de la plante, de cycle infectieux

en cycle infectieux. Plusieurs études, notamment de modélisation, font état d'une course entre la plante et le pathogène pour la colonisation du couvert (Garin 2015, Robert et coll., 2017). En effet, la sénescence naturelle des feuilles de blé empêche l'installation du pathogène, biotrophe donc ne pouvant infecter qu'un tissu vivant, sur des tissus trop vieux. Si le pathogène n'est pas assez rapide pour coloniser les feuilles au fur et à mesure de leur émergence, il pourrait bien être rattrapé par la sénescence du couvert. Des cycles infectieux trop longs peuvent donc conduire à l'échappement de la plante face à la maladie.

Après plusieurs cycles (jusqu'à 8 d'après Agrios 2005), l'épidémie prend fin soit par la récolte de la culture, soit parce que tout le couvert a été colonisé par le pathogène (Figure 6). Le pathogène passe la période de l'interculture et/ou la mauvaise saison sur des résidus de culture ou des poacées sauvages infectées aux abords des parcelles. Cet inoculum permet le démarrage des épidémies lors de la saison suivante. Une fois l'épidémie initiée en revanche, c'est l'inoculum produit « en interne » dans le couvert qui est responsable du développement exponentiel de la maladie.

Conclusion : deux échelles sont donc à considérer absolument pour bien modéliser les interactions entre le champignon et son hôte : l'échelle du tissu/de la lésion, à laquelle ont lieu l'infection, les échanges de nutriments, la défense de la plante, la production de spores, ... , et l'échelle de la parcelle à laquelle ont lieu la croissance du couvert végétal et la dispersion des spores au cours des cycles infectieux successifs. Nous ne manquerons pas de bien prendre en compte ces deux échelles dans la construction de notre premier modèle. L'échelle du paysage transparaît également dans la description ci-dessus au travers des processus d'inoculation initiale et de survie lors de l'interculture.

Effet de la fertilisation sur les épidémies fongiques

Une bibliographie contrastée

Les liens entre fertilisation azotée et champignons pathogènes sont documentés de longue date (revue par Walters et Bingham, 2007). Smith et Blair (1950) et Last (1953) rapportent une plus grande susceptibilité du blé fertilisé au mildiou poudreux *Erysiphe graminis*. En 1962, Last note que « l'incidence du mildiou poudreux des céréales *Erysiphe graminis* est largement déterminée par le statut nutritif de son hôte. Appliquer une fertilisation azotée augmente visiblement les niveaux d'infection » (traduit de Last, 1962). D'autres travaux ultérieurs sur le même *E. graminis* confirment ces observations (Bainbridge, 1974 ; Shaner et Finney, 1977 ; Daamen et coll. 1989 ; Olesen et coll. 2003). Kürschner (1992) rapporte que la fertilisation azotée augmente la sévérité du pathogène *Magnaporthe grisea* sur riz. Howard et coll. (1994) obtiennent un résultat similaire pour trois pathogènes du blé, *Zymoseptoria tritici* et *Parastagonospora nodorum* (agents des septorioSES du blé) et *Puccinia recondita f. sp. tritici* (agent de la rouille brune du blé ; maintenant *P. triticina*). D'autres études font également état d'un accroissement de la sévérité d'épidémies de rouille avec la fertilisation (Ash et Brown, 1991 ; Danial et Parlevliet 1995 ; Devadas et coll. 2014). L'augmentation de la sévérité des épidémies de *Z. tritici* (déterminée après anthèse) avec le taux de fertilisation est également démontrée par Leitch et Jenkins (1994). Simon et coll. (2003) et Olesen et coll. (2003) montrent que la progression de la septorioSE du blé est plus rapide à forte fertilisation.

Cependant, d'autres études ne parviennent pas à établir de lien clair en fertilisation et épidémies, voire trouvent des résultats opposés. Buschbell et Hoffman (1992) et Olesen et coll. (2000) ne détectent aucun effet de la fertilisation azotée sur la septorioSE du blé. Hoffland et coll. (2000) montrent bien une susceptibilité accrue de tomates fertilisées à *Oidium lycopersicum* et à la bactérie *Pseudomonas syringae* pv. *tomato* mais aucun impact de la fertilisation sur l'infection par *Fusarium oxysporum* f. sp. *lycopersici* et même une réduction de la susceptibilité de ces mêmes plantes fertilisées à l'infection par *Botrytis cinerea*.

Ces exemples sont très illustratifs à plusieurs titres. Ils montrent tout d'abord que les effets de la fertilisation sont observables à différentes échelles : depuis le cycle infectieux (niveau de la lésion sur les feuilles) jusqu'aux épidémies. On retrouve ici les deux échelles

mentionnées précédemment. Il est également intéressant de noter à quel point ces résultats sont variés, parfois même contradictoires ! Nous interprétons cette diversité de résultats comme symptomatique d'une diversité de mécanismes par lesquels la fertilisation impacte les épidémies. Cette multiplicité d'effets fait l'objet de la suite de cette synthèse bibliographique. Elle est le point de départ de mon travail de thèse : parmi ces effets, lesquels devons-nous intégrer dans notre travail de modélisation afin de bien décrire l'effet de la fertilisation azotée sur les épidémies ?

De multiples effets de la fertilisation azotée sur les plantes.

L'impact de la fertilisation azotée sur la plante se manifeste à plusieurs niveaux.

a) A l'échelle tissulaire, sur le contenu en métabolite des organes

La fertilisation azotée augmente la concentration des métabolites primaires dans les organes tels que les feuilles. Ce phénomène a été démontré chez le blé (Spiertz et de Vos 1983 ; Robert et coll. 2002, 2006), le riz (Savary et coll. 1995), l'orge (Peros, 1990 ; Kürschner et coll. 1992 ; Jensen et Munk 1997), ou encore (hors de la famille des poacées) la tomate (Abro et coll. 2013). Dans le cas du blé, ce n'est pas seulement la quantité d'azote générale dans les feuilles qui augmente (via celle des protéines et des acides aminés), mais aussi le contenu en chlorophylle des feuilles (Filella et coll. 1995 ; Robert et coll. 2005), augmentant ainsi la capacité photosynthétique de la plante. Il est plus difficile de conclure sur l'effet de la fertilisation sur les métabolites secondaires tels que les composés de défense. Plusieurs auteurs notent chez le blé une diminution de la concentration en composés phénoliques (participant à la synthèse de composés immunitaires ou de lignines pariétales) ou de leur toxicité (Kirkham 1954 ; Király 1964 ; Matsuyama et Diamond 1973 ; Matsuyama 1975) avec la fertilisation. Cette réduction s'accompagne d'un amincissement des parois secondaires, d'une augmentation du pouvoir réducteur des organes et d'une diminution de l'activité de certaines enzymes (Király 1964). Des résultats similaires ont été montrés chez la tomate (Talukder et coll. 2005). Inversement, il semble que la fertilisation azotée favorise la synthèse de certaines protéines impliquées dans la résistance des plantes (Dietrich et coll. 2004). Comme la résistance des plantes aux champignons pathogènes

biotrophes passe par de nombreuses interactions protéine-protéines (effecteurs, facteurs de virulence, ...), il est possible que la fertilisation azotée ait un effet bénéfique sur ce sous-ensemble du système immunitaire végétal.

b) A l'échelle de la parcelle, sur l'architecture des plantes et du couvert

Chez le blé, la fertilisation azotée modifie également le nombre et la taille des organes. Ainsi, les plantes fertilisées présentent des feuilles plus grandes et conservent davantage de talles (Vos 1983 ; Lovell et coll. 1997, Robert et coll. 2004, 2006). Des résultats similaires ont été obtenus sur l'orge (Bainbridge 1974). La taille d'un couvert de blé est parfois mesurée en terme de surface foliaire totale (« leaf area index » ou LAI) ou, pour une mesure plus fonctionnelle, en terme de surface foliaire verte (« green leaf area index » ou gLAI). L'effet de la fertilisation azotée sur les couverts de blé est hautement dynamique. La formation de talles ainsi que l'augmentation de surface des feuilles rend le couvert fertilisé beaucoup plus dense. Ainsi, la vitesse de croissance du couvert augmente avec la fertilisation, conduisant à un LAI plus fort des couverts fertilisés (Cowling et Field 2003 et citations associées ; Drecce et coll. 2000 ; Yin et coll. 2003 ; Jiang et coll. 2004). Contrairement au LAI qui s'apparente à la somme des surfaces foliaires et est donc une grandeur cumulative, le gLAI atteint son maximum au cours de la saison et retombe à zéro lorsque le blé mûr. Sa valeur maximale augmente elle-aussi avec la fertilisation, mais sa dynamique change également avec le taux d'azote reçu par le couvert (Hinzman et coll. 1986 ; Benbi 1994 ; Forsman et Poutala 1997 ; Bedoussac et Justes 2010 ; Vári et Máriás 2013). Pour un blé d'hiver (celui qui nous intéressera dans nos modèles), le pic du gLAI des couverts faiblement fertilisées a lieu tard dans la saison (vers 1 300 dd après germination) tandis que le gLAI atteint son maximum plus tôt pour un couvert fortement fertilisé et plafonne entre (environ) 1 000 et 1 300 degrés-jours post germination (Hinzman et coll. 1986 ; Benbi 1994 ; Bedoussac et Justes 2010 ; Vári et Máriás 2013). Ce sont à la fois l'architecture et la dynamique de croissance du couvert qui changent avec la fertilisation et qui expliquent le taux de croissance accru d'un couvert fertilisé.

c) A l'échelle de la plante, les feuilles sont vertes plus longtemps

Chez l'orge (Marschner 1986) comme chez le blé, les feuilles de plantes fertilisées ont, en plus d'une concentration en azote plus forte, une durée de vie plus longue. Cet effet explique en partie que les couverts fortement fertilisés restent verts plus longtemps.

Nous retiendrons de l'ensemble de ces études que la fertilisation a trois effets principaux sur le blé en tant que ressource pour les pathogènes foliaires :

- sur la concentration en nutriments dans les feuilles
- sur la taille et la densité du couvert
- sur la durée de vie des feuilles.

De la plante fertilisée aux épidémies

Dans cette partie, nous analysons comment la fertilisation azotée peut impacter les épidémies de champignons pathogènes foliaires à travers ses différents effets sur la plante (présentés ci-dessus) aux deux échelles du tissu et du couvert soulignées précédemment.

a) Effet de la concentration en métabolites primaires dans les feuilles

Quels composés constituent la base du régime azoté des champignons pathogènes foliaires reste encore obscur (Solomon et coll. 2003 ; Divon et Fluhr 2006). Néanmoins, quels que soient ces composés, il est vraisemblable que l'augmentation de la concentration en métabolites des feuilles de blé avec le taux de fertilisation de la plante donne accès à davantage de ressources au pathogène. C'est en tout cas l'une des hypothèses centrale de notre travail. Cette hypothèse est supportée par les travaux de Robert et coll. (2002, 2004, 2006) qui parviennent à lier fertilisation azotée, quantité de métabolites dans les feuilles de blé et intensité de la production de spores. Utilisant le modèle FSPM Septo3D, Baccar et coll. (2011) montrent un effet de la concentration des feuilles en azote sur le développement des lésions de *Z. tritici*. Cette hypothèse selon laquelle

l'augmentation des ressources intra-tissulaires avec la fertilisation bénéficie au champignon est également supportée par Leitch et Jenkins (1995), Jensen et Munk (1997), Neumann et coll. (2004), Walters et Bingham (2007) et Lecompte et coll. (2010).

D'autres effets de l'azote sur le cycle infectieux ont été mis en évidence. Arora et coll. (1985) et Schisler (1990) notent que les spores de pathogènes produites dans des conditions de stress azoté germent moins bien (respectivement conidies de *Bipolaris sorokiniana* et *Colletotrichum truncatum*). Savary et coll. (1995) notent que la fertilisation du riz accélère la croissance des lésions du pathogène racinaire *Rhizoctonia solani*. Bainbridge (1974) montre un résultat similaire pour *Erysiphe graminis* sur orge. Verhoeff (1968) trouve davantage de lésions de *Botrytis cinerea* sur des tomates fortement fertilisées. Des résultats similaires sont rapportés par Bainbridge (1974) pour *E. graminis* sur orge et Kürschner et coll. (1992) pour *Magnaporthe oryzae* sur riz. Jensen et Munk (1997) quant à eux montrent une efficacité d'infection accrue de l'orge au mildiou poudreux lorsque le taux de fertilisation augmente. Plusieurs études font aussi état d'un effet de la fertilisation sur la durée de latence, mais les résultats dépendent là encore du type de pathogène. Bainbridge (1974) et Jensen et Munk (1997) trouvent une latence d'*E. graminis* sur orge plus courte lorsque la fertilisation augmente (et donc des cycles infectieux qui se succèdent plus rapidement). En revanche, Lecompte et coll. (2010) rapportent une latence de *Botrytis cinerea* sur tomate plus longue à forte fertilisation. Mais de tous les paramètres du cycle infectieux, c'est la production de spores qui présente la réponse la plus forte à la fertilisation, quel que soit le pathogène : plus la fertilisation est élevée, plus la production de spores augmente (Bainbridge 1974 ; Jensen et Munk, 1997 ; Lovell et coll. 1997 ; Robert et coll. 2002, 2004 ; Yermiyahu et coll. 2006 ; Abro et coll. 2013).

De cette dense bibliographie, nous retiendrons que le niveau de ressources global (quels que soient les composés en jeu) favorise le développement du pathogène à l'échelle du cycle infectieux, augmentant notamment la production de spores. On négligera pour le moment l'effet de la fertilisation sur la défense de l'hôte.

b) Effet de la durée de vie des feuilles

L'effet de l'augmentation de la durée de vie des feuilles avec la fertilisation sur le cycle infectieux des pathogènes foliaires n'a, à notre connaissance pas encore fait l'objet d'études spécifiques. Cet effet est néanmoins pris en compte comme réponse à la fertilisation dans certaines études théoriques. En effet, par des travaux de modélisation, Robert et coll. (2017) montrent l'existence d'une course à l'échelle des organes entre la sénescence naturelle qui remobilise les ressources de la plante pour elle-même et l'exploitation par le champignon. Dans ce contexte, la durée d'exploitation de l'hôte par le pathogène est conditionnée par la durée de vie des feuilles.

c) Effet de la densité du couvert

Les différences d'architecture et de dynamique du couvert liées à la fertilisation peuvent impacter le développement des maladies foliaires d'une part en modifiant les conditions de dispersion des spores dans le couvert et d'autre part en y modifiant le microclimat.

Augmenter la densité du couvert favorise la dispersion via le rapprochement des feuilles les unes par rapport aux autres (Lovell et coll. 1997, Calonnec et coll. 2008, Robert et coll 2008, Garin et coll. 2014). Cet effet est spécialement marqué pour des pathogènes qui, comme la septoriose du blé, sont dispersés par les éclaboussures consécutives à l'impact des gouttes de pluie sur les feuilles. Notons toutefois que des feuilles plus proches les unes des autres impliquent une pénétration moindre de la pluie dans le couvert, ce qui *in fine* limite la dispersion du pathogène (Rapilly et Jolivet 1976 ; Saint-Jean et coll. 2004). Cet « effet parapluie » par lequel des feuilles plus proches dans un couvert plus dense seraient en réalité moins accessibles pour le pathogène n'est pas pris en compte dans notre modèle, les rouilles étant dispersées par le vent. En l'absence de cet effet, la densité du couvert détermine donc le nombre de feuilles accessibles au pathogène à un moment donné. Elle détermine également la distance entre les feuilles infectées, source de spores et les feuilles qui émergent, nouvelles cibles des champignons (Savary et coll. 1995 ; Lovell et coll. 1997).

Bien que les conséquences de tels changements soient difficiles à saisir d'un point de vue épidémiologique, l'augmentation de densité des couverts avec la fertilisation s'accompagne généralement d'une augmentation de leur humidité. Cet effet, considéré comme favorisant le déroulement du cycle infectieux des pathogènes, est invoqué dans plusieurs études faisant état d'une corrélation entre densité du couvert et épidémies (Darwinkel 1980, Daamen et coll. 1989, Danial et Parlevliet 1995, Savary et coll. 1995, Jensen et Munk 1997, Lovell et coll. 1997). Nous ne tenons pas compte de cet effet microclimatique dans la version actuelle de nos modèles.

Plus récemment, Robert et coll. (2017) ont montré qu'il existe une course entre le couvert et le champignon à deux niveaux : (1) une course locale entre sénescence naturelle et exploitation des feuilles par le pathogène et en conséquence (2) une course entre le pathogène et la plante pour la colonisation/l'échappement du couvert. La fertilisation, en changeant la dynamique de croissance du couvert, aura certainement des répercussions sur cette course pour l'acquisition/la conservation des ressources. Afin de pouvoir prendre en compte cet aspect dans notre travail, nous aurons besoin de deux échelles de modélisation, une locale (échelle du tissu) où opèrent les processus trophiques, et une plus large (échelle du couvert) où opèrent les processus de dispersion.

Plus globalement, nous retiendrons dans nos modèles que l'augmentation de la taille et de la densité du couvert en réponse à la fertilisation se traduit par une surface accrue de tissu vert susceptible d'être colonisé par le champignon. L'accessibilité de cette ressource dépendra néanmoins de la dynamique de croissance du couvert et de la localisation du tissu au sein du couvert, elles-mêmes dépendantes de la fertilisation (échappement possible).

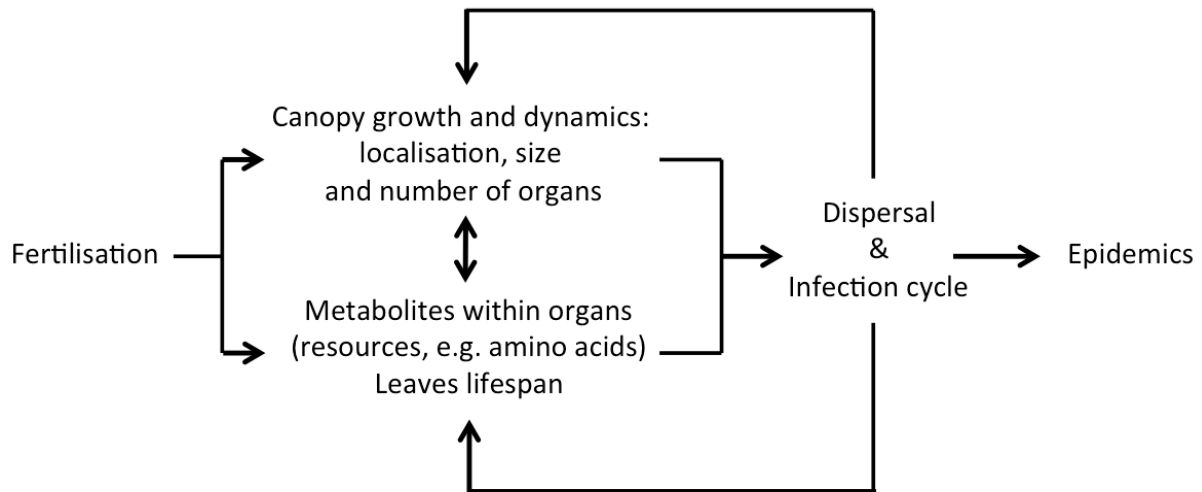


Figure 7 : résultat de notre synthèse bibliographique sur l'impact de la fertilisation sur le pathosystème.

Conclusion : d'un point de vue expérimental, il est difficile de séparer les effets qu'a la fertilisation sur le pathosystème (Lovell et coll. 1997). Cela devient beaucoup plus facile avec des modèles mathématiques. En cela, la modélisation est un outil précieux qui pourra nous aider à comprendre ces effets, à les décorrérer et à les hiérarchiser. Dans ce travail de thèse nous avons choisi de modéliser l'effet de la fertilisation via la quantité de ressources à laquelle le pathogène peut avoir accès à un moment donné (Figure 7). Nous considérerons ainsi que la quantité de métabolites dans les tissus (concentration de métabolites foliaires), la quantité de tissu colonisable (dynamique et taille du couvert) ainsi que sa durée de vie des feuilles déterminent la quantité des ressources « végétales » potentiellement utilisables par le pathogène. Pouvoir séparer ces trois effets dans notre modèle passe à nouveau par la prise en compte d'au moins deux échelles : celle du tissu/de la lésion et celle du couvert/des épidémies.

Références

1. Abro, M.A. (2013). Nitrogen fertilization of the host plant influences susceptibility, production and aggressiveness of *Botrytis cinerea* secondary inoculum and on the efficacy of biological control.
2. Agrios, G. N. (2005). Plant diseases caused by fungi. Pages 562–582 in: *Plant Pathology*, 5th ed. Academic Press, Cambridge, MA.
3. Altieri, M.A. (1994). Biodiversity and pest management in agroecosystems. New York: Haworth Press
4. Altieri, M.A., Nicholls, C.I., Henao, A., and Lana, M.A. (2015). Agroecology and the design of climate change-resilient farming systems. *Agronomy for Sustainable Development* 35, 869–890.
5. Arora, D.K., Filonow, A.B., and Lockwood, J.L. (1985). Decreased aggressiveness of *Bipolaris sorokiniana* conidia in response to nutrient stress. *Physiological Plant Pathology* 26, 135–142.
6. Ash, G.J., and Brown, J.F. (1991). Effect of nitrogen nutrition of the host on the epidemiology of *Puccinia striiformis* f.sp. *tritici* and crop yield in wheat. *Australasian Plant Pathology* 20, 108–114.
7. Baccar, R., Fournier, C., Dornbusch, T., Andrieu, B., Gouache, D., and Robert, C. (2011). Modelling the effect of wheat canopy architecture as affected by sowing density on *Septoria tritici* epidemics using a coupled epidemic/virtual plant model. *Annals of Botany* 108, 1179–1194.
8. Bainbridge, A. (1974). Effect of Nitrogen Nutrition of the Host on Barley Powdery Mildew. *Plant Pathology* 23, 160–161.
9. Bedoussac, L., and Justes, E. (2010). Dynamic analysis of competition and complementarity for light and N use to understand the yield and the protein content of a durum wheat-winter pea intercrop. *Plant and Soil* 330, 37–54.
10. Beman, J.M., Arrigo, K.R., and Matson, P.A. (2005). Agricultural runoff fuels large phytoplankton blooms in vulnerable areas of the ocean. *Nature* 434, 211–214.
11. Benbi, D.K. (1994). Prediction of leaf area indices and yields of wheat. *Journal of Agricultural Science* 122, 13–20.
12. Berraies, S., Gharbi, M.S., Rezgui, S., and Yahyaoui, A. (2014). Estimating grain yield losses caused by septoria leaf blotch on durum wheat in Tunisia. *Chilean Journal of Agricultural Research* 74, 432–437.
13. Berry, P.M., Kindred, D.R., and Paveley, N.D. (2008). Quantifying the effects of fungicides and disease resistance on greenhouse gas emissions associated with wheat production. *Plant Pathology* 57, 1000–1008.
14. Brent, K. J., and Hollomon, D. W. 2007. Fungicide Resistance in Crop Pathogens: How Can It Be Managed? FRAC Monogr. No. 1 (second, revised edition). Fungicide Resistance Action Committee 2007, CropLife International, Brussels.
15. Brisson, N., Gate, P., Gouache, D., Charmet, G., Oury, F.X., and Huard, F. (2010). Why are wheat yields stagnating in Europe? A comprehensive data analysis for France. *Field Crops Research* 119, 201–212.
16. Brotman, Y., Makovitzki, A., Shai, Y., Chet, I., and Viterbo, A. (2009). Synthetic ultrashort cationic lipopeptides induce systemic plant defense responses against bacterial and fungal pathogens. *Applied and Environmental Microbiology* 75, 5373–5379.
17. Bruce, T.J.A. (2010). Tackling the threat to food security caused by crop pests in the new millennium. *Food Security* 2, 133–141.

18. Buschbell T., Hoffmann G.M. (1992) The effects of different nitrogen regimes on the epidemiologic development of pathogens on winter-wheat and their control. *Journal of Plant Diseases and Protection*, 99, 381–403.
19. Calonnec, A., Cartolaro, P., Naulin, J.M., Bailey, D., and Langlais, M. (2008). A host-pathogen simulation model: Powdery mildew of grapevine. *Plant Pathology* 57, 493–508.
20. Chen, Y.L.L., Chen, H.Y., Karl, D.M., and Takahashi, M. (2004). Nitrogen modulates phytoplankton growth in spring in the South China Sea. *Continental Shelf Research* 24, 527–541.
21. Chuwa, C.J., Mabagala, R.B., and Reuben, M.S.O.W. (2015). Assessment of grain yield losses caused by rice blast disease in major rice growing areas in Tanzania. *International Journal of Science and Research* 4(10), 2211-2218.
22. Claessen, D., de Roos, A.M., and Persson, L. (2000). Dwarfs and Giants: Cannibalism and Competition in Size-Structured Populations. *The American Naturalist* 155, 219–237.
23. Cohen, D. (1976). On the Optimal Timing of Reproduction. *The American Naturalist*, 110(975), 801–807. <https://doi.org/10.1086/283495>
24. Collinge DB. (2016) Biotechnology for Plant Disease Control, New York and London: Wiley 440 pages.
25. Comby, M., Gacoin, M., Robineau, M., Rabenoelina, F., Ptas, S., Dupont, J., Profizi, C., and Baillieul, F. (2017). Screening of wheat endophytes as biological control agents against Fusarium head blight using two different in vitro tests. *Microbiological Research* 202, 11–20.
26. Cowling, S.A., and Field, C.B. (2003). Environmental control of leaf area production: Implications for vegetation and land-surface modeling - art. no. 1007. *Global Biogeochemical Cycles* 17, 1007.
27. Danial, D.L., and Parlevliet J.E. (1995). Effects of nitrogen fertilization on disease severity and infection type of yellow rust on wheat genotypes varying in quantitative resistance, *J. Phytopathology* 143 679–681.
28. D'Onofrio, A. (2002). Stability properties of pulse vaccination strategy in SEIR epidemic model. *Mathematical Biosciences* 179, 57–72.
29. Daamen, R.A., Wijnands, F.G., and Vliet, G. vander (1989). Epidemics of Diseases and Pests of Winter Wheat at Different Levels of Agrochemical Input: A study on the possibilities for designing an integrated cropping system. *Journal of Phytopathology* 125, 305–319.
30. Darwinkel A 1980 Grain production of winter wheat in relation to nitrogen and diseases. Relationship between nitrogen dressing and yellow rust infection. *Z. Acker Pflanzenbau* 149,299-308.
31. De Roos, A.M., Diekmann, O., and Metz, J.A.J. (1992). Studying the Dynamics of Structured Population Models: A Versatile Technique and Its Application to Daphnia. *The American Naturalist* 139, 123–147.
32. De Roos, A.M. A Gentle Introduction to Physiologically Structured Population Models. *Structured-Population Models in Marine, Terrestrial, and Freshwater Systems* 119-204 (1997).
33. De Schrijver A. 2007. Acidification and eutrophication of forests on sandy soil: effects of forest type and deposition load. Ph.D. thesis, Ghent University, Belgium, 189p.
34. De Schutter, O.S. (2010). Rapport du Rapporteur spécial sur le droit à l'alimentation. *Production* 17850, 1–4.
35. Deising, H. B., Reimann, S., and Pascholati, S. F. 2008. Mechanisms and significance of fungicide resistance. *Braz. J. Microbiol.* 39:286-295.

36. Devadas, R., Simpfendorfer, S., Backhouse, D., and Lamb, D.W. (2014). Effect of stripe rust on the yield response of wheat to nitrogen. *Crop Journal* 2, 201–206.
37. Dietrich, R., Ploß, K., and Heil, M. (2004). Constitutive and induced resistance to pathogens in *Arabidopsis thaliana* depends on nitrogen supply. *Plant, Cell and Environment* 27, 896–906.
38. Dirnböck, T., Grandin, U., Bernhardt-Römermann, M., Beudert, B., Canullo, R., Forsius, M., Grabner, M.-T., Holmberg, M., Kleemola, S., Lundin, L., et al. (2014). Forest floor vegetation response to nitrogen deposition in Europe. *Global Change Biology* 20, 429–440.
39. Divon, H.H., and Fluhr, R. (2007). Nutrition acquisition strategies during fungal infection of plants. *FEMS Microbiology Letters* 266, 65–74.
40. Dreccer, M. (2000). Dynamics of Vertical Leaf Nitrogen Distribution in a Vegetative Wheat Canopy. Impact on Canopy Photosynthesis. *Annals of Botany* 86, 821–831.
41. Duvivier, M., Dedeurwaerde, G., Bataille, C., De Proft, M., and Legre've, A. 2016. Real-time PCR quantification and spatio-temporal distribution of airborne inoculum of *Puccinia triticina* in Belgium. *Eur. J. Plant Pathol.* 145:405-420.
42. Edwards-Jones, G. (2008). Do benefits accrue to “pest control” or “pesticides?”: A comment on Cooper and Dobson. *Crop Protection* 27, 965–967.
43. El Jarroudi, M., Kouadio, L., Delfosse, P., and Tychon, B. 2014. Brown rust disease control in winter wheat: I. Exploring an approach for disease progression based on night weather conditions. *Environ. Sci. Pollut. Res.* 21:4797-4808.
44. Engen, S., and Saether, B. (1994). Optimal allocation of resources to growth and reproduction. *Theoretical Population Biology* 46, 232–248.
45. Esmaeel, Q., Pupin, M., Kieu, N.P., Chataigné, G., Béchet, M., Deravel, J., Krier, F., Höfte, M., Jacques, P., and Leclère, V. (2016). Burkholderia genome mining for nonribosomal peptide synthetases reveals a great potential for novel siderophores and lipopeptides synthesis. *MicrobiologyOpen* 5, 512–526.
46. Evenson, R. (2003). Assessing the impact of the Green Revolution, 1960 to 2000. *Science* 300, 758–763.
47. Evers, J.B., Vos, J., Fournier, C., Andrieu, B., Chelle, M., and Struik, P.C. (2007). An architectural model of spring wheat: Evaluation of the effects of population density and shading on model parameterization and performance. *Ecological Modelling* 200, 308–320.
48. Eyal, Z., A.L. Scharen, J.M. Prescott, and M. van Ginkel. 1987. The *Septoria* Diseases of Wheat : Concepts and methods of disease management. Mexico, D.F. : CIMMYT.
49. FAO (2014) FAOSTAT. Available at: <http://faostat3.fao.org/home/index.html> (accessed 20 May 2014).
50. Fenn, M., Baron, J., Allen, E., Rueth, H., Nydick, K., Geiser, L., Bowman, W., Sickman, J., Meixner, T., Johnson, D., et al. (2003). Ecological Effects of Nitrogen Deposition in the Western United States. *BioScience* 53, 404–420.
51. Filella, I., Serrano, L., Serra, J., and Peñuelas, J. (1995). Evaluating Wheat Nitrogen Status with Canopy Reflectance Indexes and Discriminant-Analysis. *Crop Science* 35, 1400–1405.
52. Fones, H., and Gurr, S. (2015). The impact of *Septoria tritici* Blotch disease on wheat: An EU perspective. *Fungal Genetics and Biology* 79, 3–7.
53. Food and Agriculture Organization of the United Nations (2006). *World Agriculture: Towards 2030/2050* (Food and Agriculture Organization of the United Nations, Rome).

54. Ford Denison, R., and McGuire, A.M. (2015). What should agriculture copy from natural ecosystems? *Global Food Security* 4, 30–36.
55. Forsman, K., and Poutala, T. (1997). Crop Management Effects on Pre- and Post-Anthesis Changes in Leaf Area Index and Leaf Area Duration and their Contribution to Grain Yield and Yield Components in Spring Cereals. *Journal of Agronomy and Crop Science* 61, 47–61.
56. Garin G. 2015. Vers la compréhension des épidémies fongiques foliaires par modélisation multi-échelle dans les couverts architecturés. Thèse de Doctorat soutenue le 11 décembre 2015.
57. Geritz, S.A.H., Kisdi, É., Meszéna, G., and Metz, J.A.J. (1998). Evolutionarily singular strategies and the adaptive growth and branching of the evolutionary tree. *Evolutionary Ecology* 12, 35–57.
58. Gilchrist, M. A., Sulsky, D. L., and Pringle, A. 2006. Identifying fitness and optimal life-history strategies for an asexual filamentous fungus. *Evolution* 60:970-979.
59. Godin, C., and Sinoquet, H. (2005). Functional-structural plant modelling. *New Phytologist* 166, 705–708.
60. Gullino, M.L., Leroux, P., and Smith, C.M. (2000). Uses and challenges of novel compounds for plant disease control. *Crop Protection* 19, 1–11.
61. Hayes, L.E., Sackett, K.E., Anderson, N.P., and Flowers, M.D. (2016). Evidence of Selection for Fungicide Resistance in *Zymoseptoria tritici* Populations on Wheat in Western Oregon. *Plant Disease* 100, 483–489.
62. Hewitt, H. G. 1998. *Fungicides in Crop Protection*. CAB International, Wallingford, UK.
63. Hinzman, L.D., Bauer, M.E., and Daughtry, C.S.T. (1986). Effects of Nitrogen-Fertilization on Growth and Reflectance Characteristics of Winter-Wheat. *Remote Sensing of Environment* 19, 47–61.
64. Horbach, R., Navarro-Quesada, A.R., Knogge, W., and Deising, H.B. (2011). When and how to kill a plant cell: Infection strategies of plant pathogenic fungi. *Journal of Plant Physiology* 168, 51–62
65. Hoffland, E., Jeger, M.J., and van Beusichem, M.L. (2000). Effect of nitrogen supply rate on disease resistance in tomato depends on the pathogen. *Plant and Soil* 218, 239–247.
66. Howard, D., Chambers, A., and Logan, J. (1994). Nitrogen and Fungicide Effects on Yield Components and Disease Severity in Wheat. *Journal of Production Agriculture* 7, 448–454.
67. Howarth, R.W., and Marino, R. (2006). Nitrogen as the limiting nutrient for eutrophication in coastal marine ecosystems: Evolving views over three decades. *Limnology and Oceanography* 51, 364–376.
68. Jensen, B., and Munk, L. (1997). Nitrogen-induced changes in colony density and spore production of *Erysiphe graminis* f.sp. *hordei* on seedlings of six spring barley cultivars. *Plant Pathology* 46, 191–202.
69. Jiang, D., Dai, T., Jing, Q., Cao, W., Zhou, Q., Zhao, H., and Fan, X. (2004). Effects of long-term fertilization on leaf photosynthetic characteristics and grain yield in winter wheat. *Photosynthetica* 42, 439–446.
70. Jones, E.O., Webb, S.D., Ruiz-Fons, F.J., Albon, S., and Gilbert, L. (2011). The effect of landscape heterogeneity and host movement on a tick-borne pathogen. *Theoretical Ecology* 4, 435–448.
71. Király, Z. (1964). Effect of Nitrogen Fertilization on Phenol Metabolism and Stem Rust Susceptibility of Wheat. *Journal of Phytopathology* 51, 252–261.
72. Kirkham, D.S. (1954). Significance of the ratio between the water-soluble aromatic and nitrogen constituents of apple and pear in the host-parasite relationships of *venturia* species [16]. *Nature* 173, 690–691.

73. Koch, A., Biedenkopf, D., Furch, A., Weber, L., Rossbach, O., Abdellatef, E., Linicus, L., Johannsmeier, J., Jelonek, L., Goesmann, A., et al. (2016). An RNAi-Based Control of *Fusarium graminearum* Infections Through Spraying of Long dsRNAs Involves a Plant Passage and Is Controlled by the Fungal Silencing Machinery. *PLoS Pathogens* 12.
74. Kou, Y., and Wang, S. (2010). Broad-spectrum and durability: understanding of quantitative disease resistance. *Current Opinion in Plant Biology* 13, 181–185.
75. Kozlowski, J. (1992). Optimal allocation of resources to growth and reproduction: Implications for age and size at maturity. *Trends in Ecology & Evolution* 7, 15–19.
76. Kürschner, E., Bonman, J., Garrity, D.P., Tamisin, M.M., Pabale, D., and Estrada, B. (1992). Effects of nitrogen timing and split application on blast disease in upland rice. *Plant Disease* 76, 384–389.
77. Laursen, K., and Møller, A.P. (2014). Long-term changes in nutrients and mussel stocks are related to numbers of breeding eiders *Somateria mollissima* at a large baltic colony. *PLoS ONE* 9.
78. Last, F.T. (1953). Some Effects of Temperature and Nitrogen Supply on Wheat Powdery Mildew. *Annals of Applied Biology* 40, 312–322.
79. Last, F.T. (1962). Effects of Nutrition on the Incidence of Barley Powdery Mildew. *Plant Pathology* 11, 133–136.
80. Lecompte, F., Abro, M.A., and Nicot, P.C. (2010). Contrasted responses of *Botrytis cinerea* isolates developing on tomato plants grown under different nitrogen nutrition regimes. *Plant Pathology* 59, 891–899.
81. Leitch, M.H., and Jenkins, P.D. (1994). Influence of nitrogen on the development of *Septoria* epidemics in winter wheat. *Journal of Agricultural Science* 124, 361–368.
82. Li, M. Y., and Muldowney, J. S. 1995. Global stability for the SEIR model in epidemiology. *Math. Biosci.* 125:155-164.
83. Loeuille, N., Barot, S., Georgelin, E., Kyafis, G., and Lavigne, C. (2013). Eco-evolutionary dynamics of agricultural networks: Implications for sustainable management. *Advances in Ecological Research* 49, 339–435.
84. López-Ráez, J.A., Bouwmeester, H., and Pozo, M.J. (2012). Communication in the Rhizosphere, a Target for Pest Management. *Agroecology and Strategies for Climate Change* 8, 109–133.
85. Lovell, D.J., Parker, S.R., Hunter, T., Royle, D.J., and Coker, R.R. (1997). Influence of crop growth and structure on the risk of epidemics by *Mycosphaerella graminicola* (*Septoria tritici*) in winter wheat. *Plant Pathology* 46, 126–138.
86. Khush, G.S., and Jena, K.K. (2009). Current Status and Future Prospects for Research on Blast Resistance in Rice (*Oryza sativa* L.). *Advances in Genetics, Genomics and Control of Rice Blast Disease* 1–10.
87. Ma, Z.H., and Michailides, T.J. (2005). Advances in understanding molecular mechanisms of fungicide resistance and molecular detection of resistant genotypes in phytopathogenic fungi. *Crop Protection* 24, 853–863.
88. Marschner H. (1986). *Mineral Nutrition of Higher Plants*. London: Academic Press.
89. Matsuyama, N., and Dimond, A.E. (1973). Effect of nitrogenous fertilizer on biochemical processes that could affect lesion size of rice blast. *Phytopathology* 63, 1202–1203.
90. Matsuyama, N. (1975). The effect of ample nitrogen fertilizer on cell wall materials and its significance to rice blast disease. *Annual Phytopathological Society of Japan* 41, 56–61.

91. McDonald, B.A., and Linde, C. (2002). Pathogen population genetics, evolutionary potential, and durable resistance. *Annual Review of Phytopathology* 40, 349–379.
92. Mendgen, K., and Hahn, M. (2002). Plant infection and the establishment of fungal biotrophy. *Trends in Plant Science* 7, 352–356
93. Metz, J.a.J., Nisbet, R.M., and Geritz, S.a.H. (1992). How should we define 'fitness' for general ecological scenarios? *Trends in Ecology & Evolution* 7, 198–202.
94. Møller, A.P., Flensted-Jensen, E., and Mardal, W. (2007). Agriculture, fertilizers and life history of a coastal seabird. *Journal of Animal Ecology* 76, 515–525.
95. Neumann, S., Paveley, N.D., Beed, F.D., and Sylvester-Bradley, R. (2004). Nitrogen per unit leaf area affects the upper asymptote of *Puccinia striiformis* f.sp. *tritici* epidemics in winter wheat. *Plant Pathology* 53, 725–732.
96. Oerke, E. C., & Dehne, H. W. (1997). Global crop production and the efficacy of crop protection - Current situation and future trends. *Eur. J. Plant Pathol.*, 103(3), 203–215.
97. Oerke, E.-C., and Dehne, H.-W. (2004). Safeguarding production—losses in major crops and the role of crop protection. *Crop Protection* 23, 275–285.
98. Olesen, J.E., Mortensen, J.V., Jørgensen, L.N., and Andersen, M.N. (2000). Irrigation strategy, nitrogen application and fungicide control in winter wheat on a sandy soil. I. Yield, yield components and nitrogen uptake. *Journal of Agricultural Science* 134, 1–11.
99. Olesen, J.E., Jørgensen, L.N., Peterson, J., and Mortensen, J.V. (2003). Effects of rate and timing of nitrogen fertilizer on disease control by fungicides in winter wheat. 1. Grain yield and foliar disease control. *Journal of Agricultural Science* 140.
100. Papaïx, J., Adamczyk-Chauvat, K., Bouvier, A., Kiêu, K., Touzeau, S., Lannou, C., and Monod, H. (2014). Pathogen population dynamics in agricultural landscapes: The Ddal modelling framework. *Infection, Genetics and Evolution* 27, 509–520.
101. Papaïx, J., Burdon, J.J., Zhan, J., and Thrall, P.H. (2015). Crop pathogen emergence and evolution in agro-ecological landscapes. *Evolutionary Applications* 8, 385–402.
102. Park, A., Gubbins, S., and Gilligan, C. (2001). Invasion and Persistence of Plant Parasites in a Spatially Structured Host Population. *Oikos* 94, 162–174.
103. Peros JP, 1990. Relations entre les teneurs en minéraux des limbes de canne à sucre et l'infection par *Puccinia melanocephala* II—Essais au champ. *Agronomie Tropicale*.
104. Pimentel, D., and Burgess, M. (2014). Environmental and economic costs of the application of pesticides primarily in the United States. In *Integrated Pest Management*, (Springer Netherlands), pp. 47–71.
105. Poland, J.A., Balint-Kurti, P.J., Wisser, R.J., Pratt, R.C., and Nelson, R.J. (2009). Shades of gray: the world of quantitative disease resistance. *Trends in Plant Science* 14, 21–29.
106. Plantegenest, M., Le May, C., and Fabre, F. (2007). Landscape epidemiology of plant diseases. *Journal of The Royal Society Interface* 4, 963–972.
107. Pretorius, Z.A., Singh, R.P., Wagiore, W.W., and Payne, T.S. (2000). Detection of virulence toward stemrust resistance gene Sr31 in *Puccinia graminis* f. sp. *tritici* in Uganda. *Plant Disease* 84, 203.
108. Rapilly, F., and Jolivet, E. (1976). Construction d'un modèle (episept) permettant la simulation d'une épidémie de *Septoria nodorum* BERK. sur blé. *Revue* 4, 5–15.

109. Ray, D.K., Ramankutty, N., Mueller, N.D., West, P.C., and Foley, J.A. (2012). Recent patterns of crop yield growth and stagnation. *Nature Communications* 3.
110. Robert, C., Bancal, M.-O., and Lannou, C. (2002). Wheat Leaf Rust Uredospore Production and Carbon and Nitrogen Export in Relation to Lesion Size and Density. *Phytopathology* 92, 762–768.
111. Robert, C., Bancal, M.-O., and Lannou, C. (2004). Wheat Leaf Rust Uredospore Production on Adult Plants: Influence of Leaf Nitrogen Content and *Septoria tritici* Blotch. *Phytopathology* 94, 712–721.
112. Robert, C., Bancal, M.-O., Ney, B., and Lannou, C. (2005). Wheat leaf photosynthesis loss due to leaf rust, with respect to lesion development and leaf nitrogen status. *New Phytologist* 165, 227–241.
113. Robert, C., Fournier, C., Andrieu, B., and Ney, B. (2008). Coupling a 3D virtual wheat (*Triticum aestivum*) plant model with a *Septoria tritici* epidemic model (Septo3D): A new approach to investigate plant-pathogen interactions linked to canopy architecture. *Functional Plant Biology* 35, 997–1013.
114. Roelfs AP, Singh RP, Saari EE (1992) Rust diseases of wheat: concepts and methods of disease management Mexico, 81 pp. Mexico, DF (Mexico), CIMMYT
115. Roff, D. A. 2002. Life history evolution. Sinauer Associates, Sunderland, Massachusetts.
116. Roux, F., Voisin, D., Badet, T., Balague, C., Barlet, X., Huard-Chauveau, et al. (2014). Resistance to phytopathogens e tutti quanti: placing plant quantitative disease resistance on the map, *Molecular Plant Pathology* 15 427–432.
117. Saint-Jean, S., Chelle, M., and Huber, L. (2004). Modelling water transfer by rain-splash in a 3D canopy using Monte Carlo integration. *Agricultural and Forest Meteorology* 121, 183–196.
118. Savary, S., Castilla, N., and Elazegui, F. (1995). Direct and indirect effects of nitrogen supply and disease source structure on rice sheath blight spread. *Phytopathology* 85, 959–965.
119. Schisler, D. (1990). Influence of Nutrition During Conidiation of *Colletotrichum truncatum* on Conidial Germination and Efficacy in Inciting Disease in *Sesbania exaltata*. *Phytopathology* 81, 458–461.
120. Shaner, G., and Finney, R.E. (1977). The Effect of Nitrogen Fertilization on the Expression of Slow-Mildewing Resistance in Knox Wheat. *Phytopathology* 77, 1051–1056.
121. Sierotzki, H., and Scalliet, G. 2013. A review of current knowledge of resistance aspects for the next-generation succinate dehydrogenase inhibitor fungicides. *Phytopathology* 103:880-887
122. Sievänen, R., Godin, C., De Jong, T.M., and Nikinmaa, E. (2014). Functional-structural plant models: A growing paradigm for plant studies. *Annals of Botany* 114, 599–603.
123. Simón, M.R., Cordero, C. a., Perelló, a. E., and Struik, P.C. (2003). Influence of Nitrogen Supply on the Susceptibility of Wheat to *Septoria tritici*. *Journal of Phytopathology* 151, 283–289.
124. Skelsey, P., Rossing, W. a H., Kessel, G.J.T., and van der Werf, W. (2010). Invasion of Phytophthora infestans at the landscape level: how do spatial scale and weather modulate the consequences of spatial heterogeneity in host resistance? *Phytopathology* 100, 1146–1161.
125. Smith, H.C., and Blair, I.D. (1950). Wheat Powdery Mildew Investigations. *Annals of Applied Biology* 37, 570–583.
126. Snoeijers, S.S., Pérez-García, A., Joosten, M.H.A.J., and De Wit, P.J.G.M. (2000). The effect of nitrogen on disease development and gene expression in bacterial and fungal plant pathogens. *European Journal of Plant Pathology* 106, 493–506.
127. Solomon, P.S., Tan, K.C., and Oliver, R.P. (2003). The nutrient supply of pathogenic fungi; a fertile field for study. *Molecular Plant Pathology* 4, 203–210.

128. Spiertz, J.H.J., and De Vos, N.M. (1983). Agronomical and physiological aspects of the role of nitrogen in yield formation of cereals. *Plant and Soil* 75, 379–391.
129. Stadnik, M.J., and Freitas, M.B. de (2014). Algal polysaccharides as source of plant resistance inducers. *Tropical Plant Pathology* 39, 111–118.
130. Stearns, S.C. (1989). Trade-Offs in Life-History Evolution. *Functional Ecology* 3, 259.
131. Stevens, C.J., Thompson, K., Grime, J.P., Long, C.J., and Gowing, D.J.G. (2010). Contribution of acidification and eutrophication to declines in species richness of calcifuge grasslands along a gradient of atmospheric nitrogen deposition. *Functional Ecology* 24, 478–484.
132. Talukder, Z.I., McDonald, A.J.S., and Price, A.H. (2005). Loci controlling partial resistance to rice blast do not show marked QTL x environment interaction when plant nitrogen status alters disease severity. *New Phytologist* 168, 455–464.
133. Tilman, D. (1999). Global environmental impacts of agricultural expansion: The need for sustainable and efficient practices. *Proceedings of the National Academy of Sciences* 96, 5995–6000.
134. Tuljapurkar S., Caswell H. (eds) Structured-Population Models in Marine, Terrestrial, and Freshwater Systems. Population and Community Biology Series, vol 18. (1997) Springer, Boston, MA
135. Urech, P. A., Staub, T., and Voss, G. 1997. Review: Resistance as a concomitant of modern crop protection. *Pestic. Sci.* 51:227-234.
136. Vári, E., and Máriás, K. (2013). The Impact of Crop Rotation and N Fertilization on the Leaf Area Index , Leaf Disease and Yield of Winter Wheat. *International Scholarly and Scientific Research & Innovation* 7, 1031–1034.
137. Verhoeff, K. (1968). Studies on Botrytis cinerea in tomatoes. Effect of soil nitrogen level and of methods of defoliation upon the occurrence of B. cinerea under commercial conditions. *Netherlands Journal of Plant Pathology* 74, 184–192.
138. Vos, J., Evers, J.B., Buck-Sorlin, G.H., Andrieu, B., Chelle, M., and De Visser, P.H.B. (2010). Functional-structural plant modelling: A new versatile tool in crop science. *Journal of Experimental Botany* 61.
139. Walters, D.R., and Bingham, I.J. (2007). Influence of nutrition on disease development caused by fungal pathogens: Implications for plant disease control. *Annals of Applied Biology* 151, 307–324.
140. Wezel, A., Bellon, S., Doré, T., Francis, C., Vallod, D., and David, C. (2009). Agroecology as a science, a movement and a practice. In *Sustainable Agriculture*, (Springer Netherlands), pp. 27–43.
141. Wilson, C., and Tisdell, C. (2001). Why farmers continue to use pesticides despite environmental, health and sustainability costs. *Ecological Economics* 39, 449–462.
142. Yermiyahu, U., Shamai, I., Peleg, R., Dudai, N., and Shtienberg, D. (2006). Reduction of Botrytis cinerea sporulation in sweet basil by altering the concentrations of nitrogen and calcium in the irrigation solution. *Plant Pathology* 55, 544–552.
143. Yin, X., Schapendonk, A.C.M., Kropff, M.J., Van Oijen, M., and Bindraban, S. (2000). A Generic Equation for Nitrogen-limited Leaf Area Index and its Application in Crop Growth Models for Predicting Leaf Senescence. *Annals of Botany* 85, 579–585.
144. Zadoks, J.C. (2008). On the political economy of plant diseases epidemics – Capita selecta in historical epidemiology. Wageningen Academic Publishers. pp 39-119. ISBN 978-90-8686-086-9.
145. Zhang, T., Yang, X., Wang, H., Li, Y., and Ye, Q. (2014). Climatic and technological ceilings for Chinese rice stagnation based on yield gaps and yield trend pattern analysis. *Global Change Biology* 20, 1289–1298.

Chapter 1: Modelling physiologically structured crop epidemics and the pathogen's life history problem

ABSTRACT

In this work we have developed a model to study the epidemiology of fungal foliar crop pathogens. This model deals with spatial scales ranging from a few square millimeters (one patch, the size of a lesion) to a crop field (multi-patch). It stands at the crossroads between (i) physiologically structured population models (PSPM) and (ii) susceptible, exposed, infected, and removed (SEIR) models. In our model, the classical epidemiological compartments benefit from a double age structure (in terms of both age of the host tissue and age of the infection) that allows studying the interactions and feedbacks between the plant and the pathogen. We use the model to explore the existence of putative optimal latent periods at the scale of a lesion as well as at the scale of the crop canopy. At each scale, a trade-off emerges that influences the optimal latent period. At the lesion scale, the latent period drives a trade-off between resources allocated to mycelium growth vs spores production. At the canopy scale, the latent period drives a second trade-off between spores production and speed of canopy colonization. The value of the optimal latent period that maximizes spores production is much lower when estimated at the canopy scale than at the lesion scale.

INTRODUCTION

In this chapter, we present a model designed for the study of the epidemics of polycyclic fungal crop pathogens, explicitly taking into account the pathogen life history at the scale of single lesions, as well as seasonal crop dynamics. We keep in mind the pathosystem consisting of wheat and a biotrophic foliar, wind-dispersed pathogen such as leaf rust (presented previously in the Introduction). Yet we expect this model should hold for more general cases. Our main focus is on the plant-pathogen interaction in terms of a consumer-resource interaction. We start out with a simple model describing the within-host growth of a lesion, depending on available resources within the plant tissue. The pathogen's life history is defined in terms of the infection cycle, including the latent period, mycelium growth, and sporulation. A second model scales up the life history model to the canopy-level dynamics of a population of lesions, the dynamics of which depends on the growth dynamics of its host, the canopy and spores dispersal. We are interested in the two-way interactions between pathogens and plants at both the lesion scale and the canopy scale. Using the models, we will explore the question of an optimal latent period, at the lesion scale and at the canopy scale.

Specifically, we address the question of how to find the optimal latent period of fungal crop pathogens. We consider the pathogen's life history problem of the allocation of energy between growth and reproduction, in analogy with the classical problem of optimization of the age at maturation studied in life history theory (Cohen, 1976; Stearns and Koella, 1986; Engen and Saether, 1994). Within-host pathogen dynamics depend on resource competition between pathogen populations and the host's nutrient requirements (Smith and Holt, 1996). The energy allocation trade-off has been studied for filamentous saprophytic fungi living in a patchy environment of localized patches of resources, interconnected by spores dispersal (Gilchrist et al., 2006), a class of organisms similar to fungal crop pathogens. The first main result of these authors is a rigorous definition of fitness, based on invasion analysis as commonly used in adaptive dynamics theory (Metz et al., 1992), which is shown to be the steady-state lifetime reproduction of spores by a single patch. In their study, the spatial structure of the patches is simple (all patches are equally connected) and constant (the in- and outflow of patches are constant). In fungal crop pathogens the spatial organization is more complex, in particular due to local spores dispersal and the seasonal dynamics of the crop both in terms of the overall quantity of available plant tissue and in terms of crop architecture

(Robert et al., 2008). Epidemics and evolution of fungal crop pathogens are hence characterized by spatiotemporal forcing and non-steady state dynamics. This complicates the tasks of computing their dynamics and of defining pathogen fitness. One goal of our study is to evaluate different ways to quantify fitness in this more complex setting, starting from the fitness definition of Gilchrist et al. (2006) as a first approximation, but considering non-equilibrium dynamics as well.

The second main result of Gilchrist et al. (2006) is that the optimal allocation strategy is of the “bang-bang” type, i.e., allocate all energy in somatic growth before the optimal age at maturation and all energy in reproduction after the optimal age at reproduction (Cohen, 1976; Schaffer et al., 1982; Engen and Saether, 1994; Gilchrist et al., 2006). Based on this result, we will use the assumption that the fungus life cycle can be approximated by a simple bang-bang strategy of a latent period followed by a sporulation phase, at least during the growing season of the crop. The interpretation of the latent period as a juvenile growth period, thus indirectly determining the body size of the adult (sporulating) organisms, naturally invites to consider a number of life history trade-offs constraining the evolution of fungal pathogens (Pringle and Taylor, 2002). Empirical studies have revealed trade-offs between latent period and transmission success (Heraudet et al., 2008) and spores production (Pariaud et al., 2013). These studies show that strains with longer latent periods produce more spores at the lesion scale and have a higher transmission success. The trade-off results from the temporal cost of a longer latent period: strains with a shorter latent period produce fewer spores but may colonize susceptible tissue more quickly (Pringle and Taylor, 2002). Note that this interpretation of latent period is very different from the “latent cycle” as opposed to the “lytic cycle”, as used by Sasaki and Iwasa (1991) in the context of human diseases. In the latter article’s terminology, the latent cycle corresponds to phases during an infection without any pathogen growth whereas the lytic cycle corresponds to pathogen growth causing virulence (defined as host damage).

It has been suggested that short latent periods result in higher disease severity than long latent periods (Lehman and Shaner, 1996), although this should depend on the trade-off between latent period and other parameters such as sporulation rate and longevity (Lehman and Shaner, 1997; Pringle and Taylor, 2002; Heraudet et al., 2008; Lannou, 2012; Pariaud et al., 2013). Latent period may also play a role in the competition among and between different strains on the same crop: according to Newton et al. (1999), early sporulation favors epidemic

growth under low densities, whereas late sporulation allows epidemic growth under high pathogen densities. Note that in this experimental observation trade-offs with other life history parameters could play a role. A theoretical example of such a trade-off was studied by Damgaard and Ostergard (1997) who found, in an explicit simulation of competition between strains of fungal pathogens, that the strain with the highest infection density outcompeted the other strain. Assuming that a strategy of fast sporulation is associated with a lower spores production, they found that a slow strain outcompetes a fast strain although the fast strain dominates the early phase of competition (while the densities are still low). These results suggests that an analogy of the classical “r-K” continuum of life history strategies (MacArthur and Wilson, 1967; Pianka, 1970) may exist for fungal plant pathogens, in which short latent periods corresponds to an “r-strategy” and a long latent period to a “K-strategy”.

Our starting point is the study by Gilchrist et al. (2006) on saprophytic fungi and we extend the model in order to correspond better to our biological system. The epidemiological model of Gilchrist et al. (2006) is an age-structured susceptible-infected (SI) model (Hethcote, 2000) in which the “infected” compartment is age-structured, accounting for the time since colonization by the fungus of a local patch. This allows for an explicit description of the within-patch dynamics of resources, mycelium and sporulation. Whereas this may be a fair representation of the spatial structure of saprophytic resources, the structure within a growing crop is more complex. We therefore extend the model by accounting for age-structure in the “susceptible” compartment: the susceptible patches in our model correspond to the (yet uninfected) growing crop canopy in which older patches are situated at or close to the ground and the youngest patches are newly created leaf area at the top of the canopy. We therefore use an approach with a double age structure (leaf patch age a and lesion infection age b) similar to Zhou et al. (2002).

Another important aspect that we take into account is the seasonal growth dynamics of the canopy, instead of the steady-state approach used by Gilchrist et al. (2006). At the end of the growing season the crop is removed, and we assume a constant survival rate of remaining spores over the unfavourable season. This results in a primary inoculum possibly initiating the next year’s epidemics. With simpler, unstructured models the consequences of seasonal crop dynamics and in particular the presence of an “overwintering” season in which the host is absent, has recently been studied. It has thus been shown that seasonality may be important in

the coexistence and evolutionary dynamics of sympatric pathogen strains (Hamelin et al., 2011; van den Berg et al., 2011; Mailleret et al., 2012).

Finally, we define the within-patch dynamics of healthy and infected patches in a way to capture a number of biologically relevant aspects of the system, including: local photosynthetic resource production; age- and resource-dependent senescence (possibly accelerated by the presence of a pathogen, van den Berg et al. (2007)); a biotrophic infection cycle including a latent period and a sporulating period.

Our model appears rather complex, in comparison to classical SIR models, and this follows from our interest in pathogen life history traits in the context of a growing crop. Whereas simple epidemiological models can teach us interesting results on the inherent dynamical aspects of epidemics such as invasion thresholds (R_0), periodicity of outbreaks, the evolution of virulence and more (Gandon et al., 2016); they are not suitable for the study of life history traits such as the latent period. In order for a model to account for life history, it needs to be age-structured. In order to capture the limited life span of the pathogen's substrate (plant tissue senescence), the latter needs to be age-structured, too. In order to capture crop growth, the population of pathogen substrate needs to be dynamic and seasonally forced. Finally, in order to capture localized spores dispersal and the consequent disease progress through the growing canopy, a minimum level of spatial structure is required. In order to answer to our specific question, we believe our model is the simplest possible model able to capture the essential aspects.

In this work we focus on the optimization of the latent period. Note that we do not assume any fixed, *a priori* trade-off with other traits. Rather, trade-offs emerge from the process-based modelling strategy; for example, a longer latent period will lead to a larger mycelium size and by consequence a higher sporulation rate, but only if sufficient resources are left at the time of sporulation. Our objective is to use our model for predicting the long-term dynamics of the crop-pathosystem, in terms of annual epidemics and the annual spores production over the growing season. By computing these dynamics for a range of latent periods we can assess the optimal latent period, assuming a particular fitness measure. In this chapter we use a simple “empirical” fitness measure (in the sense that it is potentially observable in the field): total spore production. We will analyse the model first at the lesion scale, before analysing the canopy-level dynamics.

MATERIALS AND METHODS

Model overview

We first present an overview of our model before specifying the equations. Our model represents the within and between-seasonal dynamics of a growing canopy (wheat), reseeded at the start of each new season, that provides the substrate for the dynamics of a polycyclic disease (leaf rust), that feeds on the resources within the canopy's leaf tissue. The pathogen is supposed to be inoculated from a spore pool that itself depends on the preceding season's epidemics. This dependence between subsequent years is essential for computing the steady state long-term dynamics and the pathogen's invasion fitness. The model accounts for the age-structured life cycle of the lesions in terms of a latent period and a sporulation period, as well as for the resource-dependent growth of mycelium (during the latent period) which influences the spore production rate during the reproductive phase. Based on the results of Gilchrist et al. (2006), we suppose a bang-bang resource allocation strategy, i.e., the pathogen allocates all consumed resources to growth during the latent period and all resources to reproduction during sporulation. We assume that spores dispersal decreases with increasing distance between patches in terms of patch age: the simplest way to incorporate spatial structure is to assume that patch age correlates with distance between patches. In other words, patches closer to the soil are generally older than patches closer to the top of the canopy (Figure 1).

Our model accounts for two levels of organization: within-patch dynamics and the dynamics of the number of patches. A patch is defined as a unit of leaf tissue the size of a mature infection ("lesion", about 0.1 cm^2 for leaf rust on wheat), characterized by patch-level state variables that define patch age, time since infection, within-patch resource level and pathogen biomass. At the patch scale we model physiological processes such as within-plant nutrient dynamics including nutrient inflow and outflow, photosynthesis and nutrient exploitation by the pathogen, mycelium growth, spores production and senescence (Figure 2). Resource flow connects all patches with a central resource compartment (denoted by A) that is assumed to represent the resources present in the rest of the plant (roots, shoots, grains). Inflow to a patch occurs instantaneously at the moment of patch creation, whereas outflow

from a patch is continuous over its lifespan. Patches do not communicate directly between each other.

At the canopy scale (multi-patch level) we model the growth of plants in terms of the number of patches and their age-structure, and the dynamics of the epidemics including spores dispersal and the infection of healthy patches. The spatial scale of the multi-patch level is not explicitly specified, but is large enough to allow for a steady state year-to-year dynamics of the crop (and hence at least a regional scale of multiple crop fields). Canopy growth is modelled as an increase in the number of patches and the ageing of patches (Figure 1). At any given time the youngest patches represent the top of the canopy and the oldest the bottom. Canopy growth is a seasonal process and we assume three different phases. At the start of the growing season a single patch of age 0 is introduced, representing the emerging seedlings. During the first phase the number of patches increases, representing the canopy growth phase. The growth rate of the number of patches is assumed to depend on the common resource pool and hence indirectly on the resource production by the patches. The patch production rate is proportional to $A/(A+A_H)$ with A_H a half-saturation constant. During the first phase, the epidemics is initiated by a primary inoculum that is introduced at a fixed date, infecting a number of patches with a level of spores depending on last-year's total spores production. During the second phase the number of patches remains constant and all export from the patches accumulates in the compartment A (mimicking grain production). The third phase represents the harvest and the absence of the host. We model this phase as an instantaneous projection of the total spores pool at harvest to the start of the next year's growing season.

Time in our model is measured in degree-days (Table 1), which is the most relevant way to model both crop development and their pathogens' life cycle (Agrios, 2005). We denote time by t and use T to denote the time since the start of the current year (i.e., the “date” in degree days).

We present the model in two steps: first the within-patch dynamics, second the canopy-level dynamics. The model is formulated within the framework of physiologically structured population models (PSPM) (De Roos, 1997; De Roos and Persson, 2013) which provides a rigorous model formalism and analysis tools that allow one to formulate the model making the main assumptions at the “individual level” (here: within patch level) and then to scale up to the population level (here: canopy level).

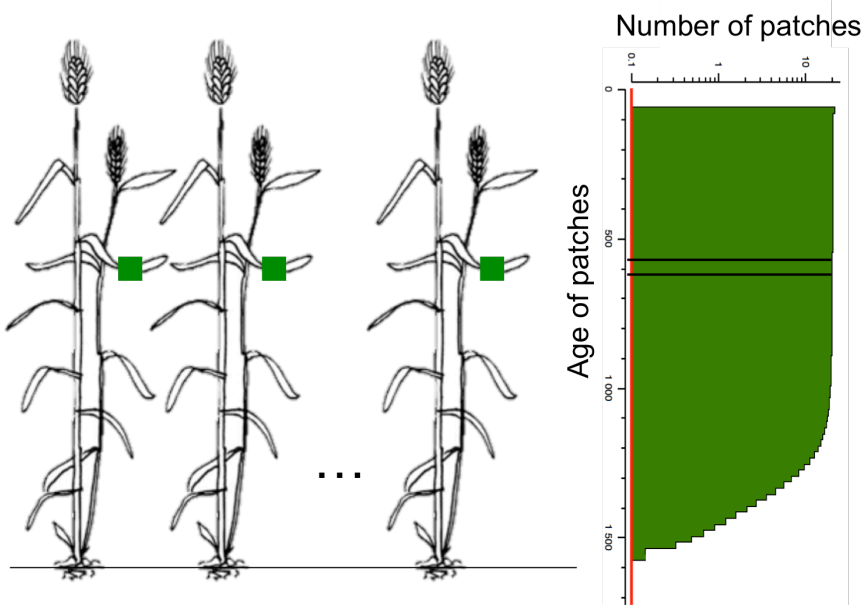


Figure 1: crop canopy abstract representation. In our model, we do not simulate individual plants, rather a distribution of leaf fragments we call patches that represent the crop canopy. Considering the semi-determined mode of development of wheat and under the hypothesis of synchronous plant growth, patches with the same age also share the same position in the canopy. The canopy can thus be depicted by a distribution of age-classes of patches we call cohorts. Left: theoretical plants with patches (green rectangles) with the same age. Right: patch age distribution of a healthy canopy. Black lines mark out one cohort with age about 700 dd.

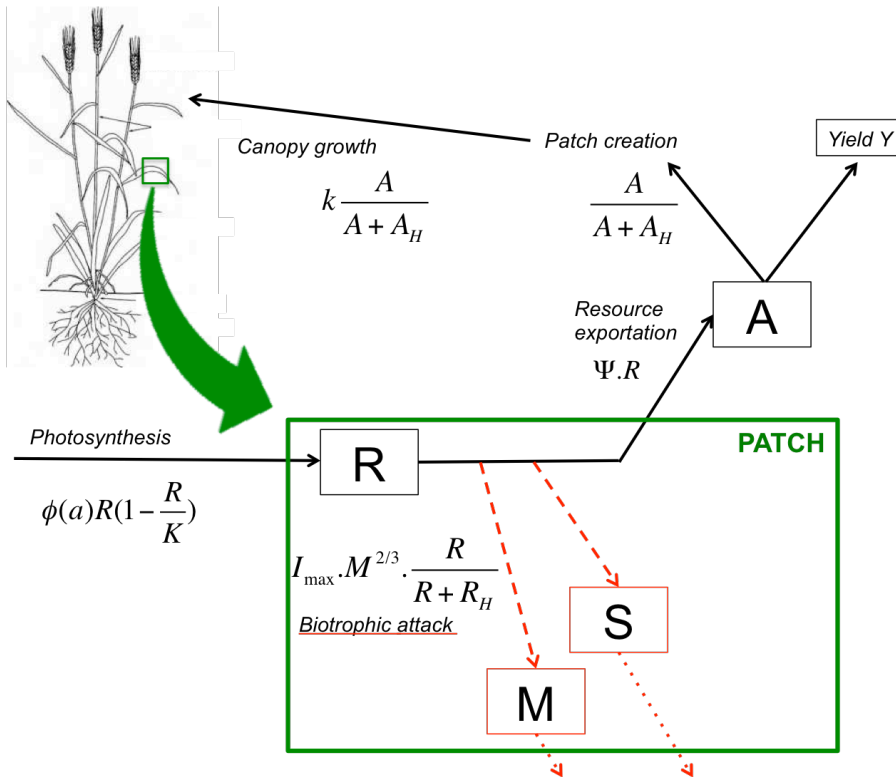


Figure 2: schematic view of patch functioning and of the role of patches in the building-up of a healthy canopy. A patch is defined as a unit of leaf tissue the size of a mature lesion (about 0.1 cm^2). It is characterized by patch-level state variables that define patch age a , time since infection b , within-patch resource level R and pathogen biomass M and S . Resources created in all patches are in part exported towards a common resource

pool named A that serves as a plant resource reservoir for plant growth (i.e. new patches creation). See also Equations 1 to 5.

Within-patch dynamics (lesion model)

We consider two kinds of patches, healthy and infected ones. Each healthy patch, identified by an index ι , is characterized by two patch-level state variables: patch age a_ι and the within-patch resource level R_ι . For notational simplicity we will drop the patch index ι in the remainder of the model definition, except where using the index seems necessary for good understanding. Patches are created with age 0 and an initial resource level R_{ini} (corresponding to the resource inflow from the common stem resource A). Age increases unsurprisingly like $da/dt=1$. Local resource dynamics depend on the balance of resource production through photosynthesis and export to the common resource pool A . We assume a simple logistic functional relationship between R and the production of R , modulated by an age-dependent senescence function:

$$\frac{dR}{dt} = R \left(1 - \frac{R}{K}\right) \phi(a) - \Psi R \quad (1)$$

where ΨR is the rate of resource export and $\phi(a)$ is the age-dependent senescence function. The function $\phi(a)$ mimics in a simple way the process of leaf senescence (which in wheat is gradual and starts once a leaf becomes ligulated (Gregerson et al., 2008)). It results in a decreasing photosynthesis rate with age. We assume that $\phi(0)=\phi_0$, that $\phi(a)$ decreases linearly with age, reaches zero at age τ and $\phi(a) = 0$ for $a > \tau$. A patch is considered to die when its resource contents drops below a critical threshold denoted by R_{\min} . Without infection, this occurs slightly before age τ that corresponds to the onset of necrosis due to natural leaf senescence (natural green lifespan of leaf tissue). An example of the seasonal dynamic of R is given in Figure 3. Note that in the canopy model, dead patches are not removed from the population; mimicking the persistence of necrotic leaves in the crop field.

Infected patches are characterized by a , R and three additional patch-level state variables: the age of the infection b , the mycelium density M and the accumulated spores production S . The double age structure along the axes a and b allows us to distinguish patches of the same age but that have been infected at different times, whose physiological states are

likely to be different. From the moment that a patch becomes infected, the age of the infection b is initialized at $b=0$ and then increases linearly ($db/dt=1$). The actual patch age a continues to increase. The mycelium density is initialized at $M(a, 0) = M_0$. The dynamics of R in an infected patch is now also influenced by resource consumption by the pathogen, which depends on the mycelium biomass M and resource availability. Uptake is assumed to increase with the surface area of mycelium and hence in proportion to $M^{2/3}$. Mycelium is assumed to take up the resource following a Holling type 2 functional response. The dynamics of R then become:

$$\frac{dR}{dt} = R \left(1 - \frac{R}{K}\right) \phi(a) - \Psi R - I_{\max} M^{2/3} \frac{R}{R+R_H} \quad (2)$$

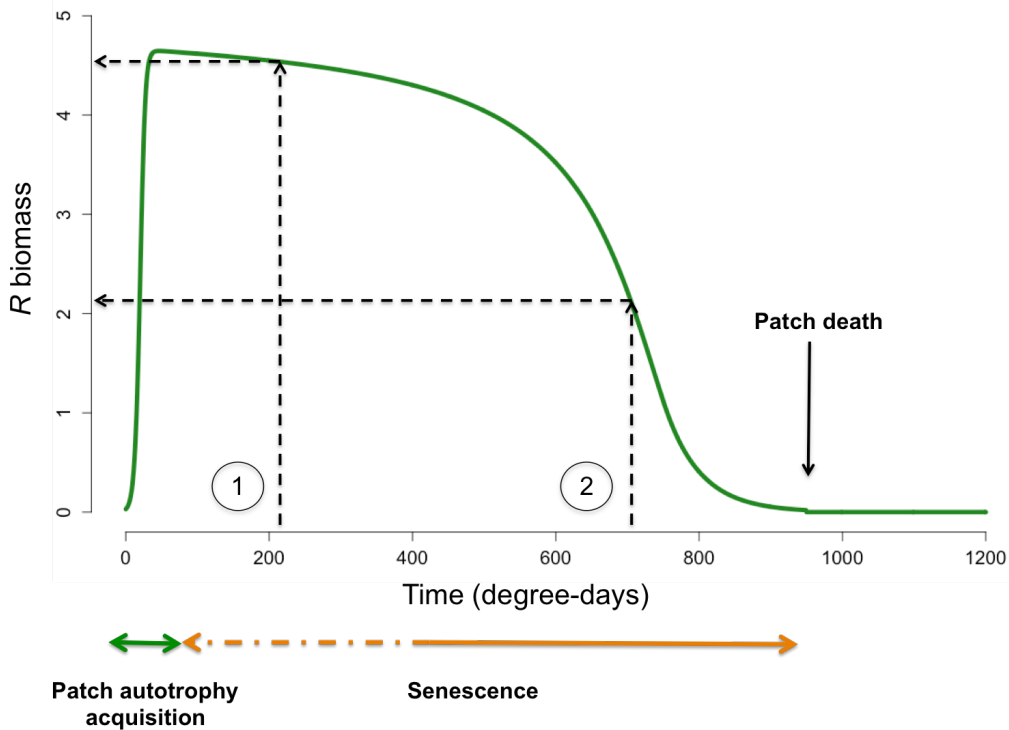


Figure 3 : within (healthy) patch dynamics of resources R . After patch creation, R increases simulating patch development and acquisition of patch autotrophy to carbon and nitrogen. Once the patch becomes mature, R starts decreasing mimicking patch senescence and patch resource re-allocation to other patches in younger organs higher in the canopy. Patch death occurs after R drop under a viability threshold R_{min} . Pathogens infecting at different times (1 and 2 for example) do not encounter the same resource environment: the pathogen infecting in (1) having access to twice the resource level of a pathogen infecting in (2).

The consumed resources are converted into mycelium tissue with efficiency c_m . The pathogen life cycle consists of a latent period ($b < \lambda$) during which all consumed energy is

allocated to mycelium growth, followed by a sporulation phase during which all energy is allocated to spores production. Mycelium tissue is assumed to decay with rate γ_m . These assumptions lead to the following equation for the mycelium dynamics:

$$\frac{dM}{dt} = \begin{cases} c_m I_{\max} M^{2/3} \frac{R}{R+R_H} - \gamma_m M, & \text{if } b < \lambda \\ -\gamma_m M, & \text{otherwise} \end{cases} \quad (3)$$

where λ is the latent period. The resulting mycelium growth dynamics are similar to Von Bertalanffy growth dynamics that result from the assumption that consumption is proportional to organisms surface area while loss is proportional to organism biomass (Claessen and Dieckmann, 2002). Such equations are sometimes used for computing growth rates for 3-dimensional organisms that absorb nutrients through their surface (Kooijman 2000). We are aware of no empirical relation between mycelium biomass and fungus uptake rate. Moreover, several authors have established that rust mycelium have a 3-dimensional growth and occupies the whole mesophyll volume under a lesion, sometimes even creating lesions on both sides of leaves (Garnica et al., 2014, Haueisen and Stukenbrock, 2016). For these reasons, we chose to use this classical model of isomorphic growth rather than a model of planar growth of mycelium dictated by leaf morphology.

The cumulative spores biomass production S increases according to:

$$\frac{dS}{dt} = \begin{cases} 0, & \text{if } b < \lambda \\ c_s I_{\max} M^{2/3} \frac{R}{R+R_H}, & \text{otherwise} \end{cases} \quad (4)$$

Equation 4 implies that spore production is (non-linearly) proportional to mycelium biomass. This mimics the fact that urediospores are produced by budding of the infection hyphae that form the sporogenous zone of uredinia (Beckett and Woods 1987).

Note that we assume that a lesion matures at a fixed latent period whereas theoretically the reaction norm of maturation could be more complex. We have also studied an alternative assumption, in which maturation occurs upon reaching a fixed mycelium density M_{mat} instead of at the fixed age λ . In this case the latent period is variable, depending on the parameter M_{mat} and the mycelium growth rate. The consequences of this alternative assumption, which are negligible, are mentioned in the Appendix of Chapter 2.

Canopy-level dynamics

The canopy-level model describes the dynamics of the age-distributions of healthy and infected patches. The canopy level can be seen as a structured population of patches of different ages and different physiological states in terms of resource content and pathogen life history. Following De Roos (1997), such a structured population can be described using partial differential equations (PDEs) or, by approximation, using a set of ordinary differential equations (ODEs). Here we will first present the formal model in terms of PDEs. Next we will show how the PDEs can be represented by a set of ODEs that corresponds to the so-called Escalator Boxcar Train (EBT) approximation of the PDEs. The numerical calculations are all based on the EBT formulation of the model.

The age distribution of healthy patches at time t is denoted by $h(t,a)$. The age distribution changes due to (i) ageing of existing patches; (ii) removal of patches due to infection, and (iii) the birth of new patches. Infection of patches depends on the force of infection $F(t,a)$, defined below. Note that we keep track of alive and dead patches. The dynamics of h are given by the partial differential equation:

$$\frac{\partial h(t,a)}{\partial t} + \frac{\partial h(t,a)}{\partial a} = -F(t,a)h(t,a) \quad (5)$$

$$h(t,0) = \begin{cases} \rho \frac{A}{A+A_H}, & \text{if } 0 < T < T_{\text{grow}} \\ 0, & \text{otherwise} \end{cases} \quad (6)$$

where the second line is the boundary condition accounting for the birth of new patches, the rate of which depends on the amount of resource in the common pool A . For unlimited resources, the patch apparition rate is ρ . Note that new patches are created only during the canopy growing phase (i.e. dates T between between 0 and T_{grow}).

The two-dimensional age distribution of infected patches at time t is denoted by $n(t,a,b)$. This distribution changes due to (i) ageing of existing patches in terms of patch age

and age of infection; (ii) arrival of newly infected patches of age a at coordinates $(t,a,0)$. Again, we keep track of alive and dead patches. The dynamics of n are given by the partial differential equation:

$$\frac{\partial n(t,a,b)}{\partial t} + \frac{\partial n(t,a,b)}{\partial a} + \frac{\partial n(t,a,b)}{\partial b} = 0 \quad (7)$$

$$n(t, a, 0) = F(t, a)h(t, a) \quad (8)$$

$$n(t, 0, 0) = 0 \quad (9)$$

where the second line is the boundary condition accounting for the flux of newly infected patches ($b=0$) and the third line is a boundary condition specifying that all newborn patches ($a=0$) are healthy by definition. Note again that dead patches are not removed.

The dynamics of the common resource pool A depends on the resource export (ΨR) from all patches and the resources used for making new patches:

$$\frac{dA}{dt} = \int_a \Psi R(t, a, 0)h(t, a)da + \iint_{a,b \neq 0} \Psi R(t, a, b) n(t, a, b) db da - \rho \frac{kA}{A+A_H} H(T_{\text{grow}} - T) \quad (10)$$

where k represents the cost (in terms of A) of producing a new patch, and $H(\cdot)$ is the Heaviside step function making sure the cost of canopy growth is deducted only for $T < T_{\text{grow}}$.

Throughout the season infected patches produce spores and we keep track of the within-season cumulative spores production, P , that is needed to compute next year's primary inoculum.

$$\frac{dP}{dt} = \int_{a=0}^{\infty} \int_{b=\lambda}^{\infty} \sigma(t, a, b)n(t, a, b) db da - \gamma_s P \quad (11)$$

where λ is the latent period, γ_s is the per capita spore death rate and $\sigma(t, a, b)$ is the patch-level sporulation rate,

$$\sigma(t, a, b) = c_s I_{\max} M(t, a, b)^{\frac{2}{3}} \frac{R(t, a, b)}{R(t, a, b) + R_H} \quad (12)$$

The force of infection, F , is the rate at which healthy patches become infected. For a given patch, it depends on the spore production rates of infected patches in the patch's neighbourhood, weighted by a dispersal kernel:

$$F(t, a) = \frac{\beta}{\Delta} \int_{x=0}^{\infty} \int_{b=0}^{\infty} \max(0, 1 - \left| \frac{x-a}{\Delta} \right|) \sigma(t, x, b) n(t, x, b) db dx \quad (13)$$

with β the dispersal efficiency, Δ the maximum dispersal distance (in terms of patch age), $\sigma(t, x, b)$ and $n(t, x, b)$ the spore production rate and abundance of patches of age x and age of infection b , respectively. For each healthy patch exposed to sporulating neighbours, this corresponds to a dispersal kernel centred on its age, as represented in Figure 4.

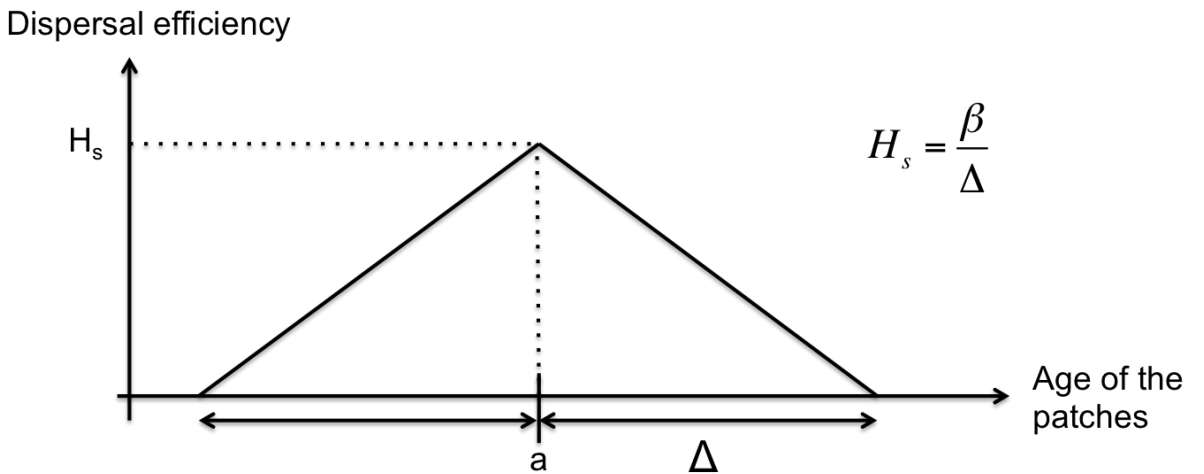


Figure 4: dispersal kernel at the vicinity of patches cohort of age a . β is the dispersal efficiency, Δ the maximum dispersal distance and H_s an area-conservation value. Patches in a cohort of age a receive spores from cohorts of age $a \pm \Delta$. Dispersal efficiency linearly decreases with distance to reference cohort of age a .

Biologically, the parameter β incorporates the probability of dispersing spores to encounter healthy tissue and to successfully infect the encountered patch. Since patches have the size of a single lesion, we assume that a patch can be infected once only.

Year-to-year dynamics

The epidemics are initialized by the arrival of a primary inoculum in the early phase of the growing season. The amount of primary inoculum depends on last year's total spores production $P(T_{end})$, the spore survival rate over the unfavourable season ω and the spores mortality rate per time unit γ_s over the period from the start of the growing season until the start date of the epidemics (T_{inoc}). Primary inoculum is assumed to arrive in the canopy on the date T_{inoc} at which time a fraction of the patches in all cohorts with ages in the interval $(a_{inoc,min}, a_{inoc,max})$ are infected. This mimics the arrival of the first spores, by wind dispersal, in the top of the canopy. In these cohorts, the fraction of patches that become infected is

$$\theta = \theta_{max} \frac{P(T_{inoc})}{P_H + P(T_{inoc})} \quad (14)$$

where θ_{max} is the maximum fraction that can be inoculated, $P(T_{inoc})$ is the spores biomass present in the soil at the moment of primary inoculation, and P_H a half-saturation constant.

Practical implementation and parameterization

In this subsection, we present the second, more intuitive formulation, which is also the one used in numerical computations. The ODE approximation is referred to as the Escalator Boxcar Train (EBT) method developed by De Roos (1988) to numerically integrate physiologically structured population models.

The central idea of the EBT method is to discretize the structured population (the canopy) into age-classes that are called “cohorts”. Each cohort represents all patches that have been created during a particular time interval (that we assume to last 10 dd). A cohort is described by the number N_i of patches, as well as the mean of the patch-level state variables a_i , b_i , R_i , M_i and S_i (i.e., the mean age of the patches within the cohort, the mean resource level, etc). We distinguish between “internal cohorts” and the “boundary cohort”. The latter is the cohort that contains the youngest patches, i.e., the patches that are being created during a

fixed time interval lasting 10 dd. In our model, this cohort can be thought of as the “meristem cohort”: the only growing part of the canopy. The internal cohorts contain all older patches.

The dynamics of the cohorts are described using ODEs that are integrated using the EBTtool, a numerical implementation of the EBT method (De Roos, 1997). We use a variable time step (the adaptive Runge-Kutta-Cash–Karp method (RKCK) for ODE integration, see Cash and Karp, 1990). The integration is stopped every 10 dd in order to (i) transform the current meristem cohort into an internal cohort, (ii) to initialize a new meristem cohort, and (iii) to create new cohorts into which we transfer the newly infected patches from each uninfected cohort. Values of 2, 5, 10 and 20 dd have been tested with no notable effect on the results. The value of 10 dd was chosen because it offers a compromise between speed of the simulations and precision of the graphical results. Here are how Equations 1 to 14 are implemented in the EBT method.

Uninfected canopy dynamics

The meristem cohort

The growth rate of the population of patches depends on the amount of resource in the common resource pool $A(t)$. Since the patch production rate follows a Michaelis-Menten equation with maximum patch creation rate ρ and half-saturation coefficient A_H (subsection *Overview* page 55), the rate of change of patches in the meristem cohort thus equals:

$$\frac{dN_0}{dt} = \rho \frac{A}{A + A_H} \quad (15)$$

Note that we use index 0 for the meristem cohort. The meristem cohort is thus filled with patches during each fixed time interval of 10 dd. At the end of this interval, the meristem cohort becomes an internal cohort and a new meristem cohort is created. The dynamics of the mean patch age, a_0 , and the mean resource level, R_0 , for the meristem cohort are computed as for the internal cohorts (see below), using the appropriate implementation as outlined by De

Roos (1997). Note also that since we assume the meristem cannot become infected, we have no equations for the variables b_0 , M_0 and S_0 .

The common resource pool

In turn, the dynamics of the common resource pool A results from the export from all patches minus the cost of patch creation. Equation 10 then becomes:

$$\frac{dA}{dt} = \sum_{i=0}^k \psi R_i N_i - c_A \rho \frac{A}{A + A_H} \quad (16)$$

where k is the number of cohorts, ψ the export coefficient per patch, and c_A the cost of producing a new patch. In absence of an epidemic, the canopy at the end of the season will consist of $k=150$ cohorts, since every 10 dd a new cohort is created during the growth phase that lasts 1500 dd.

The internal cohorts

For a healthy canopy, the number of patches in an internal cohort stays constant since we count both alive and dead patches. Patch senescence does hence not result in removal from the cohort: it only changes the status of the patches in the cohort. For the internal cohorts, the dynamics of N_i is hence given by:

$$\frac{dN_i}{dt} = 0 \quad (17)$$

for $i=1,\dots,k$. The dynamics of the patch age is

$$\frac{da_i}{dt} = 1 \quad (18)$$

and following Equation 2 the dynamics of patch resource level is:

$$\frac{dR_i}{dt} = \phi(a_i)R_i \left(1 - \frac{R_i}{K}\right) - \psi R_i \quad (19)$$

where the function $\phi(a_i)$ simulates the effect of senescence. We assume that a patch's intrinsic photosynthetic activity decreases linearly with patch age:

$$\phi(a_i) = \begin{cases} \phi_0(1 - \frac{a_i}{\tau}) & \text{if } a_i \leq \tau \\ 0 & \text{otherwise} \end{cases} \quad (20)$$

where τ is the maximum patch age for photosynthesis. We choose a linear decrease as a first approximation in the absence of detailed experimental data. In the absence of the pathogen, the variables b_i , M_i and S_i all remain at 0 (but see “Infected canopy dynamics” below).

Infected canopy dynamics

The dynamics of the meristem cohort and of the common resource pool are the same for infected canopies. We assume that the meristem cannot become infected.

In case of an epidemic, the internal cohorts are further divided into uninfected and infected cohorts. Uninfected cohorts contain no mycelium or spores and hence $M_i = 0$ and $S_i = 0$, whereas $b_i = 0$ until infection. In case of an epidemic, a given uninfected cohort i may receive spores from surrounding, infected cohorts. During each fixed time interval of 10 dd, we keep track of the number of patches in cohort i that gets infected, denoted by Y_i . By the end of the 10 dd time interval, these newly infected patches are transferred into a new cohort j that will have its own dynamics, independent of its “parent” cohort i . The new, infected cohort j is initialized with the variables:

$$N_j = Y_i,$$

$$\begin{aligned} a_j &= a_i, \\ R_j &= R_i, \\ b_j &= 0, \\ M_j &= M_0, \\ S_j &= 0. \end{aligned}$$

Thus, the infected cohort inherits the patch age and resource level of the parental cohort whereas age of infection, mycelium biomass and spores biomass are initialized at the conditions of a new infection (see Table 1 in the text). The parental cohort continues its trajectory after removal of the transferred patches.

Uninfected cohorts

In an infected canopy, the number of patches in a still uninfected cohort may decrease due to infection, according to the local force of infection:

$$\frac{dN_i}{dt} = -F_i N_i \quad (21)$$

The thus newly infected patches are accounted for within the current cohort until the next opportunity to create a new, infected cohort, which is at the end of the fixed time interval (every 10 dd). In order to keep track of the number of patches that become infected, we use the following ODE for Y_i :

$$\frac{dY_i}{dt} = F_i N_i \quad (22)$$

where F_i is the force of infection experienced by cohort i , which is a function of the sporulation rates and abundance of patches of neighbouring infected cohorts (Equation 13). In this formulation of the model, it is defined as:

$$F_i = \beta \sum_{j \neq i}^k (1 - d_{ij}) \sigma_j(R_j, M_j, b_i) N_j \quad (23)$$

where β is the spore dispersal efficiency incorporating the probability of spores emitted in the canopy to encounter and infect healthy tissue, σ_j is the sporulation rate in cohort j , and the distance between cohorts i and j in terms of age is computed as:

$$d_{ij} = \begin{cases} \frac{|a_i - a_j|}{\Delta} & \text{if } |a_i - a_j| \leq \Delta \\ 1 & \text{otherwise} \end{cases} \quad (24)$$

Here, Δ is the maximal dispersal distance in terms of patch age. (Remember that we assume that a patch's birth date corresponds to its vertical position). Hence, the infected cohorts nearest to a given healthy cohort will contribute most to its infection.

For uninfected internal cohorts, the ODEs for age and the resource are the same as for the internal cohorts of a healthy canopy (Equations 18 to 20).

Infected cohorts

Since we assume multiple infections are impossible the number of patches in infected cohorts cannot change. For infected internal cohorts, the dynamics of N_i and a_i are given by Equations (17) and (18) respectively. The dynamics of the age of infection is:

$$\frac{db_i}{dt} = 1 \quad (25)$$

In accordance with Equation 2, the dynamics of the patch-level resource now depend on the presence of the pathogen:

$$\frac{dR_i}{dt} = \pi(a_i)R_i \left(1 - \frac{R_i}{K}\right) - \psi R_i - u(R_i, M_i, b_i) \quad (26)$$

where the function u is the resource uptake rate by the pathogen, defined as:

$$u(R_i, M_i, b_i) = I_{max} \frac{R_i}{R_i + R_H} M_i^{2/3} \quad (27)$$

This equation reflects our assumption that resource uptake is proportional to the surface area of mycelium biomass (Equation 3). The dynamics of mycelium is given by

$$\frac{dM_i}{dt} = g(R_i, M_i, b_i) - \gamma_M M_i \quad (28)$$

where $\gamma_M M_i$ is the mycelium loss rate. It can be interpreted as the sum of mycelium maintenance and decay. The mycelium growth rate is positive during the latent period and zero afterwards:

$$g(R_i, M_i, b_i) = \begin{cases} c_M u(R_i, M_i, b_i) = c_M I_{max} \frac{R_i}{R_i + R_H} M_i^{2/3} & \text{if } 0 < b_i \leq \lambda \\ 0 & \text{otherwise} \end{cases} \quad (29)$$

In accordance with Equation 4, the dynamics of total spores produced per patch is

$$\frac{dS_i}{dt} = \sigma(R_i, M_i, b_i) \quad (30)$$

where the sporulation rate σ is zero during the latent period and positive afterwards:

$$\sigma(R_i, M_i, b_i) = \begin{cases} c_S u(R_i, M_i, b_i) = c_S I_{max} \frac{R_i}{R_i + R_H} M_i^{2/3} & \text{if } b_i > \lambda \\ 0 & \text{otherwise} \end{cases} \quad (31)$$

Canopy-level output variables

At the canopy scale in our model, the total number of patches at a given time is denoted by $X(t)$ and is computed as the sum of the number of patches in all cohorts:

$$X(t) = \sum_{i=0}^k (N_i + Y_i) \quad (32)$$

The number of infected patches at a given time is denoted by $X_{inf}(t)$ and is computed as:

$$X_{inf}(t) = \sum_{i=1}^n Y_i + \sum_{i=n+1}^k N_i \quad (33)$$

where cohorts with index $i=1, \dots, n$ are the uninfected cohorts and cohorts with index $i=n+1, \dots, k$ are the infected cohorts (i.e., cohorts with $b_i > 0$).

The canopy level cumulative spores production (see Equation 11) is now computed as:

$$\frac{dP(t)}{dt} = \sum_{i=1}^k \sigma_i(R_i, M_i, b_i) N_i - \gamma_S P \quad (34)$$

where γ_S is the spores loss rate due to mortality, germination in unfavourable locations, etc.

Parameterization

The model is designed to represent, in a simplified way, the interaction between wheat (*Triticum aestivum*) and a biotrophic foliar pathogen such as leaf rust (*Puccinia triticina*). The biological model parameters are summarized in Table 1 and are based on the current knowledge of the pathosystem.

Analysis methods

We study the model dynamics using numerical simulations. The within-patch level model (Equations 2 to 4) was implemented in Matlab for numerical integration of the three ODEs. The full, canopy-level model was implemented using the Escalator Boxcar Train method (De Roos, 1997) and the *EBTtool* software package. The total number of cohorts typically reaches in the 100s without pathogen or in the 1000s with pathogen.

Symbol	Value	Unit	Interpretation
Seasonal dynamics			
T_{end}	2500	dd	End of season
T_{grow}	1500	dd	End of period of canopy growth
τ	750 (varied)	dd	Maximum patch age for photosynthesis
T_{inoc}	1000 (varied)	dd	Date of primary inoculum (annual start date of epidemic)
ω	0.1	-	Spore survival probability over the unfavorable season
Plant dynamics			
K	1	g	Within patch resource carrying capacity
Ψ	0.02	/dd	Export rate of resource from patch to common pool
R_0	0.03	g	Initial resource level at patch creation
ϕ_0	0.3	/dd	Intrinsic rate of photosynthesis (at age $a=0$)
R_{\min}	0.02	g	Minimum resource level for patch survival
ρ	1	/dd	Maximum rate of patch creation
k	1	g/dd	Cost of patch creation
A_H	100	g	Half-saturation pool resource level for patch creation
Pathogen Dynamics			
λ	150 (varied)	dd	Latent period
M_0	0.0001	g	Initial mycelium biomass at patch infection
I_{\max}	0.06	g/dd	Maximum resource uptake rate per unit of mycelium biomass
R_H	0.25	g	Half-saturation constant for functional response
c_m	0.2	-	Conversion coefficient resource-mycelium
c_s	0.2	-	Conversion coefficient resource-spores
γ_m	0.001	/dd	Mycelium decay rate
γ_s	0.001	/dd	Spores decay rate
c_{LTR}	50	/g	Constant for computation of LTR
Dispersal			
β	100	-	Dispersal efficiency
Δ	250	dd	Maximum dispersal distance (in terms of patch age)
H_S	0.4	/dd	Area conservation value
$a_{\text{inoc, min}}$	20	dd	Minimum patch age to receive primary inoculum
$a_{\text{inoc, max}}$	250	dd	Maximum patch age to receive primary inoculum

θ_{max}	0.02	-	Maximum fraction of patches per cohort that can be inoculated
P_H	10	g	Half-saturation spores biomass for spores-limited inoculation

Table 1. Biological model parameters and their default values, representing the wheat-brown rust pathosystem.

RESULTS

Within-patch dynamics

In this section, we explore within-patch model simulations, the basic features of the life history model and the influence of the latent period (λ) and of the age at infection (a_I) on the diseased patch functioning.

Figure 5 shows three runs of the within-patch level dynamics for standard parameter values (Table 1) and three different values of the latent period ($\lambda=90, 150$ or 240 dd). The infection is assumed to arrive at patch age $a_I=100$ dd. In all cases, the resource in the patch initially increases quickly to a value close to the carrying capacity ($K=1$). The resource level starts dropping when the sum of export and uptake by the pathogen exceeds the rate of resource production by photosynthesis (the latter decreasing linearly with age, see also Figure 3). As the mycelium grows, the fungus' uptake rate increases, resulting in a higher resource loss and hence lower resource level. By the end of the latent period, the mycelium mass stays almost constant (except from a small loss rate) and, by consequence, the resource level declines less quickly. The cumulative spores production increases almost linearly as long as the resource level remains well above the pathogen's half-saturation level (i.e. as long as $R(a) \gg R_H = 0.25$). The sporulation rate under resource saturation is higher when mycelium density is higher: the curve of spores production hence increases faster with higher latent period. Spore production goes to zero when patch photosynthesis declines to zero due to resource depletion and age-dependent shading. Patch senescence occurs when R drops below $R_{min}=0.03$. Comparison of the three columns in Figure 5 illustrates the pathogen's life history problem: given the finite amount of resources and time to complete its life history in the patch, the length of the latent period is a critical trait. When λ is low (e.g. $\lambda=90$, left column in Figure 5), the pathogen starts sporulating with plenty of resource and time left but with a low sporulation rate due to its small size. When λ is high (e.g. $\lambda=240$, right column in Figure 5), the pathogen sporulates at a large size and hence a high rate, but with only little resources and

time left. This defines a natural trade-off, at the within-patch level, between a high sporulation rate (with a long latent period, high mycelium content) and a long, resource-rich sporulation period (with short latent period, low mycelium content). Clearly, an intermediate latent period is optimal, with an intermediate mycelium size and an intermediate sporulation period, as suggested by results with $\lambda=150$ (Figure 5).

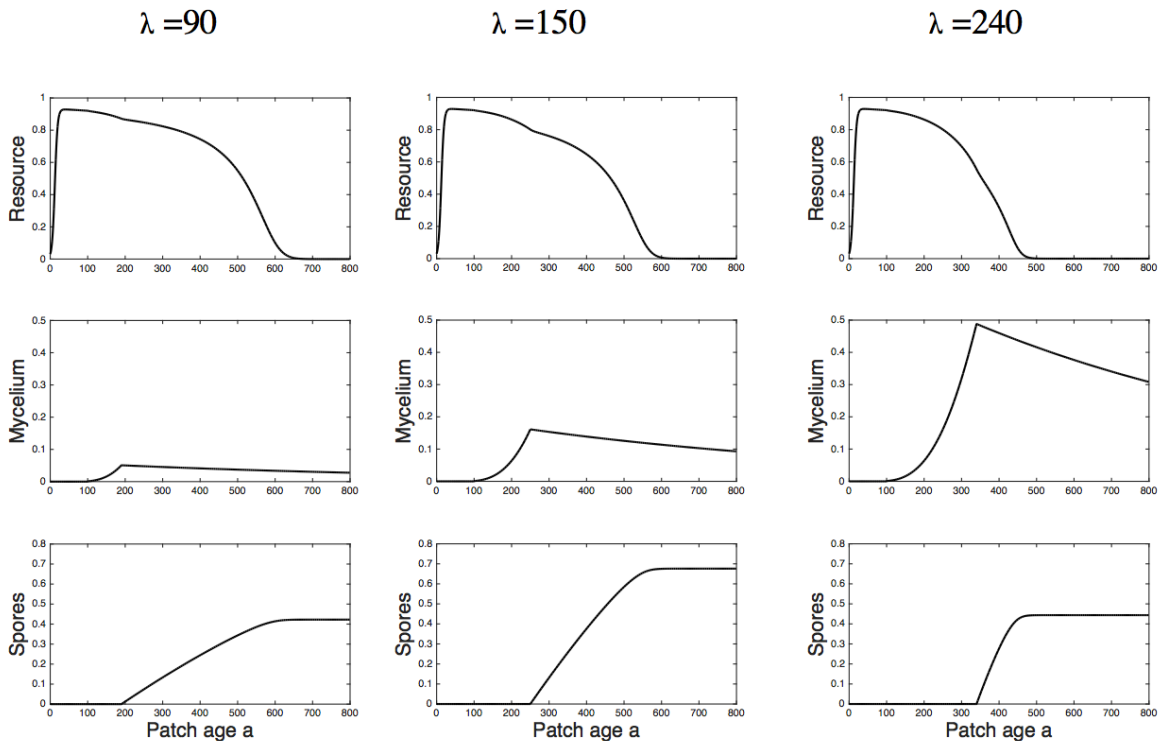


Figure 5 : The effect of latent period on within patch dynamics of resource R , mycelium M and cumulative spores production S , for different latent periods ($\lambda = 90$, $\lambda = 150$, $\lambda = 240$, respectively). **Top:** Dynamics of $R(a)$. **Middle:** Dynamics of $M(a)$. **Bottom:** Dynamics of $S(a)$. Parameters: $a_I = 100$ and see Table 1.

However, as suggested by Figure 3, the age of the patch at infection also influences the outcome of the infection: since pathogens infecting similar patches at different dates encounter different resource environments, the age at infection likely influences the within-patch growth-reproduction trade-off.

Figure 6 shows three time series for different ages at infection. The figure shows that the age at infection a_I has little effect on the size of the mycelium, due to the relatively constant resource level for a large part of the patch' life span. Total spores production, on the other hand, decreases with the age at infection. Figure 7 shows that this decrease is roughly

linear with the age at infection. Considering the life history problem described above, this comes at no surprise: with a finite time for sporulation, delaying the onset of sporulation simply reduces the period over which spores are produced. So there is likely an interaction between age at infection and the latent period in the patch-level reproduction success of the pathogen. Note however that the age at infection has little effect on the patch age at senescence (Figure 6).

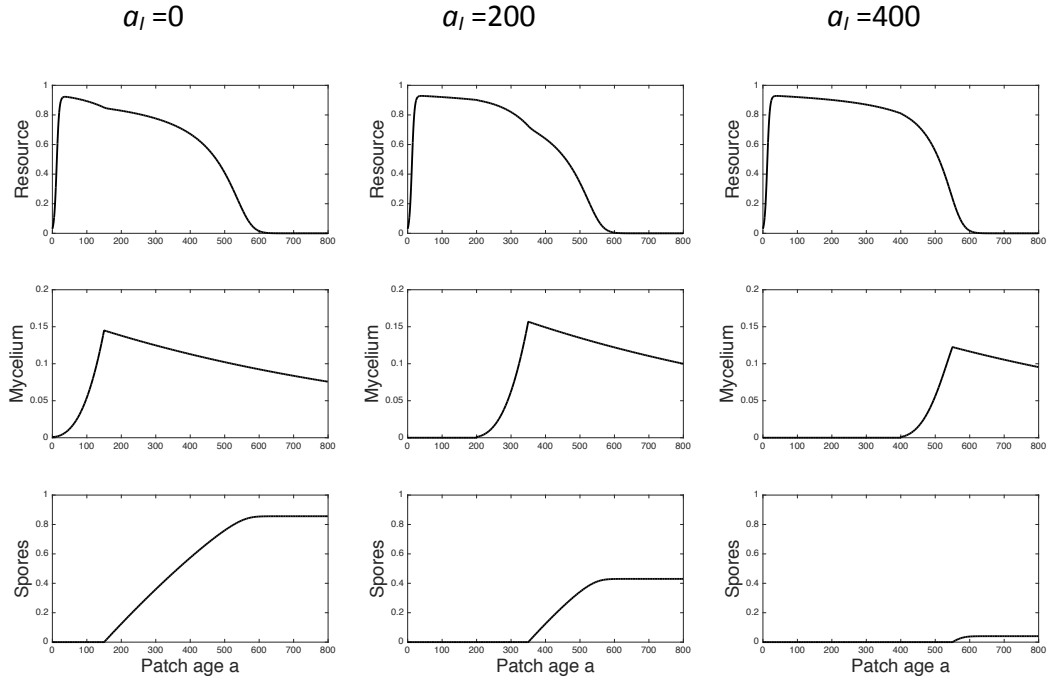


Figure 6. The effect of the age-at-infection on within patch dynamics of resource R , mycelium M and spores production S , representing time series for a given patch. **Top:** Dynamics of $R(a)$ for a patch becoming infected at patch age $a_I = 0, 200, 400$, respectively. **Middle:** Idem, dynamics of $M(a)$. **Bottom:** Idem, dynamics of $S(a)$. Parameters: $\lambda = 100$ and see Table 1.

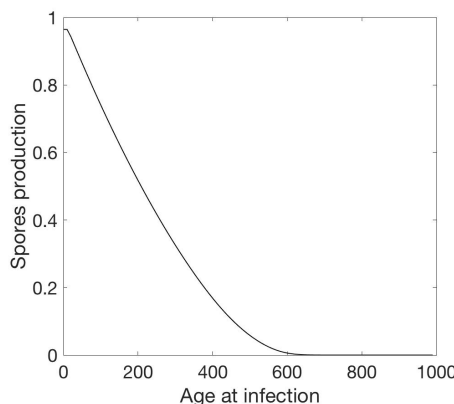


Figure 7. The effect of the age-at-infection a_I on within patch spores production S for a latent period of 150 dd.

In order to visualise the growth-reproduction trade-off at the lesion level, we plot the relationship between total spores production and the latent period (Figure 8). Since the spores production depends on the age at infection, we first plot the curve for a selection of different values of a_l (Figure 8, black curves). In order to summarize the result, we also plot the mean relationship, averaged over the different a_l (Figure 8, red curve). In the absence of a-priori knowledge of the age at infection, using the mean a_l seems a natural first approximation. Below we will show that the canopy dynamics will provide us with the relevant distribution of a_l . Figure 8 clearly shows that the trade-off results in a bell-shaped relationship, with an intermediate optimal latent period. The optimal value is highest ($\lambda > 200$ dd) for the lowest age at infection a_l . Averaging over the age at infection a_l the optimal latent period is $\lambda = 190$ dd.

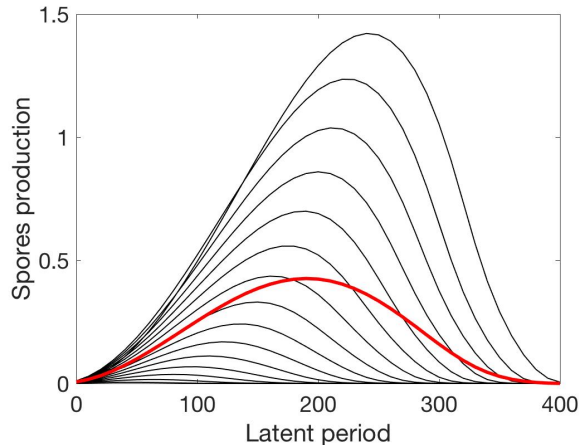


Figure 8: patch-level spore production depending on latent period and age at infection. Black curves: each curve represents a specific age at infection ($a_l=0, 50, 100, \dots$). The upper curve is for $a_l=0$. Each subsequent curve represents the data for an infection occurring 50 dd later. Red curve: the mean spores production, averaged over all a_l . See Table 1 for other parameter values.

Canopy-level model simulations

In this section, we explore the model dynamics of the full canopy-level model, along with the relations existing between some patch-scale infection properties (such as age of the patch at infection) and canopy-scale epidemics. We first present results of an example simulation, in order to illustrate a number of key aspects of the model structure and its typical dynamics.

Canopy level dynamics

Figure 9A shows the overall patch dynamics of a healthy canopy. Note that healthy canopy dynamics are highly constraint by our assumptions and parameter values. During a first phase (date $T=0$ to 1500 dd) the canopy grows (creation of patches). There is a gradual increase in growth rate of the number of patches at low patch numbers, which reflects the dependence of canopy growth on the common resource pool $A(t)$ which gradually accumulates by resource from exporting patches (Figure 9C, upper curve). During a second phase the canopy size remains constant and the number of green patches decreases due to senescence. At the end of the season ($T=2500$), the patches are removed and replaced by next year's initial patches.

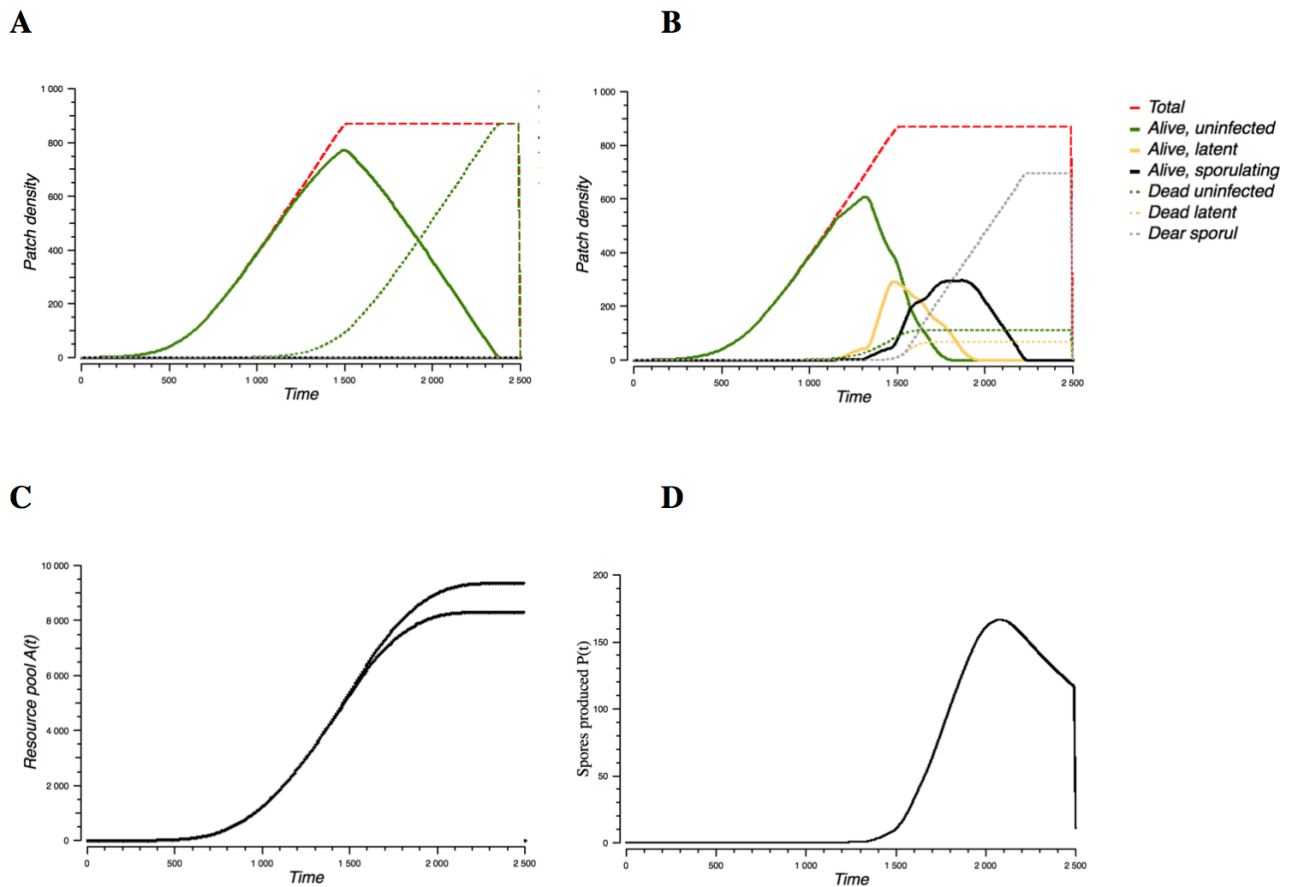


Figure 9: Single-year dynamics of the canopy level model, for a latent period of $\lambda = 150$. **A:** Simulation of canopy without disease, showing the dynamics of healthy, senesced and all patches. **B:** Simulation of canopy with epidemics, showing the dynamics of healthy, latent and sporulating patches. Inoculum arrives at date $T=1000$ dd. For dead patches, the curves distinguish between patches according to their status at the onset of their senescence. **C:** the accumulated resource in the common pool $A(t)$, for the runs in A (upper curve) and B (lower curve), showing the disease's impact on yield. **D:** The dynamics of the total spores pool $P(t)$, for the run in panel B. Parameters: default values in Table 1.

Figure 9B shows the dynamics in the presence of pathogens with a latent period of $\lambda = 150$ dd. Each year, an inoculum (primary infection) is introduced at date $T_{\text{inoc}} = 1000$ dd, moving a small fraction (<2%) of healthy patches into the latent state. The density of primary infections is too small to be seen in Figure 9B; the first sign of the epidemics is the appearance of the second generation of latent patches around $T = 1150$, that are the descendants of the primary infections. One latent period later ($T = 1300$), this generation of infections starts sporulating (Figure 9B). The polycyclic nature of the epidemic is evident from the within-seasonal step-wise dynamics of the densities of latent and sporulating patches: steps are roughly one latent period apart. Roughly two latent periods after the end of the canopy growth phase (i.e., $T = 1800$) the latest green patches become infected. One latent period later, the density of latent patches drops to zero too, since there are no more green patches to be colonized. Subsequently the density of sporulating patches gradually drops to zero as sporulating patches become senescent through ageing and resource depletion. The figure shows that not all patches become infectious; about 15% of patches reach senescence uninfected. About 10% of patches reach senescence while being latent.

Figure 9C shows the impact of the epidemics in Figure 9B on the common resource pool $A(t)$. If yield is assumed to be proportional to the final resource pool, it would hence be reduced by about 10% by the disease, in this example. Figure 9D shows the increase of the total spores pool during the phase with sporulating patches. At the end of the season the spores pool is reduced instantaneously, representing mortality during the unfavorable season. The final value of the spores pool is used to initialize next year's epidemics by determining the fraction of healthy patches to be inoculated.

Figure 10 illustrates the dynamics of the patch age distributions, revealing some of the complexity of the model structure at patch level. The shape of the distribution of healthy (green) patches at $T=1000$, just before the primary infection, reflects the increasing canopy growth rate: the number of patches per age class is higher for more recent age classes (younger ages) than for the oldest age classes. The canopy growth is also illustrated by the progressive movement of the age distribution towards older ages (compare $T=1000, 1150, 1300$, etc). The first pathogen generation sporulates at $T=1150$ but is barely visible. The second generation is clearly visible at $T=1300$ (two latent periods after primary infection). This generation is sporulating at $T=1450$, producing an abundant third generation. The diagram at $T=1600$ shows that infected patches become senescent before healthy patches: some patches are dead before $a=750$ dd, whereas uninfected patches die around $a=880$ dd (see

$T=1150$). Note that the canopy becomes clearly age-stratified by $T=1600$ with green patches remaining exclusively in the top of the canopy (ages near $a=0$). As the canopy stops growing, eventually the entire canopy becomes sporulating or senescent ($T=1750$).

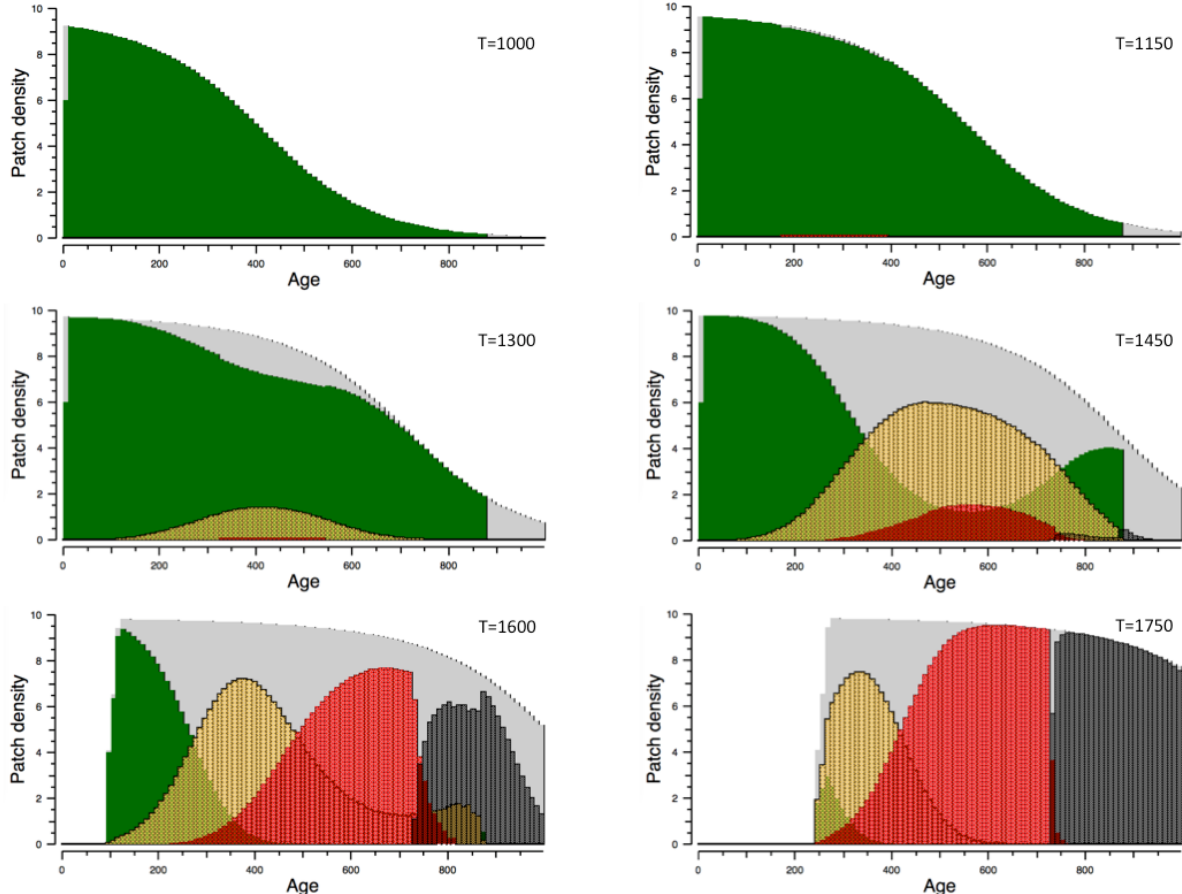


Figure 10. The dynamics of the infection-specific age-structure of the canopy, illustrated by snapshots at 150dd intervals, for the run in Figure 9B ($\lambda = 150$, $T_{\text{inoc}} = 1000\text{dd}$). Green: uninfected patches. Yellow: latent patches. Red: sporulating patches. Black: dead infected patches. Grey: the sum of all types of patches in a given age interval.

The distributions in Figure 10 do not distinguish between patches of different infection age b . Figure 11 shows the double age structure. Each dot corresponds to a cohort of patches of the same patch age and the same infection age, given by its coordinate (a, b) . At $T=1150$ the primary infections are visible as the upper horizontal line whereas the healthy patches are represented by the horizontal line at $b=0$. The second generation of infections is visible at $T=1300$, the third generation at $T=1450$, etc. The figure shows that the subsequent

generations are not discrete age classes, rather each generation covers a range of ages. Furthermore, a given patch may sporulate over a period longer than one latent period so the different generations overlap, and progressively so throughout the season.

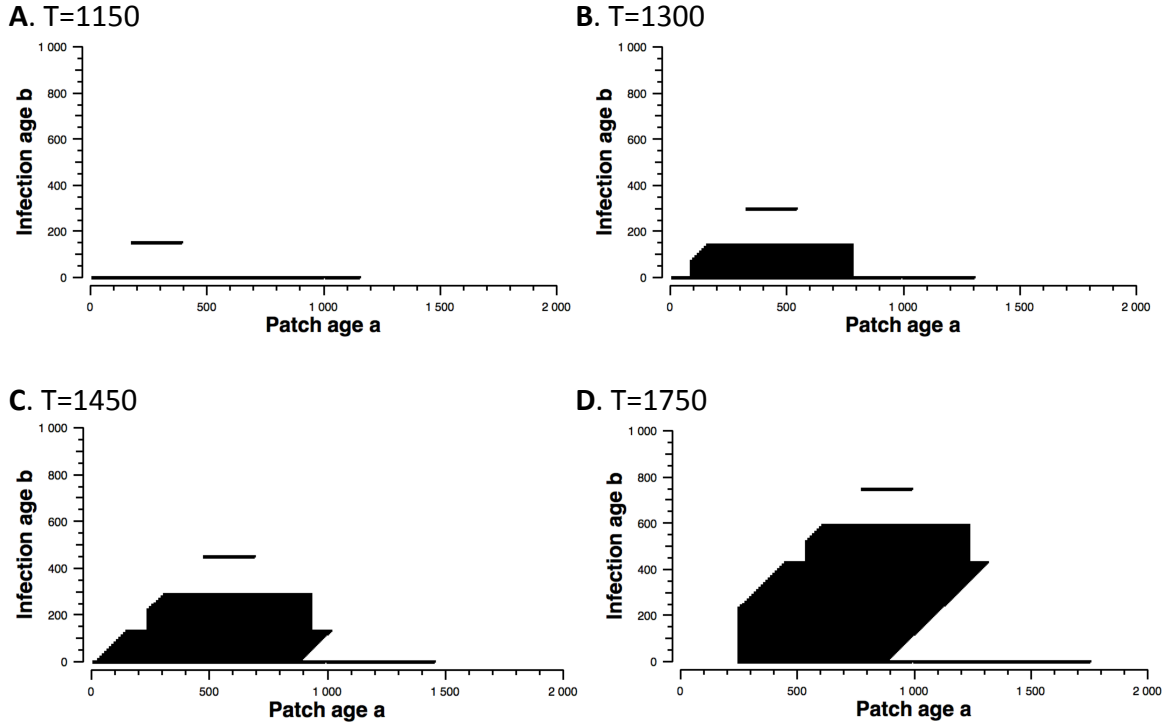


Figure 11. Snapshots of the double age structure of the population, in terms of patch age a , and infection age b , for the same run as in Figs 9B and 10 ($\lambda = 150$). The black region is made up of discrete dots representing the cohorts that make up the canopy. The number of cohorts k increases over time: at times $T=1150$, 1300 , 1450 , and 1750 dd, the number of cohorts is, respectively: $k=140$, 1000 , 2188 , and 3826 . At $T=1150$, the horizontal line at $b=150$ dd corresponds to the primary infections resulting from inoculation at $T=1000$. The line at $b=0$ corresponds to the uninfected population (infection age is arbitrarily set to $b=0$) and span the range $a=(0,1150)$. At $T=1300$ the second generation of (still latent) patches is visible as the black area between $b=0$ and $b=150$. At $T=1450$ this generation is sporulating and a new generation of latent patches is visible. At $T=1500$ the canopy stops growing and thus by $T=1750$ no patches younger than $a=250$ dd exist. The right-hand side limit of the black area results from the assumption that dead patches cannot be infected.

The values of the within-patch variables $R(a)$, $M(a)$ and $S(a)$ for all patches in the canopy are plotted against patch age in the scatter plots in Figure 12. The figure reveals the finer complexity of the model: patches of the same patch age (a) may have different values of these three variables. These differences are explained by the differences in infection age (b) between the patches. For a given patch age a , the patches with the lowest resource level (top panel) generally have the highest mycelium level (middle panel), resulting from an earlier infection (higher b). Note that the figure also reveals a consequence of our numerical approximation of the PDEs using the EBT method, lumping patches of similar ages (a and b)

into age classes (cohorts). The dots are aligned along curves that correspond to patches that have the same infection age b but different patch age. For the simulation in Figure 12 the discretization parameter was 10 dd; the dots are hence 10 dd apart in terms of infection age and/or patch age.

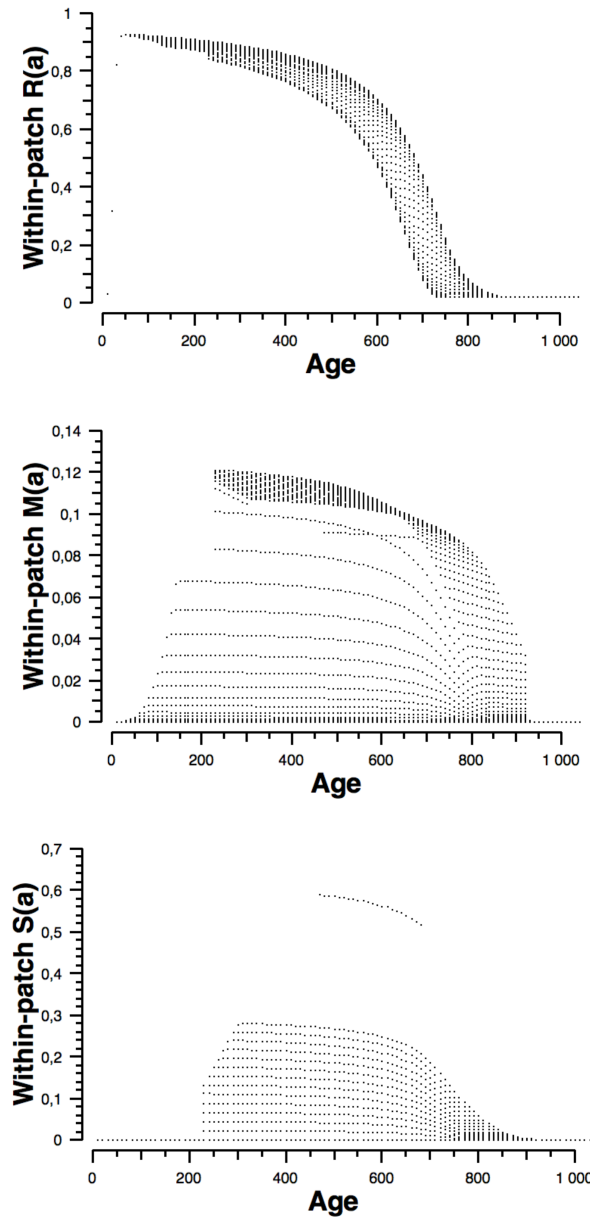


Figure 12: Scatter plots of the patch-level variables $R(a)$, $M(a)$ and $S(a)$ versus patch age a ($T=1450$ dd). Same run as in Figure 9B, 10 and 11.

Figure 12 (lower panel) shows the range of spore production in the canopy. Again, the range of $S(a)$ is the consequence of differences in infection age between patches. This

becomes evident when plotting the total spores production at the end of the season (i.e., $S(a)$ for $a = T_{\text{end}}$) of all patches in the canopy (Figure 13A). All values fall on an almost linear relationship. (This effect was already apparent in Figure 7, comparing the final values of $S(a)$ for different ages at infection). Apparently, in order to predict the patch-level spores production, the only unknown we need to know is the age at infection.

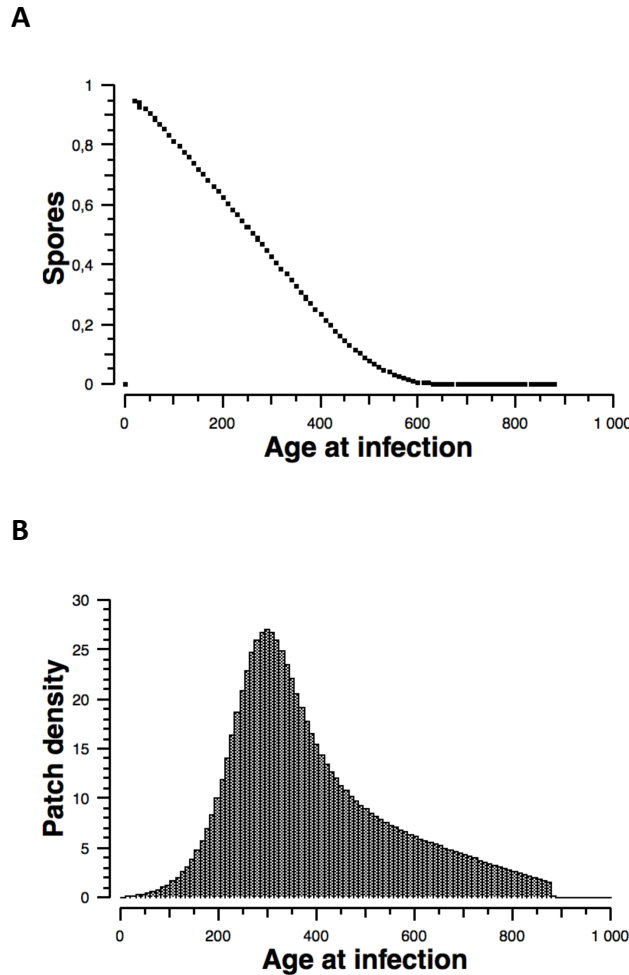


Figure 13. A: The relation between the end-of-season, within-patch cumulative spore production $S(T_{\text{season}})$ and age at infection for all patches in the population. NB patches with the same age at infection (a_i) need not have the same patch age a nor infection age b . (cf Figure 11). **B:** The distribution of patch age at infection (a_i) on the final day in the time series of Figure 9B and Figure 10. The distribution peaks at 300 dd. Parameters: $\lambda = 150$, $\Delta = 250$ and Table 1.

Age at infection (a_I) and epidemics

The age at infection a_I is not a life history trait but rather a consequence of a range of circumstances. For a sporulating patch, the ages of infection of its spores depend on the age distribution of uninfected patches in the dispersal neighbourhood of the patch at the time of dispersal. It hence depends on the current state of the canopy and of the epidemics, as well as on the maximum dispersal distance Δ . It furthermore depends indirectly on canopy growth and the pathogen life history traits (see below). The age at infection is highly variable among

patches: 13B shows the a_I -distribution of all patches, at the end of the season of our example simulation. Note that patches do not disappear from the canopy even after senescence and hence the distribution in Figure 13B includes all patches from the entire season. Due to its critical influence on patch-level spores production, the a_I distribution can be used to characterize the epidemics of a given season or the steady-state dynamics of a given combination of parameters. For example, the total, canopy-level spores production can be obtained by multiplying the a_I -distribution (Figure 13B) with the a_I -specific spores production (Figure 13A). Interestingly, the curve in Figure 13A depends on the parameters of the infection cycle (e.g., latent period) but not on the canopy-level parameters such as dispersal distance, canopy growth rate, length of the growing season, (which do influence the a_I -distribution). It can be thus inferred from Figure 13A that a canopy trait that shifts the a_I -distribution to the right will result in lower epidemics. Similarly, a pathogen dispersal trait that shifts the a_I -distribution to the left will increase spores production. Pathogen life history traits simultaneously affect the a_I -specific spores production and the a_I -distribution and hence the net effect cannot be easily predicted.

Optimal latent period for canopy-level (epidemic) spores production

The effect of latent period on epidemics

Figure 14 shows three simulations for different latent periods (same values as in Figure 5). The figure shows that the pathogen with a short latent period ($\lambda=90$) reaches higher densities of sporulating patches than the intermediate latent period ($\lambda=150$), but the total spores production is higher for the latter strategy ($\lambda=150$). This is due to the higher within-patch sporulation rate obtained with a higher mycelium size. However, the highest latent period ($\lambda=240$) produces too few spores to maintain a stable year-to-year dynamics: the epidemic is ephemeral and goes extinct within three years. Interestingly, at the patch level the spores production for $\lambda=90$ and $\lambda=240$ (and $a_I=100$) are almost identical (Figure 5) and averaged over all a_I spores production is even higher for $\lambda=240$. Yet at the epidemic level, the two trait values give completely different dynamics. This can be understood by considering the spatio-temporal dynamics of the epidemics. With a short latent period ($\lambda=90$) the epidemic moves up quickly through the canopy towards the youngest patches: by $T=1600$ we observe infected patches in the top (lowest age a) of the canopy (Figure 15A). With $\lambda=240$ the epidemic does

not succeed in moving up due to the long delay between infection and sporulation (Figure 15C). The ensuing lower number of generation cycles results in a poorer dispersal across the canopy and a bias towards a higher age at infection (Figure 15). By consequence, a considerable part of infected patches senesce during the latent period and hence without sporulating (Figure 14C). These results suggest that a second trade-off emerges at the canopy level, between high sporulation rate (for longer latent periods) *versus* faster propagation (for lower latent periods).

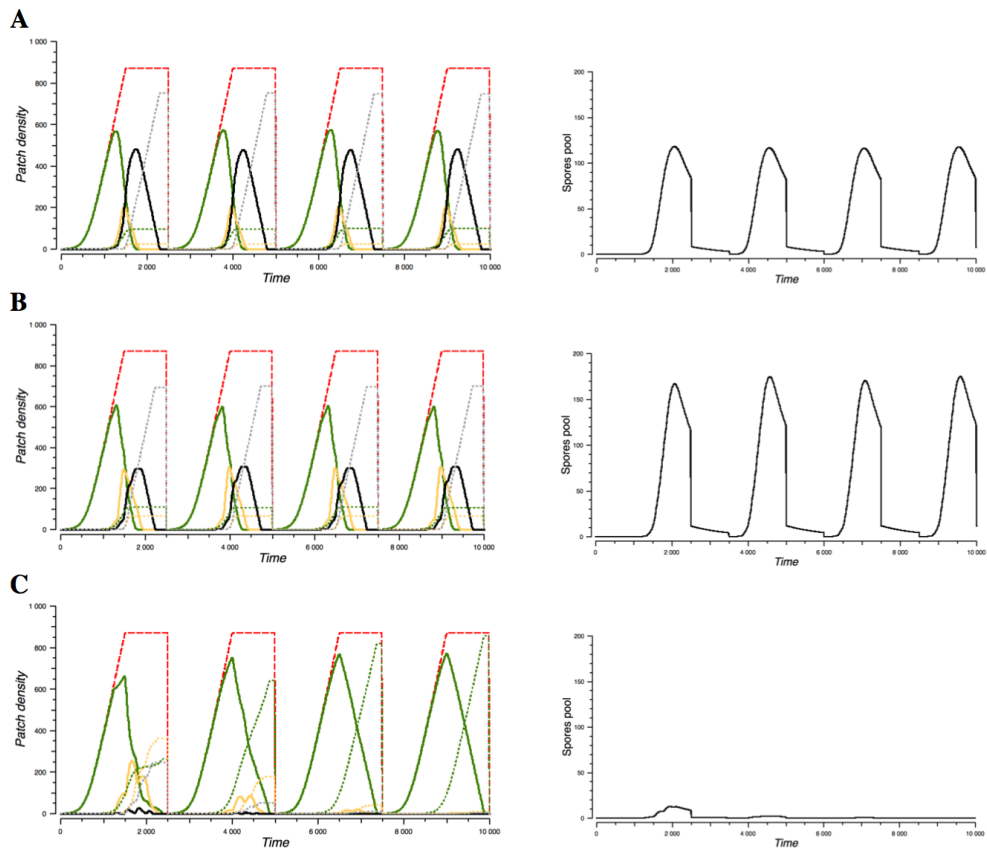


Figure 14. Times series for three values of the latent period. Left panels: canopy and epidemics. Right panels: dynamics of the spores pool $P(t)$. **A:** $\lambda=90$. **B:** $\lambda=150$. **C:** $\lambda=240$. The epidemics are stable from year to year in panels A and B whereas it is ephemeral in panel C. Parameters: $T_{\text{inoc}} = 1000$, and see Table 1.

The results above suggest that there are two trade-offs that together influence the canopy level spores production over a season: at the patch level, there is a trade-off of resource allocation between mycelium and spores; and at the canopy level, a trade-off between sporulation rate (favoured by intermediate latent periods) and propagation speed (favoured by shorter latent periods). Here we explore the net effect of the latent period on these trade-offs, by computing spores production, $P(T_{\text{end}})$, over a range of latent periods

(Figure 8). The epidemics are persistent only for latent periods in the interval $25 < \lambda < 225$. Strains with too long or too short latent periods cannot maintain a stable population in the long run, although they may produce ephemeral epidemics (such as $\lambda=240$ in Figure 14C and Figure 15C). To maximize annual spores production, ($P(T_{end})$) the optimal latent period is around 135 dd.

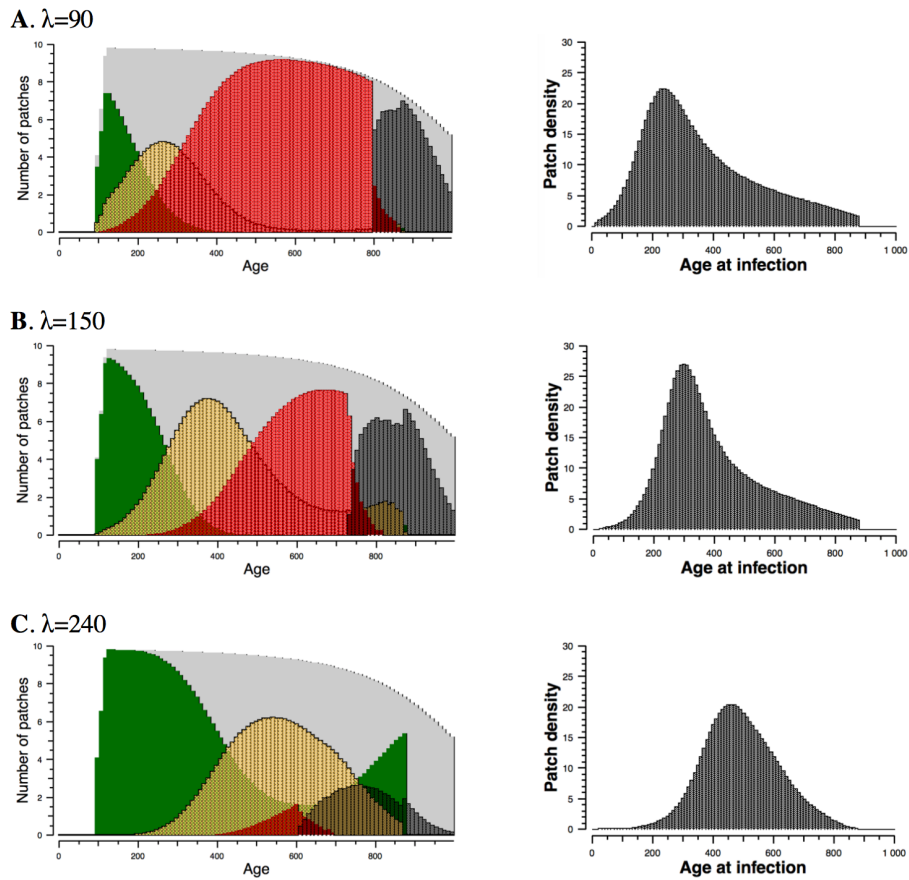


Figure 15. Left column: the canopy age structure of healthy, latent, sporulating and dead infected patches at date $T=1600$ dd. Right column: the distribution of age at infection (a_i) at the end of the season. **A:** $\lambda=90$. **B:** $\lambda=150$. **C:** $\lambda=240$. In A and B the epidemics are stable from year to year whereas it is ephemeral in panel C. Note that A, B and C correspond to Figure 14A, B and C. Parameters: $T_{inoc}=1000$, and see Table 1.

DISCUSSION

In order to account explicitly for (i) age-dependent lesion development; (ii) within-tissue plant physiology (resource dynamics); and seasonal canopy growth, we have developed a model in the framework of Physiologically Structured Population Models. Our model is of intermediate complexity, in between classical SIR models and the very detailed Functional-Structural Plant Models (FSPM) that use highly detailed descriptions of plant architecture and development. The advantage of our approach is that it does take into account a relevant level of low-level detail (i and ii above) yet enables us to do long term studies (multiple year epidemiology and invasion dynamics, see Chapters 2 and 3) which is still impossible for FSPMs due to numerical limitations and the daunting task of their analysis. An additional original aspect of our model is the ecological view of the pathosystem, with the plant and its pathogen being “equally” modelled and interacting in both directions.

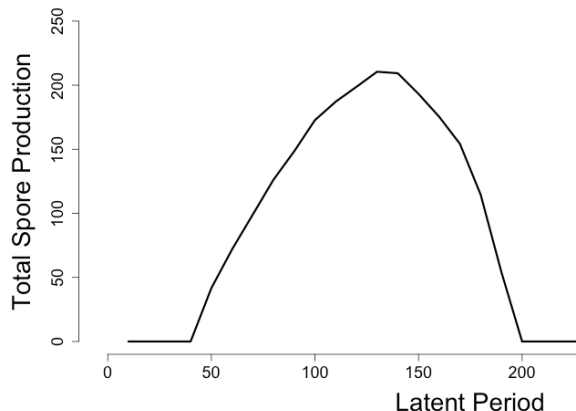


Figure 16. Total spores production at canopy level, over a range of latent periods λ .

Using a lesion-level model and a canopy-level model, both relating a crop pathogen’s latent period to its spore production, we have been able to identify two trade-offs between these important infection cycle traits. The first trade-off, which is apparent at the within-patch level, is analogous to the classical life history problem of optimizing the age at maturation given finite availability of time and resources: the optimal maturation strategy is a compromise between using resources for juvenile growth and keeping resources for reproduction. Reproducing too early results in low sporulation rates due to small mycelium

density, whereas reproducing too late means too little time and resources left for reproduction. This trade-off is apparent at the smallest spatial scale of a single lesion (a single patch).

Extrapolating to the leaf scale, our lesion scale model suggests a strong impact of leaf age on disease severity: the older a leaf is when infection occurs, the less disease will develop. This results from decreasing resources and time available for lesion development. It has been shown that leaf age does indeed decrease the foliar metabolite concentration and the remaining lifespan (Howarth, Parmar et al., 2008; Allwood, Chandra et al., 2015), corroborating our model assumptions. Recent experimental results by Farber, D. H. and C. C. Mundt (2016) support our model prediction showing that inoculated younger leaves have significantly greater disease severity of wheat stripe rust than older inoculated leaves. It is also consistent with simulations of Garin et al. (2014) and Robert et al. (2017) showing that the delay between date of infection and foliar senescence strongly impacts the lesion development and the resulting epidemics.

The second trade-off emerges from the pathogen dynamics at the larger spatial scale: the resulting epidemics and pathogen spread through the canopy. We have shown that a strategy with a relatively high patch-level spores production (i.e., $\lambda = 240$ in Figure 5) may be inefficient at the canopy scale due to inefficient spread through the canopy (i.e., Figure 14C). We have shown that earlier maturation (shorter latent period) results in a more rapid dispersal to the top of the canopy than late maturation (i.e., $\lambda = 90$ in Figure 15A), despite a possibly lower within-patch sporulation rate (cf. examples cited in Pringle and Taylor, 2002). This second trade-off is less predictable than the first one since it depends on the indirect effects of the pathogen's life history traits on the canopy-level population dynamics of the epidemics. In particular, the epidemics depend on the time between subsequent pathogen generations, which corresponds to the latent period. Thus a shorter latent period results in faster succession of generation and hence potentially faster population growth. This second trade-off explains why the optimal latent period (for spore production) is considerably lower at the canopy-level (Figure 16) than at the lesion-level (Figure 6).

The second trade-off also depends on the canopy growth dynamics and on dispersal parameters. It is possible to interpret these results in the light of the effects of plant architecture on foliar fungus development. Several experimental studies have shown that wheat architectures with more distance between the leaves decrease the epidemic

development (Tavella 1978; Danon et al., 1982; Camacho-Casas et al., 1995; Simón et al., 2005). Increasing the distance between diseased leaves and healthy emerging ones allows the plant to escape the disease (Lovell et al., 2004; Robert et al., 2008). We observe the same mechanism in our simulations, with a longer latent period inducing a slower rate of dispersal and therefore smaller epidemics. This slowing down effect of the latent period explains the inability of the strain with $\lambda = 240$ to persist (Figure 14C). It is interesting to note that this disease escape mechanism has been demonstrated for rain-splash dispersed disease such as septoria, but it is a new suggestion for wind-dispersed diseases. It would be interesting to test how the optimal latent period responds to changes in crop architecture.

The existence of two trade-off, one at the local, foliar scale, and one at the canopy scale is consistent with a recent modelling study on the race between wheat growth and septoria epidemics (Robert et al., 2017). Indeed, the authors show that there are two types of race that both impact the epidemics: a local race at the tissue scale, that concerns competition for foliar metabolites, and a vertical race in the canopy with the disease being able or not to reach the new upper leaves as leaves appear and grow apart.

These two trade-offs are expected to influence the pathogen's life history problem of "optimizing" its life history, in an evolutionary context. Our results are based on a simple optimization approach, using an ad-hoc "fitness" measure (total spore production), and cannot be interpreted as predictions of the outcome of evolutionary dynamics without a solid argument why this quantity would be a good fitness measure (Metz, Mylius and Diekmann 2008). For this, a more rigorous analysis can be used, such as invasion analysis based on the theory of adaptive dynamics (Metz et al 1992). The next two chapters explore the evolutionary question in more depth.

Several simplifying assumptions are made in the model. First, it should be noted that climatic factors do not directly influence epidemic development. Temperature scenarios are implicitly considered because plant growth and latent period are expressed in degree-days. Based on the results of Sache et al. (2000), we have considered regular (continuous) events of dispersal. However, we do not simulate other effects of abiotic factors such as variable wind, rain and humidity, that are known to influence foliar crop epidemics (Savary and Janeau 1986; Geagea et al., 1999; Sache et al., 2000), as this was not the main question of our work. In order to introduce effects of climatic factors, one way is to run simulations for varied start

dates of the epidemics, that correspond to favourable (early start date) or unfavourable (late start date) weather conditions. We have investigated such scenarios and simulations show similar results and a dependence of the optimal latent period on the start date (data not shown). Another interesting possibility would be to link the weather scenario to the probability of infection (Del Ponte et al., 2006).

As mentioned in the section “Material and Methods”, we have tested two different assumptions concerning the switch from mycelium growth to sporulation. Above we have assumed that a lesion becomes sporulating upon reaching a fixed age, the latent period. Alternatively we have investigated the assumption that lesions mature upon reaching a fixed size in terms of mycelium density M . We have found that both assumptions lead to nearly identical predictions in terms of the optimal switch from latent to sporulating (see the Appendix of Chapter 2). That is, the mycelium size that corresponds to the optimal latent period (averaged over all patches across a season) under the former assumption is the same as the optimal mycelium density when using the latter assumption of maturation at a fixed mycelium density. Symmetrically, the average latent period observed under the latter assumption is the same as the optimal latent period under the former assumption. The equivalence of the results under the two assumptions can be explained by the fact that the within-patch resource density is fully determined by the within-patch dynamics. Given that all other parameters are equal, the dynamics of R , M and S are identical up to maturation, whichever assumption is made. Our results are hence robust to this detail of the life history model.

The key to our model is the double age structure, which allows us to account for two kinds of population structure at the same time: life history structure in the pathogen population (mycelium growth with age, a latent period, sporulation) and physiological structure in the canopy (within-patch age-dependent resource dynamics, patch senescence). This double age structure enables us to account for a high degree of biologically relevant variability between patches of different age and of different infection status. A further source of structure is the seasonal dynamics of the canopy, imposing constraints on the availability of healthy patches on the pathogen population. This level of population structure poses numerical challenges in terms of managing the dynamics of a large number of types of patches at the same time. We have formulated the model in terms of partial differential equations (PDEs) for mathematical simplicity, and have used the numerical technique called

the “escalator boxcar train” (EBT) to implement the equations for computation. This method is well suited for the implementation of physiologically structured population models (De Roos, 1997; De Roos and Persson, 2013). The application of the EBT method to an epidemiological problem is original, and our choice of using pathogen structure and host structure simultaneously is particularly original. The implementation required making the assumption that new infected cohorts are created only once every 10 dd. In between theses dates, the number of newly infected patches is accounted for within the healthy cohorts, but they are not yet visible or active in terms of infection. This rather elegant modeling trick allowed us to construct the numerical approximation of the PDEs but imposed a limited precision in terms of some results: e.g., it results in the appearance of regular white spaces in Figure 12 (corresponding to a 10 dd interval between infected cohorts) and the discrete steps of 10 dd in the latent period in the Figure 16.

REFERENCES

1. Agrios, G. N. 2005. Plant diseases caused by fungi. Pages 562-582 in: Plant Pathology, 5th ed. Academic Press, Cambridge, MA.
2. Allwood, J.W., Chandra, S., Xu, Y., Dunn, W.B., Correa, E., Hopkins, L., Goodacre, R., Tobin, A.K., and Bowsher, C.G. (2015). Profiling of spatial metabolite distributions in wheat leaves under normal and nitrate limiting conditions. *Phytochemistry* 115, 99–111.
3. Beckett, A. & Woods, A.M. The pattern of colony development and the formation of the uredinium of *Uromyces viciae-fabae* on *Vicia faba*. *Canadian Journal of Botany* 65: 1998-2006 (1987)
4. Cash, J.R. & Karp. A.H. A variable order Runge-Kutta method for initial value problems with rapidly varying right-hand sides. *ACM Transactions on Mathematical Software* 16: 201-222 (1990)
5. Camacho-Casas MA, Kronstad WE, Scharen AL. 1995. Septoria tritici resistance and associations with agronomic traits in a wheat cross. *Crop Science* 35: 971–976.
6. Claessen, D., and Dieckmann, U. (2002). Ontogenetic niche shifts and evolutionary branching in size-structured populations. *Evolutionary Ecology Research* 4, 189-217.
7. Cohen, D. (1976). On the Optimal Timing of Reproduction. *The American Naturalist* 110, 801–807.
8. Damgaard, C., and Østergård, H. (1997). Density-dependent growth and life history evolution of polycyclic leaf pathogens: A continuous time growth model. *Journal of Phytopathology* 145, 17–23.
9. Danon T, Sacks JM, Eyal Z. 1982. The relationships among plant stature, maturity class, and susceptibility to *Septoria* leaf blotch of wheat. *Phytopathology* 72: 1037–1042.
10. Del Ponte, E.M., Godoy, C.V., Li, X., and Yang, X.B. (2006). Predicting Severity of Asian Soybean Rust Epidemics with Empirical Rainfall Models. *Phytopathology* 96, 797–803.
11. De Roos, A.M. Numerical methods for structured population models: The Escalator Boxcar Train. *Numerical Methods for Partial Differential Equations* 4: 173-195 (1988)
12. De Roos, A.M. A Gentle Introduction to Physiologically Structured Population Models. *Structured-Population Models in Marine, Terrestrial, and Freshwater Systems* 119-204 (1997).
13. De Roos, A.M. & Persson, L. Population and community ecology of ontogenetic development. *Monographs in population biology* 448 (2013).
14. Engen, S., and Saether, B. (1994). Optimal allocation of resources to growth and reproduction. *Theoretical Population Biology* 46, 232–248.
15. Farber, D., and Mundt, C. (2016). Effect of Plant Age and Leaf Position on Susceptibility to Wheat Stripe Rust. *Phytopathology PHYTO-07-16-0284-R*.
16. Gandon, S., Day, T., Metcalf, C.J.E., and Grenfell, B.T. (2016). Forecasting Epidemiological and Evolutionary Dynamics of Infectious Diseases. *Trends in Ecology and Evolution* 31, 776–788.
17. Garin, G., Fournier, C., Andrieu, B., Houlès, V., Robert, C., and Pradal, C. (2014). A modelling framework to simulate foliar fungal epidemics using functional-structural plant models. *Annals of Botany* 114, 795–812.
18. Garnica, D.P., Nemri, A., Upadhyaya, N.M., Rathjen, J.P., and Dodds, P.N. (2014). The Ins and Outs of Rust Haustoria. *PLoS Pathogens* 10.

19. Geagea, L., Huber, L., and Sache, I. (1999). Dry-dispersal and rain-splash of brown (*Puccinia recondita* f.sp. *tritici*) and yellow (*P. striiformis*) rust spores from infected wheat leaves exposed to simulated raindrops. *Plant Pathology* *48*, 472–482.
20. Gilchrist, M. a, Sulsky, D.L., and Pringle, A. (2006). Identifying fitness and optimal life-history strategies for an asexual filamentous fungus. *Evolution; International Journal of Organic Evolution* *60*, 970–979.
21. Greenhalgh, D. Hopf bifurcation in epidemic models with a latent period and nonpermanent immunity. *Mathematical and Computer Modelling* *25*, 85-107 (1997).
22. Gregersen, P.L., Holm, P.B., and Krupinska, K. (2008). Leaf senescence and nutrient remobilisation in barley and wheat. *Plant Biology* *10*, 37–49.
23. Hamelin, F.M., Castel, M., Poggi, S., Andrivon, D., and Mailleret, L. (2011). Seasonality and the evolutionary divergence of plant parasites. *Ecology* *92*, 2159–2166.
24. Haueisen, J., and Stukenbrock, E.H. (2016). Life cycle specialization of filamentous pathogens - colonization and reproduction in plant tissues. *Current Opinion in Microbiology* *32*, 31–37.
25. Héraudet, V., Salvaudon, L., and Shykoff, J.A. (2008). Trade-off between latent period and transmission success of a plant pathogen revealed by phenotypic correlations. *Evolutionary Ecology Research* *10*, 912–924.
26. Hethcote, H. W. 2000. The mathematics of infectious diseases. *SIAM Review* *42*:599–653.
27. Howarth, J. R., S. Parmar, et al. (2008). "Co-ordinated expression of amino acid metabolism in response to N and S deficiency during wheat grain filling." *Journal of Experimental Botany* *59*(13): 3675-3689.
28. Kooijman, S.A.L.M. & Metz, J.A.J. On the dynamics of chemically stressed populations: The deduction of population consequences from effects on individuals. *Hydrobiological Bulletin* *17*, 88-89 (1983).
29. Kooijman, S.A.L.M. (2000). Dynamic Energy and Mass Budgets in Biological Systems. Cambridge University Press, Great Britain
30. Lannou, C. (2012). Variation and Selection of Quantitative Traits in Plant Pathogens. *Annual Review of Phytopathology* *50*, 319–338.
31. Lehman, J., and Shaner, G. (1996). Genetic Variation in Latent Period Among Isolates of *Puccinia recondita* f. sp. *tritici* on Partially Resistant Wheat Cultivars. *Phytopathology* *86*, 633–641.
32. Lehman, J.S., and Shaner, G. (1997). Selection of Populations of *Puccinia recondita* f. sp. *tritici* for Shortened Latent Period on a Partially Resistant Wheat Cultivar. *Phytopathology* *87*, 170–176.
33. Li, M.Y. & Muldowney, J.S. Global stability for the SEIR model in epidemiology. *Mathematical Biosciences* *125*, 155-164 (1995).
34. Lovell, D.J., Hunter, T., Powers, S.J., Parker, S.R., and Van Den Bosch, F. (2004). Effect of temperature on latent period of septoria leaf blotch on winter wheat under outdoor conditions. *Plant Pathology* *53*, 170–181.
35. MacArthur, R.M., and Wilson, E.O. (1967). The Theory of Island Biogeography.
36. Mailleret, L., Castel, M., Montarry, J., and Hamelin, F.M. (2012). From elaborate to compact seasonal plant epidemic models and back: Is competitive exclusion in the details? *Theoretical Ecology* *5*, 311–324.

37. Metz, J.a.J., Nisbet, R.M., and Geritz, S.a.H. (1992). How should we define 'fitness' for general ecological scenarios? *Trends in Ecology & Evolution* 7, 198-202.
38. Metz J.A.J., Mylius S.D., Diekmann O. (2008). When does evolution optimize? *Evol Ecol Res* 10:629–654
39. Newton, M.R., Wright, A.S., Kinkel, L.L., and Leonard, K.J. (1999). Competition alters temporal dynamics of sporulation in the wheat stem rust fungus. *Journal of Phytopathology* 147, 527–534.
40. Pariaud, B., Van den Berg, F., Van den Bosch, F., Powers, S.J., Kaltz, O., and Lannou, C. (2013). Shared influence of pathogen and host genetics on a trade-off between latent period and spore production capacity in the wheat pathogen, *Puccinia triticina*. *Evolutionary Applications* 6, 303–312.
41. Pianka, E. (1970). On r and K selection. *American Naturalist*, 104 :592–597.
42. Pringle, A., and Taylor, J.W. (2002). The fitness of filamentous fungi. *Trends in Microbiology* 10, 474–481.
43. Robert, C., Fournier, C., Andrieu, B., and Ney, B. (2008). Coupling a 3D virtual wheat (*Triticum aestivum*) plant model with a *Septoria tritici* epidemic model (Septo3D): A new approach to investigate plant-pathogen interactions linked to canopy architecture. *Functional Plant Biology* 35, 997–1013.
44. Robert C., Garin G., Pradal C., Fournier C. 2017. A plant-pathogen model reveals how plant architecture and foliar senescence impact the race between wheat growth and *Zymoseptoria tritici* epidemics. *Annals of Botany*. (In press).
45. Sache, I. (2000). Short-distance dispersal of wheat rust spores. *Agronomie* 20 (7),757-767.
46. Sasaki, A., and Iwasa, Y. (1991). Optimal growth schedule of pathogens within a host: Switching between lytic and latent cycles. *Theoretical Population Biology* 39, 201–239.
47. Savary, S., and Janeau, J.L. (1986). Rain-induced dispersal in *Puccinia arachidis*, studied by means of a rainfall simulator. *Netherlands Journal of Plant Pathology* 92, 163–174.
48. Schaffer, W.M., Inouye, R.S., and Whittam, T.S. (1982). Energy allocation by an annual plant when the effects of seasonality on growth and reproduction are decoupled. *American Naturalist* 120, 787.
49. Simon MR, Perello AE, Cordo CA, Larran S, van der Putten PEL, Struik PC. 2005. Association between *Septoria tritici* blotch, plant height, and heading date in wheat. *Agronomy Journal* 97: 1072–1081.
50. Smith, V.H., and Holt, R.D. (1996). Resource competition and within-host disease dynamics. *Trends in Ecology and Evolution* 11, 386–389.
51. Stearns, S.C., and Koella, J.C. (1986). The evolution of phenotypic plasticity in life-history traits: predictions of reaction norms for age and size at maturity. *Evolution* 40, 893–913.
52. Tavella CM. 1978. Date of heading and plant height of wheat varieties, as related to *Septoria leaf blotch* damage. *Euphytica* 27: 577–580.
53. Van Den Berg, F., Robert, C., Shaw, M.W., and Van Den Bosch, F. (2007). Apical leaf necrosis and leaf nitrogen dynamics in diseased leaves: A model study. *Plant Pathology* 56, 424–436.
54. van den Berg, F., Bacaer, N., Metz, J.A.J., Lannou, C., and van den Bosch, F. (2011). Periodic host absence can select for higher or lower parasite transmission rates. *Evolutionary Ecology* 25, 121–137.
55. Zhou, Y.C., Song, B.J., and Ma, Z. (2002). "The global stability analysis for an SIS model with age and infection age structures," in Mathematical Approaches for Emerging and Reemerging Infectious Diseases: Models, Methods, and Theory, eds. C. Castillochavez, S. Blower, P. Vandendriessche, D. Kirschner & A.A. Yakubu.), 313-335.

Chapter 2: Crop fertilisation impacts epidemics and optimal latent period of biotrophic fungal pathogens

ABSTRACT

Crop pathogens are known to rapidly adapt to agricultural practices. Although cultivar resistance breakdown and resistance to pesticides have been broadly studied, little is known about the adaptation of crop pathogens to fertilization regimes and no epidemiological model has addressed that question. However this is a critical issue for developing sustainable low-input agriculture. In this paper, we use a model of life history evolution of biotrophic wheat fungal pathogens aiming to understand how they could adapt to changes in fertilization practices. We focus on a single pathogen life history trait, the latent period, which directly determines the amount of resource allocated to growth and reproduction alongside the speed of canopy colonization. We implemented three modelling scenarios corresponding to major effects of increased nitrogen fertilization on crops: (i) increase in nutrients concentration in leaves, (ii) increase of leaf lifespan and (iii) increase of leaf number (tillering) and size that leads to a bigger canopy size. For every scenario, we used two different fitness measures to identify putative evolutionary responses of latent period to changes in fertilization level. We observe that annual spore production increases with fertilization, because it results in more resources available to the pathogens. Diminishing the use of fertilizers could then reduce biotrophic fungal epidemics.

INTRODUCTION

In contrast to plants or animals whose life history has long been studied (Cohen 1971, 1976, Engen and Saether 1994, Kozlowski 1992), fungi received much less attention in life history theory (Gilchrist et al., 2006), possibly because there is still no consensual fitness measure for these organisms (Pringle and Taylor 2002). However, both multiple crop resistance breakdown (Biffen 1905, Kilpatrick 1975, McDonald and Linde 2002, McIntosh and Brown 1997) and the broad development of pesticide-resistant pathogen strains (Fraaije et al., 2001) have made it very clear that fungal crop pathogens rapidly adapt to cultural practices. Life history evolution of fungal crop pathogens is then a key factor to take into account for designing sustainable agriculture. In this paper, we use the ecological framework of life history theory and a consumer-resource-based structured population model to study the response of biotrophic fungal crop leaf pathogens to changes in crop fertilization level.

Most fungal crop pathogens are of real concern because of their propensity to rapidly colonize the crop canopy through successive infection cycles, a phenomenon called polycyclic epidemics. Early in the season, when the canopy is still small, plants get first infected by a primary inoculum. An infection takes place after a spore germinates on the leaf surface. The infection cycle can then be divided into two different steps: the mycelium starts growing during a somatic growth period called the latent period, which precedes the reproduction period. Spores get dispersed and deposited on still healthy leaves, often at higher, younger parts of the growing canopy, where they initiate new infections and the infection cycle repeats itself until the end of the growing season (Agrios 2005).

From that picture, one may hypothesize that resources available to the fungus due to fertilization practices modulate the severity of epidemics either at the leaf tissue scale (modifying the infection cycle) or at the canopy scale (modifying the epidemic propagation). Canopies with different densities or architectures may be more or less susceptible to colonization by the pathogen. Numerous studies have documented the impact of fertilization on cereals and their growth and on plant pathogens (reviewed by Dorda 2008 and Walters and Bingham 2007). Although processes occurring at the leaf scale are rather well studied thanks to many greenhouse experiments, the interplay with canopy-scale processes remains difficult to disentangle. At the leaf scale, the concentration of leaf metabolites and their

dynamics vary with fertilization level. It has been shown that fertilization increases the amount of within-leaf nutrients, hence worsening disease severity (Neumann et al., 2004; Olesen et al., 2003b). Several studies have established a correlation between leaf metabolite content and spore production (Kürschner et al., 1992; Robert et al., 2004, 2006). In several cereal species, leaves of plants exposed to low nitrogen levels also undergo natural senescence sooner than those of plants exposed to high nitrogen levels (Jensen and Munk 1997; Robert et al., 2005). Natural leaf senescence can also be accelerated by nutrient uptake by leaf pathogens (van den Berg et al., 2007). Shorter leaf lifespan likely means that resources are available to the pathogen for a shorter time period, as modelled in Robert et al. (2008). At the canopy scale, fertilization increases both the number and size of plant organs (leaves and tillers, Bainbridge 1974; Naseri et al., 2010; Robert et al., 2006), that one can see as a global level of resource available to the pathogen. The plant organs are possible infection sites whose abundance, shape and spacing also influence spore dispersal and microclimate within the crop canopy. Several authors have demonstrated a correlation between canopy architecture and epidemiological development (Lovell et al., 2004; Calonnec et al., 2012; Robert et al., 2008). It remains difficult to determine which plant effects of fertilization (local- versus canopy-scale) stimulate epidemic development most. Modelling approaches could help tackling this question since they allow computing scenarios that are impossible or very long and difficult to implement in the field or in the greenhouse. However, to our knowledge, no epidemiological model has addressed the question of either epidemiology and adaptation of crop pathogens to fertilization.

To explore the response of fungal crop pathogens to changes in fertilization levels, we opted for a modelling approach using tools and concepts from ecological life history theory and from consumer-resource theory in periodically forced systems (Grover, 1997). There is a limited amount of resource accessible to the fungus within the colonized host tissue. Moreover, the amount of resource is decreasing over time because of leaf senescence (and associated metabolite remobilisation). Under such constraints, life history theory predicts the pathogen will face an age-at-maturation evolutionary dilemma (Roff 2002). It must indeed successfully partition that finite amount of resource between three functions that are key to all organisms: growth, maintenance and reproduction. Reproduction must be efficient enough to ensure canopy colonisation during the polycyclic epidemics, but not at the expense of growth and maintenance. We thus expect strong resource allocation trade-offs to constrain the evolution of fungi life history traits such as age at maturation, referred to as latent period in

fungal pathogens. Latent period is a critical fungal aggressiveness trait in phytopathology research (Lehman and Shaner 1997; Setti et al., 2009; Xue and Hall 1992). Empirical studies have demonstrated the existence of a trade-off between latent period and epidemiological variables such as transmission success (Heraudet et al., 2008) or spore production (Pariaud et al., 2013). The relative latent period of a pathogen strain on different crop cultivars is considered to be a measure of quantitative resistance of the cultivar: the longer the relative latent period, the more resistant the cultivar (Parlevliet 1979; Roumen and Boef 1993; Shaner and Finney 1980).

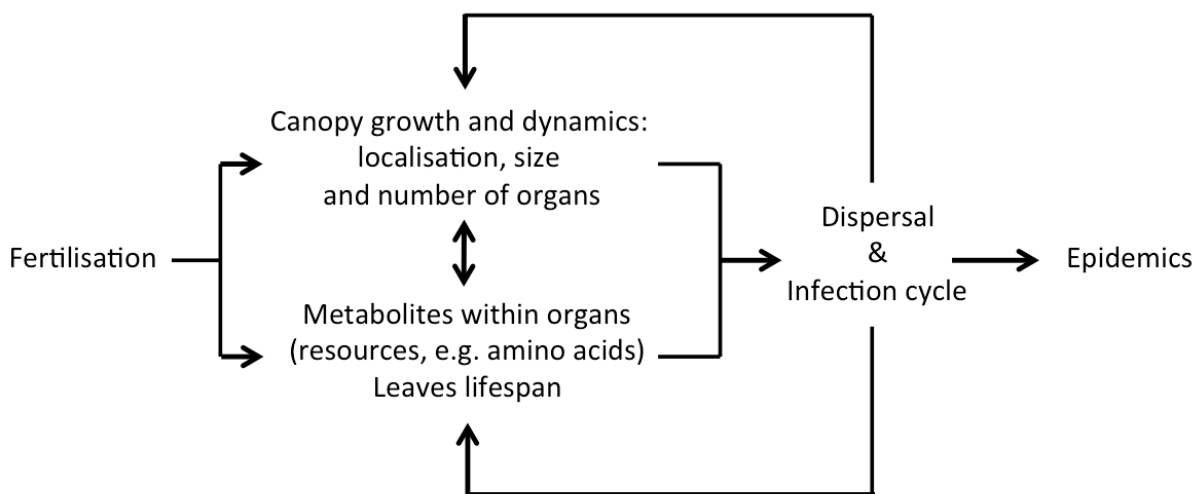


Figure 1: Effects of fertilization on a foliar pathosystem. In our study, fertilization increases both the number and size of plant organs (leaves and tillers), their metabolite content, and their green lifespan. Leaf and canopy scales interact because emergence of new leaves is dependent on resource production by photosynthesis in older leaves. Leaf status affects infection cycle variables such as lesion growth whereas canopy size influences spores dispersal of the pathogen. Both processes have negative feedback on leaf status and canopy growth because they decrease resource level. Therefore, we distinguish between effects of fertilization on the local infection cycle and on the global epidemiological dynamics in our modeling framework.

To address the question of pathogen possible adaptation to crop fertilization, we use two different possible fitness measures. The first one is the annual total spores production. A closely related fitness measure, life time reproductive success, has already been proposed for several filamentous fungi (Gilchrist et al., 2006; Pringle and Taylor 2002). We argue that the within-season exponential growth rate of the pathogen may also be an potential fitness measure since there is a seasonal chase of plant growth and canopy colonization by the fungus (Garin et al., 2014; Robert et al., 2008). The value of the latent period maximizing either of these quantities is called the optimum latent period. If the pathogen strains currently found in the field were indeed adapted to intensive agricultural practices, one could expect them to be

near the optimal latent period for high fertilization levels. If the availability of resource changed in the environment, one can expect the resource allocation trade-offs of these pathogens to also change along with the optimal latent period. In this paper, we are interested in the effect of crop fertilization on the pathosystem through changes in resource availability for both the consumer (pathogen) and the resource (plant). Using a model of crop and pathogen dynamics, we study how changing the resource affects the pathogen's sporulation and optimal latent period. The processes involved in linking fertilization to epidemics, considered in our model are summed up in Figure 1. We consider changes in optimal latent period in response to changes in fertilization to be an indicative direction of pathogen adaptation to changes in fertilization practices.

In our study, we focus on the consumer-resource aspects of fertilization, ignoring other aspects such as defense mechanisms and microclimate. We implement three modelling scenarios mimicking the three main effects of fertilization on the pathosystem (Figure 1): (i) within-leaf nutrient concentration; (ii) leaf lifespan and (iii) canopy size and density (Ferrise et al., 2010; Filella et al., 1995; Hinzman et al., 1986). We simulate these three effects of fertilization on epidemics and the optimal latent period using the two different fitness measures introduced above.

MATERIALS AND METHODS

Pathosystem biology

Our model is inspired by biological knowledge of the pathosystem of a wheat crop and a biotrophic fungal pathogen such as leaf rust (*Puccinia triticina*), although we believe the model is sufficiently generic to apply to other pathosystems as well, in particular to other cereal-fungi pathosystems. In this section, we gather some biological knowledge we think useful to the understanding of our model. More details about the pathosystem can be found in Agrios (2005).

Wheat has a semi-determined developmental schedule: ten to twelve alternate leaves develop on the main axis, the upper-next leaf starting to emerge after the lower one has fully extended. New leaves are created about every 100 degree-days (duration of one phyllochroone, see Lovell et al., 2004). Thus, the age of the leaves approximately reflects their position in the canopy: older leaves near the ground and younger leaves close to the ear. Mature (ligulated) leaves function as source organs for the plant, exporting primary metabolites towards other plant organs. Metabolites are also stored in other organs such as roots or stem. The leaf senescence process begins at ligulation of the leaf (the date on which the leaf becomes entirely mature) and lasts until final leaf death (varying from 700 to 1300 degree-days in wheat). Concentration of primary metabolites in the leaf decreases over senescence. These metabolites are reallocated to new (upper) leaves creation or to grain filling. Hence, the amount of primary metabolites in a leaf decreases with leaf age, allowing canopy growth by creation of new upper leaves and ear development.

Wheat leaf rust is caused by the biotrophic basidiomycete *Puccinia triticina* Eriks. This fungus reproduces mostly asexually on wheat, urediospores being the commonest form of spores produced during polycyclic epidemics. Infection takes place at a local scale on wheat leaves. Lesions on leaves are a few mm² large (Robert et al., 2002). Spores germinate and mycelium starts developing, breaking through the epidermis and colonizing living host tissue in all three dimensions (Garnica et al., 2014; Haueisen and Stukenbrock 2016). During that somatic growth phase (latent period), it develops differentiated intracellular hyphae called haustoria somehow silencing the host immune system and taking up nutrients directly from

the plant cell's cytoplasm (Mendgen and Hahn 2002). Once the latent period has been completed, the fungus differentiates asexual reproductive structures named uredinia. Uredinia are considered mature when they rupture the epidermis allowing spore dispersion by wind. In standard wheat canopies, urediospores produced on a leaf are able to reach two leaves above and two leaves below them (Frejal et al., 2009). Sporulation goes on during an infectious period up to three weeks long for some rust fungi. Spores on leaves impede light reception for photosynthesis. In the fall, urediospore production stops, and a last asexual reproduction cycle leads to the production of rare teliospores able to overwinter. Teliospore germination on wheat residues make the fungus enter a sexual reproduction cycle. Sexual reproduction is associated with overwintering. Sexual basidiospores produced in early spring infect an alternative host, the barberry shrub *Berberis vulgaris* L., from which asexual ecidiospores will colonize wheat seedlings later in spring. In the north-west of Europe, polycyclic epidemics due to urediospores traditionally start in April/May (1000 to 1300 dd after crop sowing depending on numerous factors such as climate or year, Duvivier et al., 2016; El Jarroudi et al., 2014). It may start up to 250 dd earlier in the south-west of Europe.

To adequately model the pathosystem and its particularities, we need to distinguish between the developmental schedule of the plant and the one of the pathogen, which are likely to diverge. In other words, we need a theoretical framework capable of integrating these two developmental scales in the same model over several vegetative seasons.

Model overview

In this part we present the main features of the model that are required to understand how we implement our main assumptions. The complete model is presented in details in Chapter 1.

Our model belongs to the class of physiologically structured populations models (De Roos 1997, De Roos and Persson 2013), which are individual-based models that are well suited to formulate model assumptions at the individual scale (here: patch scale) and to integrate the collective dynamics at the population scale (here: canopy scale). We adopt a strategy with two levels of organization: (i) plant physiology and plant-pathogen interactions at the mm² scale (referred to as the “patch submodel”); and (ii) multi-annual, seasonally

forced patch dynamics and pathogen dispersal at the level of the whole wheat canopy (“canopy-level” model). These two scales of modelling allow us to represent within and between seasonal dynamics of plant-pathogen interactions. To some extent, our model is a structured SEIR epidemiological model (Gilchrist et al., 2006; Greenhalgh 1997; Li and Muldowney 1995). In our case, the host population is structured in terms of patch age a and patch age of infection b as well as in terms of within-tissue resource level, mycelium and spores biomass.

In our model, we consider the fungus has a “bang-bang” resource allocation strategy. Its life cycle is split into two distinct phases. First, the latent period is entirely devoted to somatic growth: resources derived from the host are allocated to mycelium biomass production. Second, the infectious period is entirely devoted to reproduction: resources derived from the host are only allocated to spore production. Concerning lesion maturation, we have modelled two assumptions: lesions mature either at (i) a fixed latent period (fixed age) or at (ii) a fixed mycelium size. We found that the overall results do not differ significantly between these rules (See the Appendix of this chapter). Here we only present the results with fixed latent period.

Patch submodel

In our model, a patch represents a small portion of photosynthesizing leaf (1 mm^2 of leaf surface). The state of a patch is characterized by the variables patch age a and resource concentration R . Infected patches are additionally characterized by the variables age since infection b , mycelium biomass M and spores produced S . Patch resource renewal is governed by a logistic equation with carrying capacity K . Renewal is thought to result from photosynthesis whose intensity $P(a)$ is a decreasing function of age a throughout the patch lifespan τ . The rate of photosynthesis decreases with age in a wheat leaf because of (i) shading by upper leaves; and (ii) apical leaf senescence. In the absence of detailed experimental data on the combined effect of these processes, we have decided to use a linear model as a first approximation, which is the simplest possible model. Note however that the actual resource level R does not follow this linear decrease since it is limited by the carrying capacity, not photosynthesis, in young patches. The resource dynamics are hence insensitive

to the precise shape of the photosynthesis function up to the point where photosynthesis becomes a limiting factor.

Resources created in a patch are exported towards other plant organs (global stored resource pool A) at a rate proportional to patch resource level R and coefficient ψ .

In an infected patch, the mycelium M develops during the somatic growth phase, i.e. the latent period, competing with the plant for resources. Once the latent period has been completed, the mycelium stops growing and the resources acquired by the fungus are allocated to spore production (“bang-bang” resource allocation strategy). Resource uptake by the fungus follows Michaelis-Menten kinetics with asymptotic growth rate $I_{max} M^{2/3}$ and half-saturation R_H , but only a fraction of that energy is converted into either mycelium (M) or spores (S). The rest is lost. The term $\gamma_M M$ is the mycelium loss rate and can be interpreted as the sum of mycelium maintenance and decay. All these biological processes stop when the patch resource level drops below a critical level R_{min} corresponding to patch death. These within-patch processes are described by the following set of ODEs:

$$\frac{dR}{dt} = P(a)R \left(1 - \frac{R}{K}\right) - \psi R - I_{max}M^{2/3} \frac{R}{R + R_H} \quad (1)$$

with

$$P(a) = \begin{cases} 1 - \frac{a}{\tau} & \text{if } a \leq \tau \\ 0 & \text{otherwise} \end{cases} \quad (2)$$

During the latent period ($0 < b \leq \lambda$):

$$\begin{aligned} \frac{dM}{dt} &= c_M I_{max} M^{2/3} \frac{R}{R + R_H} - \gamma_M M \\ \frac{dS}{dt} &= 0 \end{aligned} \quad (3)$$

During the infectious period ($b > \lambda$):

$$\frac{dM}{dt} = -\gamma_M M \quad (4)$$

$$\frac{dS}{dt} = c_S I_{max} M^{\frac{2}{3}} \frac{R}{R + R_H}$$

We assume that the pathogen can only infect healthy patches (no multiple infections). Note that the size of a patch approximates the size of a single lesion. The pathogen acts as a nutrient sink reducing patch lifespan. Once a patch is infected, it is not contagious until the latent period has been completed. Further, the length of the infectious period depends on the amount of resource left in the patch for spore production, hence it also depends on the age at which the patch has been infected.

Patches get infected when reached by spores emitted by nearby (age-similar) infectious patches. Spores dispersal decreases with increasing age-distance to sporulating patches. The probability for a patch to become infected is proportional to the sum of the sporulation rates of patches within a range of Δ degree-days around the patch (maximum dispersal distance) inversely weighted by the age difference between source and target patches. Such dispersion kernel corresponds to having the maximum chance of dispersing to tissue on the same leaf (same age of leaf in the model) (Frejal et al., 2009).

For a more detailed presentation of the patch submodel, see Chapter 1.

Canopy-level model

We consider two populations: a single crop and a single biotrophic fungal pathogen strain.

We model wheat crop as a collection of 1 mm^2 leaf patches. Age is a handy trait to structure the population of plant patches: the younger the patch, the higher its position in the canopy and the higher its concentration of primary metabolites. All patches are thus characterized by their age a . This simplification is central in our model. Note that we do not model any intermediate structure such as leaves or plants. Our canopy-level model may thus be regarded as spatially uni-dimensional since patch age is inclusive of patch height in the canopy and since there is neither individual plant modelling nor “horizontal” field structure. Healthy patches are characterized by their age a only.

Infected (latent or infectious) patches are characterized both by their age a (like any other patch) but also by their age of infection b . Since patches with different ages have different resource levels, patches infected at two different ages will not offer the pathogen the same amount of resource, nor the same time, to develop. Both variables a and b are thus required to fully describe the physiological state of infected patches.

Healthy patches (“susceptible” in terms of SEIR models terminology) colonized by the pathogen become infected but remain non-infectious (exposed) during the latent period. They become able to infect neighbouring patches. Spore produced by infectious patches (infected) decay at a rate γ_s . The total of spores produced during a growing season constitutes a spore pool, whose end-of-the-season value is used to calculate both measures of the pathogen's fitness. The spore quantity that remains at the end of each growing season and overwinters determines, if sufficient, the intensity of the next season's epidemics. Dead patches (removed) are neither susceptible nor infectious anymore since biotrophic pathogens can only develop on living tissues. With healthy, latent, infectious and dead patches possibly co-occurring in the same patch-age class, our model resembles a structured SEIR epidemiological model.

For more details regarding the model functioning and equations, see Chapter 1.

Pathogen fitness and optimal latent period

Following Gilchrist et al. (2006) and Pringle and Taylor (2002), we consider the total annual production of spores at the epidemic scale to be potential putative fitness measures for our fungal pathogen. Moreover, in periodically growing populations, the within-seasonal exponential growth rate may be a critical fitness measure (?opportunist strategy?, Grover 1997). For foliar fungal pathogen, it has been shown by numerical simulations that a race occurs between plant growth and the colonization of the canopy by the pathogen (Garin et al., 2014; Robert et al., 2008). If the pathogen is not fast enough in the canopy colonization process, the plant may even escape the disease. We thus argue that the within-season exponential growth rate of the pathogen may represent another potential fitness measure in our system. In the following, we refer as “optimal latent period” to the value of the latent period parameter maximizing either of these two quantities.

The total annual production of spores at the epidemic scale $P(T_{end})$ is measured at the end of the last year of a ten year simulation (ten years is long enough for the system to reach a stationary year-to-year dynamics).

The within-season exponential growth rate of the pathogen is computed as follows:

$$r = \frac{\log(LTR)}{\lambda} \quad (5)$$

with $LTR = c_{LTR} S(a_\infty)$, λ the latent period serving as a minimum generation time, $S(a_\infty)$ the patch-level, average, lifetime spore biomass production and c_{LTR} the number of patches infected by one unit of spore biomass. The quantity LTR can be regarded as the patch-level lifetime reproductive success.

For more details about r calculation, see Chapter 1.

Effects of fertilization

To model the effect of nitrogen fertilization on crop resource and physiology, we implemented three modelling scenarios mimicking three main effects of fertilization on the crop (Figure 1): (i) within-leaf metabolite concentration; (ii) leaf lifespan and (iii) canopy size. In the first two ones, we change the resource level at the leaf scale.

To simulate the effect of fertilization on within-leaf metabolite concentration (“MC” effect), we change within-patch resource level by artificially increasing or decreasing the patch carrying capacity K (Equation 1), e.g. the maximum amount of resource in the patch. This mimics the increased concentration of primary metabolites in leaves of higher fertilized crops.

To simulate the effect of fertilization on leaf lifespan (“LL” effect), we artificially change patch lifespan by varying the parameter τ (Equation 2): the longer the patch lives, the more resource it produces by photosynthesis. This mimics the increased leaf lifespan in leaves of higher fertilized crops.

Symbol	Value	Unit	Interpretation
T_{season}	2 500	dd	End of season
T_{grow}	1 500	dd	End of period of canopy growth
T_{inoc}	1 000	dd	Date of primary inoculation (annual start date of epidemic)
K	0.1 to 2	g	Within-patch resource carrying capacity
P_0	0.3	dd ⁻¹	Intrinsic rate of photosynthesis
τ	400-1300	dd	Maximum patch age for photosynthesis (patch lifespan)
Ψ	0.02	dd ⁻¹	Export rate of resource from patch to common pool
R_0	0.03	g	Initial resource level at patch creation
M_0	0.0001	g	Initial mycelium biomass at patch infection
R_{min}	0.02	g	Minimum resource level for patch survival
I_{max}	0.06	g · dd ⁻¹	Maximum resource uptake rate per unit of mycelium biomass
R_H	0.25	g	Half-saturation coefficient for functional response of resource uptake
c_M	0.2	-	Conversion coefficient for resource-mycelium conversion
c_S	0.2	-	Conversion coefficient for resource-spores conversion
c_{LTR}	50	g ⁻¹	Constant for computing LTR
λ	10 to 350	dd	Latent Period
γ_m	0.001	dd ⁻¹	Mycelium decay rate
γ_s	0.001	dd ⁻¹	Spores decay rate
A_H	100	g	Half-saturation coefficient of pool resource level for patch creation
ρ	0.1 to 2	dd ⁻¹	Maximum rate of patch creation
k	1	g · dd ⁻¹	Cost of patch creation
β	100	dd ⁻¹	Dispersal efficiency
Δ	250	dd	Maximum dispersal distance
ω	0.1	-	Spore survival probability over the unfavorable season
$a_{inoc,min}$	20	dd	Minimum patch age to receive primary inoculum
$a_{inoc,max}$	250	dd	Maximum patch age to receive primary inoculum
θ_{max}	0.02	-	Maximum fraction of patches per cohort that can be inoculated
P_H	10	g	Half-saturation coefficient of spore biomass for spores-limited inoculation

Table 1: Biological model parameters and their default values, representing the wheat–brown rust pathosystem

Contrary to the two previous effects of fertilization, the third one, corresponding to changes in the leaf area index (“LAI” effect), leads to changes in resource levels at the canopy scale. We change the canopy leaf area index (LAI) by changing the maximum patch creation rate ρ (Equations 6, 10, 15 and 16 in Chapter 1). This mimics the increase in leaves surface and tillers numbers in high-fertilized crops, which results in increased LAI.

Analysis methods and simulations

We study the model dynamics using numerical simulations. The patch submodel was implemented in Matlab for numerical integration of the ODEs for R , M and S (equations 1 to

4). The canopy-level model was implemented using the Escalator Boxcar Train method (De Roos 1997) and the *EBTtool* software package. This method discretizes the continuous patch distributions into cohorts of patches of similar patch ages a and similar infection ages b . Each cohort is characterized by the total number of patches in the corresponding age interval and the cohort's average patch-level state variables (a , b , R , M and S) of the patches. The dynamics of each cohort are described by the ODEs that describe the dynamics of its patch-level state variables and the number of patches in each cohort. In our simulations, new cohorts are created every 10 time units where the time unit is one degree-day (dd). The number of cohorts increases during the growing season via the creation of newborn healthy cohorts (cohorts with $a=0$) and via the creation of newly infected cohorts (cohorts with $b=0$). The total number of cohorts typically reaches in the 100s without pathogen or in the 1000s with pathogen. See Chapter 1 for detailed description of the EBT formulation of our model.

To study the impact of fertilization on epidemics and on optimal latent period, we carry out sensitivity analysis for each of the three fertilization parameters K , ρ and τ . Results of Figure 2 and 3 are from the Matlab implementation of the patch submodel. Results of Figure 4, 5, 6 and 7 are from the *EBTtool* implementation of the canopy-level model. In Figure 4, the amount of R produced over an epidemic is calculated by integrating the photosynthesis term in equation 1 for every patch between infection start T_{inoc} and the end of the growing season (T_{season}). In Figure 7, optimal latent period can only be a multiple of 10 because of time scale of new cohorts creation (see above). Regressions have been added to these data to emphasize the relationship between fertilization parameters and optimal latent periods.

RESULTS

Effect of resource level at the patch scale

Figure 2 shows the effect of an increase in fertilization parameters K (patch resource carrying capacity) and τ (patch lifespan) on resource allocation in a single infected patch for different latent periods λ .

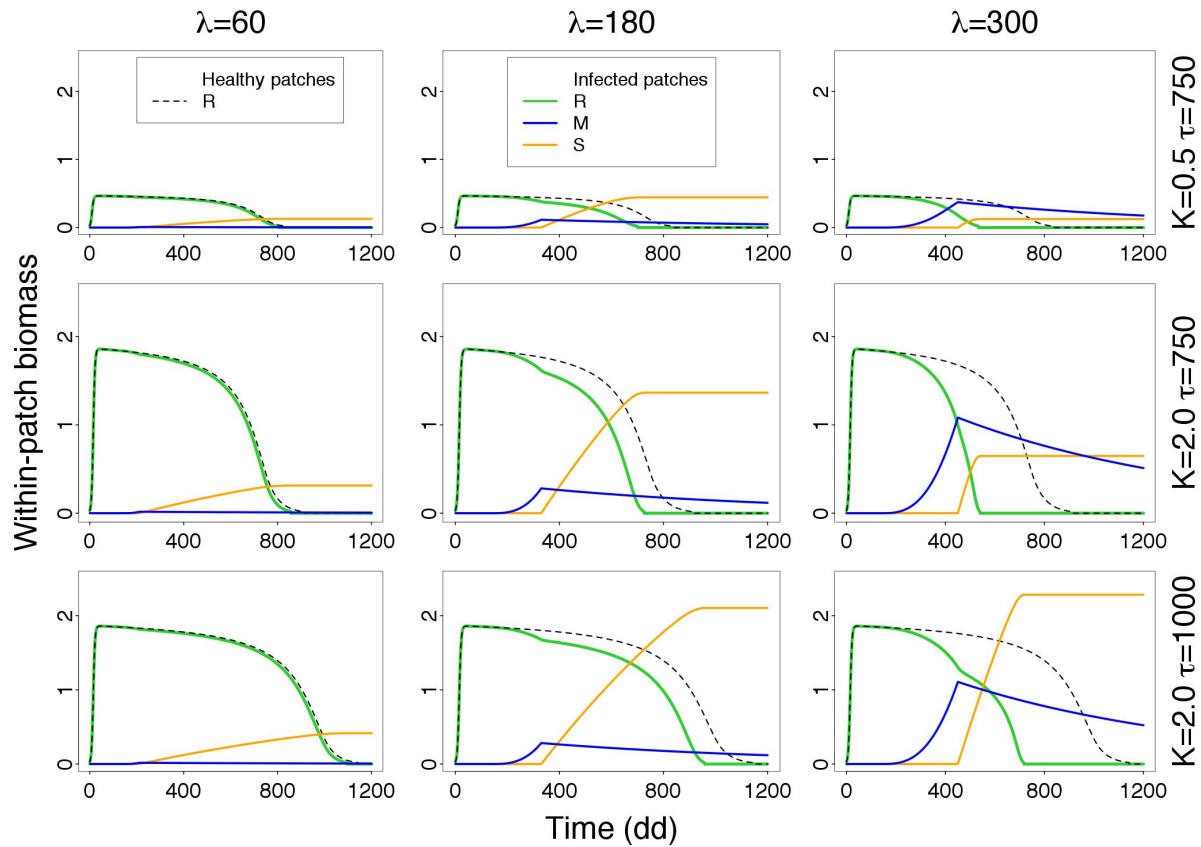


Figure 2: Variation over the lifespan of a patch infected at 200 degree-days (dd) of the patch biomass (medium gray curves), mycelium biomass (dark gray curves), and spore biomass (light gray curves). Black dotted lines represent the biomass of a corresponding healthy patch for the sake of comparison. Areas between the black dotted lines and the medium lines represent the effect of the fungus on the resource dynamics. Latent period (λ) is constant in columns, varying from 60 dd (left) to 180 dd (middle) and 300 dd (right). Upper row, $K = 0.5$, $\tau = 750$ dd. Middle row, $K = 2$, $\tau = 750$ dd. Bottom row, $K = 2$, $\tau = 1,000$ dd.

For every combination of these parameters, the longer the latent period, the more the pathogen depletes the patch resource and therefore the sooner the patch dies (difference between green solid and black dotted curves increases). Mycelium biomass always increases with latent period.

Increasing K increases the amount of resource within the patch (compare upper and middle panels). For each latent period value, increasing K increases the amount of mycelium and spore produced. Maximum spore production occurs at intermediate latent period.

Increasing τ leads to longer-lasting patches, with no increase in the patch maximum resource concentration (compare middle and bottom three panels, $K=2$ and $\tau = 750$ or 1000 dd). There is no visible difference in mycelium biomass production, but spore production is higher than in the previous simulations. For the last parameter combination, spore production is maximum at long latent period, showing the optimal latent period is longer than in previous simulations.

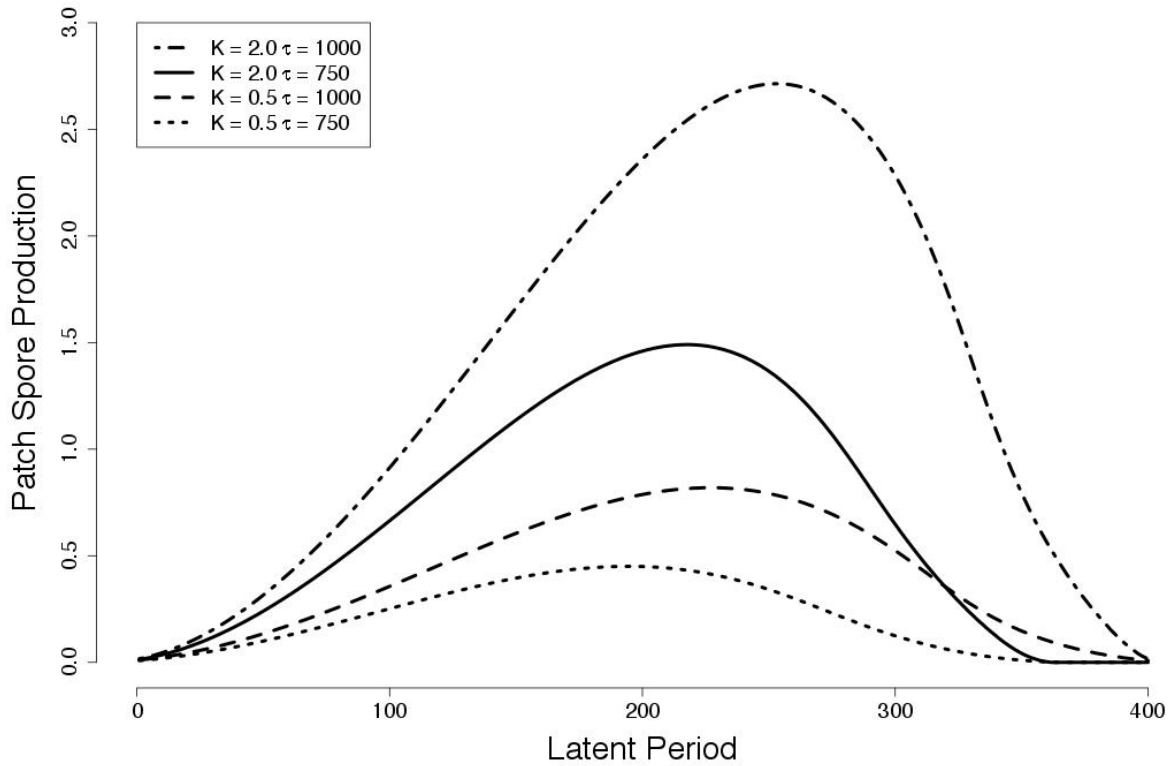


Figure 3: Spore production of a patch infected at 200 degree-days (dd) for a range of latent periods. Dotted line, $K = 0.5$, $\tau = 750$ dd; solid line, $K = 2$, $\tau = 750$ dd; and mixed line, $K = 2$, $\tau = 1,000$ dd. A fourth parameter combination has been added for the sake of comparison: dashed line, $K = 0.5$, $\tau = 1,000$ dd. Maximum values of these curves are the optimal latent periods (for spore production) at the patch level and reflect a trade-off in resource allocation between mycelium growth and spore production. Typically, a latent period shorter than optimal results in a too-low sporulation rate due to small mycelium size, whereas a latent period longer than optimal suffers from too little resources left for spore production.

Figure 3 shows the effect of the latent period on the spores production at the patch level for two values of τ and K and for a single age at infection (200 dd). Spores production increases with both τ and K . Spores production also strongly depends on the latent period with an optimal period that varies with resource conditions: the more resource, the longer the optimal latency. For very long latent periods, the spores production decreases to zero.

Effect of fertilization at the canopy level

Figure 4 shows the impact of fertilization parameters K , τ and ρ on canopy size, primary production and resource allocation at the wheat canopy scale. Canopy size increases linearly with ρ whereas it has a sigmoid response to a change in K and τ (Figure 4A, B and C). In the latter case (Figure 4C), canopy size is less sensitive to an increase of patch lifespan τ for biologically realistic parameter values (600 to 1000 dd).

The three effects of nitrogen fertilization tested in our work are not entirely independant in our model because of canopy functioning feedbacks. The “MC” effect is simulated via an increase of the patch resource carrying capacity. This also leads to an indirect increase in canopy size via leaf resource exportation and resource allocation to patch creation. More resource in patches means more resource exported towards plant nutrient sinks A and then more resource available for canopy growth. Canopy growth in the “MC” effect simulations remains however less sensitive to fertilization than in “LAI” effect simulations (compare Figure 4A and C). Similarly, patches lifespan in “MC” effect simulations increases with K ; a healthy patch living about 500 dd at $K = 0.1$ and about 800 dd at $K = 2$ (theoretical value $\tau = 750$ dd, data not shown). In “LAI” effect simulations, maximum patch creation rate is the only parameter to change, with no feedback on patch lifespan (constant at 750 dd for all values of ρ tested, data not shown). Patch maximum resource concentration does not change in “LAI” effect simulations either.

Total resource produced (primary production) during a growing season increases linearly with fertilization level (Figure 4D, E and F). Annual primary production is quantitatively similar in all three modelling scenarios, though a bit less regarding the “LL”

effect. Total primary production is slightly higher in infected canopies than in healthy canopies, up to 2%, 5% and 9% for “MC” and “LAI” and “LL” effects respectively. Nevertheless, the amount of resource exported by the plant for its own functioning (export towards A) is a 10 to 30% less in infected canopies than in healthy canopies (data not shown).

Both spore and mycelium biomass production increase with K , ρ and τ . Spore biomass increases faster than mycelium biomass. The proportion of total produced biomass of mycelium is at most 3% for the “LL” effect and 4% for the “MC” and “LAI” effects. The proportion of total produced biomass of spores is at most 15% for the “MC” and “LAI” effects, and 25% for the “LL” effect.

For the three effects of fertilization on the pathosystem tested, more resource is usually allocated to spores than to mycelium production. Increasing each of the fertilization parameters ends up favouring spore production over mycelium production.

Figure 5 shows the impact of a change in each fertilization parameter on the temporal dynamics of the infected canopy. Two-year time series of the asymptotic dynamics allow comparison of the proportion of healthy, latent and infected patches over time.

In all four panels, patches are healthy (green lines) until 1000 degree-days after the start of the growing season, date at which the canopy is first inoculated. The increase of healthy patches is followed by an increase of latent patches as they become infected (blue lines), those same becoming infectious a latent period later (orange lines). Patches finally die, whether they have been infected or not (dotted lines).

Canopy size does not change when doubling the patch resource carrying capacity K (cf. Figure 5A and B), slightly increases when increasing patch lifespan τ from 750 to 1000 dd (cf. Figure 5A and C), and more than doubles when doubling the maximum patch creation rate ρ (cf. Figure 5A and D).

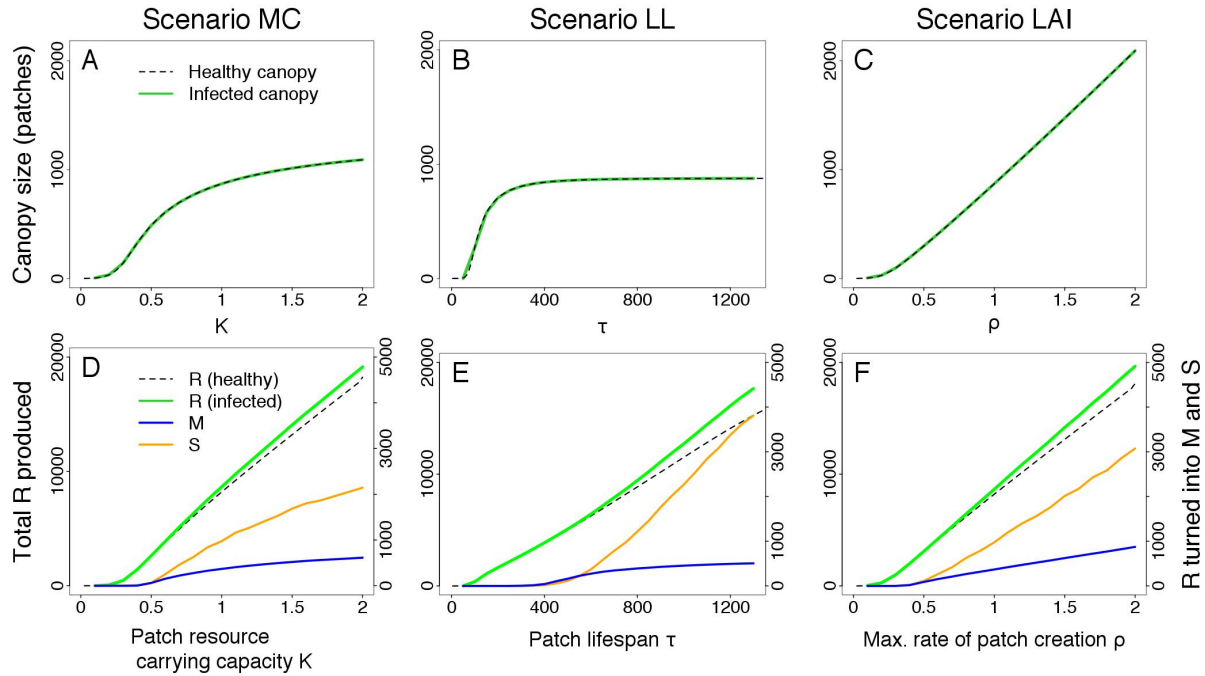


Figure 4: **A, B, and C,** Relation between canopy size (number of patches) and fertilization level for each the three main effects of fertilization on crops. K = patch resource carrying capacity (metabolite concentration [MC] effect), τ = patch lifespan (leaf lifespan [LL] effect), and ρ = maximum patch creation rate (leaf area index [LAI] effect). Black dotted lines refer to canopies without pathogens and solid lines refer to infected canopies. **D, E, and F,** Relation between resources (R) produced by an infected canopy over an epidemic (medium gray) and total resource transformed into mycelium (M, dark gray) or spores (S, light gray) to variable fertilization level for fertilization effects MC, LL, and LAI, respectively. Medium gray curves = patch biomass, dark gray curves = mycelium biomass, and light gray curves = spore biomass. Black dotted lines represent the amount of R produced by a healthy canopy over the same time for the sake of comparison.

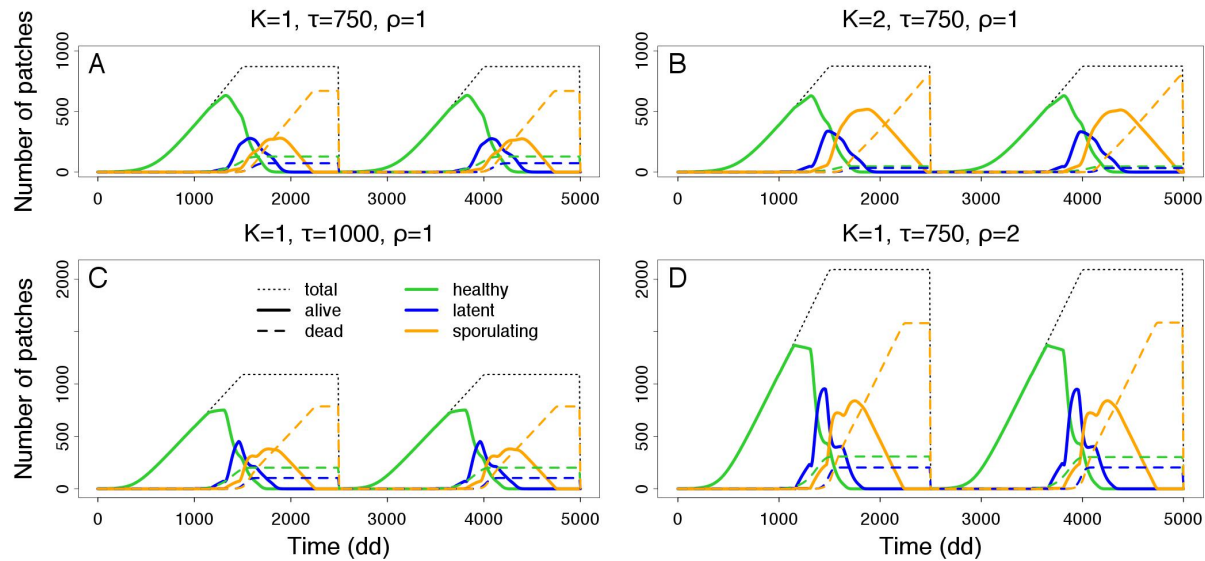


Figure 5: Two-year time series showing the impact of increasing fertilization parameters on epidemics. Solid lines indicate the number of alive patches (black = total number of patches, green = healthy patches, blue = latent patches, and orange = sporulating patches). Dotted lines indicate the number of dead patches. Their color indicate the state they were in at the moment of death. **A,** Reference case. $K = 1, \rho = 1, \tau = 750$. **B,** Increase in resource carrying capacity. $K = 2, \rho = 1, \tau = 750$. **C,** Increase in patch lifespan. $K = 1, \rho = 1, \tau = 1000$. **D,** Increase in maximum patch creation rate. $K = 1, \rho = 2, \tau = 750$.

Increasing any of the fertilization parameters K , ρ and τ lead to an increase of the number of latent and sporulating patches, but with different consequences. Doubling K increases the proportion of infected patches (more than 90% of patches ever become infected in Figure 5B) whereas it does not when doubling ρ or increasing τ (less than 80% of patches ever become infected in Figure 5A, C and D). Epidemic development is faster when increasing K compared to τ or ρ . In these latter cases, more patches die at the latent state and the maximum number of infected patches (both latent and sporulating) is reached earlier and levels off, whereas it does not when increasing K (compare Figure 5B to 5C and 5D).

Effect of fertilization on optimal latent period

Figures 6 and 7 show the impact of fertilization on the optimal latent period. For the three effects of fertilization, at every latent period, increasing the fertilization parameter increases spore production (Figure 6A, C and E) and within-season exponential growth rate of the pathogen (Figure 6B, D and F). Epidemics are not sustainable if K is less than 0.5 and if ρ is less than 0.4 because spore production is not sufficient for enough spores to overwinter and create a new infection the next growing season (dashed areas in Figure 7). This phenomenon does not occur for the “LL” effect (Figure 7, middle panel). At a given resource level, epidemics can not take place if the latent period is too short or too long. If the latent period is too short, mycelium concentration remains very low and hence the spore production rate is too low for epidemics to be perennial. If the latent period is too long, all resources taken up by the pathogen are allocated in mycelium growth and the resource pool is depleted when it turns to sporulation. As a result of this resource allocation trade-off, the value of the latent period maximizing either the annual spore production $P(T_{end})$ or the within-season exponential growth rate of the pathogen r is intermediate between these two extreme cases.

The optimal latent period maximizing spore production increases with the fertilization parameters (Figure 7, filled circles). It varies from 110 dd to 150 dd as K or ρ increases from 0.5 to 2. The optimal latent period is most sensitive to τ over the range of values tested, more than doubling between $\tau = 400$ ($\lambda = 80$) and $\tau = 1300$ ($\lambda = 200$). The optimal latent period

maximizing within-season exponential growth rate of the pathogen always decreases with the fertilization parameters (Figure 7, empty diamonds). It is divided by two over the range of parameter values tested (from about 100 dd at $K = 0.5$, $\rho = 0.4$ and $\tau = 400$ to about 50 dd at $K = 2$, $\rho = 2$ and $\tau = 1300$). The difference between the latent periods calculated with either fitness measures increases with the fertilization parameters. Both fitness measures give similar optimal latent periods at low resource level ($K = 0.5$, $\rho < 0.6$ and $\tau < 500$).

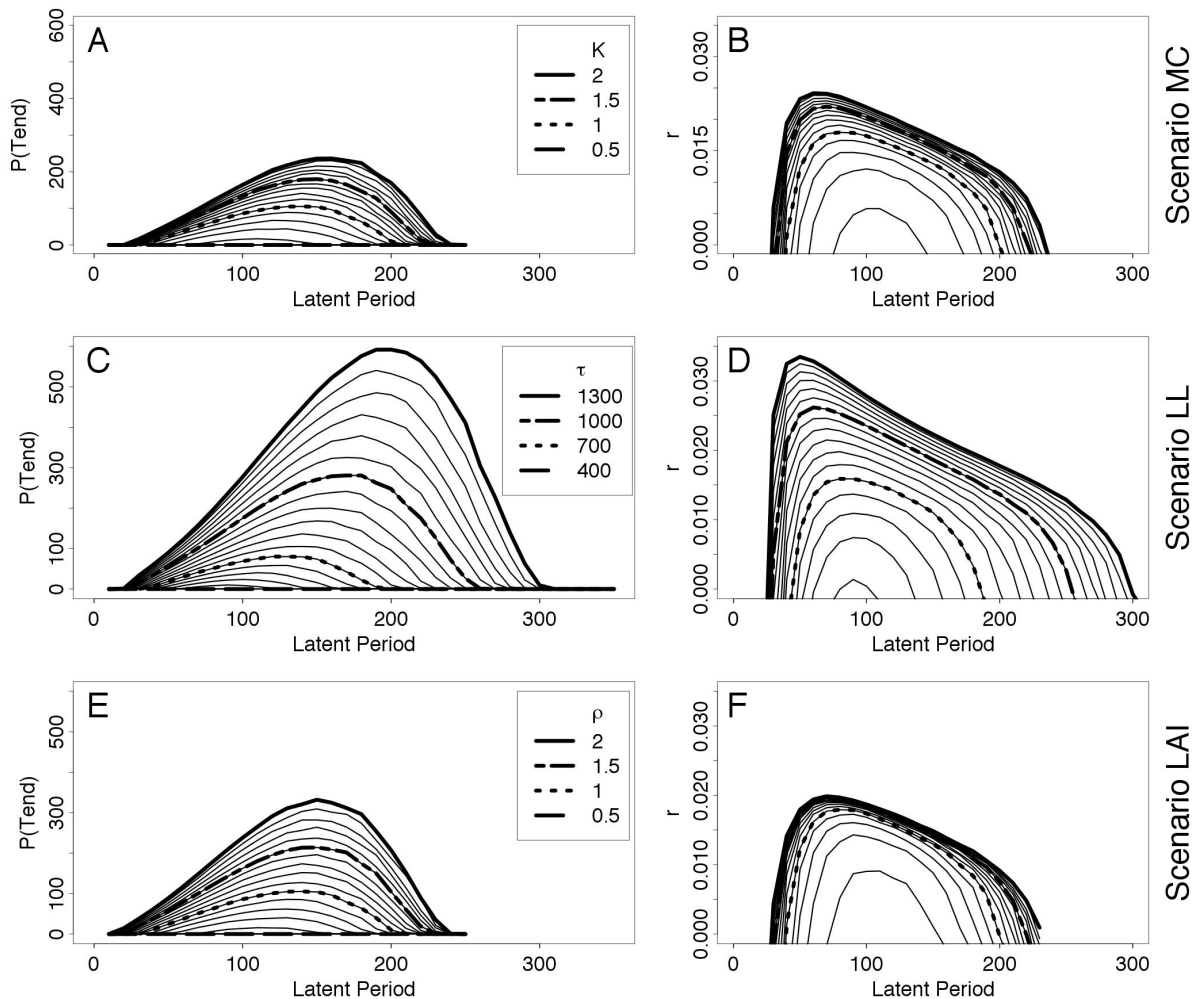


Figure 6: Fitness curves for range of fertilization and for two different fitness definitions. The summit of each curve indicates the optimal latent period. **A, C, and E**, Variation of total seasonal spore production $P(T_{end})$ with pathogen's latent period. **B, D, and F**, Variation of within-season exponential growth rate of the pathogen r with latent period (see equation 5 in the text for r calculation). K = patch resource carrying capacity, ρ = maximum patch creation rate, and τ = patch lifespan.

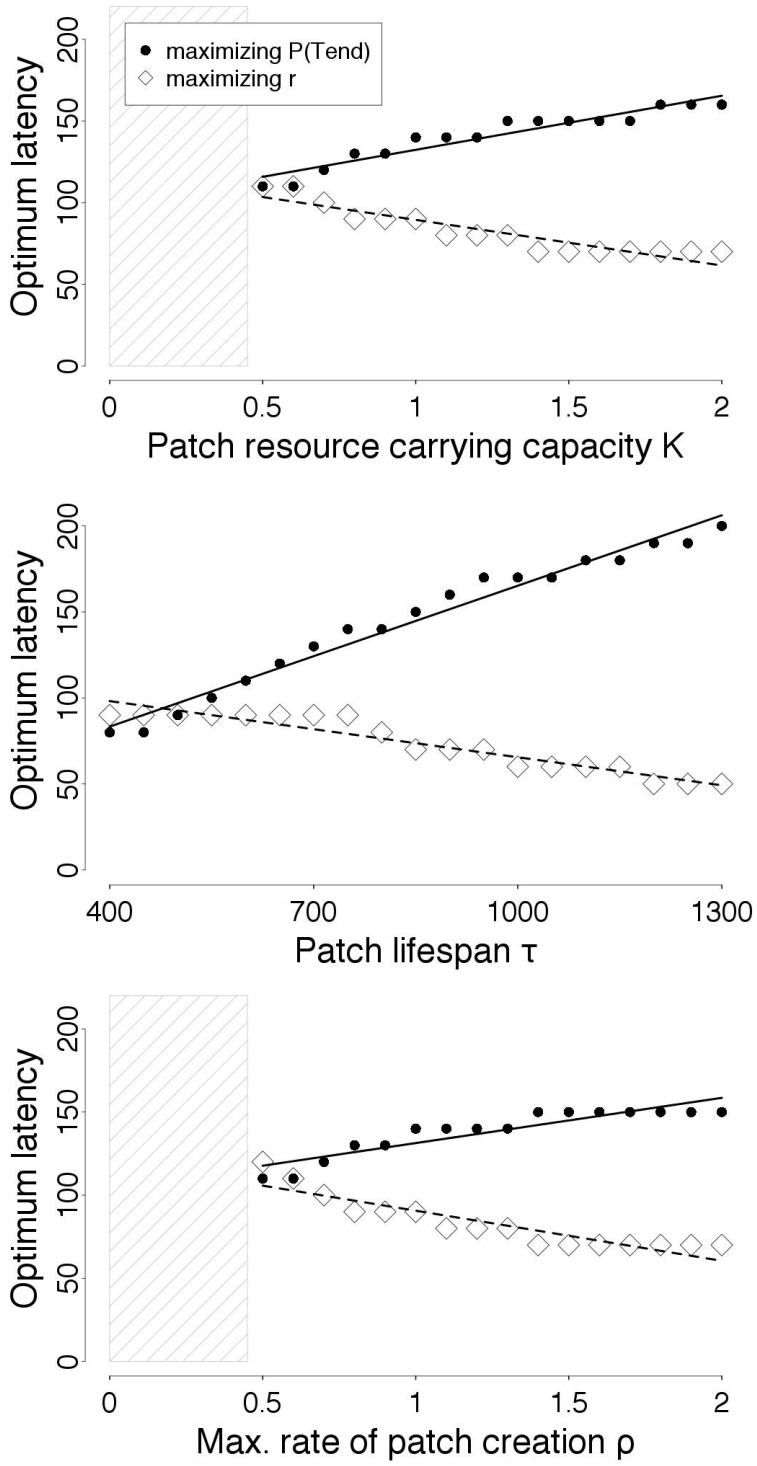


Figure 7: Variation of optimal latent periods with fertilization in the metabolite concentration (MC, upper panel), leaf lifespan (LL, middle panel), and leaf area index (LAI, lower panel) fertilization effects. Full circles and solid lines are optimal latent periods corresponding to seasonal spore production as a fitness measure. Open diamonds and dotted lines are optimal latent periods corresponding to within-season exponential growth rate as a fitness measure of the pathogen. Dots and diamonds correspond to maximum values of curves in Figure 6. Lines are linear regressions added for the sake of clarity. There are no sustainable epidemics in the striped areas of the parameter space. K = patch resource carrying capacity, ρ = maximum patch creation rate, and τ = patch lifespan.

DISCUSSION

Nitrogen fertilization is known to change crop physiology and architecture in three major ways by changing amount and/or dynamics of (i) within-leaf metabolites, (ii) leaf lifespan and (iii) number and size of leaves and tillers, hence modifying canopy size and architecture (Ferrise et al., 2010; Filella et al., 1995; Hinzman et al., 1986, Walters and Bingham 2007). We designed three modelling scenarios to study these three effects in our model. Each of these changes influences the quantity of host resource available to leaf pathogens. In our study, an increase in fertilization leads to an increase of resource quantity available for crop pathogens. We found that spores production and severity of epidemics are predicted to increase with fertilization for the three tested scenarios. This is consistent with many experimental studies (see for example Daamen et al., 1989; Jensen and Munk 1997; Kürschner et al., 1992; Lovell et al., 1997; Neumann et al., 2004; Olesen et al., 2003a; Robert et al., 2002, 2004; Walters and Bingham 2007).

We used two different fitness measures to identify the pathogen optimal latent period under different fertilization levels. When pathogen fitness is defined as the annual spore production, we found a positive relationship between optimal latent period and fertilization. On the contrary, when pathogen fitness is defined as the within-season exponential growth rate of the pathogen, we found a negative relationship between optimal latent period and fertilization. Depending on which fitness measure is best suited for the considered pathosystem and its environment, one can thus make different hypothesis regarding the consequences of reducing fertilization. Our study shows that change in fertilization practices may change pathogen life history, possibly altering aggressiveness profiles of the different pathogen species and strains.

Effect of fertilization on optimal latent period and consequences

One main result of our theoretical study is the establishment of a relationship between a pathogen's optimal latent period and fertilization. The optimal latent period is the latent period that maximizes pathogen fitness. It therefore indicates a putative direction of evolution of the latent period if the fertilization changes over the years. We used two different fitness

measures to predict the optimal latent period. We defined the optimal latent period as the value of the latent period maximizing either annual spore production at the epidemic scale (fitness defined as spore production over an entire season) or canopy colonization through several infection cycles (fitness defined as within-season exponential growth rate).

We argue that annual spore production could be an appropriate fitness measure in systems where the initial colonization of new fields (the next season) and overwintering are more limiting factors than within-season, between-strain competition. We found that this fitness measure tends to favor long latent periods (Figure 7) that have a high sporulation rate. Under low fertilization, we predict that strains with shorter latent periods will be positively selected, resulting in pathogens with shorter infection cycles. In terms of plant-pathogen interactions, the number of leaves that emerge per latent period (the so-called pathochron of Lovell et al., 2004) would decrease, leading to pathogens spreading upward more rapidly in the canopy, but producing fewer spores. By contrast, the within-season exponential growth rate could be an appropriate fitness measure in systems where between-strain competition is a more limiting factor than initial colonization. We found that this fitness measure tends to favor short latent periods (Figure 7) that have a short generation time and hence spread rapidly though the canopy. Under low fertilization, we predict that strains with longer latent period will be positively selected.

It is interesting to note that at high fertilization the two predicted optimal latent periods for either fitness measure strongly differ, suggesting there is room for multiple pathogen strains with different life history strategies. In such environments, the existence of distinct local maxima in the fitness landscape could indicate that fast colonizing strains (with short latent period) and more reproductive strains (longer latent period) may be able to co-occur. Pathogen subpopulations of *Erysiphe necator* and *Zymoseptoria tritici* with distinct latent periods have indeed been identified in the field by Montarry et al. (2008) and Suffert et al. (2015) respectively. On the contrary, at low fertilization, both fitness measures lead to similar predictions of the optimal latent period (Figure 7). This suggests that reducing crop fertilization may result in a greater homogeneity of pathogen populations in the field. This result is consistent with classical foodweb theory predicting a positive relationship between diversity and primary productivity (Loreau 1998, Tilman et al., 2001).

Data and optimal latent period

The data available in the literature show contrasting results on the relationship between latent period and fertilization treatment. On the one hand, Lecompte et al. (2010) showed that high nitrate nutrition of tomato increased latent period of the necrotrophic pathogen *Botrytis cinerea*. Similar results were obtained by Abro et al. (2013) for two strains of the same pathogen, alone or together with bio-control agents. On the other hand, Jensen (1995) showed that a reduction in nitrogen treatment on barley prolonged latent period of biotrophic *Erysiphe graminis*. These latter results are in the line of Bainbridge (1974), arguing that with more nitrogen, the generation interval of *Erysiphe graminis* was smaller. Lovell et al. (1997) observed a lag in the progression of *Zymoseptoria tritici* incidence in low-nitrogen and suggested that latent period should be shorter in high-nitrogen crops. These differences may reflect antagonistic host exploitation strategies of biotrophic and hemibiotrophic versus necrotrophic fungi. However these experiments show the physiological response of a fungal strain to different levels of fertilization but do not teach us anything about the optimal latent period. They cannot be used to test our results on the impact of fertilization on potential fungal adaptation.

Our predictions on the optimal latent period could be compared with observations of latent periods of pathogens that, for long periods, have infected crops cultivated under different levels of fertilization. In such cases, fungal populations could tend to be close to their evolutionary optimum for the local fertilization level. One could compare the distribution and the peaks of measured latent periods in these different fertilization conditions to estimate an empirical measure of the optimal latent period. Estimating experimentally the optimal latent period is rather difficult. We are not aware of such studies either in the field or in the greenhouse. Protocols in controlled conditions could be used to test whether pathogens adapt to the resource level of their environment, by comparing latent period and spore production of in vitro cultures of pathogen strains grown for many generations on agar complemented media at different resource levels or, even better, on plants grown with varied fertilization levels. Such protocols have been used by Alexander et al. (1985) and Lehman and Shaner (1997) to study adaptation of biotrophic pathogens *Uromyces appendiculatus* and *Puccinia recondita f. sp. tritici* to partially resistant bean and wheat cultivars respectively. Field measurements of latent periods and spore production in crops that have experienced different fertilization levels would also prove very interesting (but possibly confounded by

interactions with other environmental factors such as climate, initial inoculum, cultivars?). In this perspective, it is interesting to note that fertilization practices have changed a lot in western Europe after World War Two but that change has been more recent in eastern Europe where cereals culture still remains quite unchanged in some places. Measuring latent period and spore production for several varieties during several years in these different environments could allow us to test the hypothesis of evolving infection cycles under different fertilizations.

Our model predicts a fairly strong effect of the leaf lifespan on pathogen development and on the optimal latent period. This has previously been predicted in the wheat 3D modelling work done by Robert et al. (2008). Unfortunately there are only a few experimental data on this aspect. Yet few empirical studies have shown a negative effect of leaf age on pathogen lesion development (Farber and Mundt 2016). Our work suggests that the effect of leaf age could be explained by earlier senescence. Furthermore, Suffert et al. (2015) have shown that the latent period of the fungal population increases from winter to spring conditions. They propose that this variation is driven by seasonal fluctuations in environmental conditions. Our study suggests an alternative additional explanation: crop physiology. We hypothesize that this type of variation could impact which pathogen strain dominates in which part of the year. The competition between multiple pathogen strains is the subject of the next Chapter (Chapter 3).

Spore production under varied fertilization levels

In our model, we show that annual spore production increases with foliar resource concentration, leaf lifespan and canopy size (Figure 4). Over the explored area of the parameter space, spore production is most sensitive to canopy size and leaf lifespan. Several empirical data on spore production are consistent with our prediction of an increased spore production under higher fertilization level. At the leaf scale, Robert et al. (2004, 2006) established a positive correlation between leaf nitrogen content and spore production by *Puccinia tritici*. Increase of spore production with canopy size has also been observed (Daamen et al., 1989; Jensen and Munk 1997; Smith and Blair 1950). It was sometimes hypothesized that this increase could be linked to favorable microclimate. Our results show that increasing canopy size and the associated level of resource for the pathogen could play a role to explain this effect. From an epidemiological point of view, bigger canopies represent a

higher concentration of putative infection sites. In classic SIR models, there is always a minimum number of putative infection sites necessary for epidemic development (Heesterbeek 2002). We observe the same effect in our simulations under very low fertilization where no epidemic can develop due to insufficient canopy size (Figures 4D and F and 7, dashed area). We found a strong effect of patch lifespan on spore production. Until now, this has not been studied experimentally. In recent modelling studies, leaf lifespan has however been identified as a sensitive host parameter for determining disease severity of *Zymoseptoria tritici* (Garin et al., 2014; Robert et al., 2008).

Of the three different effects of fertilization we have considered, two are at the foliar scale (changing metabolites and senescence), one at the canopy scale. Different crops do not respond the same way to fertilization: wheat, barley and rice respond to fertilization first through their canopy size, while maize responds mainly by within leave nitrogen content (Robert et al., 2004; Savary et al., 1995). The theoretical framework we have developed should therefore allow comparing different species strategies.

Modelling choices and hypothesis

A major assumption in our model is that fertilization impacts pathogen development by increasing the level of resource available to the pathogen by increasing both the canopy size and the within leaf nutrient concentration. By doing so, we do not consider other possible processes that could be influenced by fertilization such as plant immunity and changes in microclimate due to variation in crop architecture (Walters and Bingham 2007). By changing canopy architecture, fertilization may impact spores dispersal (Garin et al., 2014; Gigot et al., 2014; Robert et al., 2008; Saint-Jean et al., 2004). Increasing leaves density can influence spores dispersal around a sporulating lesion. Bigger and more numerous leaves decrease distance between leaves possibly thus favouring local dispersal of the fungus (Garin et al., 2014). But within-canopy long distance dispersal could be reduced in denser canopies. These entangled antagonistic processes can be approximated in our model by making the dispersal parameter Δ (Table 1) dependent on the canopy density. Moreover, canopy architecture also influences microclimate that could impact lesion (Bernard et al., 2013) and disease development (Aust and Hoyningen-Huene 1986; English et al., 1989; Lemmens et al., 2004). For example, denser rice canopies are moister and likely more favourable to sporulation of the

hemibiotrophic rice blast agent *Pyricularia oryzae* (Kürschner et al., 1992). Here again, this might be included in the model by an effect on the infection strength (θ_{max} in Table 1).

Since many plant defense compounds contain nitrogen, especially anti-fungi protein effectors, one would expect a positive correlation between nitrogen fertilization and leaf concentration of defense compounds. The picture seems however more complicated (see review by Fagard et al., 2014). Although nitrogen starvation has been shown to increase rice susceptibility by reducing cell wall thickness and lignification (Matsuyama and Dimond 1973, Matsuyama 1975), it has also been shown to increase the concentration of leaf phenolic compounds and to lower the level of epidemics in wheat (Kiraly 1964). These contrasted empirical data support the hypothesis formulated by ecologists of a trade-off between plant growth and defense (Herms and Mattson 1992, Walters and Heil 2007). Including such trade-off in our theoretical framework is possible and would add biological realism. To do so, one possibility is to perform the analyses simulating more aggressive strains or more resistant plants dependent on fertilization level, by changing the resource conversion coefficients of the pathogen (c_M and c_S in Table 1) or its maximal uptake rate (I_{max}). This could test the hypothesis of Hoffland et al. (2000) suggesting that susceptibility of disease is the result of the source of nutrients available to the pathogens and the presence of secondary host metabolites.

In our study, we consider a sensitive cultivar. It is an interesting perspective to test how pathogens would behave with more resistant cultivars under varied fertilization. Performing similar analyses but changing the infection cycle parameters would give us an insight of possible interactions between host resistance and fertilization. In our model, we assume that all patches are equally susceptible to infection by the pathogen. But in the field, leaf susceptibility may decrease with leaf age and increase with leaf rank on the main stem (Farber and Mundt 2016). The existence of two separate scales in our model, the patch scale and the canopy scale, would make it easy to take such time-dependent susceptibilities into account.

Fungal crop epidemics are dependent on climatic and weather conditions. For instance, under warmer climate, leaf rust epidemics start earlier in spring, even in the fall (Duvivier et al., 2016; El Jarroudi et al., 2014). The current parametrization of our model simulates epidemics starting around late April (for Northern France, about 1000 dd post-

sowing in general) with a fungus that does not significantly hamper plant architecture (patch creation, Figure 4). This resembles an “average” epidemics currently occurring in north-western Europe. Although our model does not allow us to explicitly change weather and climatic conditions, we can simulate more favourable climatic scenarios by advancing the starting date of the infection parameter and/or the infection strength of patches.

Few studies have so far addressed the question of optimal resource allocation strategy of filamentous fungi. Using a modelling approach on saprophytic fungi, Gilchrist et al. (2006) found the optimal strategy for these organisms was to allocate 100% of the resource first into growth (during the latent period) then into reproduction. That strategy, that we use in our model, is common amongst holometabolous insects and annual plants growing in a “constant” environment (Cohen 1971, 1976). It has been named “bang-bang” strategy by Vincent and Pulliam (1980). By contrast, rust lesions on wheat leaves do not stop growing after the first uredia have broken through the epidermis. Lesions continue to spread laterally during the whole infectious period. We intend to relax this hypothesis in future versions of our model by allowing the mycelium to still get a fraction of the derived resource during the sporulating period using an alternative rule for energy allocation.

We studied two versions of the model with lesions maturation either at a fixed age or at a fixed size (Appendix of this chapter). Maturity occurs thus at a given age size or at a given size. In the second version of the model, the latent period is a variable that changes with resource level. Interestingly we observed that the latent period at the optimal size at maturation was nearly identical to the optimal latent period in the first model. In brief, assuming either a fixed age at maturation or for fixed size at maturation does not change our results.

CONCLUSION

Our modelling results suggest that effects of fertilization on within-leaf resource level, leaf lifespan, and canopy size all contribute to worsening biotrophic fungal epidemics in high fertilization by increasing the level of resource available to the pathogen. Depending on what fitness measure we use, we get contrasted results regarding the relationship of the optimal latent period with fertilization. We predict that high resource levels would allow more strains with different latent periods to coexist in the field than low resource levels. Since the optimal latent period changes with resource level, we expect that reducing fertilization will change the aggressiveness profiles of different biotrophic pathogen species or strains in the field. In the future, it would be interesting to generalize our results to other types of crop pathogens such as necrotrophs or hemibiotrophs.

APPENDIX: comparison of two maturation rules

In this appendix, we relax one of the major biological assumptions of our model. So far we have assumed that the pathogen matures at a given age, that is, the latent period has a fixed duration for a given pathogen. Here we study a version of the model in which the fungus matures at a given size rather than at a given age.

The evolution of maturation has long been studied in life history theory (Cole, 1954, Gadgil and Bossert, 1970). Two extreme cases are often recognized: either organisms mature at a given age, or at a given size. These extreme strategies sometimes coexist within populations of the same species, depending of their environment (Kawecki, 1993). The current view tends to consider that no organism matures at a given age or size, rather along an age-size trajectory in between these extreme cases (Stearns et Koella, 1986).

In the core of this paper, we presented what we call here the “Timer” version of our model. In the “Timer” version, maturity occurs at a given age, after the latent period has been completed. This is described by:

$$\frac{dM_i}{dt} = g(R_i, M_i, b_i) - \gamma_M M_i$$

with

$$g(R_i, M_i, b_i) = \begin{cases} c_M I_{max} \frac{R_i}{R_i + R_H} M_i^{2/3} & \text{if } 0 < b_i \leq \lambda \\ 0 & \text{otherwise} \end{cases}$$

where the mycelium growth rate, $g(R_i, M_i, b_i)$ is positive during the latent period λ and zero afterwards, and by:

$$\frac{dS_i}{dt} = \sigma(R_i, M_i, b_i)$$

with

$$\sigma(R_i, M_i, b_i) = \begin{cases} c_S I_{max} \frac{R_i}{R_i + R_H} M_i^{2/3} & \text{if } b_i > \lambda \\ 0 & \text{otherwise} \end{cases}$$

where the sporulation rate σ is zero during the latent period and positive afterwards (See Appendix 1 for more details about these equations).

In this version of the model, the latent period of the pathogen is a controlled parameter (λ). We can thus identify values of this parameter that maximize pathogen fitness measures (total annual spore production or within-season exponential growth rate). We named these values optimal latent periods.

To simulate size-dependent maturation, we assume that maturity occurs when the mycelium reaches a given size, denoted by M_S . We call this the “Sizer” version of the model. In this second version, the latent period is the time needed for the pathogen to reach the critical size for maturation. The equations above remain the same for the “Sizer” version, except that the latent period is now variable and depends indirectly on the mycelium growth rate and hence, in turn, on the resource level. Consequently, patches with different ages at infection, that typically have different resource levels by the time of their infection, will have different latent periods. In the canopy model, there is hence a distribution of latent periods. The unique optimal latent period of the “Timer” version does not exist anymore, but can be compared with the average latent period at the optimal mycelium maturation size M_S .

Figure S1 shows a comparison of the two versions of the model. The total annual spore production computed for either optimal strategy (either fixed-age or fixed-size) is nearly identical in the two versions of the model (Figure S1A). There is also a clear overlapping between the optimal latent period in the “Timer” version and the average latent period in the “Sizer” version (Figure S1B). These similarities suggest that optimizing either the latent period or the mycelium size at maturity results in the same resource exploitation strategy of the pathogen. Hence, we argue that assuming either a fixed age at maturation or for fixed size at maturation does not change our results.

The assumption of an age-dependent maturation of the pathogen may thus not be considered a strong modelling assumption.

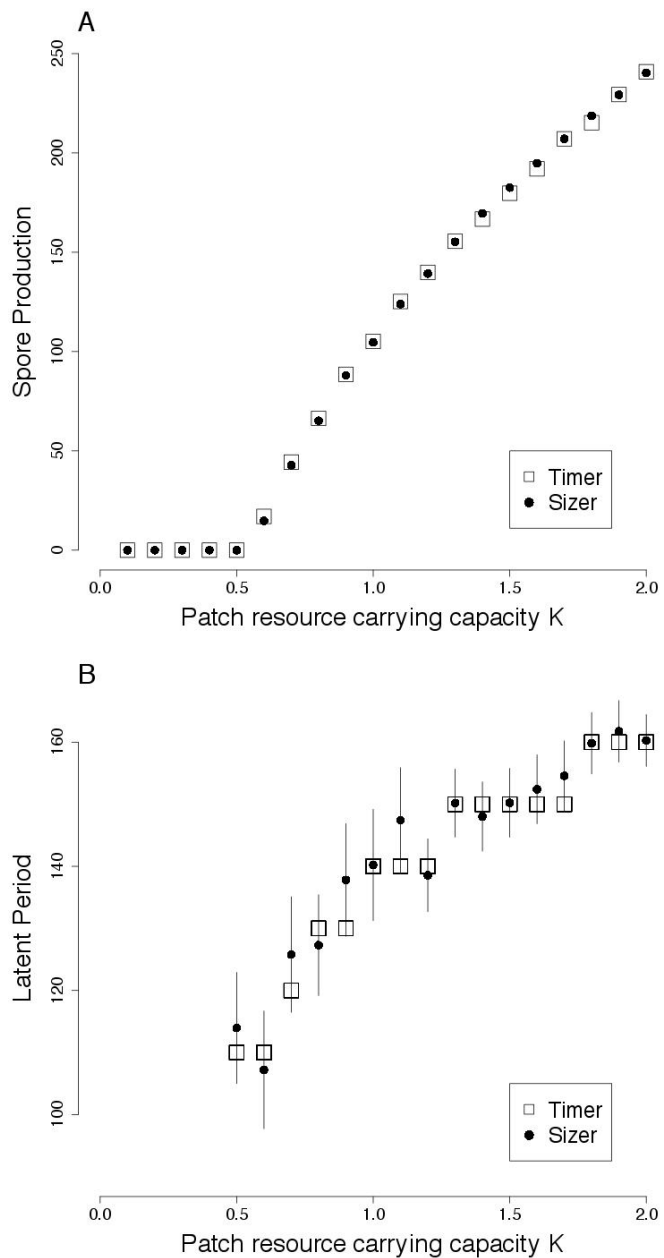


Figure S1. Comparison of fixed-size and fixed-age maturation rules. **A:** Annual spore production for different levels of patch resource carrying capacity K , and for the corresponding optimal maturation strategy. **B:** Optimal latent period for different levels of patch resource carrying capacity K . Empty squares represent the optimal latent period, i.e. the value of the parameter λ that maximizes spore production in the “Timer” version (results presented in Figure 7 of the main text). Filled circles represent the average latent period at the optimal mycelium maturation size in the “Sizer” version. Vertical bars represent standard deviations.

REFERENCES

1. *EBTtool*: Escalator Boxcar Train tool. <https://staff.fnwi.uva.nl/a.m.deroos/EBT/>
2. Abro, M. A. Nitrogen fertilization of the host plant influences susceptibility, production and aggressiveness of *Botrytis cinerea* secondary inoculum and on the efficacy of biological control. Agricultural sciences. Universite d'Avignon, 2013.
3. Abro, M.A., Lecompte, F., Bryone, F. & Nicot, P.C. Nitrogen fertilization of the host plant influences production and pathogenicity of *Botrytis cinerea* secondary inoculum. *Phytopathology* 103, 261-7 (2013).
4. Agrios, G. N. Plant Pathology, fifth edition, pp562-582. Academic Press (2005).
5. Alexander, H. M., Groth, J. V. & Roelfs, A. P. Virulence changes in *Uromyces appendiculatus* after fixed asexual generations on a partially resistant cultivar of *Phaseolus vulgaris*. *Phytopathology* 75, 449-453 (1985).
6. Aust, H & v. Hoyningen-Huene, J. Microclimate in relation to epidemics of powdery mildew. *Annual Review of Phytopathology* 24, 491-510 (1986).
7. Bainbridge, A. Effect of nitrogen nutrition of the host on barley powdery mildew. *Plant Pathology*, 23, 160?161 (1974).
8. Bernard, F., Sache, I., Suffert, F. & Chelle, M. The development of a foliar fungal pathogen does react to leaf temperature! *New Phytologist* 198, 232-240 (2013).
9. Biffen, R.H. Mendel's laws of inheritance and wheat breeding. *The Journal of Agricultural Science* 1, 4-48 (1905).
10. Büschbell T &, Hoffmann G.M. The effects of different nitrogen regimes on the epidemiologic development of pathogens on winter- wheat and their control. *Journal of Plant Diseases and Protection*, 99: 381?403 (1992).
11. Calonnec, A. et al. Impacts of plant growth and architecture on pathogen processes and their consequences for epidemic behaviour. *European Journal of Plant Pathology* 135, 479-497 (2013).
12. Cohen, D. Maximizing final yield when growth is limited by time or by limiting resources. *Journal of Theoretical Biology* 33, 299-307 (1971).
13. Cohen, D. On the Optimal Timing of Reproduction. *The American Naturalist* 110, 801-807 (1976).
14. Daamen, R. A., Wijnands, F. G., & van der Vliet, G. Epidemics of Diseases and Pests of Winter Wheat at Different Levels of Agrochemical Input. *Journal of Phytopathology*, 125, 305?320 (1989).
15. De Roos, A.M. A Gentle Introduction to Physiologically Structured Population Models. *Structured- Population Models in Marine, Terrestrial, and Freshwater Systems* 119-204 (1997).
16. De Roos, A.M. & Persson, L. Population and community ecology of ontogenetic development. *Monographs in population biology* 448 (2013).
17. Dordas, C. Role of nutrients in controlling plant diseases in sustainable agriculture. A review. *Agronomy for Sustainable Development* 28, 33-46 (2008).

18. Duvivier, M., Dedeurwaerder, G., Bataille, C., De Proft, M. & Legrèvre, A. Real-time PCR quantification and spatio-temporal distribution of airborne inoculum of *Puccinia triticina* in Belgium. *European Journal of Plant Pathology* 145(2), 405-420 (2016).
19. El Jarroudi, M., Kouadio, L., Delfosse, P. & Tychon, B. Brown rust disease control in winter wheat: I. Exploring an approach for disease progression based on night weather conditions. *Environmental Science and Pollution Research* 21, 4797-4808 (2014).
20. Engen, S. & Saether, B. Optimal allocation of resources to growth and reproduction. *Theoretical Population Biology* 46, 232-248 (1994).
21. English, J.T. Microclimates of Grapevine Canopies Associated with Leaf Removal and Control of Botrytis Bunch Rot. *Phytopathology* 79, 395 (1989).
22. Fagard, M. et al. Nitrogen metabolism meets phytopathology. *Journal of Experimental Botany* 65, 5643-5656 (2014).
23. Farber, D. & Mundt, C. Effect of Plant Age and Leaf Position on Susceptibility to Wheat Stripe Rust. *Phytopathology* (2016). doi: 10.1094/PHYTO-07-16-0284-R
24. Ferrise, R., Triossi, A., Stratonovitch, P., Bindi, M. & Martre, P. Sowing date and nitrogen fertilisation effects on dry matter and nitrogen dynamics for durum wheat: An experimental and simulation study. *Field Crops Research* 117, 245-257 (2010).
25. Filella, I., Serrano, L., Serra, J. & Penuelas, J. Evaluating wheat nitrogen status with canopy reflectance indices and discriminant analysis. *Crop Science* 35, 1400-1405 (1995).
26. Fraaije, B.A., Lovell, D.J., Coelho, J.M., Baldwin, S. & Hollomon, D.W. PCR-based assays to assess wheat varietal resistance to blotch (*Septoria tritici* and *Stagonospora nodorum*) and rust (*Puccinia striiformis* and *Puccinia recondita*) diseases. *European Journal of Plant Pathology* 107, 905-917 (2001).
27. Frezal, L., Robert, C., Bancal, M.-O. & Lannou, C. Local dispersal of *Puccinia triticina* and wheat canopy structure. *Phytopathology* 99, 1216-24 (2009).
28. Garin, G. et al. A modelling framework to simulate foliar fungal epidemics using functional-structural plant models. *Annals of Botany* 114, 795-812 (2014).
29. Garnica, D.P., Nemri, A., Upadhyaya, N.M., Rathjen, J.P. & Dodds, P.N. The Ins and Outs of Rust Haustoria. *PLoS Pathogens* 10(9): e1004329. doi:10.1371/journal.ppat.1004329.
30. Gigot, C., De Vallavieille-Pope, C., Huber, L. & Saint-Jean, S. Using virtual 3-D plant architecture to assess fungal pathogen splash dispersal in heterogeneous canopies: A case study with cultivar mixtures and a non-specialized disease causal agent. *Annals of Botany* 114, 863-875 (2014).
31. Gilchrist, M. a, Sulsky, D.L. & Pringle, A. Identifying fitness and optimal life-history strategies for an asexual filamentous fungus. *Evolution; international journal of organic evolution* 60, 970-979 (2006).
32. Greenhalgh, D. Hopf bifurcation in epidemic models with a latent period and nonpermanent immunity. *Mathematical and Computer Modelling* 25, 85-107 (1997).
33. Grover, J.P., 1997. Resource competition (Vol. 19). Springer Science & Business Media.
34. Haueisen, J. and Stukenbrock, E.H. Life cycle specialization of filamentous pathogens - colonization and reproduction in plant tissues. *Current Opinion in Microbiology* 32, 31-37 (2016).
35. Heesterbeek, J.A.P. A brief history of R₀ and a recipe for its calculation. *Acta Biotheoretica* 50, 189-204 (2002).

36. Heraudet, V., Salvaudon, L. & Shykoff, J.A. Trade-off between latent period and transmission success of a plant pathogen revealed by phenotypic correlations. *Evolutionary Ecology Research* 10, 913-924 (2008).
37. Herms, D. a & Mattson, W.J. The Dilemma of Plants: To Grow or Defend. *The Quarterly Review of Biology* 67, 283 (1992).
38. Hinzman, L.D., Bauer, M.E. & Daughtry, C.S.T. Effects of nitrogen fertilization on growth and reflectance characteristics of winter wheat. *Remote Sensing of Environment* 19, 47-61 (1986).
39. Hoffland, E., Jeger, M.J. & Beusichem, M.L. van Effect of nitrogen supply rate on disease resistance in tomato depends on the pathogen. *Plant and Soil* 218, 239?247 (2000).
40. Jensen, B. Nitrogen induced changes in the development of barley powdery mildew (*Erysiphe graminis* f.sp *hordei*). Copenhagen, Denmark: The Royal Veterinary and Agricultural University, PhD Thesis (1995).
41. Jensen, B. & Munk, L. Nitrogen-induced changes in colony density and spore production of *Erysiphe graminis* f.sp. *hordei* on seedlings of six spring barley cultivars. *Plant Pathology*, 46(2), 191?202 (1997).
42. Kilpatrick, R. A. New wheat cultivars and longevity of rust resistance, 1971-75. US Department of Agriculture. Agricultural Research Service. NE-64:1-20 (1975).
43. Kiraly, Z. Effect of nitrogen fertilization on phenol metabolism and stem rust susceptibility of wheat. *Journal of Phytopathology* 51, 252?261. (1964).
44. Koz?owski, J. Optimal allocation of resources to growth and reproduction: Implications for age and size at maturity. *Trends in ecology & evolution* 7, 15-9 (1992).
45. Kürschner, E., Bonman, J., Garrity, D. P., Tamisin, M. M., Pabale, D., & Estrada, B. A. Effects of nitrogen timing and split application on blast disease in upland rice. *Plant Disease* (1992).
46. Last, F. T. Some Effects of Temperature and Nitrogen Supply on Wheat Powdery Mildew. *Annals of Applied Biology*, 40(2), 312?322 (1953).
47. Last, F. T. Effects of nutrition on the incidence of barley powdery mildew. *Plant Pathology* (1962).
48. Lecompte, F., Abro, M.A. & Nicot, P.C. Contrasted responses of *Botrytis cinerea* isolates developing on tomato plants grown under different nitrogen nutrition regimes. *Plant Pathology* 59, 891-899 (2010).
49. Lehman, J.S. & Shaner, G. Selection of Populations of *Puccinia recondita* f. sp. *tritici* for Shortened Latent Period on a Partially Resistant Wheat Cultivar. *Phytopathology* 87, 170-176 (1997).
50. Lemmens, M. et al. The effect of inoculation treatment and long-term application of moisture on Fusarium head blight symptoms and deoxynivalenol contamination in wheat grains. *European Journal of Plant Pathology* 110, 299-308 (2004).
51. Li, M.Y. & Muldowney, J.S. Global stability for the SEIR model in epidemiology. *Mathematical Biosciences* 125, 155-164 (1995).
52. Loreau, M. Biodiversity and ecosystem functioning: a mechanistic model. *Proceedings of the National Academy of Sciences of the United States of America* 95, 5632-5636 (1998).
53. Lovell, D.J., Parker, S.R., Hunter, T., Royle, D.J. & Coker, R.R. Influence of crop growth and structure on the risk of epidemics by *Mycosphaerella graminicola* (*Septoria tritici*) in winter wheat. *Plant Pathology* 46, 126-138 (1997).

54. Lovell, D.J., Hunter, T., Powers, S.J., Parker, S.R. & Van Den Bosch, F. Effect of temperature on latent period of septoria leaf blotch on winter wheat under outdoor conditions. *Plant Pathology* 53, 170-181 (2004).
55. Matsuyama, N. The Effect of Ample Nitrogen Fertilizer on Cell-Wall Materials and its Significance to Rice Blast Disease. *Japanese Journal of Phytopathology* 41, 56-61 (1975).
56. Matsuyama, N. & Dimond, A.E. Effect of nitrogenous fertilizer on biochemical processes that could affect lesion size of rice blast. *Phytopathology* 63, 1202-1203 (1973).
57. McDonald, B. a & Linde, C. Pathogen population genetics, evolutionary potential, and durable resistance. *Annual Review of Phytopathology* 40, 349-379 (2002).
58. McIntosh, R. a & Brown, G.N. Anticipatory breeding for resistance to rust diseases in wheat. *Annual review of phytopathology* 35, 311-26 (1997).
59. Mendgen, K. & Hahn, M. Plant infection and the establishment of fungal biotrophy. *Trends in Plant Science* 7, 352-356 (2002).
60. Montarry, J., Cartolaro, P., Delmotte, F., Jolivet, J. & Willocquet, L. Genetic structure and aggressiveness of *Erysiphe necator* populations during grapevine powdery mildew epidemics. *Applied and Environmental Microbiology* 74, 6327-6332 (2008).
61. Naseri, R., Mirzaei, A., Soleimani, R. & Nazarbeygi, E. Response of Bread Wheat to Nitrogen Application in Calcareous Soils of Western Iran. 9, 79-85 (2010).
62. Neumann, S., Paveley, N.D., Beed, F.D. & Sylvester-Bradley, R. Nitrogen per unit leaf area affects the upper asymptote of *Puccinia striiformis* f.sp. *tritici* epidemics in winter wheat. *Plant Pathology* 53, 725-732 (2004).
63. Olesen, J.E., Jørgensen, L.N., Petersen, J. & Mortensen, J.V. Effects of rate and timing of nitrogen fertilizer on disease control by fungicides in winter wheat. 1. Grain yield and foliar disease control. *Journal of Agricultural Science* 140, 1-13 (2003).
64. Olesen, J.E., Jørgensen, L.N., Petersen, J. & Mortensen, J.V. Effects of rates and timing of nitrogen fertilizer on disease control by fungicides in winter wheat. 2. Crop growth and disease development. *Journal of Agricultural Science* 140, 15-29 (2003).
65. Pariaud, B., Van den Berg, F., Van den Bosch, F., Powers, S. J., Kaltz, O. & Lannou, C. Shared influence of pathogen and host genetics on a trade-off between latent period and spore production capacity in the wheat pathogen, *Puccinia triticina*. *Evolutionary Applications* 6, 303-312 (2013).
66. Parlevliet, J.E. Components of Resistance that Reduce the Rate of Epidemic Development. *Annual Review of Phytopathology* 17, 203-222 (1979).
67. Pringle, A. & Taylor, J.W. The fitness of filamentous fungi. *Trends in Microbiology* 10, 474-481 (2002).
68. Robert, C., Bancal, M.-O. & Lannou, C. Wheat leaf rust uredospore production and carbon and nitrogen export in relation to lesion size and density. *Phytopathology* 92, 762-8 (2002).
69. Robert, C., Bancal, M.-O. & Lannou, C. Wheat Leaf Rust Uredospore Production on Adult Plants: Influence of Leaf Nitrogen Content and *Septoria tritici* Blotch. *Phytopathology* 94, 712-21 (2004).
70. Robert, C., Bancal, M.-O., Ney, B. & Lannou, C. Wheat leaf photosynthesis loss due to leaf rust, with respect to lesion development and leaf nitrogen status. *The New phytologist* 165, 227-241 (2005).
71. Robert, C., Bancal, M.O., Lannou, C. & Ney, B. Quantification of the effects of *Septoria tritici* blotch on wheat leaf gas exchange with respect to lesion age, leaf number, and leaf nitrogen status. *Journal of Experimental Botany* 57, 225-234 (2006).

72. Robert, C., Fournier, C., Andrieu, B. & Ney ,B. Coupling a 3D virtual wheat (*Triticum aestivum*) plant model with a *Septoria tritici* epidemic model (Septo3D) : A new approach to investigate plant-pathogen interactions linked to canopy architecture. *Functional Plant Biology* 35, 997-1013 (2008).
73. Roff, D. A. 2002. Life history evolution. Sinauer Associates, Sunderland, Massachusetts.
74. Roumen, E.C. & Boef, W.S. de Latent period to leaf blast in rice and its importance as a component of partial resistance. *Euphytica* 69, 185-190 (1993).
75. Saint-Jean, S., Chelle, M. & Huber, L. Modelling water transfer by rain-splash in a 3D canopy using Monte Carlo integration. *Agricultural and Forest Meteorology* 121, 183-196 (2004).
76. Savary, S., Castilla, N. & Elazegui, F. Direct and indirect effects of nitrogen supply and disease source structure on rice sheath blight spread. *Phytopathology* 85, 959-965 (1995).
77. Setti, B., Bencheikh, M., Henni, J. & Neema, C. Comparative aggressiveness of *Mycosphaerella pinodes* on peas from different regions in western Algeria. *Phytopathologia Mediterranea* 48, 195-204 (2009).
78. Shaner, G. & Finney, R. E. The Effect of Nitrogen Fertilization on the Expression of Slow-Mildewing Resistance in Knox Wheat. *Phytopathology* 67, 1051-1056 (1977).
79. Shaner, G. & Finney, R.E. New sources of slow leaf rusting resistance in wheat. *Phytopath.* 70, 1183-1186 (1980).
80. Smith, H. C. & Blair, I. D. Wheat powdery mildew investigations. *Annals of Applied Biology* 37, 570. (1950).
81. Suffert, F., Ravigné, V. & Sachec, I. Seasonal changes drive short-term selection for fitness traits in the wheat pathogen *Zymoseptoria tritici*. *Applied and Environmental Microbiology* 81, 6367-6379 (2015).
82. Tilman, D. et al. Diversity and productivity in a long-term grassland experiment. *Science* (New York, N.Y.) 294, 843-845 (2001).
83. Van Den Berg, F., Robert, C., Shaw, M.W. & Van Den Bosch, F. Apical leaf necrosis and leaf nitrogen dynamics in diseased leaves: A model study. *Plant Pathology* 56, 424-436 (2007).
84. Vincent, T.L. & Pulliam, H.R. Evolution of life history strategies for an asexual annual plant model. *Theoretical Population Biology* 17, 215-231 (1980).
85. Walters, D.R. & Bingham, I.J. Influence of nutrition on disease development caused by fungal pathogens: Implications for plant disease control. *Annals of Applied Biology* 151, 307-324 (2007).
86. Walters, D. & Heil, M. Costs and trade-offs associated with induced resistance. *Physiological & Molecular Plant Pathology* 71, 3-17 (2007).
87. Xue, G. & Hall, R. Effects of surface wetness duration, temperature, and inoculum concentration on infection of winter barley by *Rhynchosporium secalis*. *Phytoprotection* 73, 61 (1992).

Chapter 3: Fertilization-triggered evolutionary changes in the latent period of leaf fungal pathogens at the scale of a crop field.

ABSTRACT

One conclusion of evolutionary ecology applied to the management of agroecosystems is that sustainable disease management strategies must be adaptive to overcome the immense adaptive potential of crop pathogens. In this context, knowledge of how pathogens will adapt to changes of cultural practices is power. In this paper, we address the question of biotrophic crop pathogens evolutionary response to changes in fertilization practices. Using the modelling framework from Précigout et al. (2017), we compare predictions of latent period evolution based on two “empirical” fitness measures (annual spore production and within-season exponential growth rate), with predictions based on the more rigorous concept of invasion fitness from adaptive dynamics. For the three main effects of fertilization on the pathosystem, we use pairwise invisibility plots to identify evolutionarily stable strategies of the latent period (ESS). The ESS responds differently to the different effets of fertilization. In such perspective, early canopy colonization during crop development might be a critical factor determining the issue of between-strain competition and shaping pathogen evolution.

INTRODUCTION

The development of sustainable agriculture requires to take into account pathogen adaptation to agricultural practices. In particular, one of the conclusions of the recent interplay between evolutionary ecology and plant pathology is that sustainable disease management strategies must be adaptive to overcome pathogen adaptation to agricultural practices (McDonald and Linde 2002, Gilligan 2008, Bousset and Chèvre 2013, Zhan et al., 2015). Theoretically, this implies manipulating the pathogens' fitness landscape to force them into patterns of disruptive selection. This could be achieved by bringing back high heterogeneity in agrosystems (cultivar mixtures, agrochemicals use mosaics, multi-species assemblages...) and making it change through space and time (McDonald and Linde 2002; Mundt 2002; Plantagenest et al., 2007; Parnell et al., 2009; Mundt et al., 2011; Djian-Caporalino et al., 2014; Mikaberidze et al., 2015; Zhan et al., 2015). Knowledge of the evolutionary responses of pathogens to cultural practices and of the trade-offs constraining their evolution is essential to design such scenarios.

In the previous chapters (Chapters 1 and 2, Précigout et al., 2017), we have developed a physiologically structured population model to identify putative evolutionary responses of leaf crop fungal pathogens' latent period to changes in crop fertilization regimes. In chapter 2, we have implemented three modelling scenarios, corresponding to major effects of increased nitrogen fertilization on wheat: (i) increase in nutrient concentration in leaves, (ii) increase of leaf lifespan, and (iii) increase of leaf number and size that leads to a bigger canopy size. For every scenario, we used two "empirical" fitness measures (resembling quantities measurable in the greenhouse or in the field), and their optimization, to identify putative evolutionary responses to changes in fertilization level in terms of adaptation of the latent period. The empirical fitness measures were (i) total spore production at the end of the crop growing season and (ii) the approximate, within-season exponential growth rate of the pathogen population (Chapters 1 and 2). The first fitness measure is a population-level extrapolation of the fitness measure derived theoretically by Gilchrist et al (2006) who have shown that in a model of a simpler structure, the correct fitness measure is the lesion-level total spores production. The second fitness measure is an attempt to account for the effect of the latent period on the generation time, by converting the lesion-level spores production into an estimate of the exponential population growth rate.

Using optimization of either of these fitness measures as a first approximation of the possible outcome of evolution, we have found that the evolution of the latent period is likely to be constrained by two trade-offs. The first trade-off concerns the optimal maturation strategy of the pathogen at the lesion scale in the case of finite availability of time and resource for completing its life cycle. In Chapter 1 we have shown that at the lesion scale the optimal maturation strategy is a compromise between using resources for juvenile growth and keeping resources for reproduction. This growth-reproduction trade-off leads to intermediate latent periods maximizing seasonal spore production and is similar to classical examples from life history theory (Stearns 1992, Roff 2002).

The second trade-off emerges from the pathogen's spread through the canopy. In our model, we can identify strategies with a relatively high lesion-scale spores production that are nevertheless ineffective at the canopy scale due to insufficient spread through the canopy. In such cases, earlier maturation (shorter latent period) results in a more rapid dispersal to the top of the canopy than late maturation despite a possibly lower lesion-scale sporulation rate (Chapter 1, cf. examples cited in Pringle and Taylor, 2002). This second trade-off also depends on the indirect effects of the pathogen's life history traits on the canopy-level population dynamics of the epidemics. In particular, the epidemics depend on the time between subsequent pathogen generations, which corresponds to the latent period. Thus a shorter latent period results in faster succession of generations and hence potentially faster population growth. This second trade-offs selects for low-intermediate latent periods.

We have defined the “optimal” latent period as the latent period that maximizes either of the above-mentioned fitness measures. In chapter 2, we have found a positive relation between the optimal latent period and fertilization when maximizing spore production at the end of the crop growing season. In contrast, we have found a negative relation between the optimal latent period and fertilization when maximizing the within-season exponential growth rate of the pathogen. These contrasting results were consistent over the three tested effects of fertilization on the pathosystem.

Both fitness measures used in the previous chapters were heuristic, *ad hoc* descriptors of the pathogen's evolutionary success, based on what traits we think to be important for epidemic development. There is however no consensus about how to define and measure fitness for leaf crop fungal pathogens and filamentous fungi in general (Pringle and Taylor

2002, Gilchrist et al 2006, Zhan and McDonald 2013), telling which of these empirical fitness measures is the most suited to describe the epidemiological system remains difficult. In this paper, we will compare model predictions based on these empirical fitness measures with predictions based on the more rigorous but empirically less tangible concept of invasion fitness from adaptive dynamics (Metz et al., 1992; Brännström and Festenberg 2006).

MATERIALS AND METHODS

Theoretical framework

In previous work (Chapter 1, Chapter 2, Précigout et al., 2017), we have developed a physiologically structured population model (PSP model) of a growing wheat crop and a biotrophic foliar fungal pathogen. We have used it to study the effect of a pathogen life history trait, the latent period on the disease development and on the pathogen. The model represents the within and between-seasonal dynamics of a growing wheat-like canopy. It provides the substrate for the dynamics of a rust-like polycyclic disease that feeds on the resources within the canopy's leaf tissue. The model was designed as a consumer-resource model with emphasis on the ecophysiological aspects we identified as important for epidemic development.

Hence, changes in (i) within-leaf metabolite concentration, (ii) leaf lifespan and (iii) canopy size represent three separate responses to changes in fertilization level. The first two ones correspond to changes in resource availability at the tissue scale (the basic entities of our model are patches, leaf fragments of the size of a rust lesion, about 0.1 cm^2). The last one corresponds to changes in canopy density (canopy is represented by the age-distribution of patches). We modelled these effects independently in three scenarios.

To simulate the effect of fertilization on within-leaf metabolite concentration (MC effect), we changed within-patch resource levels by artificially increasing or decreasing the patch resource carrying capacity K (see Précigout et al., 2017, Equation 1), e.g., the maximum amount of resources in the patches. This mimics the increased concentration of primary metabolites in leaves of more highly fertilized crops.

To simulate the effect of fertilization on leaf lifespan (LL effect), we artificially changed patch lifespan by varying the parameter τ (see Précigout et al., 2017, Equation 2): the longer the patch lives, the more resources it produces by photosynthesis. This mimics the increased leaf lifespan in leaves of more highly fertilized crops.

Finally, to simulate the effect of fertilization on the leaf area index (LAI effect), we changed the resource level at the canopy scale by changing the maximum patch creation rate

ρ (see Précigout et al., 2017 and Chapter 1, Equations 10, 15 and 16). This mimics the increase in leaf surfaces and tiller numbers in highly fertilized crops, which results in increased LAI.

Empirical fitness measures

In the first two chapters, we used two different fitness measures that we refer to as “empirical” fitness measures. The first one is the total spores production over an entire season, denoted $P(T_{end})$. It is calculated as the number of viable spores that remain at the end of the season (chapter 1, Equation 11).

The second one is the within-season exponential growth rate of the pathogen. It measures how fast the pathogen colonizes the healthy canopy at the beginning of the epidemics (see Précigout et al., 2017, Equation 5). The quantity LTR corresponds to the patch-level lifetime reproductive success, i.e. the participation of each patch in the model to the number of spores remaining at the end of the season. This second fitness measure takes into account the temporal aspect of the latent period and does hence favour strategies that have shorter generation times. This measure is particularly interesting since in our model, a race occurs between plant growth and canopy colonization by the pathogen. If the pathogen is not fast enough to keep up with canopy growth, the plant may escape the disease and die from natural senescence.

Invasion fitness

The third fitness measure we use is invasion fitness, as defined in adaptive dynamics (Metz et al 1992). This fitness measure is defined as the long-term (multi-annual) exponential growth rate of a second pathogen strain, referred to as a *mutant*, trying to invade into the system composed of the crop and the first strain, that is now referred to as the *resident* (Metz et al 1992). It requires the assumption that the mutant strain remains at a negligible population density during the invasion process, such that it does not exert any density dependence on the first strain (Geritz et al 1998). In our model, we obtain this condition by (artificially) assuming that the second strain does not influence the amount of healthy patches available for

infection. In other words, the dynamics of the mutant strain are enslaved by the dynamics of the resident strain. The interaction between the two strains occurs exclusively through the dynamics of available healthy patches, since we exclude multiple infections of single patches (which is a reasonable assumption given the size of patches). The healthy patch distribution hence represents the relevant environment (in the sense of Diekmann 2004, Metz et al 2008) for which competition between strains would take place.

Mathematically, the environment is defined as the distribution of healthy patches $h(t,a)$ (equations 5 and 6 in Chapter 1). The assumption that the mutant does not exert any density dependence on the environment therefore requires that the mutant population does not influence the dynamics of $h(t,a)$. The dynamics of the mutant are modelled identically to the resident's dynamics. We duplicate the equations describing the dynamics of the distribution of patches infected by the resident $n(t,a,b)$, see equation 7-9 (Chapter 1), in order to describe the dynamics of the mutant's distribution, denoted by $m(t,a,b)$. The assumption that the mutant does not exert any density dependence on the environment requires that (i) new infections created by mutant patches are not removed from the healthy canopy (equation 14, Chapter 1); and (ii) resources exported from patches infected by mutants do not influence the dynamics of the common resource pool $A(t)$ (equation 11, Chapter 1). In the absence of any density dependence, the dynamics of the mutant population distribution $m(t,a,b)$ are necessarily exponential, once the effect of initial conditions have dissipated. Any quantitative measure of the distribution $m(t,a,b)$ can then be used in order to estimate its exponential rate of growth or decline (Claessen 2012).

Invasion fitness of a mutant with latent period λ_2 invading into a resident with latent period λ_1 is computed as the log of the ratio of the mutant's annual spores production $P_2(T_{inoc})_y$ of two successive years (denoted by y and $y + 1$), once the system has settled in its steady state (and the mutant has reached exponential growth):

$$f(\lambda_2, \lambda_1) = \log \frac{P_2(T_{inoc})_{y+1}}{P_2(T_{inoc})_y}$$

where T_{inoc} is the quantity of spores capable of overwintering and starting the next year epidemic.

Analysis methods and simulations

The model was implemented using the Escalator Boxcar Train method (de Roos 1997) and the EBTtool software package (de Roos 2014), both designed to study the dynamics of physiologically structured population models. To determine optimal latent periods for every effect of fertilization, we carried out sensitivity analysis for each corresponding fertilization parameter (K , τ , and ρ representing MC, LL and LAI effects respectively, as defined in chapter 2). For any value of each fertilization parameter high enough to allow for epidemic development, the relation between all three fitness measures and the latent period presented a maximum value. We termed the inverse images of these maximum values the “optimal” latent periods. They are the values of the latent period maximizing the empirical fitness measures and thus represent putative evolutionary responses in case of change of fertilization level. In the presented Figures, optimal latent periods can only be a multiple of 10 because of the time scale of the EBTtool software package functioning.

In adaptive dynamics it is habitual to plot the fitness function in a so-called pairwise invisibility plot (PIP), which depicts the sign of the function $f(\lambda_2, \lambda_1)$ over the two trait axes λ_1 and λ_2 (Geritz et al., 1998). We present pairwise invisibility plots (PIPs) for a few selected values of each fertilization parameter.

RESULTS

Figure 1 presents the pairwise invisibility plots (PIPs) for different fertilization levels and different effects of fertilization. A single PIP represents the outcome of the invasion process between a resident and a mutant pathogen strain that are completely identical but in their latent period. For each value of the latent period λ_1 of the resident strain, it says which mutant strains with latent periods λ_2 are capable of invading the environment defined by the resident ($f(\lambda_2, \lambda_1) > 0$) and which are not. Note that a PIP does not show the outcome of between-strain competition since it is assumed the invader has no impact on density dependence. Following invasion, a mutant strain with positive invasion fitness may either coexist with the resident or replace it. The invasion fitness is necessarily zero along the diagonal where the resident and mutant strains have identical latent periods. The boundaries between area with positive and negative invasion fitness are called zero-isoclines. The invasion fitness is also zero along these curves. The intersection of a zero-isocline with the diagonal defines an evolutionarily singular strategy: points at which the selection gradient vanishes. Such singular points may be either attractive or repulsive (Geritz et al., 1998).

Considering any of the PIPs in Figure 1, we can deduce that starting from any resident population with $10dd < \lambda_1 < 200dd$, a trait-substitution sequence will result in convergence to the special point of λ^* . This special point is hence an evolutionary attractor of the adaptive dynamics, and is the equivalent of the optimal latent period for invasion fitness. In all the PIPs in Figure 1, the singular strategy corresponds to a fitness maximum since invasion fitness is negative both above and below the singular strategy. Theoretically, singular points that are both attractive and evolutionarily stable are referred to as Continuously Stable Strategies (CSS, Metz et al 1996). Yet since this terminology is relatively obscure, we will refer to them as Evolutionarily Stable Strategies (ESS).

Regarding the metabolite concentration (MC) effect, the PIPs are nearly identical for $K = 1, 1.5$ or 2 . Regardless of fertilization, the ESS latent period is $100 dd$ (Figure 1, upper row). For the leaf lifespan (LL) effect, the ESS increases with fertilization (middle row) and for the leaf area index (LAI) effect the ESS decreases with fertilization (lower row). The ESSs obtained from the PIPs in Figure 1 (and other PIPs not shown) have been plotted in Figure 2 alongside with the optimal latent period derived from the empirical fitness measures. Figure 2 allows for the comparison between the ESS and the optimal latent period obtained with the

empirical fitness measures. When pathogen fitness is defined as the annual spore production $P(T_{end})$, we find a positive relation between optimal latent periods and fertilization. By contrast, when fitness is defined as the within-season exponential growth rate of the pathogen, we find a negative relation between optimal latent periods and fertilization. These results are consistent for the three effects of fertilization tested (Figure 2, open and full circles). Considering the relation between ESS latent period and fertilization, we observe that the ESS is systematically in between the two first empirical fitness measures. Further, the ESS is rather insensitive to the level of fertilization.

As mentioned above, a PIP does not show the outcome of between-strain competition since it is assumed the invader has no impact on density dependence. Yet the invasion fitness concept can be used to infer conclusions about the scope for coexistence between two strains. The reason is that a minimal condition for global coexistence of two populations is that each strain can invade the steady state of the other one. In other words, *mutual invasibility* is a condition for coexistence. The PIP can hence be used to detect combinations of latent periods that can mutually invade each other's steady state. In adaptive dynamics, a useful tool to this end is the so-called “trait evolution plot” (TEP) (Metz et al 1996). It is a plot that synthesises at the same time the signs of the two fitness functions $f(\lambda_2, \lambda_1)$ and $f(\lambda_1, \lambda_2)$. Only combinations of latent periods for which both functions have positive sign correspond to pairs of mutually invading strains. In Figure 3, mutual invisibility of pairs (λ_1, λ_2) are coloured orange. The figure shows that mutual invisibility is extremely rare in our model. Coexistence is impossible at low fertilization (“Reference case” in Figure 3) and marginally possible at high fertilization for both effects of fertilization (Figure 3).

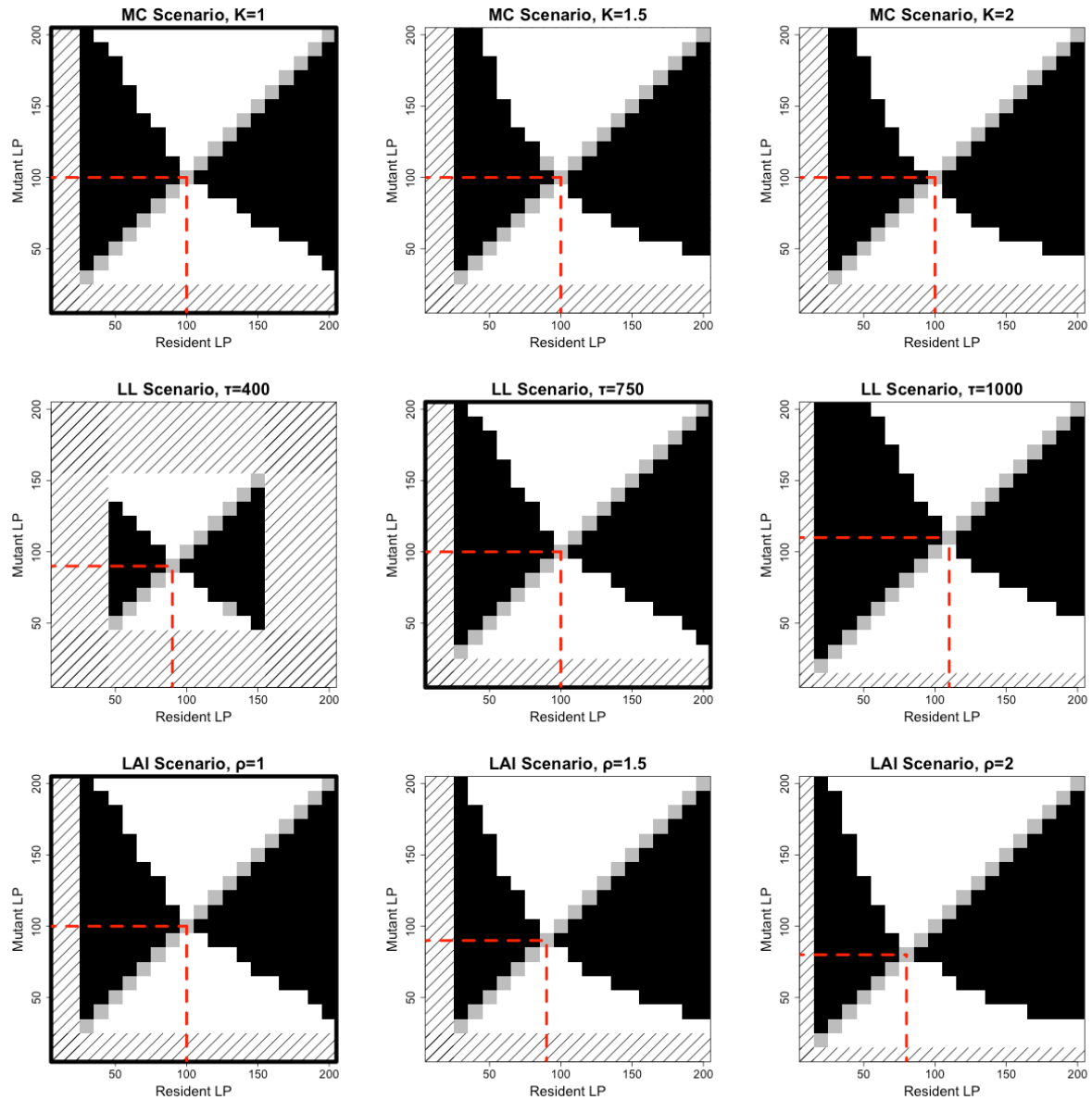


Figure 1: pairwise invisibility plots for three fertilization levels of each modelling scenario. Modelling scenarios correspond to the main effects of fertilization on the pathosystem. Upper line: “Metabolite Concentration” (MC) effect. Middle line: “Leaf Lifespan” (LL) effect. Lower line: “Leaf Area Index” (LAI) effect. Corresponding fertilization parameters (K , τ , and p respectively) increase from left to right. In black areas, mutants have a positive invasion fitness. In white areas, they have negative ones. The singular strategies are highlighted by dashed red segments. There are no sustainable epidemics in the dashed areas of the parameter space. Black boxes indicate standard parameter values in Précigout et al. (2017).

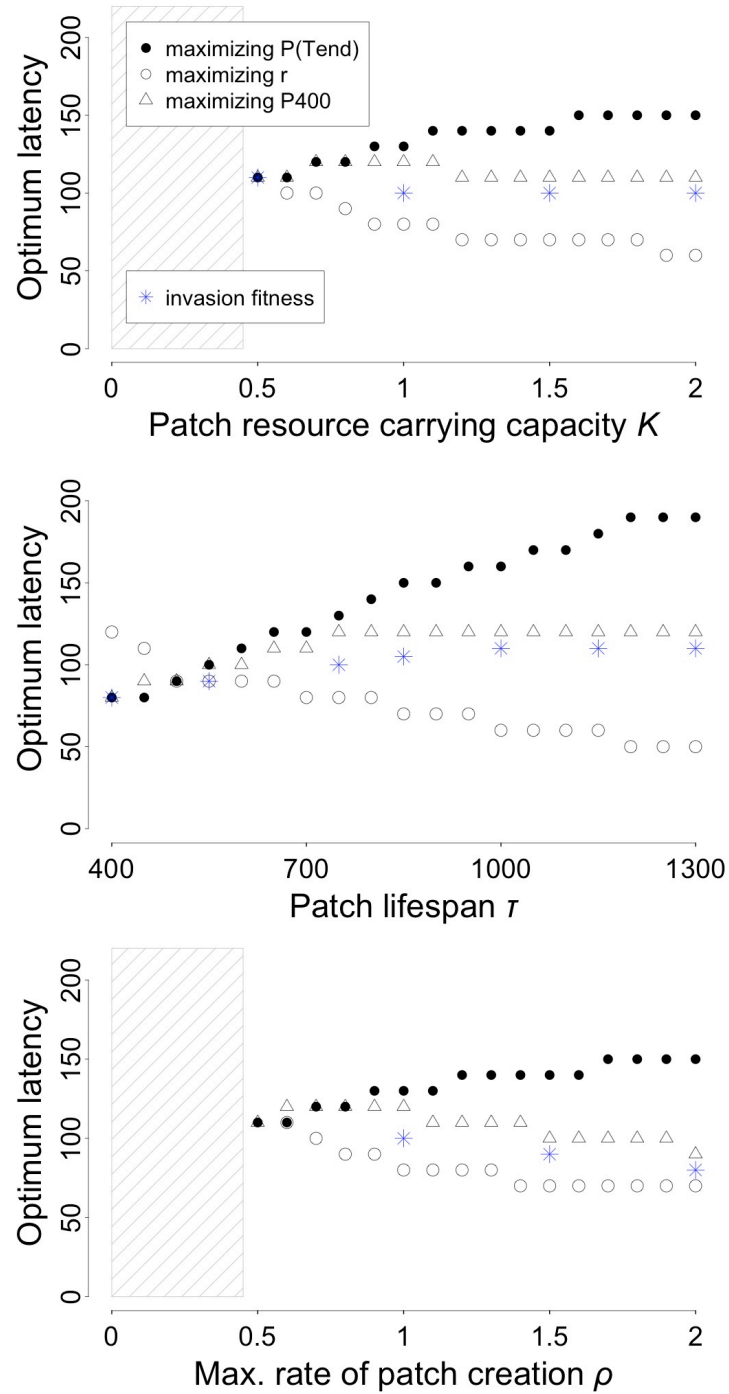


Figure 2: Variation of optimal latent periods and invasion fitness with fertilization for the metabolite concentration (MC, upper panel), leaf lifespan (LL, middle panel), and leaf area index (LAI, lower panel) effects. Full circles are optimal latent periods corresponding to seasonal spore production as a fitness measure. Open circles are optimal latent periods corresponding to within-season exponential growth rate as a fitness measure of the pathogen. Open triangles are optimal latent period corresponding to spore production at 400 dd as a fitness measure. Blue stars are invasion fitness and correspond to evolutionary singular strategies from Figure 1. There are no sustainable epidemics in the striped areas of the parameter space. K = patch resource carrying capacity, ρ = maximum patch creation rate, and τ = patch lifespan.

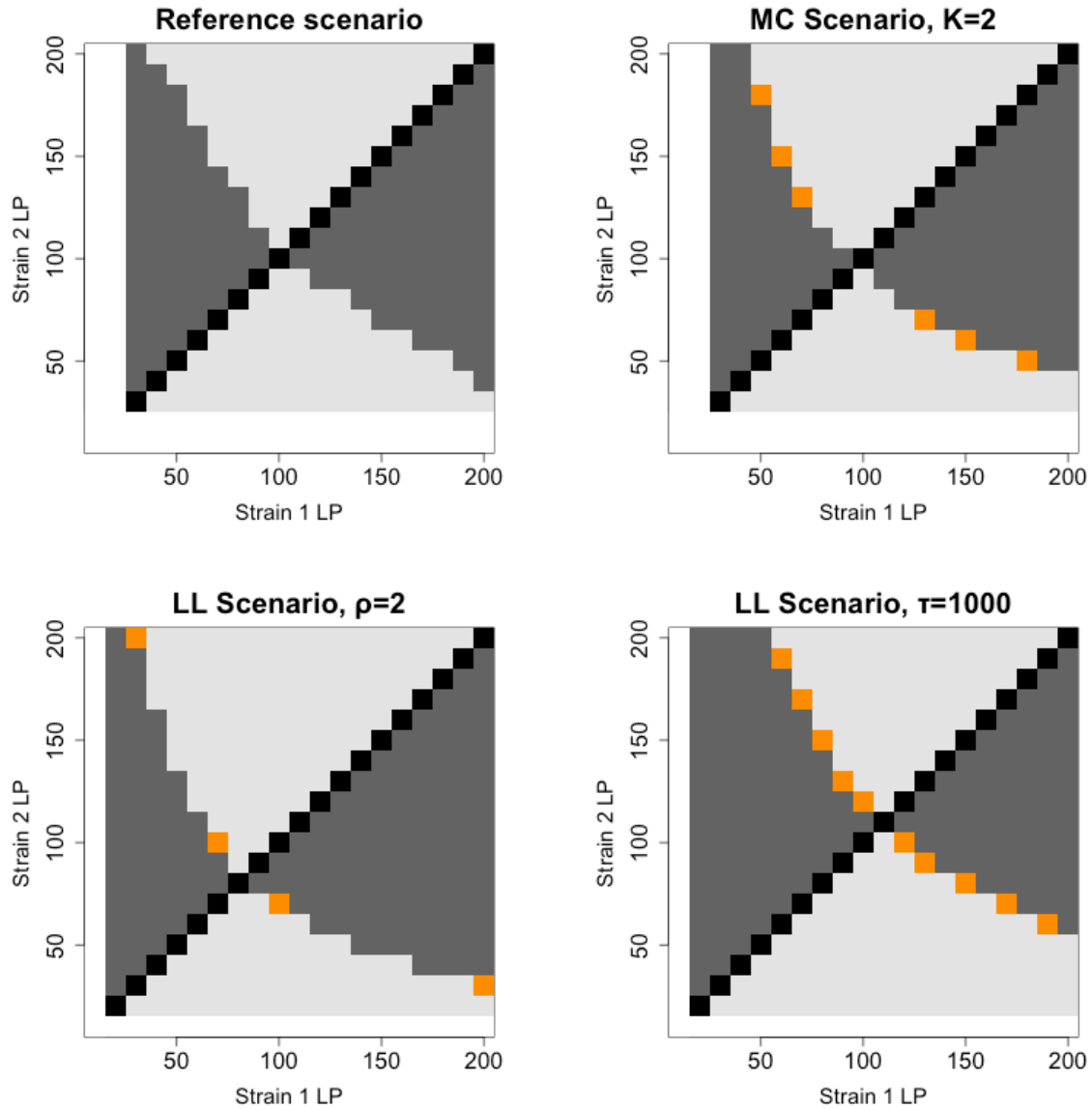


Figure 3: Graphical determination of the conditions for coexistence between two strains of pathogens. Strain 1 alone can survive in light grey areas. Strain 2 alone can survive in dark grey areas. In white areas, no strains are able to develop. Orange areas correspond to couples of latent period values allowing the two strains to coexist. Upper line: MC effect; Middle line: LL effect; Lower line: LAI effect. Left column: low fertilization level; right column: high fertilization level. K = patch resource carrying capacity, ρ = maximum patch creation rate, and τ = patch lifespan.

DISCUSSION

Using a previously developed epidemiological model of wheat rust epidemics (Chapter 1, Chapter 2, Précigout et al., 2017), we have studied the evolutionary response of such biotrophic pathogens to changes in their host's fertilization level. We use three modelling scenarios corresponding to the main effects of fertilization on the crop and three fitness measures to propose several possible evolutionary responses of the pathogen latent period to changes in fertilization regimes. Two of these fitness measures are called “empirical” fitness measures because they correspond to response variables potentially observable in experiments. They are : i) the total seasonal spore production and (ii) the within-season exponential growth rate of the pathogen population. The third one corresponds to the more theoretical invasion fitness from adaptive dynamics (Metz et al 1992). The objective of this chapter was to compare the predictions on the outcome of the evolution of the latent period based on the optimization principle, often used in classical evolutionary ecology (Stearns 1992, Roff 2002), applied to these two ad-hoc fitness measures (Chapter 2, Précigout et al 2017) with the more rigorous approach of adaptive dynamics.

Specifically, we are interested in how the different effects of fertilization on the pathosystem affect the evolution of the latent period and we have therefore focussed on the effect of fertilization on the optimal and ESS latent periods. Our results show that neither empirical fitness measure of seasonal spore production and of growth rate of the pathogen population gives the same answer as the adaptive dynamics approach based on invasion fitness. The ESS latent period is generally somewhere in between the latent periods that maximize either empirical fitness measure. That is, we can conclude that the ESS latent period does not maximize the total, seasonal spores production, nor the estimated within-seasonal exponential growth rate.

Theoretically, this is not really surprising since we know that, in general, the optimization principle gives the same answer as an invasion analysis only when the density-dependent interactions between competing strains can be characterized by a single (constant) number such as a single resource concentration (Mylius and Diekmann 1995, Metz et al 2008). In our model, the interaction environment is rather more complex, being the temporally fluctuating physiological distribution of susceptible crop patches. However the fact that we assume that the pathogen dynamics are characterised by a bottleneck passage in between years, during which the population is characterised by a single number (the amount

of spores inoculating next year's epidemic), does give some scope for a simple fitness proxy being maximized at the ESS.

It is therefore possible that another simple quantity is being maximized at the ESS, which could serve as an empirical fitness measure. Based on our experience with the model, and considering the different trade-offs at work during the epidemiological dynamics, we have learned that the dynamics are limited by both spores production and the ability to colonise the susceptible canopy structure. The two empirical fitness measures used so far are supposed to reflect these two opposite aspects. Based on our results, we can speculate that the ESS latent period finds a compromise somewhere in between in order to satisfy these different aspects.

A third empirical fitness measure

Based on these results we have designed a new empirical fitness measure that we thought may capture both aspects being like a compromise between the two first empirical fitness measures. This third empirical fitness measure is based on the idea that the growing season consists of two contrasting periods that pose different challenges to the pathogen: (1) the canopy-growth phase (from $T=0$ to 1500 dd) and (2) the fixed-canopy phase (from $T=1500$ to 2500 dd). During the first phase there is a dynamic aspect to pathogen progression since it has to keep up with the growing canopy: there is a vertical race between the canopy and the epidemics. If the pathogen is too slow, it will not colonize the green, upper part of the canopy and becomes overgrown by senescence from below. During the second phase the canopy is maximal and constant. Speed is hence of less importance during the second phase. And since the second phase is much longer than the first one, maximizing the total, annual total spores production may induce a bias towards strategies that are more successful during the second phase. This would thus reduce the importance of the dynamic aspect of the race. This is why we propose an additional empirical fitness measure that is the spores production during the early phase of the epidemic while the crop is still growing, in order to take into account the race between the crop and the epidemics. Not only would strains maximizing early spores production rapidly colonize the developing canopy, but they would also have a competitive advantage over less productive strains during the canopy colonization process. Here we briefly present some results based on the optimization of this new fitness measure,

defined as the spore production during the first 400 degree-days of the epidemics and denoted by P_{400} .

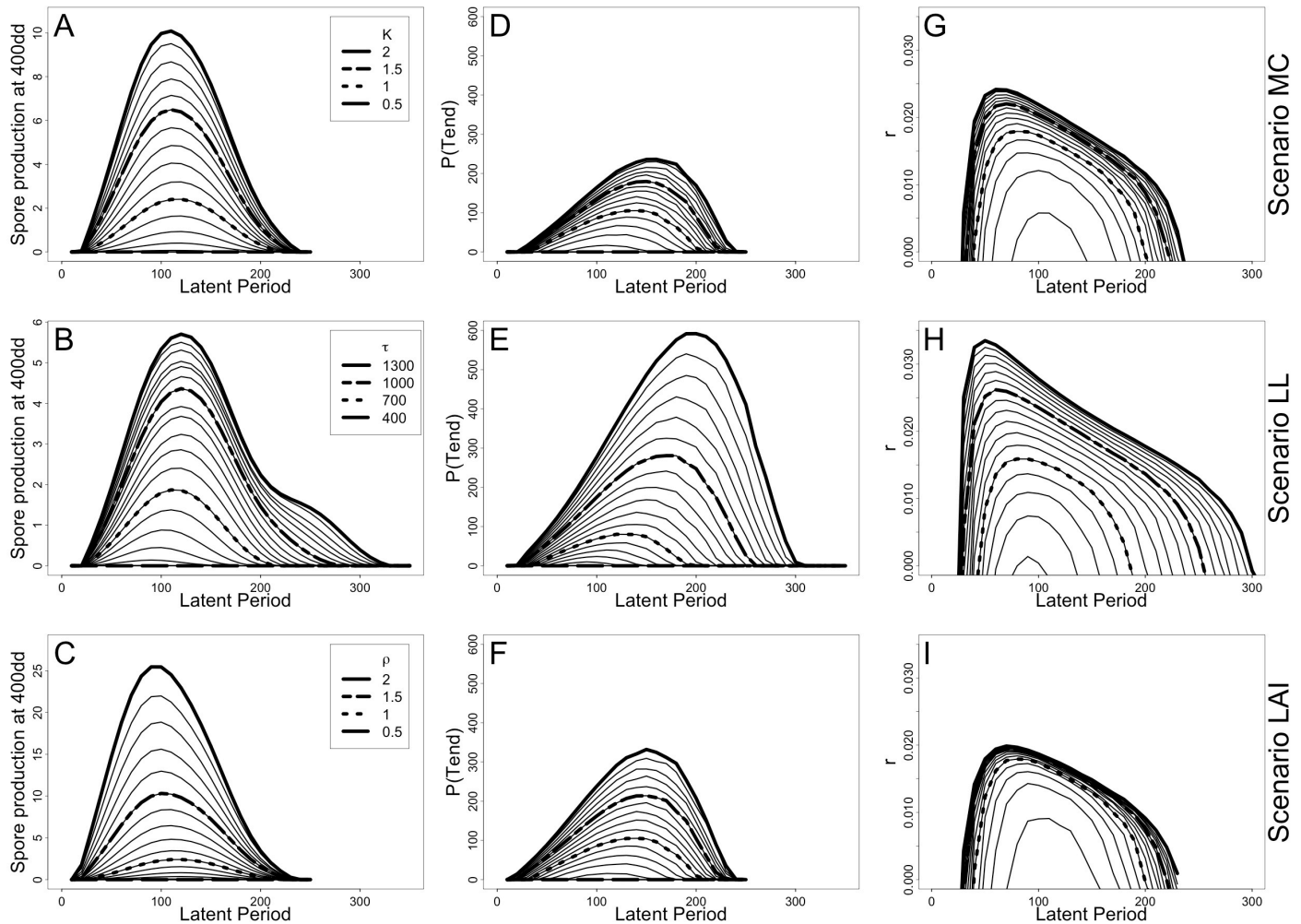


Figure 4: Fitness curves for range of fertilization corresponding to fitness measure s (spore produced at 400dd after the start of the epidemic). The summit of each curve indicates the optimal latent period. A: metabolite concentration (MC) effect. B: leaf lifespan (LL) effect. C: leaf area index (LAI) effect. K = patch resource carrying capacity, ρ = maximum patch creation rate, and τ = patch lifespan.

The impact of fertilization on P_{400} is shown in Figure 4, first column. For the three effects of fertilization, at every latent period, increasing fertilization increased spore production at 400dd. Epidemics are not sustainable if $K < 0.5$ and if $\rho < 0.4$ because spore production is not sufficient for enough spores to overwinter and create enough infection the next growing season. For a given resource level, epidemics cannot take place if the latent period is too short (10 to 30dd for both MC and LL effects, see Figure 4A and B) or too long

(more than 250dd for MC and LAI effects and more than 300dd for the LL effect). The optimal value of the latent period maximizing spore production at 400dd is intermediate between these two extreme cases.

As for the total annual spore production (Figure 4D, E and F and Chapter 2, Figure 6A, C and E) and the within-season exponential growth rate (Figure 4G, H and I and Chapter 2, Figure 6B, D and F) we find an optimal latent period that maximizes the fitness measure for the three effects of fertilisation (Figure 4A, B and C). We observe that the optimal value of the latent period for P_{400} is intermediate between the latent period maximizing the other two empirical fitness measures. But, interestingly, for this fitness measure only, the relation between the optimal latent period and fertilization depends on the effect of fertilization tested: optimal latent period does not change with the patch resource carrying capacity K (Figure 2A); it increases then levels-off with the patch lifetime τ (Figure 2B); and it decreases with the canopy growth rate ρ (Figure 2C). This suggests that the P_{400} fitness measure is more sensitive to environmental change than the two other empirical fitness measures.

Interestingly, this qualitative response of the optimum based on the P_{400} fitness measure (i.e., increase, decrease and/or no response to fertilization) is very similar to that of the ESS latent period (Figure 2). Quantitatively we observe that the optimal latent period is rather close to the ESS, with values that are 10 to 20 dd higher.

Conjecturing about pathogen latent period evolution in the field

Both ESS and P_{400} optimal latent periods present contrasted results depending on which effect of fertilization is considered. Regarding the metabolite concentration (MC) effect, we expect no evolutionary change of the latent period with a reduction of the fertilization level (Figure 2A). For the leaf lifespan (LL) effect, we expect the latent period to decrease with a reduction of the fertilization level (Figure 2B). In this case, decreasing the fertilization means reducing the leaf lifespan. This corresponds to canopies with more rapid leaf senescence, which should intensify the race between the plant and the pathogen for canopy colonization. It is then understandable that the pathogen will adapt to such increase by speeding up its infection cycle to keep pace with canopy development, hence decreasing its latent period. Finally, for the leaf area index (LAI) effect, the evolutionary response to a

decrease in fertilization is an increase of the latent period (Figure 2C). Decreasing the canopy growth rate has potentially the opposite effect to decreasing the leaf lifespan: it can slow down the race between the plant and the pathogen. This release could allow the pathogen to take more time to increase its spore production while keeping up with canopy development for tissue colonization. Decreasing the rate of canopy colonization would then allow for longer pathogen latent periods.

In the field, crops respond to changes in fertilization by changing their leaf area index, leaf lifespan and metabolite contents (Savary et al., 1995; Robert et al., 2004). Our results suggest opposite evolutionary responses of the latent period to these effects of fertilization. In this case, it would be difficult for the pathogen to adapt to changes in fertilization, and a likely outcome would be no detectable change in the latent period. However, since wheat responds to fertilization first by changing its canopy size (in particular by reducing the tillering), our results suggest that reducing fertilization could favour pathogen strains with a longer latent period. However, due to the contrasting results, an easy conclusion does not seem possible and an interesting perspective is to mimic a more realistic scenario of fertilisation with our model, accounting for the different effects at the same time. This may require including more realistic metabolite fluxes in the plant.

Evolutionary ecology: optimization or invasion analysis?

We have compared two different conceptual approaches that are both frequently used in evolutionary ecology: the optimization principle based on ad hoc fitness definitions, popular in life history theory (Roff 2002) and behavioural ecology (Stearns 1992), and an invasion analysis based on adaptive dynamics (Metz et al 2996). It is tempting to ask the question: which one is better? Which fitness definition should we use? While it is true that in adaptive dynamics fitness is rigorously defined, we argue that this does not necessarily mean that its fitness definition is more relevant than the so-called ad hoc fitness measures used in the optimization approach. The Achilles heel of fitness definitions in adaptive dynamics is that it all depends on how one chooses to model the density dependent interactions between competing strains. Had we chosen to model within-canopy competition differently, for instance by allowing for co-infection of patches, we could have obtained different results. Alternative assumptions such spatial dynamics, dispersal during the growing season,

additional host populations, a direct effect of lesions on photosynthesis, etc, are likely to influence the outcome. A second problem with invasion fitness is the difficulty to measure it in the field. We suggest that comparisons of these two approaches, invasion and old-fashioned “empirical” fitness measures, is an interesting way forward in this context. Identifying empirical fitness measures that seem consistent with invasion analysis gives us understanding of the fitness measures itself (in terms of the underlying dynamics) and can potentially provide testable predictions for field experiments.

CONCLUSIONS AND PERSPECTIVES

In this chapter we have used the model presented in Chapter 1 to study the evolutionary response of foliar biotrophic fungal pathogens to changes in their host's fertilization level. For this we have compared the predictions on the outcome of the evolution of the latent period based on the optimization principle, often used in classical evolutionary ecology, using three ad-hoc empirical fitness measures with the more rigorous approach of adaptive dynamics. We use three modelling scenarios and these four fitness measures to propose several possible evolutionary responses of the pathogen latent period to changes in fertilization regimes.

Interestingly, we found that the three empirical fitness measures give contrasting results, but that the ESS latent period is close to the latent period that maximises spores production in the early epidemics, while the crop is still growing. We found that the ESS latent period slightly changes with different effects of the fertilization-induced changes in lifespan and canopy growth rate. In order to test the robustness of our results, we propose to run similar analyses, but with varying dispersal distances (that would influence the race between the pathogen and the host), and/or the date of the epidemics onset (that would modify the length of the period with simultaneous epidemics and canopy growth), or/and the quantity of resource needed to produce spores. In particular, we will investigate (1) whether or not the ESS latent period is always close to the latent period that maximise the early spores production and (2) whether or not the changes in the responses of the ESS to fertilization depend on the effect of fertilization tested.

REFERENCES

1. Abang, M.M., Baum, M., Ceccarelli, S., Grando, S., Linde, C.C., Yahyaoui, A., Zhan, J., and McDonald, B. a (2006). Differential Selection on *Rhynchosporium secalis* During Parasitic and Saprophytic Phases in the Barley Scald Disease Cycle. *Phytopathology* *96*, 1214–1222.
2. Alstad, D.N., and Andow, D. a (1995). Managing the evolution of insect resistance to transgenic plants. *Science* (New York, N.Y.) *268*, 1894–1896.
3. Bousset, L., and Chèvre, A.M. (2013). Stable epidemic control in crops based on evolutionary principles: Adjusting the metapopulation concept to agro-ecosystems. *Agriculture, Ecosystems and Environment* *165*, 118–129.
4. Bourguet, D., Delmotte, F., Franck, P., Guillemaud, T., Reboud, X., Vacher, C., and Walker, A.S. (2010). The skill and style to model the evolution of resistance to pesticides and drugs. *Evolutionary Applications* *3*, 375–390.
5. Brännström, Å., Johansson, J., and von Festenberg, N. (2013). The Hitchhiker’s Guide to Adaptive Dynamics. *Games* *4*, 304–328.
6. Brown, S.P., Cornforth, D.M., and Mideo, N. (2012). Evolution of virulence in opportunistic pathogens: Generalism, plasticity, and control. *Trends in Microbiology* *20*, 336–342.
7. Clément, J.A.J., Magalon, H., Pellé, R., Marquer, B., and Andrivon, D. (2010). Alteration of pathogenicity-linked life-history traits by resistance of its host *Solanum tuberosum* impacts sexual reproduction of the plant pathogenic oomycete *Phytophthora infestans*. *Journal of Evolutionary Biology* *23*, 2668–2676.
8. Cowen, L.E., Kohn, L.M., and Anderson, J.B. (2001). Divergence in fitness and evolution of drug resistance in experimental populations of *Candida albicans*. *Journal of Bacteriology* *183*, 2971–2978.
9. De Roos, A.M. A Gentle Introduction to Physiologically Structured Population Models. *Structured-Population Models in Marine, Terrestrial, and Freshwater Systems* 119-204 (1997).
10. De Roos, A.M. & Persson, L. Population and community ecology of ontogenetic development. *Monographs in population biology* 448 (2013).
11. de Roos, A. M. 2014. EBTtool: Escalator Boxcar Train tool. Online publication. Institute for Biodiversity and Ecosystem Dynamics. <https://staff.fnwi.uva.nl/a.m.deroos/EBT/>
12. Diekmann, O. (2004). A beginner ’s guide to adaptive dynamics. *Mathematical Modelling of Population dynamics. Banach Center Publications*, 63:47–86.
13. Djian-Caporalino, C., Palloix, A., Fazari, A., Marteu, N., Barbary, A., Abad, P., Sage-Palloix, A.-M., Mateille, T., Risso, S., Lanza, R., et al. (2014). Pyramiding, alternating or mixing: comparative performances of deployment strategies of nematode resistance genes to promote plant resistance efficiency and durability. *BMC Plant Biology* *14*, 53.
14. Doumayrou, J., Avellan, A., Froissart, R., and Michalakis, Y. (2013). An experimental test of the transmission-virulence trade-off hypothesis in a plant virus. *Evolution* *67*, 477–486.
15. Engels, A.J.G., and de Waard, M. a. (1996). Fitness of isolates of *Erysiphe graminis* f.sp. *tritici* with reduced sensitivity to fenpropimorph. *Crop Protection* *15*, 771–777.
16. Fabre, F., Rousseau, E., Mailleret, L., and Moury, B. (2012). Durable strategies to deploy plant resistance in agricultural landscapes. *New Phytologist* *193*, 1064–1075.
17. Geritz, S.A.H., Kisdi, É., Meszéna, G., and Metz, J.A.J. (1998). Evolutionarily singular strategies and the adaptive growth and branching of the evolutionary tree. *Evolutionary Ecology* *12*, 35–57.

18. Gilchrist, M. a, Sulsky, D.L., and Pringle, A. (2006). Identifying fitness and optimal life-history strategies for an asexual filamentous fungus. *Evolution; International Journal of Organic Evolution* *60*, 970–979.
19. Gilligan, C.A. (2008). Sustainable agriculture and plant diseases: an epidemiological perspective. *Philosophical Transactions of the Royal Society B: Biological Sciences* *363*, 741–759.
20. Heraudet, V., Sauvadon, L. & Shykoff, J.A. Trade-off between latent period and transmission success of a plant pathogen revealed by phenotypic correlations. *Evolutionary Ecology Research* *10*, 913-924 (2008).
21. Kiyosawa S, 1982. Genetic and epidemiological modeling of breakdown of plant disease resistance. *Annual Review of Phytopathology* *20*,93–117.
22. Laine, A.L., and Barrès, B. (2013). Epidemiological and evolutionary consequences of life-history trade-offs in pathogens. *Plant Pathology* *62*, 96–105.
23. Lenski, R.E., and May, R.M. (1994). The evolution of virulence in parasites and pathogens: reconciliation between two competing hypotheses. *Journal of Theoretical Biology* *169*, 253–265.
24. McDonald, B.A., and Linde, C. (2002). Pathogen population genetics, evolutionary potential, and durable resistance. *Annual Review of Phytopathology* *40*, 349–379.
25. Metz, J.a.J., Nisbet, R.M., and Geritz, S.a.H. (1992). How should we define 'fitness' for general ecological scenarios? *Trends in Ecology & Evolution* *7*, 198-202.
26. Metz, J.A.J., Geritz, S.A.H., Meszena, G., Jacobs, F.J.A. & van Heerwaarden, J.S. 1996. Adaptive Dynamics, a geometrical study of the consequences of nearly faithful reproduction. In: *Stochastic and Spatial Structures of Dynamical Systems* (S. J. van Strien & S. M. Verdyen Lunel, eds), pp. 183–231. North Holland, Amsterdam, The Netherlands.
27. Metz JAJ, Gyllenberg M (2001) How should we define fitness in structured metapopulation models? Including an application to the calculation of evolutionary stable dispersal strategies. *Proc Roy Soc B-Biol Sci* *268*:499–508
28. Metz JAJ, Mylius SD, Diekmann O (2008) When does evolution optimize? *Evol Ecol Res* *10*:629–654
29. Mikaberidze, A., McDonald, B.A., and Bonhoeffer, S. (2015). Developing smarter host mixtures to control plant disease. *Plant Pathology* *64*, 996–1004.
30. Montarry, J., Hamelin, F.M., Glais, I., Corbi, R., and Andrivon, D. (2010). Fitness costs associated with unnecessary virulence factors and life history traits: evolutionary insights from the potato late blight pathogen *Phytophthora infestans*. *Bmc Evolutionary Biology* *10*, 283.
31. Mundt, C.C. (2002). Une of Multiline Cultivars and Cultivar Mixtures for Disease Management. *Annu. Rev. Phytopathol* *40*, 381–410.
32. Mundt, C.C., Sackett, K.E., and Wallace, L.D. (2011). Landscape heterogeneity and disease spread: experimental approaches with a plant pathogen. *Ecological Applications* *21*, 321–328.
33. Mykytowycz R. 1953. An attenuated strain of the myxomatosis virus recovered from the field. *Nature* *172*:448–49
34. Mylius, S.D., Diekmann, O., and Mylius, S.D. (1995). On evolutionarily stable life histories, optimization and the need to be specific about density dependence. *Oikos* *74*, 218–224.
35. Papaïx, J., Adamczyk-Chauvat, K., Bouvier, A., Kiêu, K., Touzeau, S., Lannou, C., and Monod, H. (2014). Pathogen population dynamics in agricultural landscapes: The Ddal modelling framework. *Infection, Genetics and Evolution* *27*, 509–520.

36. Pariaud, B., Van den Berg, F., Van den Bosch, F., Powers, S. J., Kaltz, O. & Lannou, C. Shared influence of pathogen and host genetics on a trade-off between latent period and spore production capacity in the wheat pathogen, *Puccinia triticina*. *Evolutionary Applications* 6, 303–312 (2013).
37. Parnell, S., Gottwald, T.R., van den Bosch, F., and Gilligan, C.A. (2009). Optimal strategies for the eradication of asiatic citrus canker in heterogeneous host landscapes. *Phytopathology* 99, 1370–1376.
38. Plantegenest, M., Le May, C., Fabre, F., Alabouvette, C., Olivain, C., Steinberg, C., Alexander, H.M., Thrall, P.H., Antonovics, J., Jarosz, A.M., et al. (2007). Landscape epidemiology of plant diseases. *Journal of the Royal Society, Interface / the Royal Society* 4, 963–972.
39. Précigout, P.-A., Claessen, D., and Robert, C. (2017). Crop Fertilization Impacts Epidemics and Optimal Latent Period of Biotrophic Fungal Pathogens. *Phytopathology PHYTO-01-17-001*.
40. Pringle, A., and Taylor, J.W. (2002). The fitness of filamentous fungi. *Trends in Microbiology* 10, 474–481.
41. Robert, C., Bancal, M.-O. & Lannou, C. Wheat Leaf Rust Uredospore Production on Adult Plants: Influence of Leaf Nitrogen Content and *Septoria tritici* Blotch. *Phytopathology* 94, 712–21 (2004).
42. Roff D. 2002. Life history evolution. Sunderland, MA: Sinauer.
43. Sapoukhina, N., Paillard, S., Dedryver, F., and de Vallavieille-Pope, C. (2013). Quantitative plant resistance in cultivar mixtures: Wheat yellow rust as a modeling case study. *New Phytologist* 200, 888–897.
44. Savary, S., Castilla, N. & Elazegui, F. Direct and indirect effects of nitrogen supply and disease source structure on rice sheath blight spread. *Phytopathology* 85, 959–965 (1995).
45. Sommerhalder, R.J., McDonald, B.A., Mascher, F., and Zhan, J. (2011). Effect of hosts on competition among clones and evidence of differential selection between pathogenic and saprophytic phases in experimental populations of the wheat pathogen *Phaeosphaeria nodorum*. *BMC Evolutionary Biology* 11, 188.
46. Stearns, S. (1992). *The Evolution of Life Histories*. Oxford ; New York: Oxford University Press.
47. Suassuna, N.D., Maffia, L.A., and Mizubuti, E.S.G. (2004). Aggressiveness and host specificity of Brazilian isolates of *Phytophthora infestans*. *Plant Pathology* 53, 405–413.
48. Walters, D., and Heil, M. (2007). Costs and trade-offs associated with induced resistance. *Physiological & Molecular Plant Pathology* 71, 3–17.
49. Zhan, J., Yang, L., Zhu, W., Shang, L., and Newton, A.C. (2012). Pathogen populations evolve to greater race complexity in agricultural systems - evidence from analysis of *Rhynchosporium secalis* virulence data. *PLoS ONE* 7.
50. Zhan, J., and McDonald, B.A. (2013). Experimental Measures of Pathogen Competition and Relative Fitness. *Annual Review of Phytopathology* 51, 131–153.
51. Zhan, J., Thrall, P.H., Papaix, J., Xie, L., and Burdon, J.J. (2015). Playing on a Pathogen's Weakness : Using Evolution to Guide Sustainable Plant Disease Control Strategies. *Annu. Rev. Phytopathol.* 53, 19–43.

Chapter 4: Influence of crop fertilization strategies at the landscape-scale on epidemiology and evolution of leaf fungal pathogens.

ABSTRACT

In this work, we address the question of the impact of crop fertilization practices at the landscape scale on the epidemiology and evolution of leaf fungal pathogens. For this we develop a model of landscape epidemiology. The landscape is depicted as a mosaic of individual fields, with either high or low fertilization and a corresponding crop dynamics. At the landscape scale, fields function like a meta-population of pathogen resource patches and are linked together through pathogen dispersal. Within each individual field, the development of the pathogen follows a classical SEIR epidemiological model. We have found that when pathogen maladaptation is possible (i.e. if a pathogen strain with a given latent period is significantly less competitive in some resource environments than in others), high aggregation landscapes and heterogeneous landscapes dominated by low fertilization patches reduce the quantity of inoculum released in the landscape and slow down the colonization of the landscape by the pathogen. These effects of maladaptation vanish when pathogens adapt to their new environment. In our model, the coexistence of two strains with different latent periods is possible and evolutionarily stable: in response to spatial fertilization heterogeneity, pathogens may undergo a process of evolutionary branching to fill the available niches in the landscape.

INTRODUCTION

The first three chapters have focused on modelling the effect of fertilization on epidemiology and evolution of fungal foliar crop pathogens at the field scale. Although the impact of nitrogen fertilization on crop fungi epidemics remains sometimes unclear (Buschbell and Hoffman, 1992; Hoffland et al., 2000; Oselen et al., 2000), many empirical and theoretical studies have shown that fertilization worsens epidemics in the field (see for example Shaner and Finney, 1977; Leitch and Jenkins, 1995; Simon et al., 2003; Walters and Bingham, 2007; Robert et al., 2008; Lecompte et al., 2010; Abro et al., 2013). In the previous chapters, using a physiologically structured population model of wheat rust epidemics, we have shown that such positive effects on epidemics can be explained by crop the availability of crop resources to the pathogen: the more the plant gains from fertilization, the more resources it represents for the pathogen to exploit in terms of both metabolite content and available tissue to colonize (Précigout et al., 2017). Decreasing fertilization should then theoretically limit pathogen incidence and reduce epidemics. In Chapter 3, we have shown several possible evolutionary outcomes of pathogen adaptation to changes in fertilization practices at the scale of a crop field. All suggest that the benefits of such a reduction could sooner or later be overcome, to some extent, by pathogen adaptation to their new less resource-rich environment. Interestingly, we have shown that the potential direction of evolution would vary according to the fitness definition such as annual spore production or rate of colonization of the canopy. On the one hand, it can be hypothesized that annual spores production is of importance when external inoculum or winter survival are limiting epidemics. On the other hand the canopy colonization rate could dominate if the within-seasonal spores production is limited and competition for green leave area is determinant for between-strain competition. These environments could therefore depend on the epidemiology around the concerned field: quantity of spores arriving in the field, in the beginning of the season or during the season should indeed depend on the epidemiology in the neighbouring fields. In this chapter we therefore ask the same question, but changing the considered spatial scale, changing from the field to the landscape scale.

A growing number of studies at the crossroads between landscape ecology and epidemiology now advocate that designing both productive and more sustainable cultural practices requires shifting the scale of crop protection from the field to the landscape and from short-term solutions to mid- to long-term ones (Holdenrieder et al., 2004; Plantagenest et al., 2007; Fabre et al., 2012; Zhan et al., 2013, 2015). At these broader scales, crop fields are not independent but rather constitute a meta-population of more or less susceptible hosts connected through pathogen dynamics and dispersal (Park et al., 2001; Burdon and Thrall, 2000, 2014; Papaïx et al., 2014a). By influencing pathogen dispersal and inoculum production, landscape architecture and heterogeneity influence population size and gene flow between pathogen populations, ultimately altering both pathogens' epidemiology and evolution (Skelsey et al., 2010; Jones et al., 2011; Papaïx et al., 2013, 2014b, 2015; Burdon et al., 2016). This has led to the idea that pest-suppressive agrosystems could be designed through cultural practices management at the landscape scale, either by impeding pathogen reproduction and dispersal or by reducing their adaptive potential (Plantagenest et al., 2007; Skelsey et al., 2010). This approach especially goes for agroecology, where interactions between species are levers to reach natural self-regulation of pest populations in agroecosystems (Nicholls and Altieri, 2004).

In this chapter, we address the question of the impact of crop fertilization practices on the epidemiology and evolution of leaf fungal pathogens at the landscape scale. In an agroecological perspective, we wish to investigate how the disease will respond to a decrease in crop fertilization but also to landscape heterogeneity in terms of fertilization levels. The basic idea is to test the effect of spatial heterogeneity of practices in order to control disease, focusing on fertilisation practices. We aim to model how landscape heterogeneity affects rust-like epidemics and their evolution. This raises the question of defining fitness for fungal crop pathogens in a heterogeneous landscape. Understanding the relation between fertilization heterogeneity and epidemics, we seek landscape configurations that limit pathogen development or cause pathogen maladaptation, as exemplified by Alstad and Andow (1995), Sapoukhina et al., 2013 or Papaïx et al. (2014a) for crop resistance breakdown.

To do this, we use a mathematical model of wheat rust epidemics at the landscape scale. This model is inspired by the more detailed theoretical framework presented in chapters 1 to 3. It comes with a simplification of the host-pathogen interaction (especially canopy growth and canopy infection have been greatly simplified) and retains only epidemiological

features of the pathosystem that are key to this change of scale. The key feature that has been used to design the field-to-landscape model is the trade-off occurring between pathogen spore production and latent period that emerges at the canopy scale (Précigout et al., 2017). The model in this chapter encompasses two scales: the field unit and the landscape. Within field-dynamics are modelled within each field (without any spatial structure), whereas the landscape-scale dynamics emerge from the connection of fields by dispersal. Heterogeneity at the landscape scale is modelled by allowing each field to have either low or high fertilization level. Different types of landscapes can be created by changing either the proportion and/or the aggregation of patches types. We focus on the colonization rate though the landscape by the pathogen, spore production and crop loss to compare epidemics at the field scale and at the landscape scale. We further identify evolutionary responses of pathogens to fertilization practices using invasion analysis from adaptive dynamics.

MATERIALS AND METHODS

Here we present the model we designed to study the epidemiological and evolutionary responses of a crop fungal pathogen to changes in fertilization regimes at the landscape scale. The model was parameterized according to biological knowledge on the wheat-rust pathosystem and previous results from Précigout et al. (2017). Although the model was made to resemble the wheat rust pathosystem, we believe it is generic enough to apply to other cereal-fungi pathosystems as well. We describe the landscape as a meta-population of crop fields. In practice, a 33-by-33 patch grid makes up the landscape. The grid is a torus to avoid boundary effects. Each patch on the grid represents a crop field with a given fertilization level. In the former three chapters, we have identified three major effects of fertilization on the pathosystem: fertilization increases (i) the within-organ metabolite concentration, (ii) the leaf lifespan and (iii) the size of crop canopy and its growth rate. As a means to simplify the host-pathogen biology to suit our needs for modelling at this wider scale, we kept only an effect of fertilization on overall canopy size. The main variable describing seasonal crop dynamics is then the green leaf area index (gLAI). To each fertilization level corresponds a dynamic of crop canopy, in terms of a canopy growth rate and a canopy final size that represent the combined effects of fertilization on the gLAI. As in our previous work, the focus of the model is on the consumer-resource aspect of the plant-pathogen interaction: the gLAI represents the amount of resources available to the pathogen in terms of susceptible tissue to colonize. From the previous model, we also keep the ecological trade-off between latent period and spore production. Whereas the trade-off emerged as a result in the former model (Chapters 1), in the present model we impose it an assumption. We assume that at the field scale the pathogen spore production rate is a direct function of the latent period, such that spore production at the patch scale is maximum at intermediate latent period. The within-field infection dynamics follow a classical SEIR epidemiological model. At the landscape scale, patches are inter-connected via air-borne spore dispersal.

Within-patch dynamics of canopy functioning and pathogen development

Patches are the elementary components of our landscape model. Each individual patch on the landscape grid represents a single (wheat) field. The dynamics of crop growth and

epidemic development are implemented at the patch scale. Time is considered discrete in the model. Seasons are indexed by t and within-season time intervals by k . A growing season starts at k_{start} which represents the sowing date of the crop. The growing season is k_{end} long. Crop harvesting and the cropless period are modelled as an instantaneous projection from k_{end} to the start of the next year.

To use the same terminology as SEIR models, susceptible host tissue is termed S , infected yet non-infectious tissue (“exposed”) is noted E , sporulating tissue (“infectious”) I and senescent tissue (“removed”) R . In our model, the quantities S , E , I and R thus refer to a field’s canopy surface area that is, respectively, susceptible, latent, sporulating or senescent.

The state of an uninfected field at time k is characterised by its green leaf area index S_k (=gLAI) and its total leaf area index $S_k + R_k$ (=LAI_{tot}). In order to obtain more or less realistic seasonal crop dynamics and a reasonable effect of fertilization on crop growth (Figure 1), we fit the dynamics of susceptible leaf area to empirical data. Following Hinzman et al. (1986), Benbi (1994), Forsman and Poutala (1997), Baccar et al. (2011) and Huang (2016), we assume that S_k increases from k_0 to $k_{switch} = 1300$ dd with growth rate $c(k)$. Leaf senescence occurs at a constant rate μ so that the dynamic of S_k is given by:

$$S_{k+1} = S_k + c(k) - \mu S_k \quad (1)$$

with

$$c(k) = \begin{cases} \beta S_k (1 - \frac{S_k}{K}) & \text{if } k \leq k_{switch} \\ 0 & \text{otherwise} \end{cases} \quad (2)$$

As nitrogen fertilization increases, winter wheat gLAI growth rate increases and levels off between (about) 1000 and 1300 dd at the highest fertilization levels (Hinzman et al., 1986; Benbi 1994; Drecce et al., 2000; Cowling and Field 2003; Jiang et al., 2004). In our model, we mimick this behaviour by assuming that fertilization \mathcal{F} has a positive effect on both the gLAI maximum value K and gLAI growth rate β . For this we use the linear relations:

$$K = \eta \mathcal{F} + \xi \quad (3)$$

and:

$$\beta = \phi \mathcal{F} + \vartheta \quad (4)$$

Note that the function $c(k)$ from equation 2 is the integrated form of a logistic growth equation. Parameters K and β can thus be related to a carrying capacity and a population growth rate respectively.

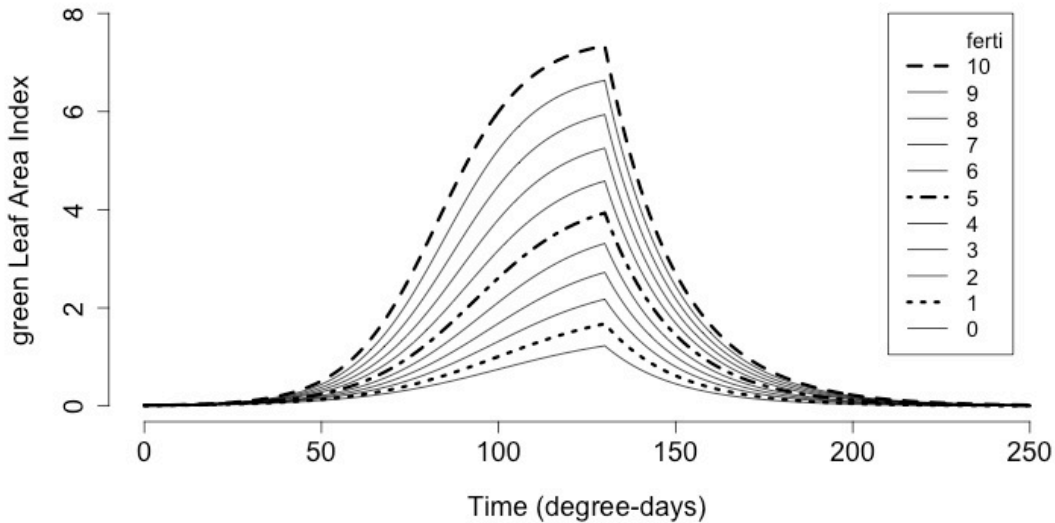


Figure 1: response of the green leaf area index (gLAI) to fertilization in our model. Results are obtained by integrating equation 1 for eleven fertilization levels. Parameter values are given in Table 1.

Crop tissue becomes senescent at rate μ . Senescent tissue is accounted for in the recovered compartment R_k . Its dynamics are described by:

$$R_{k+1} = R_k + \mu S_k \quad (5)$$

Eventually, the whole canopy will be senescent once the plant has completed its life cycle, at the end of the season. The “removed” canopy surface area R then equals the general leaf area index of the crop (LAI_{tot}).

We assume that epidemics at the field scale are initiated by the amount of pathogen inoculum that has overwintered in the patch. At date k_{inoc} , a fraction of the gLAI becomes exposed to the disease. Exposed tissue becomes infectious at a rate $1/\lambda$, being the inverse of the pathogen latent period λ . Both exposed and infected tissue E and I are subject to natural senescence at a rate μ similar to healthy tissue S . Within-field spread of the disease is proportional to the local spore production σI where σ is the pathogen spore production rate. We assume that a fraction α of the spores produced in a field are dispersed by wind towards neighbouring fields (Figure 4). The rate of spores production that remains in the field at time k

is thus $(1 - \alpha)\sigma I_k$. We further assume that a fraction ε contributes to development of the within-patch epidemic, the rest hits the soil. Since the amount of susceptible tissue that becomes infected at each time step is proportional to both the spore production and the remaining surface of susceptible tissue, we get the following equations for S, E, I and R:

$$S_{k+1} = S_k + c(k) - \varepsilon(1 - \alpha)\sigma I_k S_k - \mu S_k \quad (6)$$

$$E_{k+1} = E_k + \varepsilon(1 - \alpha)\sigma I_k S_k - \frac{1}{\lambda} E_k - \mu E_k \quad (7)$$

$$I_{k+1} = I_k + \frac{1}{\lambda} E_k - \mu I_k \quad (8)$$

$$R_{k+1} = R_k + \mu(S_k + E_k + I_k) \quad (9)$$

We assume that the remaining fraction of the spore production rate, $(1 - \varepsilon)(1 - \alpha)\sigma I_k$, build up a pool of spores that fall on the ground or cause lesions on local weeds, feral plants, or wild grasses. The dynamics of this spore pool is given by:

$$P_{k+1} = P_k + (1 - \alpha)(1 - \varepsilon)\sigma I_k - \rho P_k \quad (10)$$

where ρ is the decay rate of spores in the spore pool. A fraction θ of this spore pool will overwinter and will be responsible for the next year's internal primary inoculum. The fraction of the gLAI that becomes exposed at the beginning of the epidemics (at k_{inoc}) is calculated as:

$$E_{k_{inoc}[t+1]} = \theta P_{k_{end}[t]} * S_{k_{inoc}[t+1]} \quad (11)$$

where t and $t+1$ are two successive growing seasons, k the time index within a season, θ the percentage of overwintering spores between year t and $t+1$ and $P_{k_{end}}^t$ the amount of viable spores at the end of season t . A summary of the within-field dynamics is given in Figure 2.

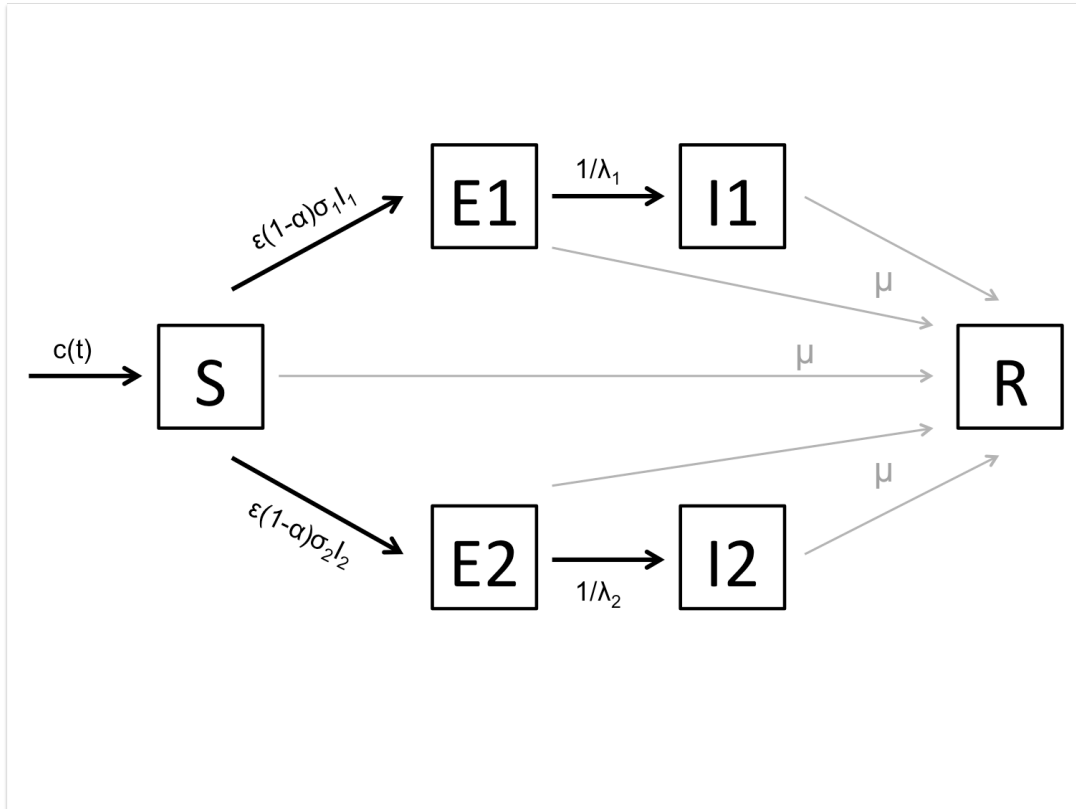


Figure 2: visual representation of the patch dynamics of the disease. Susceptible tissue S represents the canopy green leaf area index. It becomes infected (“exposed”, E) at a rate proportional to patch spore production σI . Exposed tissue E becomes infectious (I) at a rate λ corresponding to the pathogen latent period. Both S , E and I tissue become senescent at a rate μ and are thus “removed” (R) from the system. Here, we consider two separate pathogen strain 1 and 2 co-infecting the same patch.

Generalizing Equations 6 to 10 for several pathogen strains j co-infecting a field, we get:

$$S_{k+1} = S_k + c(k) - (1 - \alpha)\varepsilon S_k \sum_j \sigma_j I_{j,k} - \mu S_k \quad (12)$$

$$E_{j,k+1} = E_{j,k} + \varepsilon(1 - \alpha)\sigma_j I_{j,k} S_k - \frac{1}{\lambda} E_{j,k} - \mu E_{j,k} \quad (13)$$

$$I_{j,k+1} = I_{j,k} + \frac{1}{\lambda} E_{j,k} - \mu I_{j,k} \quad (14)$$

$$R_{k+1} = R_k + \mu(S_k + \sum_j E_{j,k} + \sum_j I_{j,k}) \quad (15)$$

$$P_{j,k+1} = P_{j,k} + (1 - \alpha)(1 - \varepsilon)\sigma_j I_{j,k} - \rho P_{j,k} \quad (16)$$

We consider the fraction of spores dispersing to neighbouring patches and the one building up the spore pool to be identical between pathogen strains in our model.

Based on the results of chapter 1 to 3, we implement a trade-off between pathogen latent period and spore production. In those chapters we have demonstrated that the relation between spore production at the canopy scale and the latent period is bell-shaped. We defined an “optimal latent period”, being the intermediate latent period value maximizing spore production. We further demonstrated that for every latent period tested, spore production increased with fertilization. We implemented this relationship in our current model by assuming that the spore production rate σ is a bell-shaped function of the latent period λ . For this trade-off to correspond to the one emerging from our model in Chapters 1 to 3, the shape parameters of the quartic function must depend on the fertilization level. For a given latent period λ and a given fertilization level \mathcal{F} , the sporulation rate of the pathogen is calculated as

$$\sigma(\lambda) = \kappa\lambda^4 + \psi\lambda^2 + \iota \quad (17)$$

with

$$\begin{aligned} \iota &= 0.12 + 0.01 * \mathcal{F} \\ \kappa &= \iota/10000 \\ \psi &= -200 * \kappa \end{aligned}$$

The relation between σ and λ is illustrated in Figure 3.

Between-field pathogen dispersal and multi-annual dynamics

At the beginning of all simulations, the landscape is composed of N healthy fields. Epidemics start with the arrival of external inoculum from outside the landscape. Arriving at time k_{init} of the first season only, this air-borne spore cloud inoculates a fraction χ of the green surface ($S_{k_{init}}$ by that time) of a percentage v of the N fields in the landscape. In the vN newly infected fields, disease development follows equations 12 to 16 while the remaining fields are still healthy (Equations 1 and 5). Successful pathogen dispersal events, which normally depend on particular weather conditions in terms of wind, humidity and rain, are assumed to take place once every τ degree-days. At each dispersal event a fraction α of the spores produced in the infected patches leave its birth patch and colonizes neighbouring ones. The maximum dispersal range is Δ patches but only a fraction φ of spores will reach a

suitable habitat and survive dispersal. Allo-infection superimposes to within-patch dynamics. Dispersal events take place from k_{init} to k_{end} during the first season and from k_{start} to k_{end} during the following seasons. The quantity of spores received by a given field thus depends on its distance to infected neighbours, on their number, on their spore production rate and on its own green leaf area.

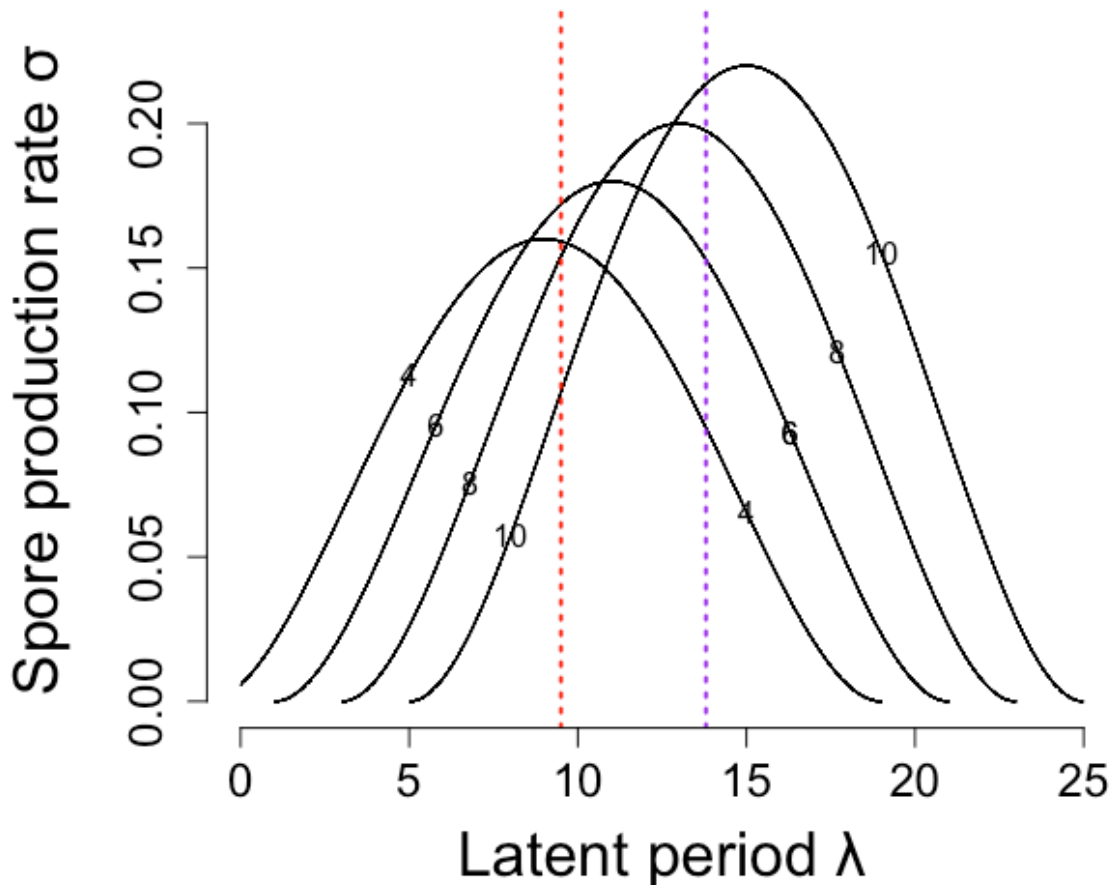


Figure 3: trade-off between latent period and spore production. In accordance with the results of chapters 1 to 3, the spore production rate of the pathogen is maximal at intermediate latent periods. These maximum values increase with fertilization levels. The curves correspond to different fertilization levels ($4 \leq \mathcal{F} \leq 10$). For the sake of comparison, vertical dotted lines have been drawn for latent periods corresponding to the ESS of field-scale invasion analysis: red line: $\mathcal{F} = 6$; purple line: $\mathcal{F} = 10$ (cf. Figure 16)

Consider an infected field denoted by A at the time of a dispersal event τ' . Let $I_{\tau'}^A$ be its sporulating leaf area at that time. The quantity of spores that will successfully disperse from patch A is then:

$$q_A = \alpha \varphi \sigma I_{\tau'}^A \quad (18)$$

Let B be a field within the dispersal range from field A. The gLAI of patch B is denoted by $S_{\tau'}^B$. Let $\delta_{BA} < \Delta$ be the distance between A and B. The crop surface becoming exposed in patch B due to spores from patch A is then:

$$E_{\tau'}^{BA} = q_A \omega_{BA} S_{\tau'}^B \quad (19)$$

with

$$\omega_{BA} = \frac{1}{\delta_{BA}} * \frac{1}{W_A} \quad (20)$$

and

$$W_A = \sum_{i=1}^n \frac{1}{\delta_{iA}} \quad (21)$$

where n is the number of neighbours of patch A (patches within a radial range Δ from A), q_A the quantity of spores dispersing from patch A from equation 18 and ω_{BA} the part of these dispersing spores successfully landing on patch B. The same surface as calculated in equation 19 is removed from $S_{\tau'}^B$.

More generally, for a given patch B, the fraction of S becoming infected due to external inoculum at time τ' is given by:

$$E_{\tau'}^B = \sum_{j=1}^m q_j \omega_{Bj} S_{k_{\tau'}}^B \quad (22)$$

where m is the number of infected neighbours of patch B. At each dispersal event, changes in S and E are calculated for all patches after the within-patch dynamics have taken place. At each dispersal event, in addition to equations (12-16) we thus add the operation:

$$E_{j,k+1}^{\tau'} = E_{j,k+1} + E_{\tau'}^B$$

where $E_{j,k+1}^{\tau'}$ denotes E after dispersal and $E_{j,k+1}$ denotes E just before dispersal.

The arrival of external inoculum (from outside the landscape) is a punctual event in our model. It occurs only once at the beginning of each simulation to initiate epidemics. Landscape colonization occurs through spore dispersal at the landscape scale. Year to year transmission occurs at the patch scale as described in Equation 11. Figure 4 gives an overview of these mechanisms.

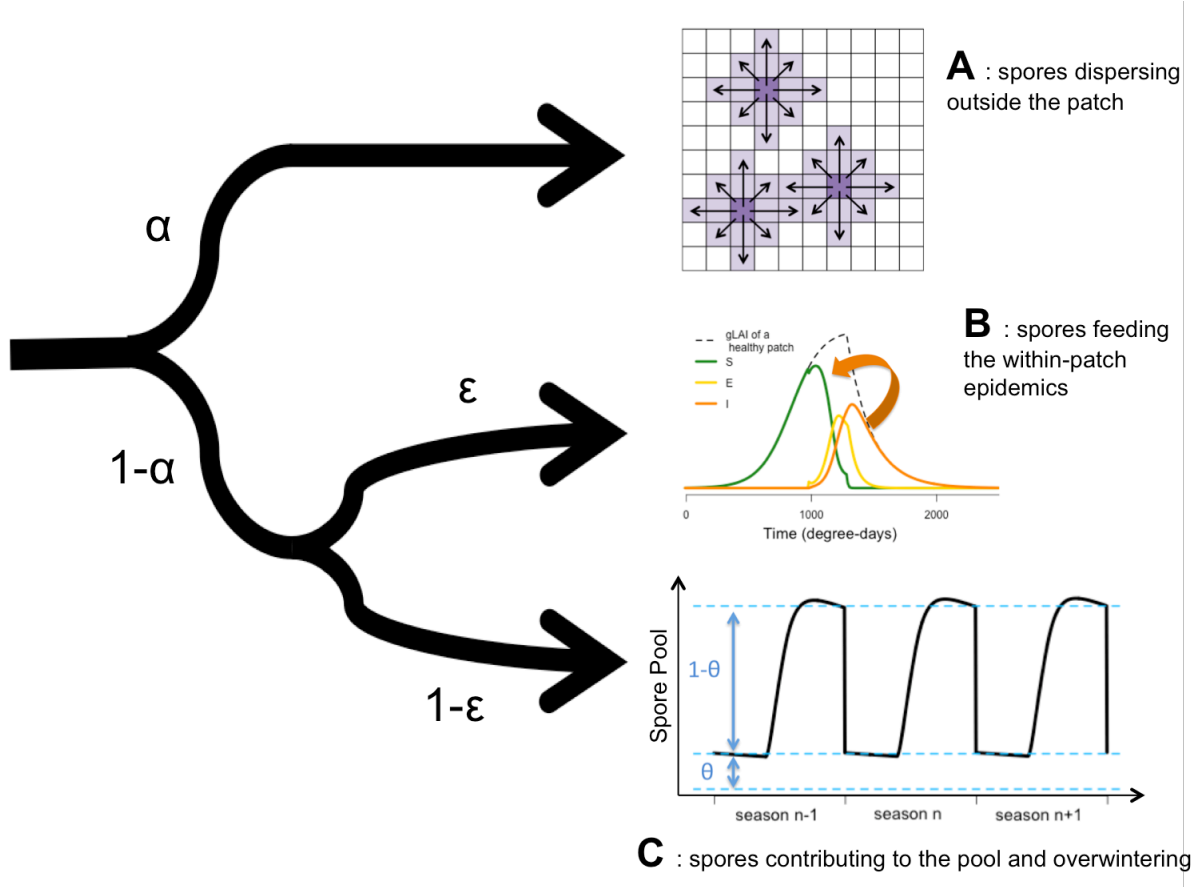


Figure 4: overview of the different fates of pathogen spores in the model. The black arrow represents the sporulation rate in a given field at a given time. A: a fraction α of spores disperses to other fields within a radius Δ . In this example, dark purple patches are already infected. Light purple ones are their - yet uninfected - neighbours within a range $\Delta = 2$. The amount of spores received by each neighbour is inversely proportional to its distance to the sporulating patch (Equations 18 to 22). B: a fraction ε of the non dispersing spores feeds the local epidemic (Equations 12 and 13 and Figure 2). C: The fraction $(1 - \varepsilon)$ enters the field's spore pool P . Spores in this compartment decay at a rate ρ . At the end of a season, only a fraction θ of the spore pool survives harvesting and the interseason and make it to the next season and form the internal primary inoculum of the new season. For more details, see Equations 11 and 16.

Analysis methods and simulations

We studied the model dynamics using numerical simulations. The model has been implemented using the NetLogo software (Wilensky, 1999). We opted for a discrete time scale with integration steps of 10 dd (i.e., time steps $k=0, 1, 2, \dots$ correspond to 0, 10, 20... degree-days into the season).

To understand the effects of fertilization patterns at the landscape scale on pathogens and their evolution, we first compare epidemic development in a single field and in a homogeneous landscape. A homogeneous landscape is nearly identical to a single patch;

except for the dispersal processes. Such comparison allows us to assess the effect of dispersal on landscape colonization, spore production and crop loss. In a second step, we compare several homogeneous landscapes (each characterized by its fertilization level) with heterogeneous landscapes with various levels of fertilization heterogeneity. For this, we use the same output variables as for the first comparison. The last step involves determining the evolutionary response of the pathogen to changes in fertilization heterogeneity at the landscape scale. To do this, we use roughly the same methods as in the previous chapters (see below).

We use several epidemiologic variables to describe the epidemics. The variables S , E , I and R represent leaf surfaces, that are green (healthy), exposed, infectious and senescent (removed) respectively. Hence, the area under the S curve (full green curves in Figures 6 and 7) corresponds to the canopy green leaf area index (gLAI). The green leaf area loss due to an epidemic (gLA loss) is defined as the difference between the gLAI of a healthy canopy and that of an infected canopy. Since both yield and biomass production are proportional to the gLAI in wheat, the variables gLAI and gLA loss can serve as proxies for epidemic intensity and crop damage respectively. In epidemiology, epidemics are often characterised by the area under disease progress curve (AUDPC), calculated as the integral of disease intensity (Madden et al 2007). We compute the AUDPC as the area under the I curve (full orange curves in Figures 6 and 7).

$$AUDPC = \sum_{k_0}^{k_{end}} I_k \quad (23)$$

Note that the area under the curve $S+E+I+R$ correspond to the total leaf area index LAItot.

Our model is able to simulate three aspects of spatial heterogeneity: (i) the number of patch types, i.e. how many different fertilization levels coexist in the landscape; (ii) the proportion of the different patch types and (iii) the level of aggregation of similar patches. We chose to work with landscapes encompassing either one type of patch (homogeneous landscape) or two (a landscape with both high and low fertilization). In heterogeneous landscapes, we assume that either 20%, 50% or 80% of fields receive high fertilization while the remaining fields receive a low treatment. Furthermore, the distribution of field types in the landscape is characterized by the level of aggregation, being low, medium or high. We quantify the level of aggregation in the landscape as the average number of neighbouring patches of the same type. To generate an aggregated landscape, a number of patches of a

given type (50% of $N = 1089$ patches, that is 544 patches of type X for example) are randomly chosen in a homogeneous landscape of patches of the other type (Y for example). For each patch, we calculate the number of patches of the same type in its immediate proximity (between 0 and 8 on the grid, see Figure 4A). While the average number of X-type neighbours of X-type patches is less than the target value, a patch of type X is randomly translocated next to another patch of type X. In our model, for an even proportion of the patch types in the landscape, a high (medium and low respectively) level of aggregation corresponds to an average number of neighbours of 7.2 (5.2 and 3.2 respectively). Examples of landscapes with various aggregation levels and several percentages of field types are given in Figure 5.

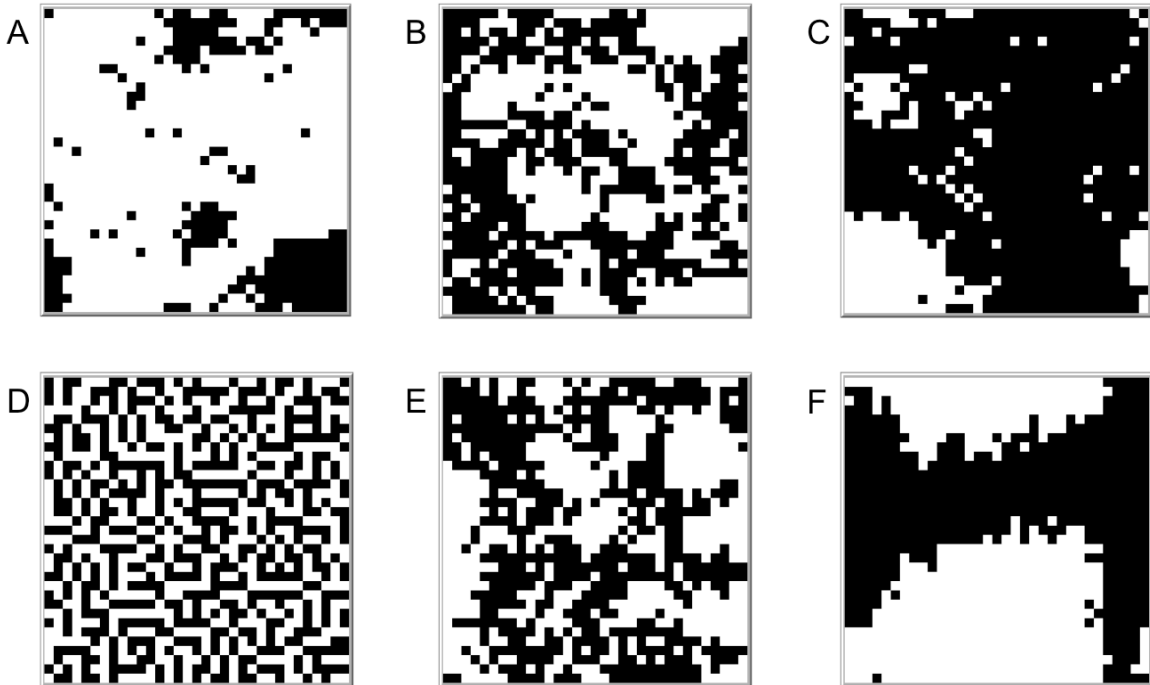


Figure 5: examples of the two scenarios of spatial heterogeneity in our model. White areas correspond to patches with a high level of fertilization. Black areas correspond to patches with a lower fertilization level. In the upper line, we change the proportion of patch type. A: 80/20%; B: 50/50% and C: 20/80% of strongly and less fertilized patches respectively. The aggregation level in landscapes A, B and C is 5.2 similar neighbours in average. In the lower line, we vary the level of patch aggregation. D: low aggregation landscape, E: average aggregation landscape and F: high aggregation landscape, corresponding to 3.2, 5.2 and 7.2 similar neighbours in average respectively.

Because of the fertilization-dependent latency-sporulation trade-off implemented at the patch scale (Figure 3), a pathogen strain with a given latent period will likely perform differently in patches with different fertilization levels. For instance, a pathogen strain with a

long latent period may proliferate in highly fertilized patches whereas it may not be able to cause epidemics in less fertilized patches. Provided that a long latent period corresponds to a well-adapted strategy in a highly fertilized environment, then this strategy is likely to be less successful in the low-fertilization fields. Such local deviation from an adaptive peak can be referred as maladaptation (Crespi, 2000). By comparing epidemics in single patches, homogeneous and heterogeneous landscapes we seek to identify spatial fertilization patterns that lead to pathogen maladaptation, as a first step to think about disease-suppressive landscapes.

But given the high adaptive potential of most crop fungal pathogens, it is likely that the advantages associated with pathogen maladaptation would only be temporary. Hence, we further seek to understand how pathogens would adapt to heterogeneous landscapes. In Chapter 3, we used four fitness measures to identify putative evolutionary responses of pathogen latent period to changes in fertilization levels. Three of them were named “empirical” fitness measures, since they correspond to experimentally measurable quantities such as annual spore production, rate of canopy colonization, or the quantity of spores produced during the canopy growth phase. We also referred to these fitness measures as “ad hoc” since none of them is canonical for filamentous fungi and since all could be potentially accurate. The fourth fitness measure was a more theoretical but more precise one: we used the invasion fitness from adaptive dynamics to draw pairwise invisibility plots and identify stable evolutionary strategies for the three main effects of fertilization on the pathosystem. In this chapter, we will use roughly the same fitness measures: total annual spore production P_{end} , spore production until 200dd post-inoculation (the canopy growth phase) P_{200} . Finally, field colonization will be approximated by the canopy-scale AUDPC, the area under disease progress curve (AUDPC, area of the curve of I). The fourth fitness measure we used in the previous chapters was a more theoretical but more precise one: we used the invasion fitness from adaptive dynamics to draw pairwise invisibility plots and identify stable evolutionary strategies for every effect of fertilization. Using the so-called empirical fitness measures, we seek to identify optimal latent periods as in the previous chapters. Optimal latent periods correspond to intermediate values of the latent period maximizing one of the above-mentioned fitness proxies. Using the invasion analysis, we seek to identify evolutionary singular strategies (evolutionarily stable strategies or evolutionary branching points, Geritz et al 1998) that would allow us to predict the direction in which pathogens would adapt to

fertilization heterogeneity at the landscape scale and see if some features of the landscape may allow us to slow down this adaptation.

Invasion analysis

Invasion analysis is a tool from adaptive dynamics that is based on the outcome of the invasion dynamics of an initially rare population of invaders (“mutants”) into the steady state of a system dominated by a “resident” phenotype. Invasion analysis allows for the identification of evolutionarily stable strategies, evolutionary branching points and scenarios of coexistence. Fitness is defined as invasion fitness, i.e., the long-term (multi-annual) exponential growth rate of the mutant phenotype trying to invade into a system dominated by the resident (Metz et al 1992). In our model, phenotypes will refer to pathogen strains with a given latent period. During invasion, the mutant strain remains at a negligible population density, such that it does not exert any density dependence on the resident strain (Geritz et al 1998). In our model, we obtain this condition by (i) inoculating the landscape with the mutant strain at low density and only once the resident strain has reached its steady state. Note that the steady state corresponds to an annual cycle. And by (ii) limiting the calculation of invasion fitness to the first five seasons after the mutant has been introduced. Invasion fitness of a mutant with latent period λ_2 invading into a resident with latent period λ_1 is then computed as the log of the ratio of the mutant’s AUDPCs of two successive seasons (denoted by t and $t + 1$), averaged over the first five seasons following the introduction of the mutant:

$$f(\lambda_2, \lambda_1) = \frac{1}{5} \sum_{t=1}^5 \log \left(\frac{\text{AUDPC}_{[t+1]}}{\text{AUDPC}_{[t]}} \right) = \frac{1}{5} \sum_{t=1}^5 \log \frac{\int_{k_0}^{k_{\text{end}}} I_{k[t+1]} dk}{\int_{k_0}^{k_{\text{end}}} I_{k[t]} dk} \quad (24)$$

The ensuing interaction between the two strains occurs exclusively through the dynamics of available S (analogous to Chapter 3). Note that according to this fitness definition, a strain identical to the resident necessarily has fitness equal to 0, corresponding to zero year-to-year population growth.

In adaptive dynamics it is usual to plot this function in a so-called pairwise invisibility plot (PIP), which depicts the sign of the function $f(\lambda_2, \lambda_1)$ in the plane of the two trait axes λ_1 and λ_2 (Geritz et al., 1998). The geometry of the PIP can be used to deduce the direction and end-point of the monomorphic dynamics (assuming a single resident population). In particular

the PIP informs us on the existence of so-called evolutionary singular points that can be attractors or repellers of the monomorphic evolution. Attracting singular points can be either evolutionarily stable (that is, uninvadable) in which case we use the terminology ESS. Or they can be evolutionarily unstable, in which case we use the term evolutionary branching point (EBP). When the resident population is attracted to an EBP, selection becomes disruptive, favouring diversification and possibly speciation (Dieckmann and Doebeli, 1999). Since simulations are much longer at the landscape scale than at the field scale, invasion analysis will be performed with latent periods varying by steps of 0.1 at the field scale and by steps of 1 at the landscape scale.

Information on the scope for coexistence between two strains with different latent periods can be deduced from a PIP by drawing a so-called trait evolution plot (TEP). A TEP corresponds to the superposition of a PIP and its transpose. The original PIP identifies which strategies y can invade which resident populations x . The transposed PIP shows which strategies x can invade which resident y . It is then possible to identify couples of mutually invasible strategies, which are pairs of strategies that are likely to coexist due to their mutual invasibility. PIPs and TEPs will be drawn for different fertilization levels and scenarios for both single patches, homogeneous and heterogeneous landscapes. They will allow us to identify evolutionary singular points that we wish to compare with the optimal latent periods obtained using the empirical fitness measures.

The question of which strain dominates or exists in the landscape in the long term is also of interest to us; we therefore complemented the PIPs and TEPs with plots that we refer to as “dominance plots”. At the field scale, we define “dominance” as the AUDPC-ratio of the mutant and the resident, computed at 100 years after the start of the epidemics (i.e., in steady state). Due to inter-field variability, the landscape is characterised by a distribution of dominance. In the dominance plots, we colour the λ_2, λ_1 plane according to a colour code based on the mode of this distribution. The colour code is defined as follows. When the dominance mode equals 1 ± 0.05 the colour code is zero (white). When the resident has an AUDPC between 1 and 2 times bigger than the mutant, the colour code is 1 (light pink). The dominance plot uses 6 colour scales for resident dominances categories 1-2 (light pink), 2-3, 3-4, 4-5, 5-10 and >10 (dark violet). In the zones where the mutant dominates, the colour code is analogous, but the colours are orange. An AUDPC ratio of more than 10 (or equivalently: less than 0.1) practically corresponds to competitive exclusion of the one strain by the other.

By contrast, dominance indices less than 5 (or more than 0.2) indicate field-scale coexistence, with both strains causing significant damage on the crop.

Symbol	Value	Unit	Interpretation
Seasonal dynamics parameters			
k_{init}	1000	dd	Date of primary inoculum arrival (inoculation of the landscape)
k_{start}	1000	dd	Annual start date of epidemic
k_{switch}	1300	dd	End of period of canopy growth
k_{end}	2500	dd	Length of a growing season
τ	50	dd	Time interval between dispersal events
Canopy growth and fertilization parameters			
S_0	0.01	[LAI]	Initial value of S
\mathcal{F}	0-10 (changed)	[\mathcal{F}]	Fertilization level
K	$f(\mathcal{F})$	[LAI]	Theoretical maximum value of the gLAI (S)
β	$f(\mathcal{F})$	[LAI]/dd	Rate of increase of the gLAI (S)
η	0.92	[LAI]/ [\mathcal{F}]	Shape parameter of the linear relation between K and \mathcal{F}
ξ	3	[LAI]	Shape parameter of the linear relation between K and \mathcal{F}
ϕ	0.003	[LAI]/ [\mathcal{F}]	Shape parameter of the linear relation between β and \mathcal{F}
ϑ	0.1	[LAI]	Shape parameter of the linear relation between β and \mathcal{F}
μ	0.05	[LAI]/dd	Canopy senescence rate
Epidemic development parameters			
N	1089	patches	Number of patches in the landscape
v	0.01	-	Fraction of the landscape infected by primary external inoculum at k_{init}
χ	$1.0 \cdot 10^{-4}$	-	Fraction of S becoming infected in the $ vN $ patches receiving external primary inoculum
λ	1-25 (changed)	dd	Latent period
σ	$f(\lambda)$	spores/[I]	Spore production rate by unit of infected canopy area
α	0 (single patch) 0.1 (otherwise)	-	Fraction of spores dispersing out of the patch
ε	0.8	-	Fraction of spores responsible for local epidemic development
θ	0.01	-	Spore survival probability over the unfavorable season
ρ	0.001	/dd	Spores decay rate related to between-patch dispersal
ι	$0.12 + 0.01 * \mathcal{F}$	spores/dd/[I]	Last order shape parameter of the relation between λ and σ
κ	$\iota/10000$	spores/dd ⁴ /[I]	Fourth order shape parameter of the relation between λ and σ
ψ	$-200 * \kappa$	spores/dd ² /[I]	Second order shape parameter of the relation between λ and σ
Δ	1	patches	Maximum dispersal distance (in terms of patch age)

Table 1: Biological model parameters and their default values, representing the wheat-brown rust pathosystem.

RESULTS

Epidemics at the scale of an isolated field

Model exploration shows that the within-field dynamics always converge to a stable 1-year cycle that we refer to as the equilibrium. We first present the results at equilibrium, then we present the results concerning the transient dynamics to the equilibrium that correspond to the infection of the field, year after to year to reach an equilibrium.

At equilibrium. Figure 6 shows the effect of fertilization on the annual epidemic for a given latent period. Fertilization increases both the total leaf area (LAI_{tot} , brown curves) and the green leaf area (gLAI , green curves) in both healthy and infected fields. We observe an increase of the diseased area with fertilization (yellow and orange curves: latent and sporulating areas). The area under disease progress curve in a field, AUDPC, increases thus strongly with fertilization, from 49.8 to 90.5 to 108.7 for $F = 6$, $F = 8$ and $F = 10$ respectively.

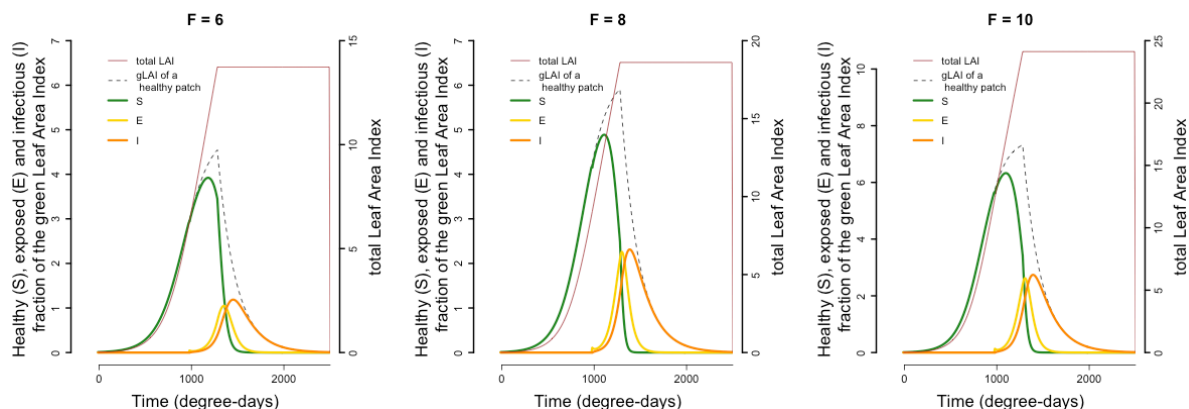


Figure 6: seasonal dynamics of within-field epidemics at equilibrium for three fertilization levels (F). Solid lines describe canopy growth and epidemic development: green = susceptible leaf area (green leaf area index, gLAI); yellow = exposed leaf area; orange = sporulating (infectious) leaf area; brown: total leaf area corresponding to the field leaf area index (LAI). Dotted lines indicate the gLAI of a corresponding uninfected field. Fertilization increases from left ($F = 6$) to right ($F = 10$). $\lambda = 130 \text{ dd}$.

Unlike fertilization, the relation between latent period and the epidemics is not monotonous. Figure 7 shows that the epidemic is maximum at an intermediate latent period. The maximum values of latent (E) and sporulating areas (I) go up to 2 for latent period $\lambda = 120$ whereas it is less than 1 at $\lambda = 80$ and $\lambda = 170$. The gLAI of infected fields is the lowest for the intermediate latent period.

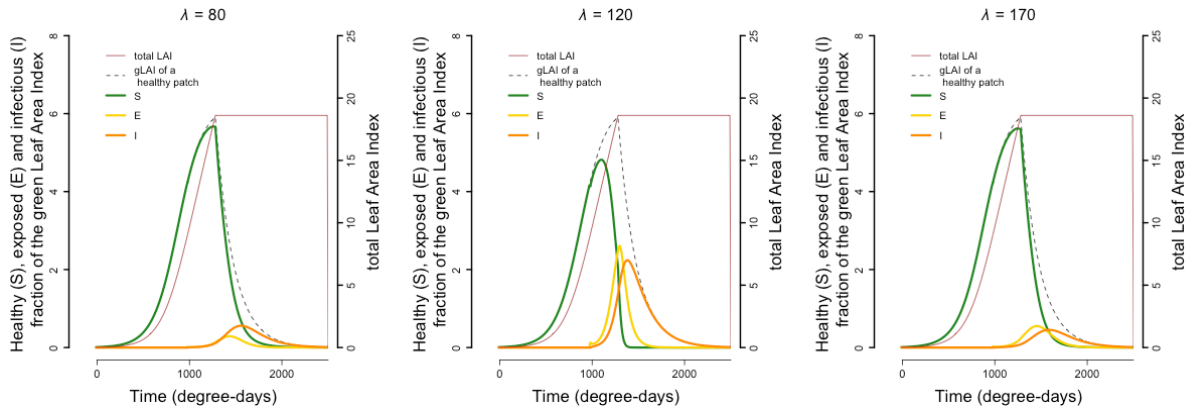


Figure 7: seasonal dynamics of within-field epidemics at equilibrium for three pathogen latent periods (λ). Solid lines describe canopy growth and epidemic development: green = susceptible leaf area (green leaf area index, gLAI); yellow = exposed leaf area; orange = sporulating (infectious) leaf area; brown: total leaf area corresponding to the field leaf area index (LAI). Dotted lines indicate the gLAI of a corresponding uninfected canopy. Latent period increases from left ($\lambda = 80$ dd) to right ($\lambda = 170$ dd). Note that the diseased surface is maximal at intermediate latent period as a result of the trade-off between spore production and latent period implemented at the field scale. $F = 10$.

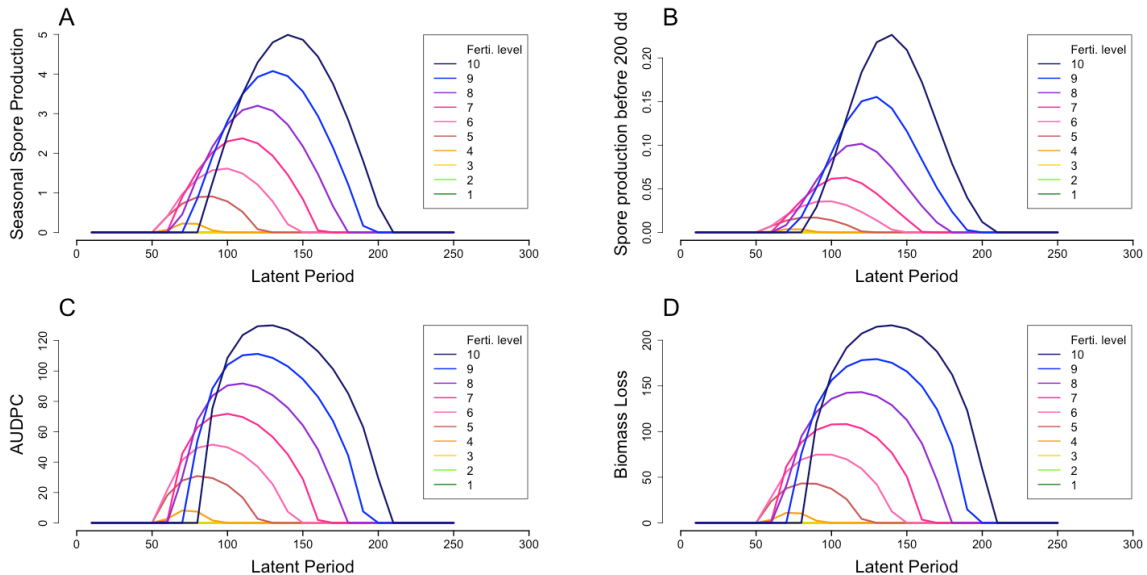


Figure 8: field-scale effect of pathogen latent period on A: seasonal spore production; B: spore production from the beginning of the epidemic to 200 dd; C: the area under disease progress curve (AUDPC) and D: biomass loss. Colors from green to blue represent a range of fertilization from $F = 1$ to $F = 10$. In panel A, B and C, the summit of each curve corresponds to the optimal latent periods (see Figure 15).

Figure 8 summarizes the effect of fertilization and latent period, for the four studied variables that are spores production (Fig 8A and 8B), AUDPC (Fig 8C) and biomass loss (Fig 8D) at the field scale. For the four variables we observe an intermediate optimal latent period

that maximizes each of the studied variable. The curves are quite similar for the studied variables with an increase in the optimal latent period with fertilization (Figure 9).

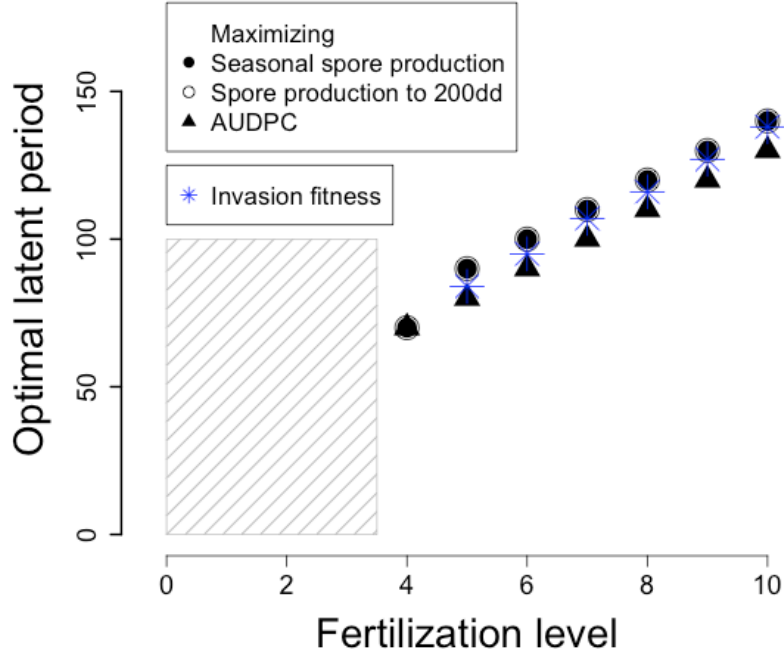


Figure 9: variation of the optimal latent periods and the ESS with fertilization at the field scale. Full circles correspond to seasonal spore production as a fitness measure (see Figure 19). Open circles correspond to spore production at the beginning of the epidemics as a fitness measure. Full triangles correspond to canopy colonization as a fitness measure (measured as the AUDPC, see Equation 23). Blue stars correspond to the evolutionary singular strategy derived from invasion analysis. There are no sustainable epidemics in the striped area of the parameter space.

Transient dynamics. Latent period and fertilization also impact the duration, in terms of the number of seasons, of the transient to reach equilibrium in term of epidemic development (Figure 10 top panels for the field scale). For instance, for a pathogen with $\lambda = 130$, it takes four seasons in a high fertilization field ($F = 10$) to reach equilibrium while it takes eight seasons for the same pathogen in a low fertilization field ($F = 6$, Figure 10 top-left panel). By contrast, a pathogen with a lower latent period, $\lambda = 90$ is quicker to reach equilibrium in a high fertilization than in a low fertilization field (5 and 7 seasons respectively, Figure 10 top-right panel).

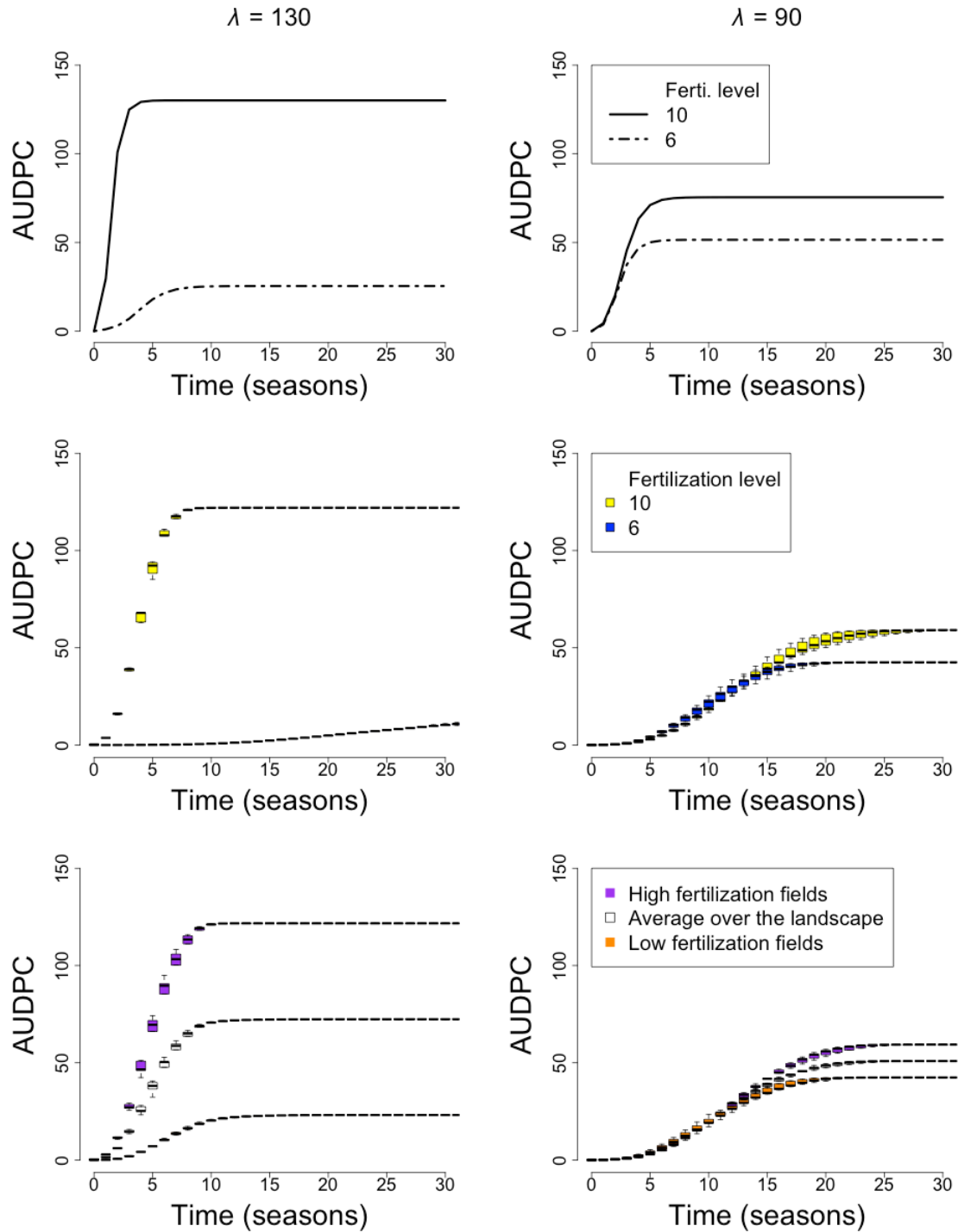


Figure 10: time series describing within-field epidemics (upper line) and landscape colonization by the pathogen (middle and lower lines). Upper line: area under disease progress curve (AUDPC) for a single field. Solid lines: high fertilization ($F = 10$)/ Dotted line: low fertilization ($F = 6$). Middle line: average AUDPC of fields in a homogeneous landscape. Boxplot represent average values for 5 repetitions. Yellow: high fertilization landscapes ($F = 10$); blue: low fertilization landscapes ($F = 6$). Lower line: average AUDPC of fields in a heterogeneous landscape. Boxplot represent average values for 5 repetitions. Aggregation index = 5.2 and there is an even proportion of both patch types. Purple: high fertilization fields within the heterogeneous landscape; orange: low fertilization fields within the heterogeneous landscape; open boxplots: AUDPC values averaged over the landscape. Latent period decreases from left to right. Left column: $\lambda = 130$ dd. Right column: $\lambda = 90$ dd.

Epidemics in a homogeneous landscape

Due to the spatial diffusion processes from patch to patch, it takes the pathogen longer to reach equilibrium in a landscape than in an isolated field (Figure 10 compare upper and middle panels). Colonization dynamics are thus a bit slower at the landscape scale with our initial conditions. Figure 10 also shows that there is variation between individual fields (box plots), during the transient phase, but that in equilibrium this variation has disappeared.

However, the epidemics in individual fields of the homogeneous landscape at equilibrium are very similar to an isolated field (with the same fertilization and latent period). As a result, the asymptotic AUDPC values are almost the same at both spatial scales (Figure 10 upper and middle panels), with AUDPC being slightly less at the landscape scale. This slight difference is due to between-field spore dispersal during which there is a slight loss of dispersing spores.

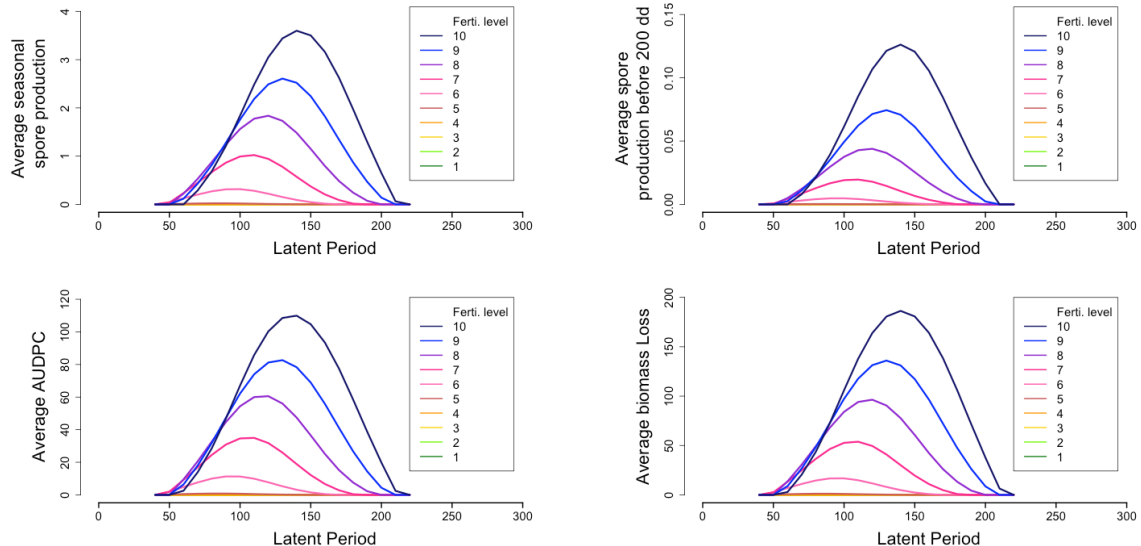


Figure 11: effect of latent period on pathogen development for different fertilization levels in a homogeneous landscape. A: seasonal spore production; B: spore production from the beginning of the epidemic to 200 dd; C: the area under disease progress curve (AUDPC) and D: biomass loss. For the sake of comparison with Figure 10, we represented per patch average values for all four quantities. In panel A, B and C, the summit of each curve corresponds to the optimal latent periods (see Figure 16).

Comparison of Figure 8 and Figure 11 shows similar results for an isolated field and a homogeneous landscape, in equilibrium. Similarly to the field scale, we observe at the landscape scale that (1) epidemics are stronger for higher fertilisation, (2) there are optimal

latent periods that maximise spores production, AUDPC or biomass for each fertilisation tested, and (3) the optimal latent periods are very similar for the four variables studied. However, it can be noted that the landscape-scale curves are flatter. Their maximum values are only very slightly less than field-scale ones. Note that despite these differences, we were still able to identify the same optimal latent periods in the homogeneous landscapes and in the isolated fields (Figure 12).

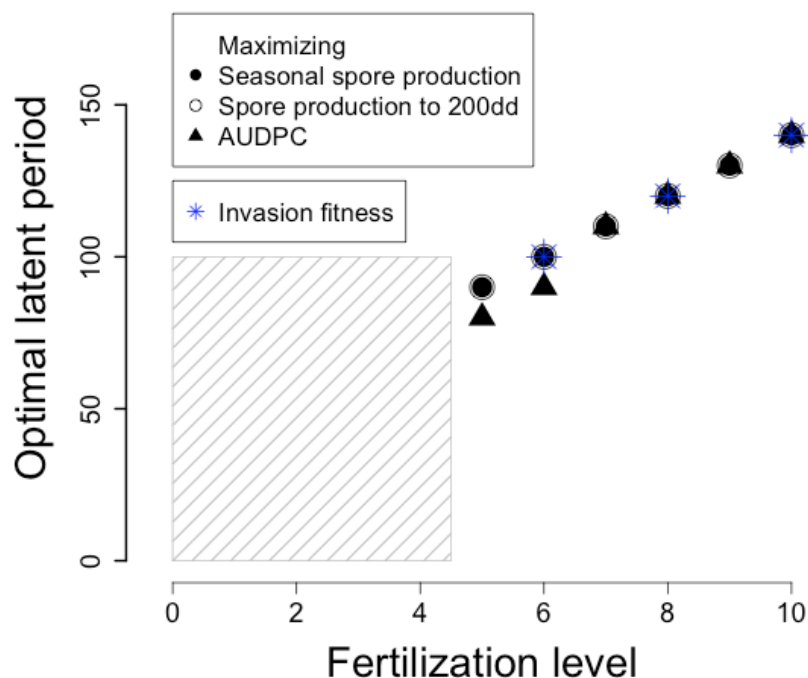


Figure 12: variation of the optimal latent periods and the ESS with fertilization in a homogeneous landscape. Full circles correspond to seasonal spore production as a fitness measure. Open circles correspond to spore production at the beginning of the epidemics as a fitness measure (see Figure 20). Full triangles correspond to canopy colonization as a fitness measure (measured as the AUDPC, see Equation 23). Blue stars correspond to the evolutionary singular strategy derived from invasion analysis. There are no sustainable epidemics in the striped area of the parameter space

Landscape heterogeneity and epidemics

Here we compare epidemics in homogeneous and heterogeneous landscapes in order to analyse the potential of heterogeneity to decrease or slow down the epidemics. In the previous paragraphs, we have shown that both the latent period and the fertilisation level impact disease development in the fields. So for the sake of simplicity and understanding, in this part of the results we first focus on the effect of fertilisation heterogeneity for a pathogen

with a latent period of 130 dd (Figures 8, 13 and 14). This latent period is very close to the optimum for maximizing spores production for a fertilization level of $F=10$ at the field scale and the homogeneous landscape (Figure 8, 9, 11 and 12). Fertilisation heterogeneity is obtained by using two types of fields with either high ($F=10$) or low ($F=6$) fertilization.

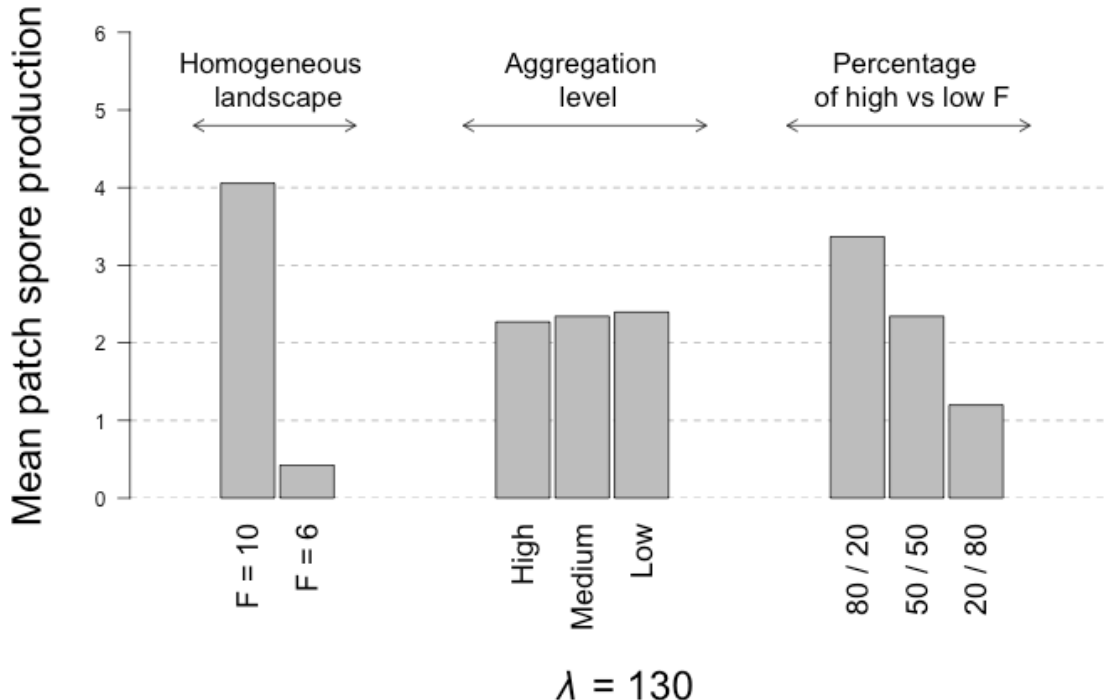


Figure 13: effect of spatial heterogeneity on landscape-scale spore production at equilibrium for $\lambda = 130$ dd. Here, we compare homogeneous landscapes with high ($F = 10$) and low ($F = 6$) fertilization and heterogeneous landscapes with various aggregation levels or various proportions of field types. The aggregation level is the same in landscapes with different field type proportions (medium aggregation) and reciprocally, the proportion of fields of each type is the same in landscapes with different aggregation levels (50/50). λ = pathogen latent period; F = fertilization level.

Our idea behind it is the following scenario. We consider an initial situation, corresponding more or less to the present situation, that is a homogenous landscape with crops being highly fertilised since a rather long time and thus with pathogens having potentially an optimal latent period for high. Then, we mimic the introduction of low fertilisation fields in the landscape ($F=6$ in the Figures 8, 9, 11 and 12) and we simulate the effects on the epidemics. In particular, we analyse (1) the effects of the proportion of the two types of fertilisation but also (2) the effect of the location (aggregation) of both types. We analyse epidemics at the equilibrium and also during the seasons to reach the equilibrium. Results for a lower latent period ($\lambda = 90$ dd, close to the optimum for $F=6$) are shown in supplementary figures SM1 and SM2.

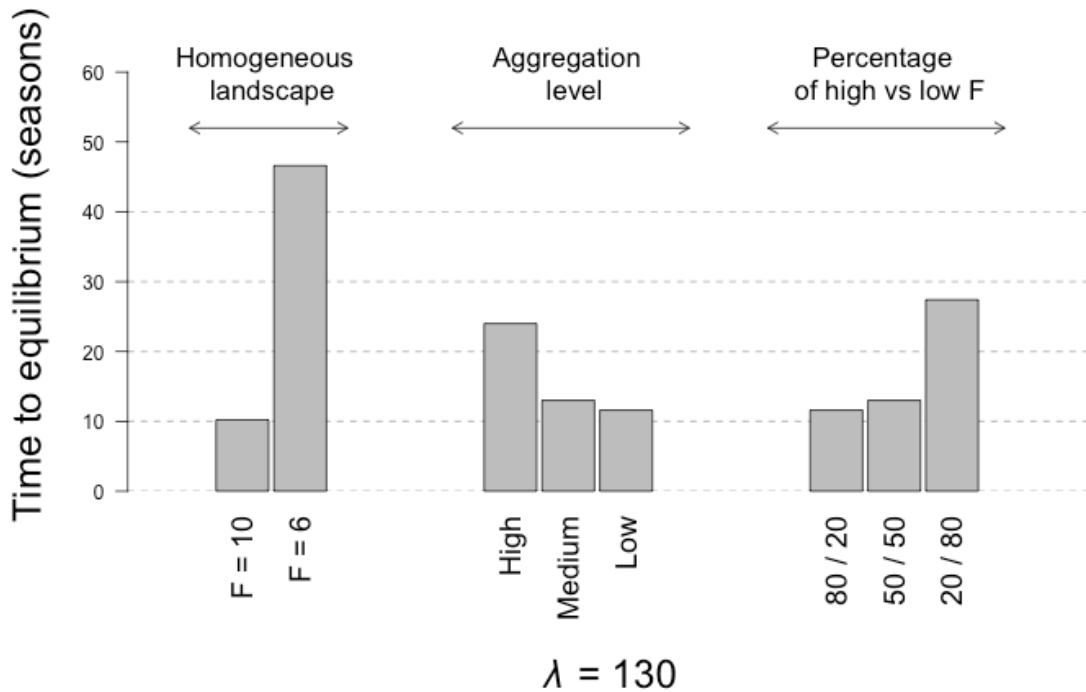


Figure 14: effect of spatial heterogeneity on the speed of landscape colonization by the pathogen with $\lambda = 130$ dd, measured as the time for the epidemics to reach a steady state. Here, we compare homogeneous landscapes with high ($F = 10$) and low ($F = 6$) fertilization and heterogeneous landscapes with various aggregation levels or various proportions of field types. The aggregation level is the same in landscapes with different field type proportions (medium aggregation) and reciprocally, the proportion of fields of each type is the same in landscapes with different aggregation levels (50/50). Data are average values from 5 repetitions. λ = pathogen latent period; F = fertilization level.

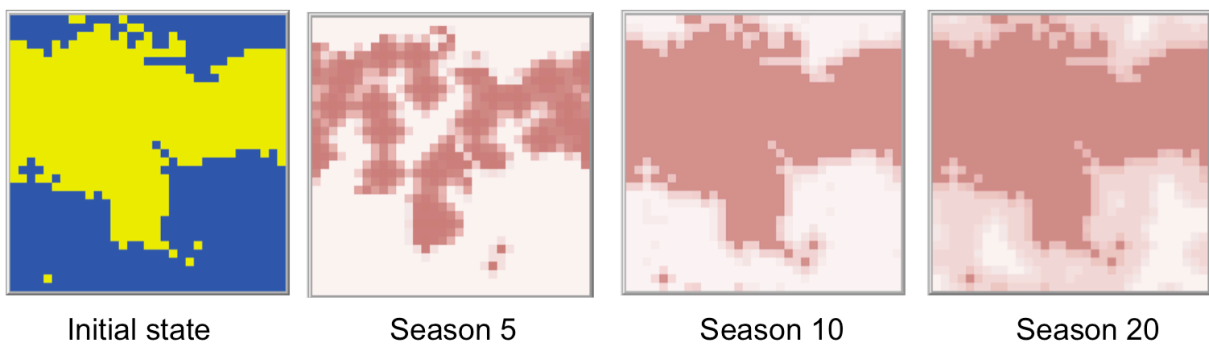


Figure 15: high spatial aggregation in a heterogeneous landscape impedes pathogen development in low fertilization areas. Except for the initial state, the red colour scale corresponds to field-scale spore production and thus represents the intensity of the epidemics: the darker the field, the stronger the epidemic. First panel: initial state. High fertilization fields have been coloured in yellow, low fertilization fields in blue. The aggregation level is 7.2 identical neighbours in average. The whole landscape has been colonized by the pathogen during the first season (data not shown). At the end of the fifth cropping season (Second panel), the pathogen causes consequent epidemics in almost all the high fertilization fields, while epidemics remain limited in low fertilization ones. After 10 seasons (Third panel), all high fertilization fields house strong epidemics. Low fertilization patches at the edge of the high fertilization clusters show a higher spore production than those further from the high fertilization clusters. This “ring” extends towards the centres of the low fertilization clusters (Fourth panel) until the system reaches a steady state.

Figure 10 (lower line) shows the dynamics of AUDPC in a heterogeneous landscape with 50% high and 50% low fertilized fields with medium aggregation. The figure shows the AUDPC for each type of field (high and low) and the overall average AUDPC of a pathogen with a latent period of 130 dd. Once the equilibrium has been reached the AUDPC values in high and low fertilization fields in a heterogeneous landscape, are very similar to high and low fertilization homogeneous landscapes respectively for this latent period (Figure 10, left column). Thus, in our model, the equilibrium outcome, in terms of AUDPC, in a heterogeneous landscape by a pathogen strain with a given latent period can almost be deduced from the individual properties of its basic entities. Moreover, the global average response of the heterogeneous landscape appears to be the average between the responses in the two types of fields (Figure 10, lower panels). These results also hold for other epidemiologic variables such as seasonal spore production.

Figure 13 shows the annual spore production per field (P_{end}) at equilibrium, in homogeneous and heterogeneous landscapes. In the homogeneous landscape (Figure 13, left column), P_{end} is almost 10 times higher in a high fertilization ($F=10$) than in a low fertilization ($F=6$). In the heterogeneous landscape, the annual spores production averaged over all fields shows an intermediate values between the two field types. The proportion of each field type has a clear and logical effect, directly linked to the proportion of each type in the landscape and the associated spores production (Figure 13, middle and right columns). This effect will ultimately vanish if both types of fields display similar spore productions (Supplementary Figure SM1 with $\lambda = 90$ dd).

It can also be noted that landscape aggregation has only little impact on spore production P_{end} . For the three aggregation levels tested (Figure 13, middle column), P_{end} remains close to the average value between a high and a low homogeneous landscape. We observe however a slight increase of spores production with a lower aggregation. In this later case, low fertilization fields receive a lot of spores from highly sporulating high fertilization neighbours and this explains why mean P_{end} of the heterogeneous landscape is slightly increasing with decreasing landscape aggregation.

The effect of landscape heterogeneity in the transients, so to say the efficacy of the pathogen to colonize the landscape, shows interesting results. Figure 14 shows the effect of

landscape heterogeneity on the speed of landscape colonization (approximated by the time the system needs to reach equilibrium). A low fertilization ($F=6$) homogeneous landscape is the longest to colonize for a pathogen strain with $\lambda = 130$ dd (48 seasons, also visible in Figure 10, left column). To the contrary, a high fertilization landscape ($F=10$) is the more quickly colonized by a pathogen with this latent period (10 seasons). The colonization times of the five tested heterogeneous landscapes lay between these two values. As for AUDPC at equilibrium, the results depend on landscape composition, but here on the contrary of what has been observed of AUDPC, it also depends on landscape aggregation.

A low aggregation landscape and a 20(F6)/80(F10) landscape are almost as quickly colonized as the high fertilization homogeneous landscape. In both cases, this is because the landscape dynamics is dominated by the dynamics of the strongly sporulating fields (either because of high field types proximity in the low aggregation landscape, or because high sporulating fields occupy the majority of the landscape). However, colonization of a high aggregation or a 20(F10)/80(F6) landscape is twice as long.

The effect of high aggregation on the delayed duration to equilibrium is illustrated in the Figure 15. A gradient of epidemic intensity established between the centres of high fertilisation and low fertilization field clusters appears in the figure. Fields near the edge of the high fertilization clusters receive more spores (and thus are more rapidly infected) than fields further in the low-fertilisation part of the landscape. Within these fields, the progression of the pathogen is almost as slow as in a low fertilization homogeneous landscape. Once again, this effect vanishes if both types of fields display similar spore production (Figure SM2).

To summarise, we have found that:

- (1) Introducing low fertilisation fields in the landscape (considering a latent period of 130) allow to strongly decrease the average level of epidemics in the landscape compared to an homogenous landscape with only high fertilisation fields,
- (2) However, this decrease is almost proportional to the proportion of each fertilisation, with almost no additional (non-linear) effect of heterogeneity (with AUDPC in each fertilisation type being almost similar to a homogeneous landscape),
- (3) There is an effect of the level of aggregation and of the proportion on the duration to colonize the landscape. We found a longer transient for low aggregation and for higher

proportion of low fertilisation fields in the landscapes. This result could be interesting in the view of protecting the landscape for a certain period.

Landscape heterogeneity and crop loss

In this part of the results our aim is to pass from epidemics-oriented analyses to more damage-oriented analyses. Fungal foliar pathogens are known to reduce biomass and consequently yield by decreasing leaf area (Robert et al., 2004; Bancal et al., 2007). This is why we use the reduction in green leaf area to estimate biomass loss due to the epidemics. Here we study (1) the loss in green leaf area that we interpret as crop loss (Figure 16) and (2) the integrated green leaf area that we interpret as the accumulated biomass (Figure 17) (and therefore proportional somehow to the yield).

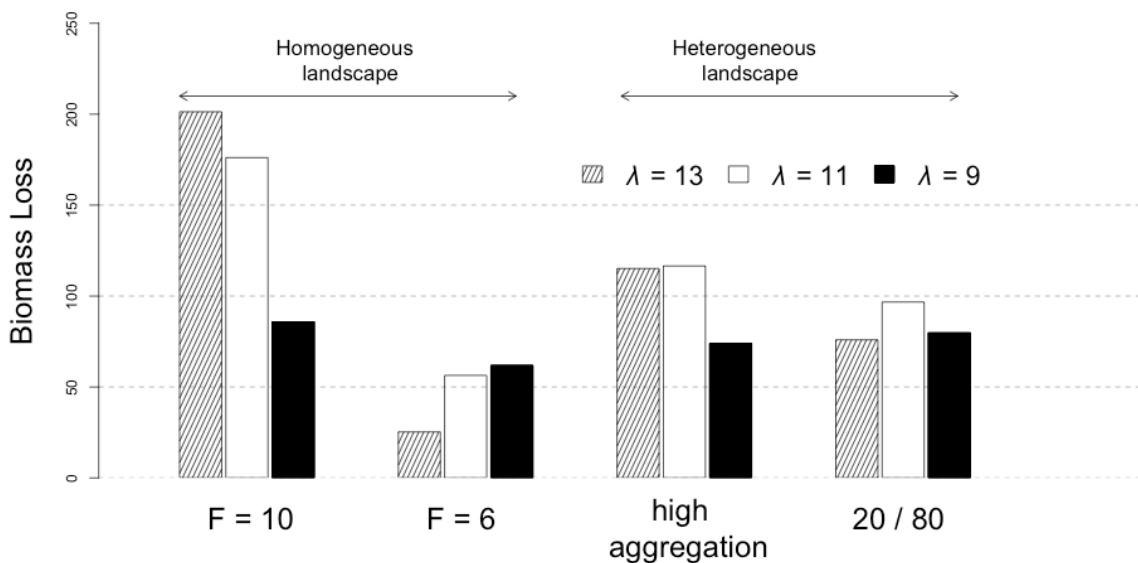


Figure 16: effect of spatial heterogeneity on disease-induced green leaf area reduction for different pathogen strains. Here we compare the reduction of green leaf area in high fertilization ($F = 10$) and low fertilization ($F = 6$) homogeneous landscapes, a high aggregation heterogeneous landscape with 50/50 field proportion and a medium aggregation landscape with 20% of high fertilization fields and 80% of low fertilization ones. The first two columns correspond to landscapes colonized by only one pathogen strain, with either $\lambda = 130$ dd or $\lambda = 90$ dd.

Figures 16 and 17 show the combined effects of latent period and fertilization on green leaf area loss (also referred to as biomass loss) and accumulated green leaf area (also referred to as accumulated biomass) respectively in both homogeneous and heterogeneous landscapes. The biomass loss is maximal in a high fertilization homogeneous landscape ($F = 10$) and

decreases with pathogen latent period. Loss is much smaller in a low fertilization homogeneous landscape and for this fertilisation it increases with latent period. For a given latent period, crop losses in heterogeneous landscape are always close to the average value of these extremes. Note that the contrast between homogeneous and heterogeneous landscapes is more pronounced as latent period increases (Figure 16).

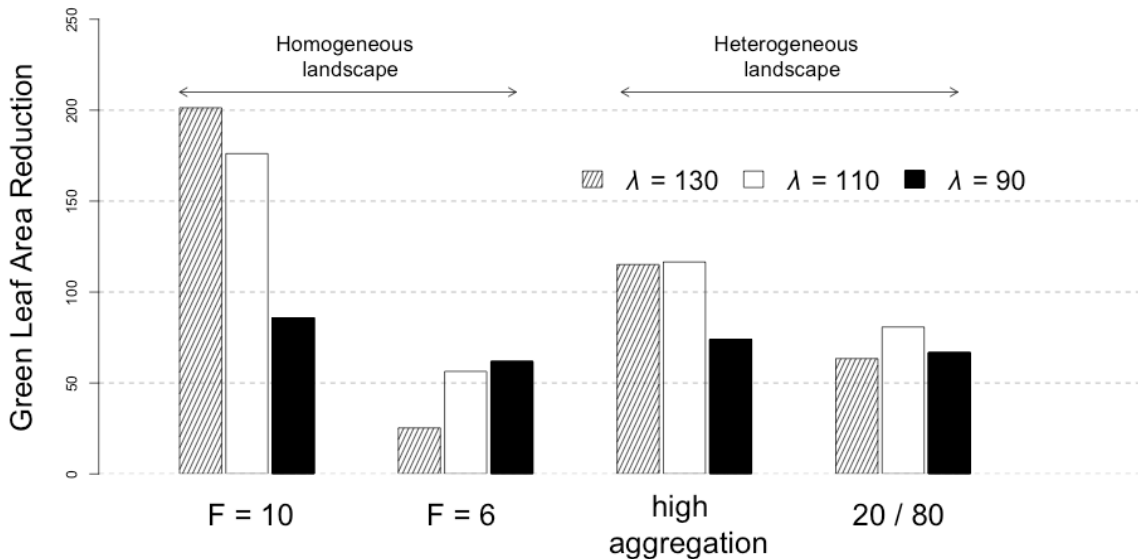


Figure 17: effect of spatial heterogeneity on infected canopy green leaf area index (GLAI) for different pathogen strains. Here we compare per patch average yields in high fertilization ($F = 10$) and low fertilization ($F = 6$) homogeneous landscapes, a high aggregation heterogeneous landscape with 50/50 field proportion and a medium aggregation landscape with 20% of high fertilization fields and 80% of low fertilization ones.

The biomass accumulated in the infected canopy (Figure 17) shows the opposite responses to latent period and sporulation to the biomass loss since given the landscape's fertilization level(s) both quantities sum up to the total biomass of the equivalent healthy landscape. Even if crop loss is much higher in high fertilisation, accumulated biomass is not so low in high fertilisation. So, what you will choose depends on what you look at.

Evolutionary responses of pathogens to fertilization

The combined effects of latent period and fertilization on the three empirical fitness measures are given in Figure 8 (for individual fields) and Figure 11 (for homogeneous landscapes). Whatever the scale and the fertilization level, these curves allow for the

identification of a latent period maximizing the fitness measures: the optimal latent periods. Provided the empirical latent periods are well suited to describe the adaptation of the pathogen to their environment, the relations between optimal latent periods and fertilization levels correspond to a putative directions of pathogen evolution.

These relations are given in Figure 9 for pathogens in individual fields. Optimal latent periods vary from 80 dd at $F = 4$ to 140 dd for $F = 10$. We thus obtain a linearly increasing relation between each of the three fitness measures and the level of fertilization. When AUDPC is used as a fitness measure, the optimal latent periods are quite consistently a bit shorter than the ones associated with spore productions (except at $F = 4$ where epidemics are of very limited magnitude). Results are very similar for optimal latent periods in homogeneous landscapes (Figure 12). Latent periods associated with both spore productions are even exactly the same as in individual fields. We then get a similar evolutionary trend at the scale of a homogeneous landscape than at the scale of a single isolated field.

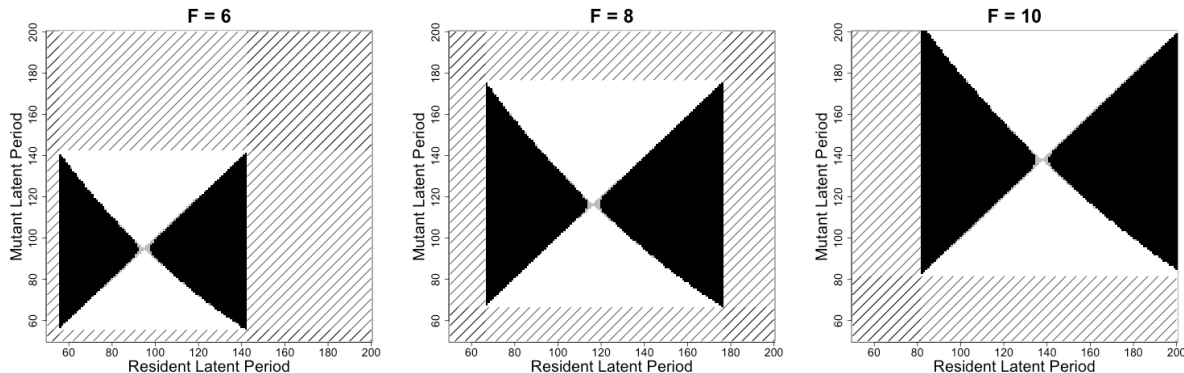


Figure 18: field-level pairwise invisibility plots for three fertilization levels. From left to right: $F = 6$; $F = 8$ and $F = 10$. Black area correspond to winning mutant strategies while white area correspond to mutants unable to invade the resident population. Similar strategies on the first diagonal have been highlighted in grey for the sake of clarity. Corresponding evolutionary singular strategies are 9.5, 11.7 and 13.8 for fertilization levels 6, 8 and 10 respectively.

Results regarding the fourth fitness measure, invasion fitness from adaptive dynamics, take the form of pairwise invisibility plots (PIPs) represented in Figures 18 (individual fields with various fertilization levels), Figure 19 (homogeneous landscapes with various fertilization levels) and Figures 20 to 22 (heterogeneous landscapes with various aggregation levels). PIPs represent the outcome of the invasion process between a resident and a mutant pathogen strain that are completely identical but in their latent period. For each value of the latent period λ_1 of the resident strain, it says which of the possible mutant strains

with latent periods λ_2 are capable of invading the environment defined by the resident. Since the resident population dynamic is at equilibrium, the fitness of the resident population is 0. Mutants capable of invading the resident population increase in frequency in the landscape, so they have a positive invasion fitness. Conversely, mutants that are not capable of invading the resident population have a negative invasion fitness. Areas of the PIPs corresponding to mutants with positive invasion fitness are in black. The areas with negative invasion fitness are left blank. By definition, the invasion fitness equals zero along the diagonal where the resident and mutant strains are identical. The limits between area with positive and negative invasion fitness are called zero-isoclines. Their intersection with the diagonal defines an evolutionarily singular point. If this singular point is attractive (convergent stable along the diagonal), it represents the latent period λ^* towards which evolution will be driven in the first place. The PIPs in Figure 18 and 19 show that the singular point λ^* is always convergent stable, as well as evolutionarily stable. These λ^* are hence all ESS. We find $\lambda^* = 95$ dd at $F = 6$, $\lambda^* = 117$ dd at $F = 8$ and $\lambda^* = 138$ dd at $F = 10$ in individual fields, and $\lambda^* = 100$ dd at $F = 6$, $\lambda^* = 120$ dd at $F = 8$ and $\lambda^* = 140$ dd at $F = 10$ in homogeneous landscapes. These values (among others) have been reported on Figures 9 and 12 (blue stars). At both scales, the ESS follow the same patterns as and are almost confounded with the optimal latent periods with either spore production as a fitness measure.

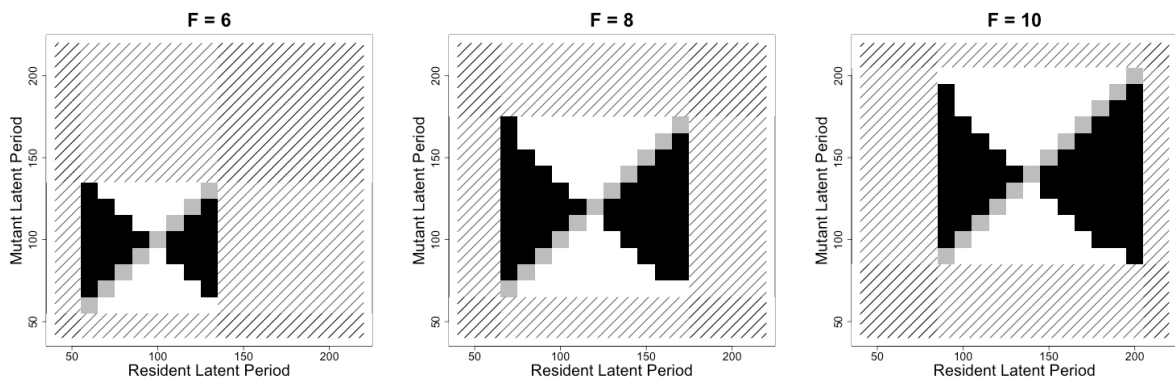


Figure 19: pairwise invisibility plots for three fertilization homogeneous landscapes. From left to right: $F = 6$; $F = 8$ and $F = 10$. Black area correspond to winning mutant strategies while white area correspond to mutants unable to invade the resident population. Similar strategies on the first diagonal have been highlighted in grey for the sake of clarity. Corresponding evolutionary singular strategies are 10, 12 and 14 for fertilization levels 6, 8 and 10 respectively.

Results regarding the fourth fitness measure, invasion fitness from adaptive dynamics, take the form of pairwise invisibility plots (PIPs) represented in Figures 18 (individual fields

with various fertilization levels), Figure 19 (homogeneous landscapes with various fertilization levels) and Figures 20 to 22 (heterogeneous landscapes with various aggregation levels). PIPs represent the outcome of the invasion process between a resident and a mutant pathogen strain that are completely identical but in their latent period. For each value of the latent period λ_1 of the resident strain, it says which of the possible mutant strains with latent periods λ_2 are capable of invading the environment defined by the resident. Since the resident population dynamic is at equilibrium, the fitness of the resident population is 0. Mutants capable of invading the resident population increase in frequency in the landscape, so they have a positive invasion fitness. Conversely, mutants that are not capable of invading the resident population have a negative invasion fitness. Areas of the PIPs corresponding to mutants with positive invasion fitness are in black. The areas with negative invasion fitness are left blank. By definition, the invasion fitness equals zero along the diagonal where the resident and mutant strains are identical. The limits between area with positive and negative invasion fitness are called zero-isoclines. Their intersection with the diagonal defines an evolutionarily singular point. If this singular point is attractive (convergent stable along the diagonal), it represents the latent period λ^* towards which evolution will be driven in the first place. The PIPs in Figure 18 and 19 show that the singular point λ^* is always convergent stable, as well as evolutionarily stable. These λ^* are hence all ESS. We find $\lambda^* = 95$ dd at $F = 6$, $\lambda^* = 117$ dd at $F = 8$ and $\lambda^* = 138$ dd at $F = 10$ in individual fields, and $\lambda^* = 100$ dd at $F = 6$, $\lambda^* = 120$ dd at $F = 8$ and $\lambda^* = 140$ dd at $F = 10$ in homogeneous landscapes. These values (among others) have been reported on Figures 9 and 12 (blue stars). At both scales, the ESS follow the same patterns as and are almost confounded with the optimal latent periods with either spore production as a fitness measure.

The PIPs obtained for heterogeneous landscapes (Figures 20 to 22, top-left panels) appear quite unusual. It is impossible to identify a singular strategy because the zero isoclines are not continuous. In fact, the PIP of Figure 20 shows that its structure corresponds to the zero isoclines of low and high fertilization field-scale PIPs from Figure 18.

To further understand the shape of these PIPs, we need a closer look at the relation between mutant and resident invasion fitness near the centre of the PIPs. For a given mutant pathogen strain ($\lambda = 100$ dd for example), the direction of evolution is decided by the slope of invasion fitness (which corresponds to the form of the selection gradient) in the vicinity of

the point Λ where $\lambda_{\text{mutant}} = \lambda_{\text{resident}}$. If invasion fitness of the mutant is negative on both sides of Λ (all mutants with $\lambda_{\text{mutant}} \sim \Lambda$ are unable to invade), then no invasion is possible and there will be no evolution. The value $\lambda = \Lambda$ is then an evolutionarily stable strategy, as in all PIPs at the field-scale and in homogeneous landscapes. If invasion fitness of the mutant is negative on the left [the right] of Λ and positive on its right [left] (only mutants with $\lambda > \Lambda$ [$\lambda < \Lambda$] can invade), then λ will evolutionarily increase [decrease]. In that case, the strategy $\lambda = \Lambda$ is not a singular strategy. Finally, if invasion fitness of the mutant is positive on both sides of Λ (all mutants with $\lambda_{\text{mutant}} \sim \Lambda$ are able to invade), the strategy $\lambda = \Lambda$ is a singular strategy that allows for the coexistence of several pathogen strains with λ close to Λ , possibly leading to speciation. Such strategy is called an evolutionary branching point (EBP).

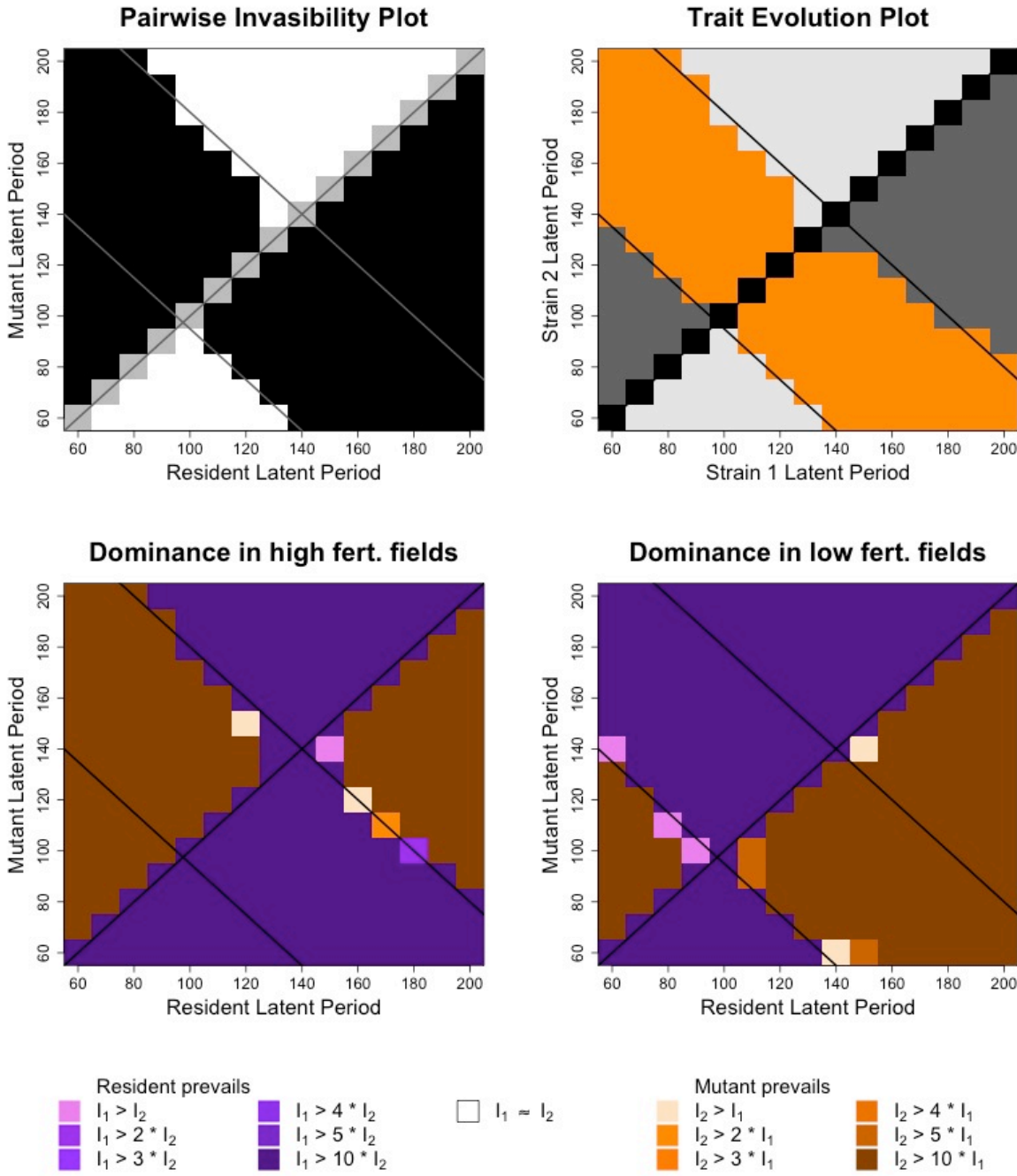


Figure 20: pairwise invasibility plot (PIP), trait evolution plot (TEP) and dominance plots for a high aggregation heterogeneous landscape with a 50/50 percentage of patch types. Top-left: PIP. Black areas correspond to mutant strategies capable to invade the resident population. White areas correspond to mutants that fail in the invasion process. The first diagonal has been highlighted in grey for the sake of clarity. Top right: TEP. Light grey areas correspond to strategies where only strain 1 can invade strain 2. Dark grey areas correspond to strategies where only strain 2 can invade strain 1. Orange areas correspond to strategies allowing for mutual invisibility, that is coexistence in adaptive dynamics. The first diagonal has been highlighted in black for the sake of clarity. Bottom left: dominance in the high fertilization fields of the heterogeneous landscape 100 seasons after the start of the epidemics. Warm colours indicate dominance by the mutant strain. Cold colours indicate dominance by the resident strain. White area indicate even coexistence. Bottom right: dominance in the low fertilization fields of the heterogeneous landscape 100 seasons after the start of the epidemics. The legend is the same for both coexistence plots. In this figure, I_1 and I_2 refer to the AUDPCs of the resident and mutant strains respectively. The first diagonal and the zero isoclines from field-scale PIPs ($F = 6$ and $F = 10$) have been superimposed as solid grey or black lines on all subplots for the sake of interpretation.

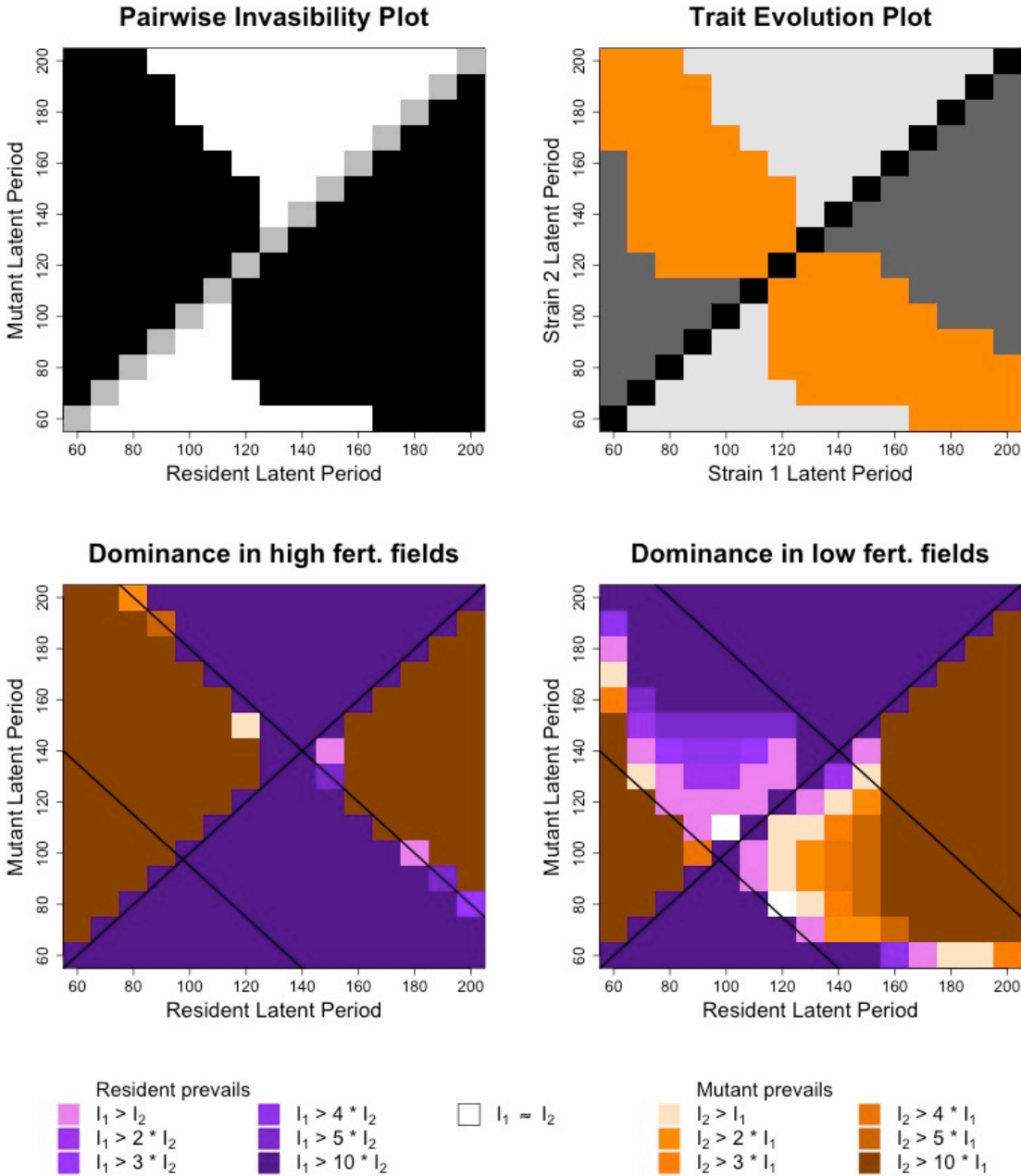


Figure 21: pairwise invasibility plot (PIP), trait evolution plot (TEP) and dominance plots for a medium aggregation heterogeneous landscape with a 50/50 percentage of patch types. Top-left: PIP. Black areas correspond to mutant strategies capable to invade the resident population. White areas correspond to mutants that fail in the invasion process. The first diagonal has been highlighted in grey for the sake of clarity. Top right: TEP. Light grey areas correspond to strategies where only strain 1 can invade strain 2. Dark grey areas correspond to strategies where only strain 2 can invade strain 1. Orange areas correspond to strategies allowing for mutual invisibility, that is coexistence in adaptive dynamics. The first diagonal has been highlighted in black for the sake of clarity. Bottom left: dominance in the high fertilization fields of the heterogeneous landscape 100 seasons after the start of the epidemics. Warm colours indicate dominance by the mutant strain. Cold colours indicate dominance by the resident strain. White area indicate even coexistence. Bottom right: dominance in the low fertilization fields of the heterogeneous landscape 100 seasons after the start of the epidemics. The legend is the same for both coexistence plots. In this figure, I_1 and I_2 refer to the AUDPCs of the resident and mutant strains respectively. The first diagonal and the zero isoclines from field-scale PIPs ($F = 6$ and $F = 10$) have been superimposed as solid grey or black lines on both dominance plots for the sake of interpretation.

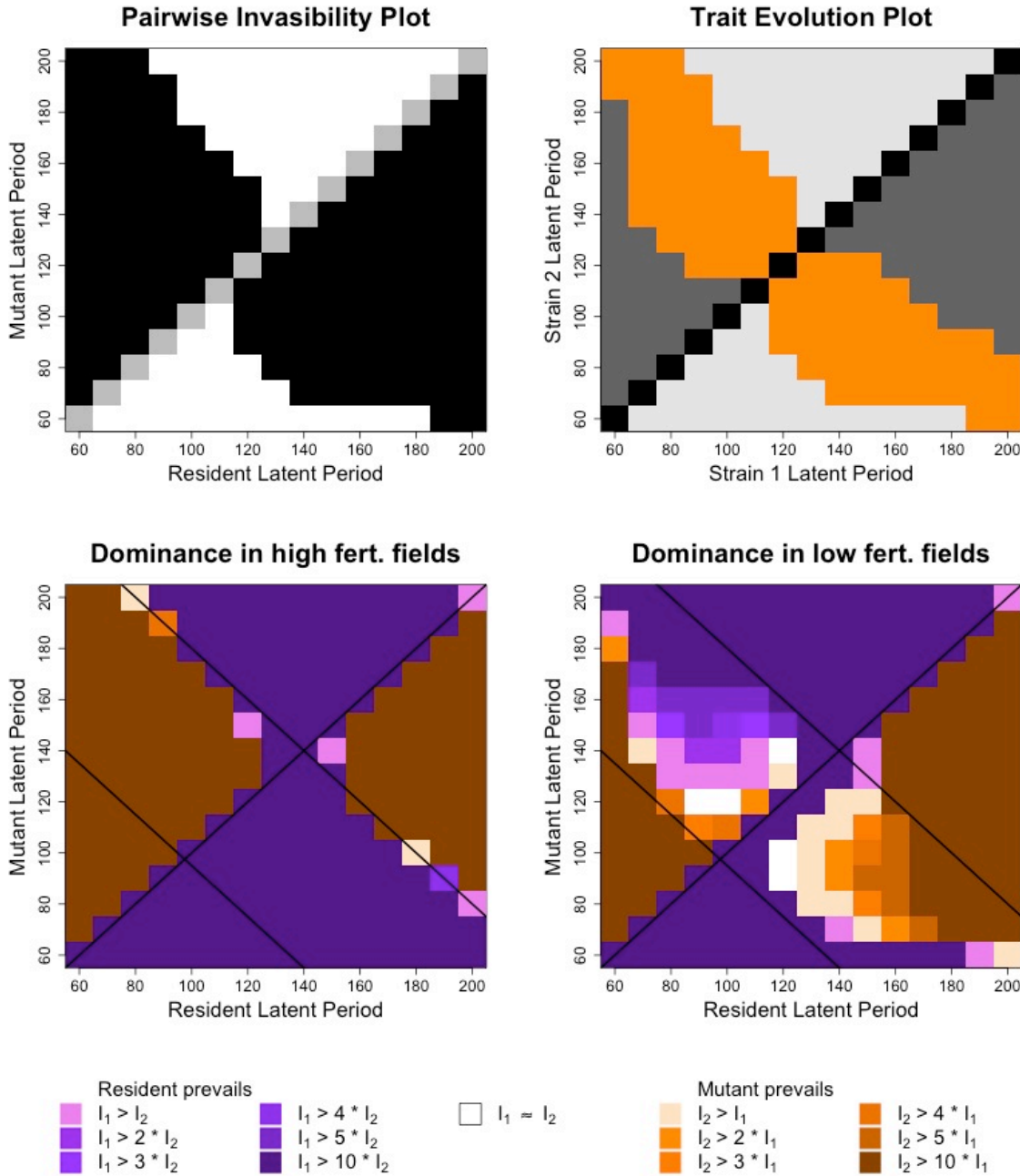


Figure 22: pairwise invasibility plot (PIP), trait evolution plot (TEP) and dominance plots for a low aggregation heterogeneous landscape with a 50/50 percentage of patch types. Top-left: PIP. Black areas correspond to mutant strategies capable to invade the resident population. White areas correspond to mutants that fail in the invasion process. The first diagonal has been highlighted in grey for the sake of clarity. Top right: TEP. Light grey areas correspond to strategies where only strain 1 can invade strain 2. Dark grey areas correspond to strategies where only strain 2 can invade strain 1. Orange areas correspond to strategies allowing for mutual invisibility, that is coexistence in adaptive dynamics. The first diagonal has been highlighted in black for the sake of clarity. Bottom left: dominance in the high fertilization fields of the heterogeneous landscape 100 seasons after the start of the epidemics. Warm colours indicate dominance by the mutant strain. Cold colours indicate dominance by the resident strain. White area indicate even coexistence. Bottom right: dominance in the low fertilization fields of the heterogeneous landscape 100 seasons after the start of the epidemics. The legend is the same for both coexistence plots. In this figure, I_1 and I_2 refer to the AUDPCs of the resident and mutant strains respectively. The first diagonal and the zero isoclines from field-scale PIPs ($F = 6$ and $F = 10$) have been superimposed as solid grey or black lines on both dominance plots for the sake of interpretation.

Figure 23 provides us with the fitness curves of mutant strains invading five resident populations whose latent period is comprised between the ESS of the field-scale PIPs. Invasion fitness of the mutant is negative for $\lambda < \Lambda = 10$ and $\lambda < \Lambda = 11$ while it is positive for $\lambda > \Lambda = 10$ and $\lambda > \Lambda = 11$ (Figures 23A and B). Mutants with longer latent periods should then be able to replace residents playing these strategies. Conversely, invasion fitness of the mutant is positive for $\lambda < \Lambda = 13$ and $\lambda < \Lambda = 12$ while it is negative for $\lambda > \Lambda = 13$ and $\lambda > \Lambda = 12$ (Figures 23D and E). Mutants with shorter latent periods should then be able to replace residents playing these strategies. Invasion fitness of the mutant is positive on both sides of $\Lambda = 11.8$ (Figure 23C) making that strategy an evolutionary branching point. We can then assume the PIPs of Figures 20 to 22 then resemble the theoretical example of Figure 24, though the rough scaling of our latent period grid (constrained by the time of simulation) does not allow to recognise it. Thus all PIPs in Figures 20 to 22 share the same EBP at $\lambda^* = 11.8$. The singular strategies in heterogeneous landscapes thus do not depend on the aggregation level, nor does it depend on the percentage of patch types (Figures SM3 and SM4). Note that this value is close to the ESS of an individual field at $F=8$ ($\lambda^* = 11.6$, Figure 9).

Following invasion, a mutant strain with positive invasion fitness may either coexist with the resident in various proportions in the field or in the landscape, or completely replace the resident. The trait evolution plots (TEPs) of Figures 20 to 22 (top-right panels) show in orange the combinations of mutant and resident latent periods that are mutually capable of invading each other. In adaptive dynamics, coexistence is defined as mutual invasibility. Thus, orange areas in TEPs correspond to coexistence domains. Coexistence is expected when the singular point is an evolutionary branching point. Theory even tells us that such coexistence will be evolutionary stable (Geritz et al 1998). Even if the EBP is the same whatever the aggregation level, we note that the size of the coexistence areas increases with the level of field aggregation. We also note that the coexistence areas are included within the space delimited by the imaginary lines corresponding to the zero isoclines of the field-scale PIPs. Finally, we note that there was no coexistence in either individual fields or homogeneous landscapes (data not shown).

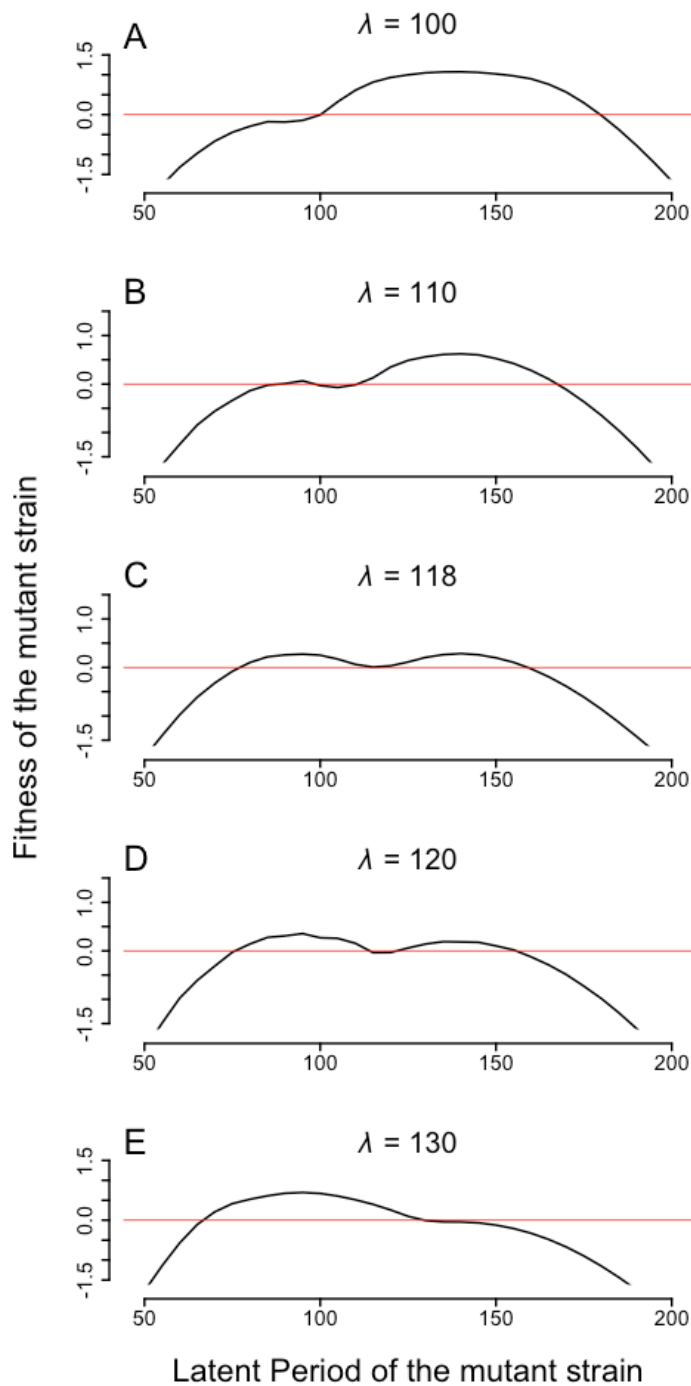


Figure 23: fitness curves of five mutant strains with various latent periods invading resident population with a given value of $\lambda_{\text{resident}}$ in a heterogeneous landscape. Landscape aggregation level is 7.3 similar neighbours in average (high aggregation) with even proportions of field types. A: $\lambda_{\text{resident}} = 10$; B: $\lambda_{\text{resident}} = 11$; C: $\lambda_{\text{resident}} = 11.8$; D: $\lambda_{\text{resident}} = 12$ and E: $\lambda_{\text{resident}} = 13$. This scenario is the same as in Figure 18.

By construction, PIPs do not show the outcome of between-strain competition since it is assumed the mutant strain has no impact on density dependence. To know the outcome of the competition between the resident and the mutant strain, we must turn to the dominance plots of Figure 20 to 22. The zero isoclines of the field-scale PIPs have been superimposed on

the dominance plots for the sake of interpretation. The high fertilization fields of the heterogeneous landscapes function like high fertilization individual fields and homogeneous landscapes (Figure 20 to 22, bottom-left panels). The mutant strain outcompetes the resident in areas where the high fertilization field-scale PIP predicts mutant invasion. The resident outcompetes the mutant in other regions. Coexistence is rare in this part of the landscape and can be found (almost) exclusively along an imaginary line corresponding to the zero isocline of the field-scale PIP. The level of landscape aggregation has little effect on this type of fields. By contrast, the low fertilization fields in the heterogeneous landscape function like low fertilization individual fields and homogeneous landscapes (Figure 20 to 22, bottom-right panels). At high landscape aggregation level, the mutant strain outcompetes the resident only in areas where the high fertilization field-scale PIP predicts mutant invasion. As previously, coexistence is rare in this part of the landscape and can be found (almost) exclusively along an imaginary line corresponding to the zero isocline of the field-scale PIP. This changes drastically when the landscape aggregation level decreases. At both medium and low aggregation, a vast area located between the imaginary lines corresponding to the zero isoclines of the field-scale PIPs allows for pathogen coexistence. The spread of this area increases with decreasing aggregation level. In the other sections of the dominance plots, exclusion takes place as at high aggregation level. We found similar results when varying the percentage of patch types in the landscape. Results in the 20(F10)/80(F6) landscape were similar to those of the high aggregation one and results in the 20(F6)/80(F10) landscape were similar to those of the low aggregation one (Figures SM3 and SM4).

DISCUSSION

Spatial fertilization heterogeneity is beneficial through maladaptation

The numerous examples of crop resistance breakdown (Pretorius et al., 2000; Gassmann et al., 2009; Carrière et al., 2010; Singh et al., 2011, ...) and the spread of resistance to pesticides (Kato et al., 1997; Urban and Lebeda, 2006; Zhan et al., 2008; Corio-Costet et al., 2010; Karaoglanidis et al., 2010; Hobbelin et al., 2014; Estep et al., 2015, ...) are testimony of the high potential of pathogens to rapidly adapt to cultural practices (McDonald and Linde, 2002). In the aforementioned examples, pathogen adaptation can be as quick as a few years. After more than fifty years of intensive use of synthetic fertilizers, it is more than likely that pathogens currently impeding crop production are adapted to these high input levels. In our model, we use four fitness measures to study the adaptation of pathogens to fertilization: (i) annual spore production, (ii) spore production during crop growth, (iii) field colonization (AUDPC) and (iv) invasion fitness from adaptive dynamics. For the four of them, pathogen adaptation to high fertilization ($F=10$) in both individual fields and homogeneous landscapes corresponds to a pathogen strain with a latent period $\lambda=130$ dd. In the following, we consider this value as the current average phenotype of pathogen populations.

Considering strains with $\lambda=130$ dd, reducing fertilization from $F = 10$ to $F = 6$ in a homogeneous landscape results in dividing by tenfold the production of inoculum in the landscape (Figure 8). Foliar fungal pathogens typically cause polycyclic epidemics: many infection cycles come one after the other leading to an exponential production of inoculum and epidemic development (Agrios 2005). Reducing the amount of pathogen inoculum released into the landscape would then result in an exponential decrease of the disease. Another consequence of a decrease in fertilization level in a homogeneous landscape is a considerable reduction in the speed of landscape colonization (Figure 14). This reduction is of course largely related to the lesser production of inoculum. From an epidemiological point of view, if pathogen strains resistant to some fungicides or virulent towards some resistant crop cultivars appear in a low fertilization landscape, their takeover of the landscape would require a much longer period of time. This reduction of epidemics also has consequences on the production of biomass. Although it would bring biomass losses (estimated from green leaf area reduction, Figure 16) from 200 to less than 40 units of biomass, it would also lead to a

(12%) decrease of net biomass production (estimated from gLAI values in Figure 17). This is due to the high biomass production potential of the most fertilized fields, so productive compared with less fertilized ones that the high reduction in disease-related biomass losses does not compensate the reduction in biomass productivity. Thus, a reduction of the fertilization level in a homogeneous landscape, though reducing epidemics, does not come along with gains in biomass production.

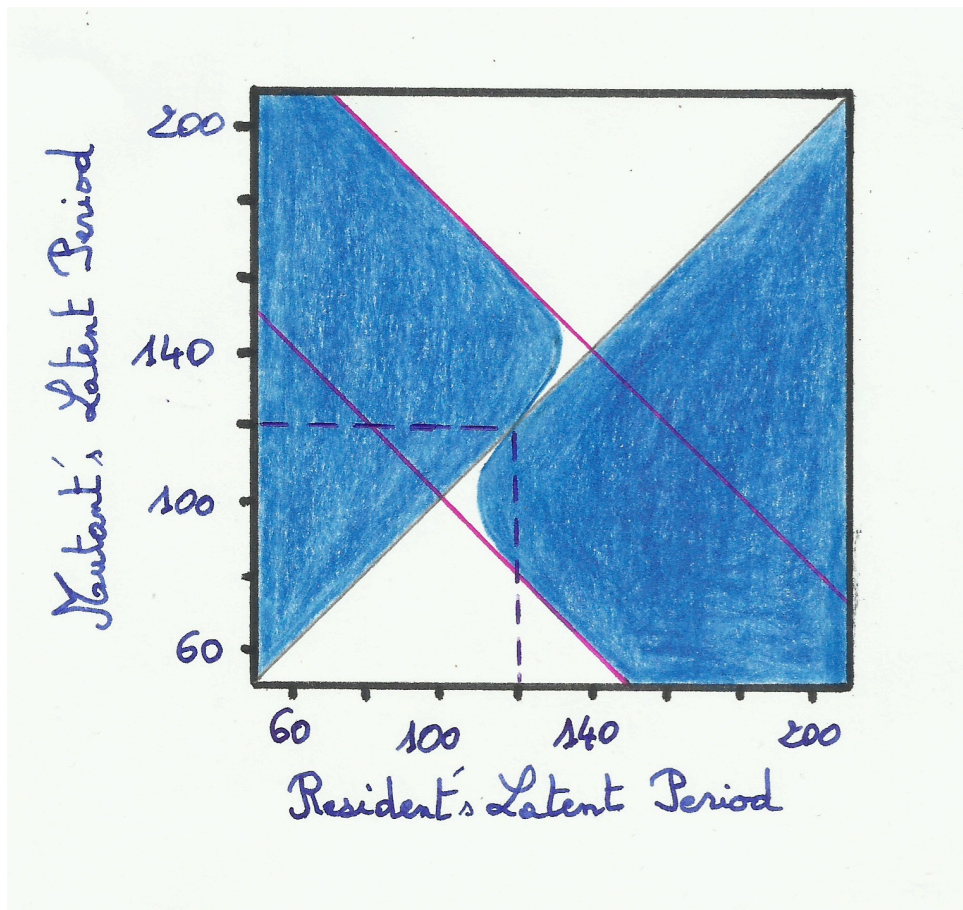


Figure 24: interpretation on the PIPs established for the heterogeneous landscapes of Figures 20 to 22. The first diagonal is in grey. Violet lines have been drawn where the zero isoclines of the field-scale PIPs (Figure 18, $F = 6$ and $F = 10$) would be. The dotted line gives the position of the evolutionary branching point ($\lambda^* \approx 12$). The blue areas represent mutant strains with positive invasion fitness, the white ones mutant strains with negative invasion fitness.

For heterogeneous landscapes we have shown that, in our model, most of the epidemiological variables behave as the average values between those in high and low fertilization homogeneous landscapes, weighted by the proportion of the landscape occupied by these types of fields (Figures 13, 14, 16 and 17). The consequences of considering a mosaic of fields with different fertilization levels will then have the same effect as reducing

the level of fertilization in a homogeneous landscape, though attenuated: the more the proportion of low fertilization fields in the landscape, the less the landscape-scale production of inoculum, and the slower the colonization of the landscape by the pathogen. Though these effects are less pronounced than in homogeneous landscapes, the exponential functioning of pathogens epidemics make it worth from an epidemiological point of view. In terms of biomass, both losses and production decrease when trading a high fertilization homogeneous landscape for a heterogeneous one. But in terms of biomass production, this corresponds to a decrease of only 6% (from 280.8 to 263.3 units of biomass, Figure 17) in a high aggregation landscape for example. Considering the costs of fertilizers and pesticides (and the environmental problems they cause) and the magnitude of losses reduction, this strategy may make sense from an sustainable point of view. Moreover, note that biomass is more sensitive to a decrease in fertilization than yield (Robert et al., 2004; Bancal et al., 2997). Moderately reducing fertilization (from $F = 10$ to $F = 6$ for instance) may cause biomass to decrease but may leave yields almost unaffected. In such a case, introducing fertilization heterogeneity in the landscape may prove to be quite advantageous.

These results are in line with several studies assessing the positive effect of landscape heterogeneity on the reduction of pest- or pathogen-induced crop damage. Using a theoretical model of pest spread, Alstad and Andow (1995) show that landscapes composed of both resistant transgenic maize and refuges of susceptible non-transgenic plants considerably slow down pest adaptation to insecticides through pest maladaptation. Papaïx et al. (2014) use a spatially explicit landscape model to show that increasing the proportion of the landscape covered with resistant crops decreases the probability of infection at the landscape scale. Sapoukhina et al. (2013) show that the careful use of several crop varieties with different levels of partial resistance can decrease epidemics up to 30%. Similarly, Garett and Mundt (1999) show that the spatial heterogeneity of a cultivar mixture creates a physical barrier to disease spread that reduce disease incidence at the landscape scale. In all cases, pathogen maladaptation in one compartment of the heterogeneous landscape is used to impede disease development, either through reduction of the production of inoculum (dilution effect) or by hindering pathogen dispersal (barrier effect) (Skelsey et al., 2010; Jones et al., 2011; Papaïx et al., 2014c). In our case, could low fertilization fields have the same effect on epidemics than crop resistance in the aforementioned models?

In our model, pathogen latent period and fertilization have a combined effect on disease development. As a result, a pathogen strain with a given latent period (let's say $\lambda=130$ dd) will perform differently in environments with different fertilization levels: its spore production will be maximum in environments with $F = 10$ but will be much less if forced into environments with $F = 6$ (Figures 8 and 11). Such local deviation from an adaptive peak due to a sudden environmental change could be referred as maladaptation (Crespi, 2000, Kalz et al., 1999; Adiba et al., 2010). Maladaptation is clearly visible in our model by comparing the green leaf area reduction or the gLAI of homogeneous landscapes attacked by pathogens with different latent periods in Figures 16 and 17. Because we constrained pathogen evolution by imposing a trade-off between latent period and spore production, for a given pathogen strain maladaptation can be defined as the difference between its spores production and its theoretically maximum spore production in its optimal environment. As pointed out in the Result section, all the benefits of landscape heterogeneity vanish when considering strains that perform quite similarly (similar spore production) in resource-rich and resource-poor environments, such as pathogen strains with $\lambda=90$ dd in SM1 and 2. Maladaptation effects are thus responsible for the beneficial effects of landscape heterogeneity.

The need to take into account pathogen adaptation

The precedent argumentation did not consider pathogen adaptation to landscape changes or heterogeneity. Figures 9 and 12 show that, considering any of the four fitness measures we used, latent period will evolutionarily decrease with fertilization in homogeneous environments (field or landscape). Given that $\lambda=130$ dd is the optimal strategy at $F = 10$, we can expect pathogen adaptation to lead to shorter latent periods, such as $\lambda=110$ dd or $\lambda=90$ dd, optimal strategies for $F = 8$ and $F = 6$ respectively. In a homogeneous environment with $F = 6$, (either homogeneous landscape or cluster of low fertilization patches in a heterogeneous landscape), decreasing latent period from 130 dd to 90 dd will result in increasing pathogen spore production. If we consider that no change in latent period has occurred for pathogens remaining in the resource-rich environments, the outcome of evolution has been a rebalancing in spore production capacity between the two strains, suppressing or strongly reducing the effects of maladaptation. In Figure 17 for example, a switch from $\lambda=130$ dd to $\lambda=90$ dd leads to a further decrease of biomass production in the $F = 6$ homogeneous landscape. From dominance plots of Figure 20, we can deduce that the outcome of the

competition between two pathogen strains with $\lambda=130$ dd and $\lambda=90$ dd respectively would be a mutual exclusion, with pathogen strain with $\lambda=130$ dd dominating the high fertilization fields and pathogen strain with $\lambda=90$ dd dominating the low fertilization ones. This scenario is represented in Figure 16 and 17 (last column). The amount of damage caused by the pathogen increases with adaptation compared with a scenario with only $\lambda=90$ dd but is always less than the losses in a high fertilization homogeneous landscape. Adaptation also reduces the gLAI in Figure 17 compared to a scenario with a single strain with $\lambda=90$ dd but interestingly, a high aggregation landscape with adaptation performs better than a high fertilization homogeneous landscape, whereas a 20/80 landscape does not.

In brief, pathogen evolution is mostly detrimental regarding the positive effects of landscape heterogeneity on epidemics. Note however that spatial heterogeneity buffers the sensibility of epidemiological variables to pathogen adaptation. For instance, the effect of latent period on both green leaf area reduction and gLAI is more pronounced in homogeneous than in heterogeneous landscapes (Figure 16 and 17).

Pathogen adaptation to landscape fertilization heterogeneity

Although the low resolution of Figures 20 to 22 does not allow to recognize it immediately, the fitness curves of Figure 23 give confirmation that the evolutionary singular point of the invasion analyses of heterogeneous landscapes is an evolutionary branching point (EBP). In Figure 24 we propose a sketch for interpreting the PIPs in Figures 20 to 22. In those figures, the position of the zero isoclines is primarily determined by the shape of the field-scale PIPs (violet lines in Fig 24), as if the PIP at the landscape scale is constructed as a superposition of the PIPs for low and high fertilization individual fields. The evolutionary branching point (EBP) is located at mid-distance between the theoretical positions of the field-scale ESSs. Interestingly, this position ($\lambda^* \approx 12$) corresponds to the ESS of a medium fertilization field ($F = 8$, Figure 12). The theory of adaptive dynamics tells us that the EBP is a convergent attractive equilibrium of the monomorphic (i.e., a single resident) dynamics. In a heterogeneous landscape composed of high and low fertilization fields, evolution thus converges to a pathogen strategy that would be optimal in medium fertilization, but that is maladapted in both high and low fertilization fields. Pathogen adaptation to spatial fertilization heterogeneity may thus be an asset for the reduction of epidemics through

maladaptation. But even if successful, would such a landscape management strategy be sustainable?

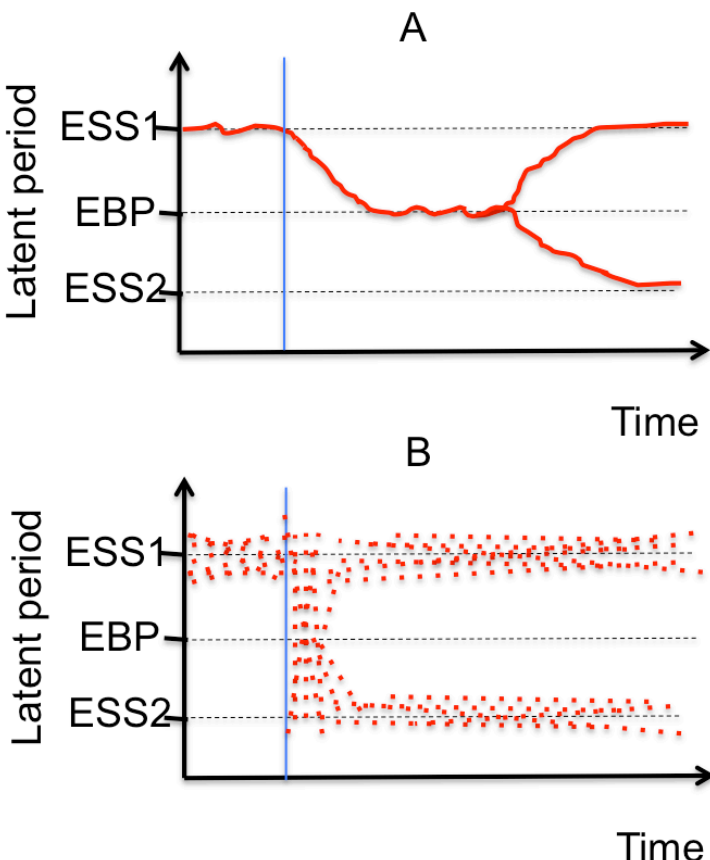


Figure 25: two scenarios of diversification in response to spatial fertilization heterogeneity depending on the size of mutation steps. A: small mutation steps; B: large mutation steps; EBP: evolutionary branching point identified in Figures 20 to 23; ESS1 and ESS2: evolutionary singular strategy identified in high ($F = 10$) and low ($F = 6$) fertilization fields in Figure 18.

If evolution proceeds only by small, rare mutations (under low genetic variation) from the initial latent period $\lambda=130$ dd, pathogen latent periods should first converge towards the EBP before evolutionary branching may potentially occur (Figure 25A). Speciation may then lead to the evolutionarily stable coexistence of two strains with distinct latent periods, with both fertilization levels corresponding to the respective niches of these strains. Depending on the duration of the pre-speciation period, during which the pathogen population converges to the EBP, and may drift around this point for extended periods (Claessen et al 2008), maladaptation is likely to occur and landscape fertilization heterogeneity may be a lever to play on the regulation of epidemics. After speciation has occurred, the protection of crops due

to maladaptation will be lost and the two “sister-strains” will likely display latent periods corresponding to the ESS of the individual fields.

If evolution proceeds by larger steps and/or at a higher rate (under high genetic variation) however, introducing heterogeneity in the landscape may immediately result in the appearance of a large spectrum of latent periods and the selection of two populations in each of the fertilization niches (Figure 25B). In that scenario, there is no period of pathogen maladaptation, and thus little positive effects of landscape heterogeneity on epidemics. It is difficult to say which scenario is the most likely. Rusts display very high genetic diversity in the field (McDonald and Linde, 2002) but their latent periods are surprisingly conserved (roughly between 150 and 200 dd, see chapter 5) for pathogens having experienced such an evolutionary radiation on very different host plants families. If increasing heterogeneity at the landscape scale comes down to providing the pathogen with a growing number of niches, we may increase even more the phenotypic and genetic diversity of pathogen populations, and thus impeding directional evolution that drives crop resistance breakdown and the evolution of resistance to fungicides. These scenarios could be explored using an eco-evolutionary modelling approach, complementary to the adaptive dynamics approach, that allows for ecological (epidemiological) and evolutionary processes on similar time scales (Lion and Gandon 2016, Sauterey et al 2017).

CONCLUSION

In this chapter, we have addressed the question of the impact of crop fertilization practices at the landscape scale on the epidemiology and evolution of leaf fungal pathogens using a model of landscape epidemiology. The landscape is depicted as a mosaic of individual fields, with either high or low fertilization and a corresponding crop dynamics. As in the previous chapters, we focus on the trophic aspects of the host-pathogen interaction: the amount of green leaf area of each field representing the resource available to the pathogen. Fields at the landscape scales are linked together through pathogen dispersal and function like a meta-population of pathogen resource patches. Within each individual field, the development of the pathogen follows a classical SEIR epidemiological model.

We use this model to investigate how the heterogeneity in landscape fertilization influences the epidemics and pathogen adaptation. We find that when pathogen maladaptation is possible (i.e. if a pathogen strain with a given latent period is significantly less competitive in some resource environments than in others), high aggregation landscapes and heterogeneous landscapes dominated by low fertilisation patches (20/80%) reduce the quantity of inoculum released in the landscape and slow down the colonization of the landscape by the pathogen. These effects vanish when pathogens adapt to their new environment. In our model, the coexistence of two strains with different latent periods is possible and evolutionarily stable in our model: in response to spatial fertilization heterogeneity, pathogens may undergo a process of evolutionary branching to fill the available niches in the landscape. It may be possible to use landscape fertilization heterogeneity as a lever to reduce pathogen epidemics, but this alone is likely not to be sufficient. It may however prove useful in combination with other types of spatial and temporal heterogeneity that promote local pathogen maladaptation.

SUPPLEMENTARY MATERIALS

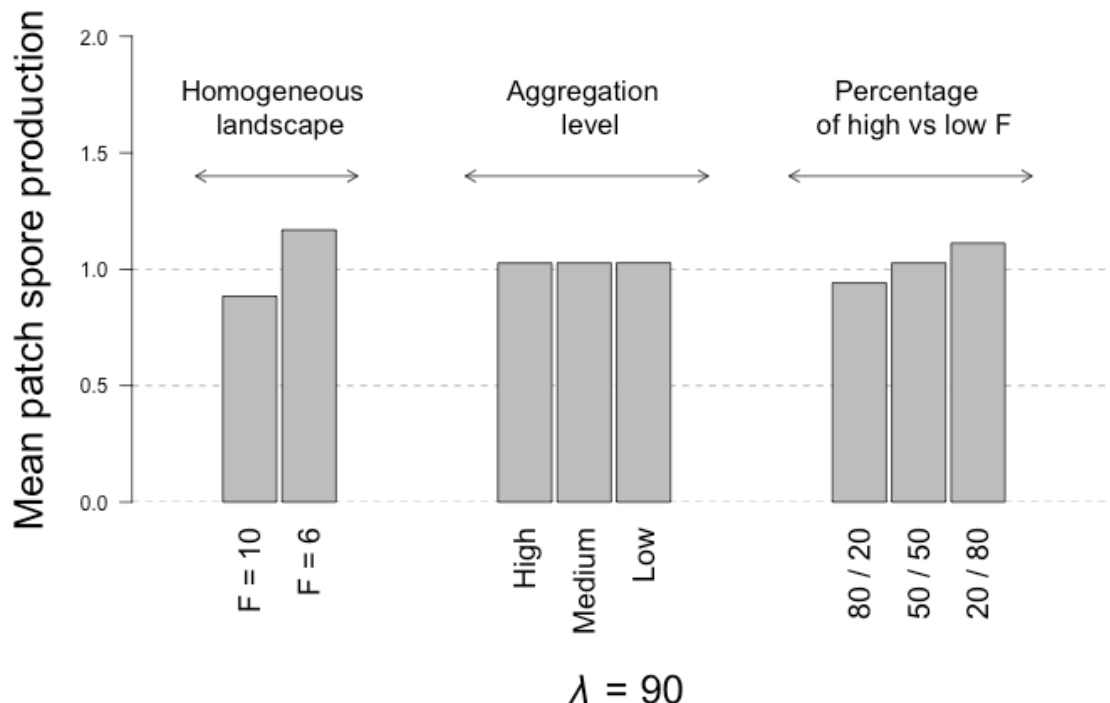


Figure SM1: effect of spatial heterogeneity on landscape-scale spore production at equilibrium for $\lambda = 90$ dd. Here, we compare homogeneous landscapes with high ($F = 10$) and low ($F = 6$) fertilization and heterogeneous landscapes with various aggregation levels or various proportions of field types. The aggregation level is the same in landscapes with different field type proportions (medium aggregation) and reciprocally, the proportion of fields of each type is the same in landscapes with different aggregation levels (50/50). λ = pathogen latent period; F = fertilization level.

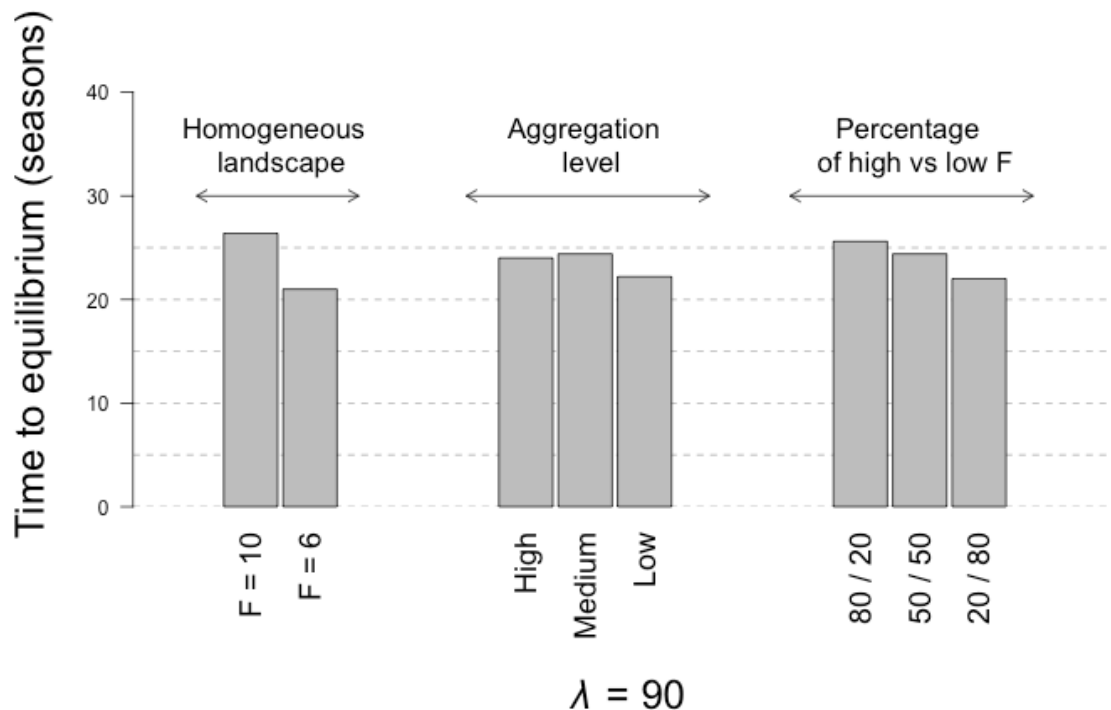


Figure SM2: effect of spatial heterogeneity on the speed of landscape colonization by the pathogen with $\lambda = 90$ dd, measured as the time for the epidemics to reach a steady state. Here, we compare homogeneous landscapes with high ($F = 10$) and low ($F = 6$) fertilization and heterogeneous landscapes with various aggregation levels or various proportions of field types. The aggregation level is the same in landscapes with different field type proportions (medium aggregation) and reciprocally, the proportion of fields of each type is the same in landscapes with different aggregation levels (50/50). Data are average values from 5 repetitions. λ = pathogen latent period; F = fertilization level.

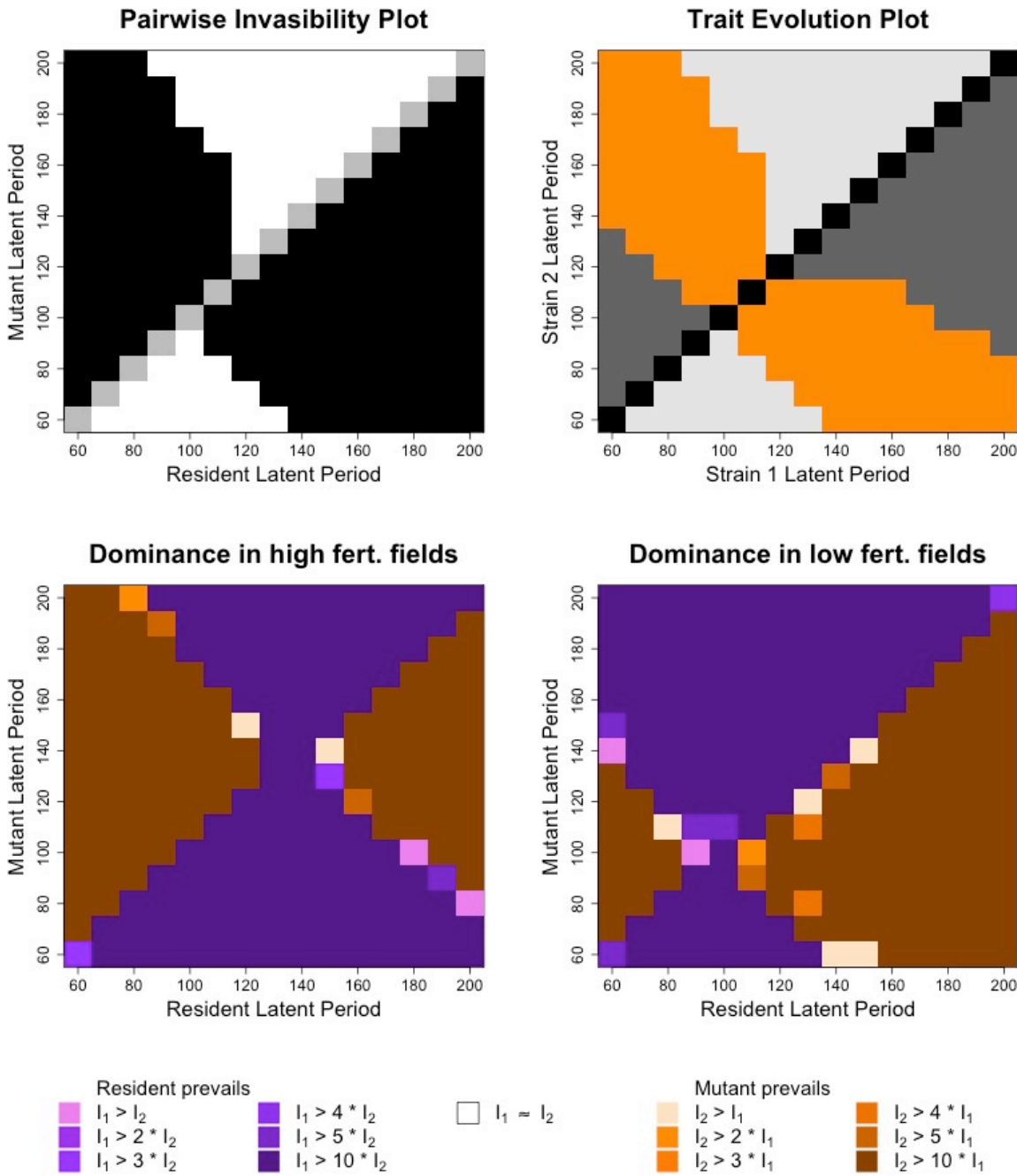


Figure SM3: pairwise invasibility plot (PIP), trait evolution plot (TEP) and dominance plots for a medium aggregation heterogeneous landscape with a 20(F10)/80(F6) percentage of patch types. Top-left: PIP. Black areas correspond to mutant strategies capable to invade the resident population. White areas correspond to mutants that fail in the invasion process. The first diagonal has been highlighted in grey for the sake of clarity. Top right: TEP. Light grey areas correspond to strategies where only strain 1 can invade strain 2. Dark grey areas correspond to strategies where only strain 2 can invade strain 1. Orange areas correspond to strategies allowing for mutual invisibility, that is coexistence in adaptive dynamics. The first diagonal has been highlighted in black for the sake of clarity. Bottom left: dominance in the high fertilization fields of the heterogeneous landscape 100 seasons after the start of the epidemics. Warm colours indicate dominance by the mutant strain. Cold colours indicate dominance by the resident strain. White area indicate even coexistence. Bottom right: dominance in the low fertilization fields of the heterogeneous landscape 100 seasons after the start of the epidemics. The legend is the same for both coexistence plots. In this figure, I_1 and I_2 refer to the AUDPCs of the resident and mutant strains respectively.

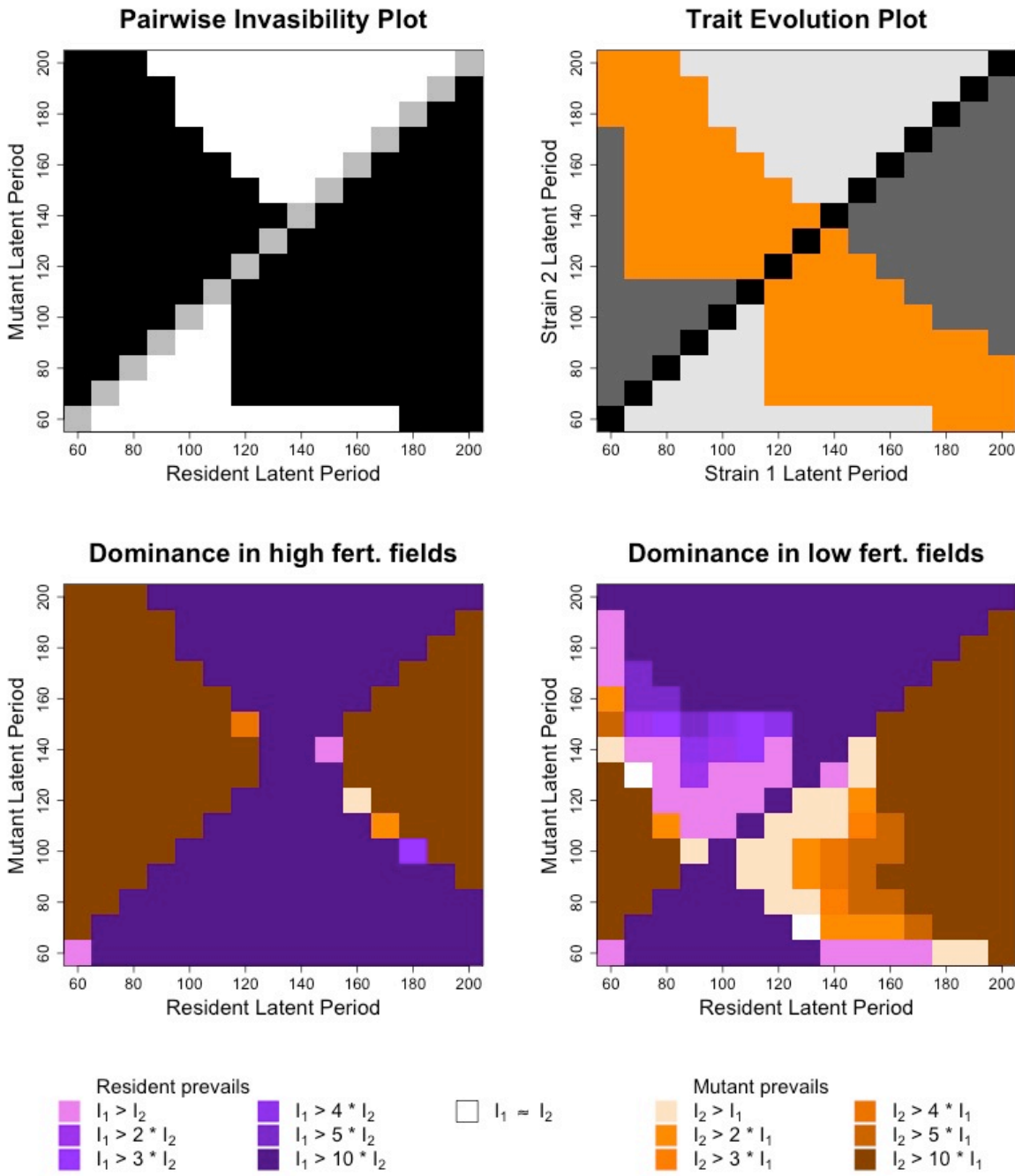


Figure SM4: pairwise invasibility plot (PIP), trait evolution plot (TEP) and dominance plots for a medium aggregation heterogeneous landscape with a 20(F6)/20(F10) percentage of patch types. Top-left: PIP. Black areas correspond to mutant strategies capable to invade the resident population. White areas correspond to mutants that fail in the invasion process. The first diagonal has been highlighted in grey for the sake of clarity. Top right: TEP. Light grey areas correspond to strategies where only strain 1 can invade strain 2. Dark grey areas correspond to strategies where only strain 2 can invade strain 1. Orange areas correspond to strategies allowing for mutual invisibility, that is coexistence in adaptive dynamics. The first diagonal has been highlighted in black for the sake of clarity. Bottom left: dominance in the high fertilization fields of the heterogeneous landscape 100 seasons after the start of the epidemics. Warm colours indicate dominance by the mutant strain. Cold colours indicate dominance by the resident strain. White area indicate even coexistence. Bottom right: dominance in the low fertilization fields of the heterogeneous landscape 100 seasons after the start of the epidemics. The legend is the same for both coexistence plots. In this figure, I_1 and I_2 refer to the AUDPCs of the resident and mutant strains respectively.

REFERENCES

1. Abro, M.A. (2013). Nitrogen fertilization of the host plant influences susceptibility, production and aggressiveness of *Botrytis cinerea* secondary inoculum and on the efficacy of biological control.
2. Adiba, S., Huet, M., and Kaltz, O. (2010). Experimental evolution of local parasite maladaptation. *Journal of Evolutionary Biology* 23, 1195–1205.
3. Agrios, G. N. 2005. Plant diseases caused by fungi. in: *Plant Pathology*, 5th ed. Academic Press, Cambridge, MA.
4. Alstad, D., and Andow, D. (1995). Managing the Evolution of Insect Resistance to Transgenic Plants. *Science* 268, 1894–1896.
5. Baccar, R., Fournier, C., Dornbusch, T., Andrieu, B., Gouache, D., and Robert, C. (2011). Modelling the effect of wheat canopy architecture as affected by sowing density on *Septoria tritici* epidemics using a coupled epidemic/virtual plant model. *Annals of Botany* 108, 1179–1194.
6. Bancal, M.O., Robert, C., and Ney, B. (2007). Modelling wheat growth and yield losses from late epidemics of foliar diseases using loss of green leaf area per layer and pre-anthesis reserves. *Annals of Botany* 100, 777–789.
7. Benbi, D.K. (1994). Prediction of leaf area indices and yields of wheat. *Journal of Agricultural Science* 122, 13–20.
8. Burdon, J.J., and Thrall, P.H. (2000). Coevolution at multiple spatial scales: *Linum marginale*-*Melampsora lini* - From the individual to the species. *Evolutionary Ecology* 14, 261–281.
9. Burdon, J.J., Zhan, J., Barrett, L.G., Papaïx, J., and Thrall, P.H. (2016). Addressing the Challenges of Pathogen Evolution on the World's Arable Crops. *Phytopathology* 106, 1117–1127.
10. Buschbell T., Hoffmann G.M. (1992) The effects of different nitrogen regimes on the epidemiologic development of pathogens on winter-wheat and their control. *Journal of Plant Diseases and Protection*, 99, 381–403.
11. Carrière, Y., Crowder, D.W., Tabashnik, B.E., 2010. Evolutionary ecology of insect adaptation to Bt crops. *Evol. Appl.* 3, 561–573.
12. Claessen, D., Andersson, J., Persson, L., De Roos, A. (2008). The Effect of Population Size and Recombination on Delayed Evolution of Polymorphism and Speciation in Sexual Populations. *The American Naturalist*, 172(1), E18-E34.
13. Corio-Costet, M.F., Dufour, M.C., Cigna, J., Abadie, P., and Chen, W.J. (2011). Diversity and fitness of *Plasmopara viticola* isolates resistant to QoI fungicides. *European Journal of Plant Pathology* 129, 315–329.
14. Cowling, S.A., and Field, C.B. (2003). Environmental control of leaf area production: Implications for vegetation and land-surface modeling - art. no. 1007. *Global Biogeochemical Cycles* 17, 1007.
15. Crespi, B.J. (2000). The evolution of maladaptation. *Heredity* 84, 623–629.
16. Dieckman, U., Doebeli, M., Dieckmann, U., and Doebeli, M. (1999). On the origin of species by sympatric speciation. *Nature* 400, 354–357.
17. Drecer, M. (2000). Dynamics of Vertical Leaf Nitrogen Distribution in a Vegetative Wheat Canopy. Impact on Canopy Photosynthesis. *Annals of Botany* 86, 821–831.

18. Estep, L.K., Torriani, S.F.F., Zala, M., Anderson, N.P., Flowers, M.D., McDonald, B.A., Mundt, C.C., and Brunner, P.C. (2015). Emergence and early evolution of fungicide resistance in North American populations of *Zymoseptoria tritici*. *Plant Pathology* *64*, 961–971.
19. Fabre, F., Rousseau, E., Mailleret, L., and Moury, B. (2012). Durable strategies to deploy plant resistance in agricultural landscapes. *New Phytologist* *193*, 1064–1075.
20. Forsman, K., and Poutala, T. (1997). Crop Management Effects on Pre- and Post-Anthesis Changes in Leaf Area Index and Leaf Area Duration and their Contribution to Grain Yield and Yield Components in Spring Cereals. *Journal of Agronomy and Crop Science* *61*, 47–61.
21. Garrett, K.A., and Mundt, C.C. (1999). Epidemiology in mixed host populations. *Phytopathology* *89*, 984–990.
22. Gassmann, A.J., Carrière, Y., and Tabashnik, B.E. (2009). Fitness costs of insect resistance to *Bacillus thuringiensis*. *Annual Review of Entomology* *54*, 147–163.
23. Geritz, S.A.H., Kisdi, É., Meszéna, G., and Metz, J.A.J. (1998). Evolutionarily singular strategies and the adaptive growth and branching of the evolutionary tree. *Evolutionary Ecology* *12*, 35–57.
24. Hinzman, L.D., Bauer, M.E., and Daughtry, C.S.T. (1986). Effects of Nitrogen-Fertilization on Growth and Reflectance Characteristics of Winter-Wheat. *Remote Sensing of Environment* *19*, 47–61.
25. Hobbelen, P.H.F., Paveley, N.D., and Van Den Bosch, F. (2014). The emergence of resistance to fungicides. *PLoS ONE* *9*.
26. Hoffland, E., Jeger, M.J., and van Beusichem, M.L. (2000). Effect of nitrogen supply rate on disease resistance in tomato depends on the pathogen. *Plant and Soil* *218*, 239–247.
27. Holdenrieder, O., Pautasso, M., Weisberg, P.J., and Lonsdale, D. (2004). Tree diseases and landscape processes: The challenge of landscape pathology. *Trends in Ecology and Evolution* *19*, 446–452.
28. Huang, J., Sedano, F., Huang, Y., Ma, H., Li, X., Liang, S., Tian, L., Zhang, X., Fan, J., and Wu, W. (2016). Assimilating a synthetic Kalman filter leaf area index series into the WOFOST model to improve regional winter wheat yield estimation. *Agricultural and Forest Meteorology* *216*, 188–202.
29. Jiang, D., Dai, T., Jing, Q., Cao, W., Zhou, Q., Zhao, H., and Fan, X. (2004). Effects of long-term fertilization on leaf photosynthetic characteristics and grain yield in winter wheat. *Photosynthetica* *42*, 439–446.
30. Jones, E.O., Webb, S.D., Ruiz-Fons, F.J., Albon, S., and Gilbert, L. (2011). The effect of landscape heterogeneity and host movement on a tick-borne pathogen. *Theoretical Ecology* *4*, 435–448.
31. Kaltz, O., Gandon, S., Michalakis, Y., and Shykoff, J.A. (1999). Local Maladaptation in the Anthracnose Fungus *Microbotryum violaceum* to Its Host Plant *Silene latifolia*: Evidence from a Cross-Inoculation Experiment. *Evolution* *53*, 395.
32. Karaoglanidis, G.S., Luo, Y., and Michailides, T.J. (2010). Competitive Ability and Fitness of *Alternaria alternata* Isolates Resistant to QoI Fungicides. *Plant Disease* *95*, 178–182.
33. Kato, M., Mizubuti, E.S., Goodwin, S.B., and Fry, W.E. (1997). Sensitivity to Protectant Fungicides and Pathogenic Fitness of Clonal Lineages of *Phytophthora infestans* in the United States. *Phytopathology* *87*, 973–978.
34. Lecompte, F., Abro, M.A., and Nicot, P.C. (2010). Contrasted responses of *Botrytis cinerea* isolates developing on tomato plants grown under different nitrogen nutrition regimes. *Plant Pathology* *59*, 891–899.
35. Leitch, M.H., and Jenkins, P.D. (1994). Influence of nitrogen on the development of *Septoria* epidemics in winter wheat. *Journal of Agricultural Science* *124*, 361–368.
36. Lion S, Gandon S. 2016 Spatial evolutionary epidemiology of spreading epidemics. *Proc. R. Soc. B* *283*: 20161170. <http://dx.doi.org/10.1098/rspb.2016.1170>

37. McDonald, B.A., and Linde, C. (2002). Pathogen population genetics, evolutionary potential, and durable resistance. *Annual Review of Phytopathology* 40, 349–379.
38. Metz, J.a.J., Nisbet, R.M., and Geritz, S.a.H. (1992). How should we define 'fitness' for general ecological scenarios? *Trends in Ecology & Evolution* 7, 198-202.
39. Nicholls, C., and Altieri, M. (2004). Designing species-rich, pest-suppressive agroecosystems through habitat management. *Agronomy* 49–62.
40. Olesen, J.E., Mortensen, J.V., Jørgensen, L.N., and Andersen, M.N. (2000). Irrigation strategy, nitrogen application and fungicide control in winter wheat on a sandy soil. I. Yield, yield components and nitrogen uptake. *Journal of Agricultural Science* 134, 1–11.
41. Papaïx, J., David, O., Lannou, C., and Monod, H. (2013). Dynamics of Adaptation in Spatially Heterogeneous Metapopulations. *PLoS ONE* 8.
42. Papaïx, J., Burdon, J.J., Lannou, C., and Thrall, P.H. (2014a). Evolution of Pathogen Specialisation in a Host Metapopulation: Joint Effects of Host and Pathogen Dispersal. *PLoS Computational Biology* 10.
43. Papaïx, J., Adamczyk-Chauvat, K., Bouvier, A., Kiêu, K., Touzeau, S., Lannou, C., and Monod, H. (2014b). Pathogen population dynamics in agricultural landscapes: The Ddal modelling framework. *Infection, Genetics and Evolution* 27, 509–520.
44. Papaïx, J., Touzeau, S., Monod, H., and Lannou, C. (2014c). Can epidemic control be achieved by altering landscape connectivity in agricultural systems? *Ecological Modelling* 284, 35–47.
45. Papaïx, J., Burdon, J.J., Zhan, J., and Thrall, P.H. (2015). Crop pathogen emergence and evolution in agro-ecological landscapes. *Evolutionary Applications* 8, 385–402.
46. Park, A., Gubbins, S., and Gilligan, C. (2001). Invasion and Persistence of Plant Parasites in a Spatially Structured Host Population. *Oikos* 94, 162–174.
47. Plantegenest, M., Le May, C., and Fabre, F. (2007). Landscape epidemiology of plant diseases. *Journal of The Royal Society Interface* 4, 963–972.
48. Précigout, P.-A., Claessen, D., and Robert, C. (2017). Crop Fertilization Impacts Epidemics and Optimal Latent Period of Biotrophic Fungal Pathogens. *Phytopathology PHYTO-01-17-001*.
49. Pretorius, Z.A., Singh, R.P., Wagiore, W.W., and Payne, T.S. (2000). Detection of virulence to wheat stem rust resistance gene Sr31 in *Puccinia graminis* f. sp. *tritici* in Uganda. *Plant Disease* 84, 203.
50. Robert C, Bancal MO, Nicolas P, Lannou C, Ney B. (2004). Analysis and modelling of effects of leaf rust and *Septoria tritici* blotch on wheat growth. *J Exp Bot*. May;55(399):1079-94.
51. Robert, C., Fournier, C., Andrieu, B., and Ney, B. (2008). Coupling a 3D virtual wheat (*Triticum aestivum*) plant model with a *Septoria tritici* epidemic model (Septo3D): A new approach to investigate plant-pathogen interactions linked to canopy architecture. *Functional Plant Biology* 35, 997–1013.
52. Sapoukhina, N., Paillard, S., Dedryver, F., and de Vallavieille-Pope, C. (2013). Quantitative plant resistance in cultivar mixtures: Wheat yellow rust as a modeling case study. *New Phytologist* 200, 888–897.
53. Sauterey, B., Rault, J., Ward, B.A., Bowler, C., and Claessen, D. (2017). The implications of eco-evolutionary processes for the emergence of marine plankton community biogeography. *The American Naturalist* 190(1):116 - 130
54. Shaner, G., and Finney, R.E. (1977). The Effect of Nitrogen Fertilization on the Expression of Slow-Mildewing Resistance in Knox Wheat. *Phytopathology* 77, 1051–1056.

55. Simón, M.R., Cordo, C. a., Perelló, a. E., and Struik, P.C. (2003). Influence of Nitrogen Supply on the Susceptibility of Wheat to *Septoria tritici*. *Journal of Phytopathology* 151, 283–289.
56. Singh, R.P., Hodson, D.P., Huerta-Espino, J., Jin, Y., Bhavani, S., Njau, P., Herrera-Foessel, S., Singh, P.K., Singh, S., and Govindan, V. (2011). The Emergence of Ug99 Races of the Stem Rust Fungus is a Threat to World Wheat Production. *Annual Review of Phytopathology* 49, 465–481.
57. Skelsey, P., Rossing, W. a H., Kessel, G.J.T., and van der Werf, W. (2010). Invasion of *Phytophthora infestans* at the landscape level: how do spatial scale and weather modulate the consequences of spatial heterogeneity in host resistance? *Phytopathology* 100, 1146–1161.
58. Urban, J., and Lebeda, A. (2006). Fungicide resistance in cucurbit downy mildew - Methodological, biological and population aspects. *Annals of Applied Biology* 149, 63–75.
59. Walters, D.R., and Bingham, I.J. (2007). Influence of nutrition on disease development caused by fungal pathogens: Implications for plant disease control. *Annals of Applied Biology* 151, 307–324.
60. Wilensky, U., 1999. NetLogo. Center for Connected Learning and Computer-Based Modeling. Northwestern University, Evanston, IL, <http://ccl.northwestern.edu/netlogo>.
61. Zhan, J., Fitt, B.D.L., Pinnschmidt, H.O., Oxley, S.J.P., and Newton, A.C. (2008). Resistance, epidemiology and sustainable management of *Rhynchosporium secalis* populations on barley. *Plant Pathology* 57, 1–14.
62. Zhan, J., and McDonald, B.A. (2013). Experimental Measures of Pathogen Competition and Relative Fitness. *Annual Review of Phytopathology* 51, 131–153.
63. Zhan, J., Thrall, P.H., Papaïx, J., Xie, L., and Burdon, J.J. (2015). Playing on a Pathogen's Weakness: Using Evolution to Guide Sustainable Plant Disease Control Strategies. *Annual Review of Phytopathology* 53, 19–43.

Chapter 5: Does latent period of leaf fungal pathogens reflects their host trophic type? A meta-analysis.

ABSTRACT

In the previous chapters, we showed that both quantity and dynamics of host resources were fundamental in the optimization of the latent period of rust-like pathogens. These pathogens engage in biotrophic interactions with their hosts, feeding only on living tissue. By contrast, other types of pathogens require dead tissue to develop and/or reproduce. Those are called necrotrophs and hemibiotrophs. It is likely that such differences between pathogen trophic types have affected the evolution of their latent period. Here, we perform a meta-analysis in search for a correlation between pathogen trophic type and latent period (defined as the elapsed time between tissue infection and appearance of the first asexual reproductive structures). We gathered latent period data from 103 studies dealing with 53 pathogen species: 26 biotrophs, 15 hemibiotrophs and 12 necrotrophs representing 2542 mean latent periods. We show that the three trophic types display significantly different latent periods. Necrotrophs have the smallest latent periods (often less than 100 dd), biotrophs have intermediate latent periods (typically between 100 and 200 dd) while hemibiotrophs have the longest latent periods (usually more than 200 dd).

INTRODUCTION

Ecologically, fungal crop pathogens can be differentiated by the nature of the trophic interaction with their host. Four types of trophic interactions are commonly distinguished: necrotrophy, biotrophy, hemibiotrophy, and saprotrophy (Divon and Fluhr, 2007). Necrotrophic pathogens kill the host tissue before being able to exploit it as a resource. They grow and sporulate only on dead tissue (Horbach et al., 2011). By contrast, biotrophic pathogens require living host tissue to feed on (Horbach et al., 2011, Mendgen and Hahn, 2002). They feed through specialized trophic structures called haustoria that draw nutrients directly from living cells cytoplasm through a specialized extracellular-matrix (Garnica et al., 2014). That matrix also plays a role in hiding the pathogen from the host immune system (Garnica et al., 2014; Oliveira-Garcia and Valent, 2015). Hemibiotrophic pathogens are first biotrophic (usually during a somatic growth stage) and then necrotrophic in a later stage (usually during a spores-producing stage), by undergoing major transcriptomic reprogramming (Lee and Rose, 2010; O'Connell et al., 2012; Palma-Guerrero et al., 2016). Some hemibiotrophs produce haustoria and a specialized extracellular-matrix (Perfect and Green, 2001; Behr et al., 2010). However these haustoria are structurally different from those of biotrophs (Kemen et al., 2015). Finally, saprotrophic fungi feed on dead host tissue without killing it themselves. As such, they may not be considered as true pathogens but rather as detritivores or scavengers. Due to our interest in true pathogens, in this article we focus on the first three trophic types of fungal crop pathogens: necrotrophic, biotrophic and hemibiotrophic. These three trophic types occur in a wide taxonomic range of fungi, including Ascomycota, Basidiomycota, and Oomycota.

Whereas ecological, pathological and biological descriptions of fungal crop pathogens generally refer to their trophic type, to our best knowledge no effort has been made to map general ecological traits to the tropic types. Such general ecological knowledge may be useful from both a fundamental and an applied point of view; increasing our basic understanding of the fungi and being able to find useful practices to control them in an agricultural context. The scope of our article is to use data currently available in the scientific literature to explore the relationship between the latent period and the trophic types. Specifically, our focus is on the latent period, which is a well-studied ecological trait of fungal crop pathogens, and which has

a direct relation with pathogenic traits such as virulence, spores production and aggressiveness. Thus our main question is whether there exist general patterns in the length of the latent period for pathogens of different trophic types.

The latent period is of key importance in the biology of fungal crop pathogens, separating a period of somatic growth from a period of spore production. It has a direct, numerical influence on the epidemiology of fungal crop pathogens due to its effect on the within-seasonal dynamics of the pathogen, notably by determining the length of the infection cycle and spore production. Most fungal crop pathogens colonize their nearby environment through repeated asexual reproduction cycles resulting in polycyclic epidemics (Agrios, 2005). Polycyclic pathogens go through up to 30 infection cycles per year (Agrios, 2005), thereby multiplying the quantity of inoculum released to the environment. An infection cycle starts with the deposition of pathogen spores on host tissue. Mycelium emerges from the germinating spores and invades the host tissue. Mycelium gathers energy from the parasitized host and, some time after infection, produces subepidermal reproductive structures. The maturation of these structures releases a new generation of spores in the crop canopy and the infection cycles repeats itself as long as there is susceptible tissue to colonize. The time interval between infection and production of new inoculum is called the latent period. It can be regarded as the minimum duration of an infection cycle.

The latent period is an important life history trait for plant fungal pathogens (Antonovics and Alexander, 1989, Pringle and Taylor, 2002, de Vallavieille-Pope et al., 2000). It is an important aggressiveness trait: pathogen strains with shorter latent periods have been demonstrated to cause more disease than strains with longer latent periods (Frenkel et al., 2010; Lehman and Shaner; 1996, Milus et al., 2006). This phenomenon is partly explained by the increased speed of canopy colonization associated with a shorter latent period (Beresford and Royle, 1988; Lovell et al., 2004; Zearfoss et al., 2011). Consequently, the latent period is involved in quantitative partial resistance of crops to pathogens. Many studies have shown that a given fungal strain has a delayed latent period when infecting a partially resistant host cultivar compared to a susceptible cultivar (see for instance Czembor et al., 2003; Habtu and Zadoks, 1995; Lehman and Shaner, 2005).

Variability of the latent period within and between populations has been reported (Lehman and Shaner, 1996, Pariaud et al., 2012, Suffert et al., 2015). Moreover, latent period

has been shown to be partially heritable (Carson, 1995; Ghannadha et al., 2005; Lehman and Shaner, 2007), making it good candidate trait for pathogen adaptation. Lehman and Shaner (1997) have demonstrated that the latent period responded to artificial selection. They transferred pathogens grown on susceptible cultivars on resistant ones and observed an increased latent period in the first pathogen generations. But after five generations on resistant cultivars, the latent period of the pathogen was already heritably shorter. These results suggest adaptation of the pathogen to its environment.

In Chapters 1, 2 and 3, we have built an epidemiological model of wheat rust showing the latent period may evolutionarily respond to changes in host resource level (Précigout et al., 2017). In this resource-based model, pathogen evolution was constrained by two trade-offs. The first trade-off was related to the pathogen's resource allocation strategy: it has to allocate enough resources to somatic growth to reproduce efficiently, but it also has to have enough resources left for sporulation. A positive correlation between the latent period and spores production, coherent with the rising part of such a trade-off (Chapter 1), has been documented by Pariaud et al. (2013) for the biotrophic wheat rust *Puccinia triticina*. The second trade-off linked the speed of within-season canopy colonization (e.g., a short latent period allows many infection cycles) and annual spore production (longer latent period allows higher sporulation rate). But these trade-offs are conditioned by the trophic type of rust, which feeds on the living resources throughout all the infection cycle. Trade-offs constraining the evolution of the latent period may very well be different for pathogens that do not continuously feed on living tissue such as necrotrophs and hemibiotrophs. One could expect the trade-offs to take different shapes according to the pathogen's trophic type.

While necrotrophs kill their host tissue by themselves, biotrophs establish a long-lasting interaction through the haustoria and extra-haustorial matrix. As for hemibiotrophs, they both produce feeding and hiding structures and undergo profound genetic reprogramming during the infection cycle. We argue that it is likely that these processes do not take the same time for the different trophic types, and do not lead to similar latent periods among necrotrophs, biotrophs and hemibiotrophs (reflecting different host exploitation strategies), hence constraining the evolution of the infection cycle of these different types of pathogens. In this paper we investigated the relationship between the trophic type and the latent period by conducting a meta-analysis of latent period data for 53 pathogen species (26 biotrophs, 15 hemibiotrophs and 12 necrotrophs) from 103 published papers.

The latent period is often measured as the time elapsed between infection and the appearance of detectable reproductive structures. The latent period usually consists of a symptomless phase, referred to as the incubation period, and a second phase with pre-sporulating disease symptoms such as chlorosis (Teng and Close, 1978). The latter phase may be absent if the first symptoms coincide with appearance of reproductive structures, in which case the incubation period is equal to the latent period. This, however, is rarely recorded. The incubation period can be considered an important aggressiveness trait, in addition to the latent period (Setti et al., 2008, 2009; Suassuna et al., 2004). We used our dataset to look for correlation between incubation and latent period in the three trophic groups of pathogens.

MATERIALS AND METHODS

Data

Studies included in the meta-analysis

A summary of the studies selection process is given in Figure 1. To gather studies reporting quantitative data on the latent period of Eumycota infecting plant leaves, we searched the Web of Science and Google Scholar data-bases with the query “fung* AND disease AND laten*”. This resulted in 531 different scientific articles. Only those dealing with fungi organisms and containing exploitable quantitative data of latent periods were kept for further investigation. We excluded articles concerning pathogens infecting other organs than leaves. Eventually, we excluded oomycete pathogens from this analysis because we did not find enough data to consider these pathogens as a separate category, which was needed given their particular biology.

We finally obtained 103 usable articles, dealing with 53 fungal pathogen species on 59 different host plants from 18 angiosperm families. It gives us 2542 latent period data. We found latent period data on 26 biotrophic pathogen species (838 data points), 15 hemibiotrophic pathogen species (1111 data points) and 12 necrotrophic (593 data points) pathogen species. These represent a biased factorial designed.

Response variable

Selecting comparable data of latent period was not straightforward. Two main definitions of the latent period can be found in the literature. On the one hand, following Parlevliet (1979), some authors define the latent period as the time interval from inoculation to initial sporulation. Similar to this definition is the one of Shearer and Zadoks (1973), defining latent period as the time interval between inoculation and appearance of first reproductive structures. From an epidemiological point of view, these studies refer to a latent period defined as the minimal possible duration for an infection cycle. On the other hand, following Johnson (1980) and Shaw (1986), some authors define the latent period as the time required for 50% of the lesions to begin sporulation. It is calculated a posteriori from pustule appearance time series. From an epidemiological point of view, this second definitions refers

to a latent period as an average duration of an infection cycle. Hereinafter, we will refer to these definitions as “minimal” and “average” latent periods respectively. Based on that dichotomy, we assigned the studies with yet slightly different definitions to one or the other group. For instance, latent periods defined as the period in which 10% of the total sporulating structures became apparent (Flier and Turkensteen, 1999) or as the time until all the leaves in a plot bear sporulating structures (Viljanen-Rollinson et al., 2005) were considered “minimal”. To the contrary, latent periods defined as the average time required for the uredinia to erupt (Lehman and Shaner, 2004) or as the time when 50% of the maximum observed disease incidence of symptomatic leaflets was achieved (Mersha et al., 2014) were considered “average”. This approach yielded to two uneven groups of latent period data. As the group “average” was small, especially for the necrotrophic fungi, only the “minimal” latent periods were further considered for the statistical analysis.

Latent period data are reported in various ways in the literature. Some studies directly give measurements from inoculation in individual leaves. Most of the time, a mean latent period is given for each repetition in a randomized (complete or incomplete) block design. In the latter case, we took them directly. In the former case, average values were calculated from individual data for each treatment, for the sake of comparison. Studies giving only a single value averaged over all treatments were also taken. All data points in our analysis are thus average values of latent period, weighted by the number of data they represent.

Latent period is known to depend on the temperature of the pathogen’s environment (Johnson, 1980, Shaw, 1986, Mersha, 2014). Several authors report a linear decrease of the latent period with increasing temperature for several pathogen species (see for example Figueroa et al., 1995a; Kolnaar and Van Den Bosch, 2001; Lovell, 2004). But studies on a wide range of temperature have demonstrated that the relationship between latent period and temperature resembles more a power function, with a possible linear approximation between 5 and 25°C (Shearer and Zadoks, 1972, Pedersen and Morrall, 1994, Sosa-Alvarez et al., 1995; Bernard et al., 2013). Many papers used this linear approximation to model plant growth and pathogen development independently from external temperature (Robert et al., 2008; Garin et al., 2014). In these models, biology of the organisms is expressed in thermal time (Lovell, 2004; Zearfoss et al., 2011). To put it in a nutshell, if at 10°C a biological process requires 10 days to complete, it will require only 5 days at 20°C. That is it requires 100 degree-days (dd) to complete. This approximation is only valid in the temperature range where the relationship

between latent period and temperature is linear, that is approximately linear, that is often between 5 and 25°C. To make our latent period data more comparable, we express them in thermal time in order to filter out the influence of temperature. Data already expressed in dd in their original paper were taken directly. Otherwise, thermal-time latent period was calculated as precisely as possible given the temperature indications available in the “Material and Methods” sections of those papers. Studies expressing latent period data in days with no temperature indication were excluded from our data set.

Our data set is composed of short latent periods expressed in degree-days.

Explanatory variables

Trophic type

We seek to investigate whether there is a correlation between the latent period of a pathogen and its trophic type, hence the due place of that variable among the explanatory variables. Levels of this categorical variable are: B (biotrophic), H (hemibiotrophic) and N (necrotrophic). Some pathogens are universally recognized as members of a given trophic group. This is true for most biotrophic fungi (with exception of *Phaeoisariopsis personata*, sometimes classified as an hemibiotroph) and for “archetypal” necrotrophs such as *Botrytis cinerea* or *Alternaria alternata*. Nevertheless, for some pathogens displaying a more or less extensive necrotrophic period (genera *Exserohilum*, *Microdochium*, *Rhynchosporium*, *Parastagonospora*, ...) are necrotrophs or hemibiotrophs remains controversial. In this study, they were classified according to the most recent papers reporting their status.

Resistance

Most fungal pathogens have an increased latent period when infecting partially resistant hosts (e.g. Czembor et al., 2003; Habtu and Zadoks, 1995; Lehman and Shaner, 2005, ...). Since some studies in this meta-analysis deal with quantitative partial resistance, resistance level of the cultivars was recorded as an explanatory variable. Depending of the studies, it is either a binary (susceptible versus partially resistant) or categorical (highly susceptible, susceptible, moderately resistant, resistant), or a semi-quantitative variable (resistance level between 1 and 10). Because most studies dealing with resistance presented

three cultivar categories, we opted for a categorical variable with three levels: S (susceptible), M (moderately resistant) and R (resistant). Wild plants and cultivars with no resistance rating were considered susceptible when not otherwise specified. None of the selected studies dealt with complete (gene for gene) resistance.

Environment of the studies

Experimental conditions have been shown to influence the parameters of the infection cycle of fungal leaf pathogens. One could mention climatic parameters (such as the level of humidity, Gilles et al., 2000; Setti et al., 2008), inoculation procedure (type of inoculum, Morais et al., 2015; Karolewski et al., 2002; inoculation technique, Giri et al., 2013, Miedaner et al., 2003; inoculum concentration, Sosnovski et al., 2005; Xue and Hall, 1992), and the environment in which the plants have been grown and/or incubated (e.g. in a climatic chamber, in a greenhouse, in the field, ... , Ohm and Shaner, 1976, Hernandez-Nopsa and Pfender, 2014). The variables from this list were only partially documented for a large proportion of the papers and thus were removed from explanatory variables for the sake of comparability of the data. We kept the environment of the study under the form of a categorical variable with four levels: D (detached leaves, leaflets or leaf disks), C (controlled environment chamber), G (greenhouse) and F (field) experiments.

We excluded studies on sexual inoculum (basidiospores and ascospores) since latent period of the sexual inoculum may significantly differ from the one of the asexual inoculum (Morais et al., 2015, but see Karolewski et al., 2002).

Incubation period

Some of the studies considered in this meta-analysis not only report latent periods, but also incubation periods. Incubation is generally defined as the time until the appearance of symptoms. It is also considered an aggressiveness trait of the pathogen (Le May et al., 2012; Setti et al., 2008; Suffert et al., 2013). As for the latent period, both a “minimal” (time from inoculation to onset of symptoms) and an “average” (time between inoculation and the development of 50% of the symptoms) definition of the incubation can be found in the literature. For the sake of comparison, we kept only the “minimal” ones.

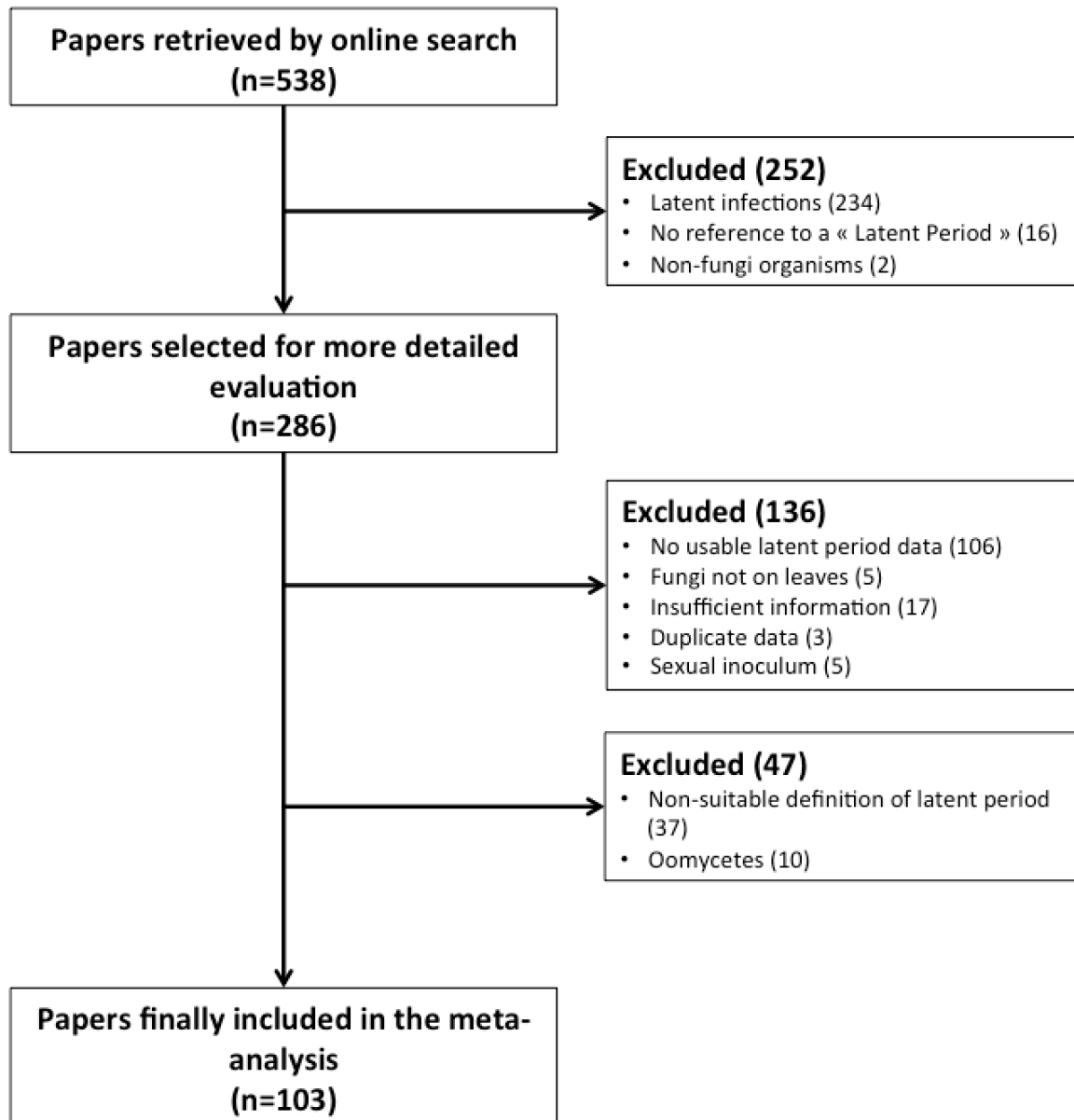


Figure 1: Study selection flow diagram. From the initial 531 different papers found on Web of Science and Google Scholar using the query “fung* AND disease AND latent*”, 250 were immediately excluded because they did not mention any latent period. Two of the 281 remaining papers were excluded because they did not focus on fungi organisms. Of the 279 remaining papers, we excluded those with no usable latent period data (106) and those not dealing with the latent period of asexual reproduction cycles of fungal pathogens infecting crop leaves (30). Seven new papers found through cross-references were added to the 143 remaining ones. We finally excluded studies about oomycetes (10) and those not dealing with a latent period such as defined in section “Response Variable.” (37).

StID	Article	Pathogen(s)	Trophic Type	Host(s)
ARM04	Armour et al. (2004)	<i>Mycosphaerella graminicola</i>	H	<i>Triticum aestivum</i>
ARS04	Arseniuk et al. (2004)	<i>Parastagonospora nodorum</i>	H	<i>Triticum aestivum</i>
ASA16	Asalf et al. (2016)	<i>Podosphaera aphanis</i>	B	<i>Fragaria x ananassa</i>
AUS12	Austin and Wilcox (2012)	<i>Erysiphe necator</i>	B	<i>Vitis vinifera</i>
BAS75	Bashi and Rotem (1975)	<i>Stemphylium botryosum</i>	N	<i>Solanum lycopersicum</i>
BOI95	Boiteux et al. (1995)	<i>Sphaerotheca fuliginea</i>	B	<i>Cucumis melo</i>
BOU03	Bouhassan et al. (2003)	<i>Botrytis fabae</i>	N	<i>Vicia faba</i>
BOU04	Bouhassan et al. (2004)	<i>Botrytis fabae</i>	N	<i>Vicia faba</i>
BOU07	Bouhassan et al. (2007)	<i>Botrytis fabae</i>	N	<i>Vicia faba</i>
BRO97	Broers (1997)	<i>Puccinia striiformis</i>	B	<i>Triticum aestivum</i>
BRO04	Browne et al. (2004)	<i>Microdochium nivale</i>	N	<i>Triticum aestivum</i>
BRO06	Browne et al. (2006)	<i>Microdochium nivale</i>	N	<i>Triticum aestivum</i>
BRC04	Browne and Cooke (2004)	<i>Microdochium nivale</i>	N	<i>Triticum aestivum</i>
CAR94	Carson and van Dyke (1994)	<i>Exserohilum turcicum</i>	H	<i>Zea mays</i>
CAS93	Casela et al. (1993)	<i>Colletotrichum graminicola</i>	H	<i>Sorghum bicolor</i>
CHH12	Chhikara et al. (2012)	<i>Alternaria brassicae</i>	N	<i>Brassica juncea</i>
CHO20	Chongo and Bernier (2000)	<i>Colletotrichum truncatum</i>	H	<i>Lens culinaris</i>
CHO14	Choudhury et al. (2014)	<i>Erysiphe necator</i>	B	<i>Vitis vinifera</i>
CRO92	Cromey (1992)	<i>Puccinia striiformis</i>	B	<i>Triticum aestivum</i>
CUN88	Cunfer et al. (1988)	<i>Parastagonospora nodorum</i>	H	<i>Triticum aestivum</i>
CZE03	Czembor et al. (2003)	<i>Parastagonospora nodorum</i>	H	<i>Triticum aestivum</i>
DAN16	Danelli and Reis (2016)	<i>Phakopsora pachyrhizi</i>	B	<i>Glycine max</i>
DEH02	Dehghani et al. (2002)	<i>Puccinia striiformis</i>	B	<i>Triticum aestivum</i>
DEH04	Dehghani and Moghaddam (2004)	<i>Puccinia striiformis</i>	B	<i>Triticum aestivum</i>
DEW03	Dewdney et al. (2003)	<i>Spilocea pomi</i>	H	<i>Malus domestica</i>
DIA99	Diamond and Cooke (1999)	<i>Microdochium nivale</i>	N	<i>Triticum aestivum</i>
DIA03	Diaz-Lago et al. (2003)	<i>Puccinia coronata</i>	B	<i>Avena sativa</i>
DOW03	Dowkiw et al. (2003)	<i>Melampsora larici-populina</i>	B	<i>Populus deltoides x trichocarpa</i>
DU014	Du et al. (2014)	<i>Parastagonospora nodorum</i>	H	<i>Triticum aestivum</i>
EAT84	Eaton et al. (1984)	<i>Puccinia graminis</i>	B	<i>Triticum aestivum</i>
ENG96	Engels and de Waard (1996)	<i>Erysiphe graminis</i>	B	<i>Triticum aestivum</i>
EVE80	Eversmeyer et al. (1980)	<i>Puccinia recondita</i>	B	<i>Triticum aestivum</i>
FIG95a	Figueroa et al. (1995a)	<i>Pyrenopeziza brassicae</i>	H	<i>Brassica napus</i>
FIG95b	Figueroa et al. (1995b)	<i>Pyrenopeziza brassicae</i>	H	<i>Brassica napus</i>
FIS08	Fisher et al. (2008)	<i>Puccinia jaceae</i>	B	<i>Centaurea solstitialis</i>
FRE10	Frenkel et al. (2010)	<i>Erysiphe necator</i>	B	<i>Vitis vinifera</i> <i>Vitis vinifera x Vitis labrusca</i>
GAL88	Galea and Price (1988)	<i>Microdochium panattoniacum</i>	N	<i>Lactuca serriola</i>
GHA95	Ghannadha et al. (1995)	<i>Puccinia striiformis</i>	B	<i>Triticum aestivum</i>
GIL00	Gilles et al. (2000)	<i>Pyrenopeziza brassicae</i>	H	<i>Brassica napus</i>
GIN95	Gingera et al. (1995)	<i>Puccinia sorghi</i>	B	<i>Zea mays</i>
GIO96	Giorcelli et al. (1996)	<i>Melampsora larici-populina</i>	B	<i>Populus x euramericana</i>
GRA11	Graichen et al. (2011)	<i>Puccinia coronata</i>	B	<i>Avena sativa</i>
HAM92	Hamelin et al. (1992)	<i>Melampsora medusae</i>	B	<i>Populus deltoides</i>
HAM94	Hamelin et al. (1994)	<i>Melampsora medusae</i>	B	<i>Populus deltoides</i>
HAZ98	Hazra (1998)	<i>Colletotrichum graminicola</i>	H	<i>Sorghum bicolor</i>
HER14	Hernandez-Nopsa and Pfender (2014)	<i>Puccinia graminis</i>	B	<i>Triticum aestivum</i>
JAC04	Jacobsen et al. (2004)	<i>Cercospora beticola</i>	H	<i>Beta vulgaris</i>
JEG82	Jeger et al. (1982)	<i>Parastagonospora nodorum</i>	H	<i>Triticum aestivum</i> <i>Triticum compactum</i> <i>Triticum dicoccoides</i> <i>Triticum dicoccum</i> <i>Triticum durum</i> <i>Triticum monococcum</i> <i>Triticum mutica</i> <i>Triticum polonicum</i> <i>Triticum spelta</i> <i>Triticum timopheevii</i> <i>Triticum turgidum</i>
JOR05	Jorge et al. (2005)	<i>Melampsora larici-populina</i>	B	<i>Populus deltoides x Populus trichocarpa</i>
KAN02	Kanrar et al. (2002)	<i>Alternaria brassicae</i>	N	<i>Brassica juncea</i>
KAR10	Karaoglanidis et al. (2010)	<i>Alternaria alternata</i>	N	<i>Pistacia vera</i>
KAR02	Karolewski et al. (2002)	<i>Pyrenopeziza brassicae</i>	H	<i>Brassica napus</i>
KAR93	Kari and Griffiths (1993)	<i>Rhynchosporium secalis</i>	H	<i>Hordeum secalinum</i>
KOC75	Kochman and Brown (1975)	<i>Puccinia graminis</i>	B	<i>Avena sterilis</i> <i>Hordeum vulgare</i>
KOL01	Kolnaar and van den Bosch (2001)	<i>Puccinia lagenophora</i>	B	<i>Senecio vulgaris</i>
LAS96	Lascoux et al. (1996)	<i>Melampsora ribesii-viminalis</i>	B	<i>Salix viminalis</i>
LEC10	Lecompte et al. (2010)	<i>Botrytis cinerea</i>	N	<i>Solanum lycopersicum</i>
LI006	Li et al. (2006)	<i>Erysiphe pulchra</i>	B	<i>Cornus florida</i>

Tableau 1: List of the studies included in this meta-analysis. Entries include citations of papers in which latent period data were taken, the pathogens the study deals with, their trophic type and the hosts on which they were grown.

StID	Article	Pathogen	Trophic Type	Host
LI007	Li et al. (2007)	<i>Puccinia hemerocallidis</i>	B	<i>Hemerocallis</i> sp
LI009	Li et al. (2009)	<i>Erysiphe polygoni</i>	B	<i>Hydrangea macrophylla</i>
LOU96	Loughman et al. (1996)	<i>Mycosphaerella graminicola</i> <i>Phaeosphaeria nodorum</i>	H H	<i>Triticum aestivum</i>
LOV04	Lovell et al. (2004)	<i>Mycosphaerella graminicola</i>	H	<i>Triticum aestivum</i>
MIL09	Milus et al. (2009)	<i>Puccinia striiformis</i>	B	<i>Triticum aestivum</i>
MON08	Montarry et al. (2008)	<i>Erysiphe necator</i>	B	<i>Vitis vinifera</i>
MOR15	Morais et al. (2015)	<i>Zymoseptoria tritici</i>	H	<i>Triticum aestivum</i>
MWA06	Mwakutuya (2006)	<i>Stemphylium botryosum</i>	N	<i>Lens culinaris</i>
NEW98	Newcombe (1998)	<i>Melampsora medusae</i>	B	<i>Populus deltoides</i>
PAR89	Park and Rees (1989)	<i>Puccinia striiformis</i>	B	<i>Triticum aestivum</i>
PED94	Pedersen and Morrall (1994)	<i>Ascochyta fabae</i>	N	<i>Lens culinaris</i>
PEE94	Peever and Milgroom (1994)	<i>Pyrenophora teres</i>	H	<i>Hordeum vulgare</i>
PRA89	Prakash and Thielges (1989)	<i>Melampsora medusae</i>	B	<i>Populus deltoides</i>
PRA13	Prasad et al. (2013)	<i>Phaeoisariopsis personata</i> <i>Puccinia arachidis</i>	B B	<i>Arachis hypogaea</i>
RAZ05	Razavi and Hugues (2005)	<i>Mycosphaerella graminicola</i>	H	<i>Triticum aestivum</i>
ROD95	Roderick and Clifford (1995)	<i>Erysiphe graminis</i>	B	<i>Avena sativa</i>
ROG99	Roger et al. (1999)	<i>Ascochyta pinodes</i>	H	<i>Pisum sativum</i>
ROS05	Rossi et al. (2005)	<i>Stemphylium vesicarium</i>	N	<i>Digitaria sanguinalis</i> <i>Festuca ovina</i> <i>Festuca rubra</i> <i>Lolium perenne</i> <i>Poa pratensis</i> <i>Pyrus communis</i> <i>Setaria glauca</i> <i>Trifolium repens</i>
ROT89	Rotem et al. (1989)	<i>Alternaria macrospora</i>	N	<i>Gossypium barbadense</i>
SET08	Setti et al. (2008)	<i>Mycosphaerella pinodes</i>	H	<i>Pisum sativum</i>
SET09	Setti et al. (2009)	<i>Mycosphaerella pinodes</i>	H	<i>Pisum sativum</i>
SHA03	Sharma and sharma (2003)	<i>Melampsora ciliata</i>	B	<i>Populus deltoides</i>
SHA90	Shaw (1990)	<i>Mycosphaerella graminicola</i>	H	<i>Triticum aestivum</i>
SHE72	Shearer and Zadoks (1972)	<i>Parastagonospora nodorum</i>	H	<i>Triticum aestivum</i>
SOM09	Sombardier et al. (2009)	<i>Podosphaera aphanis</i>	B	<i>Fragaria</i> spp
SOS95	Sosa-Alvarez et al. (1995)	<i>Botrytis cinerea</i>	N	<i>Fragaria x ananassa</i>
SOS05	Sosnowski et al. (2005)	<i>Leptosphaeria maculans</i>	H	<i>Brassica napus</i>
SOU12	Souza et al. (2012)	<i>Cercospora coffeicola</i>	H	<i>Coffea arabica</i>
STO87	Stooksbury et al. (1987)	<i>Parastagonospora nodorum</i>	H	<i>Triticum aestivum</i>
SUF13	Suffert et al. (2013)	<i>Mycosphaerella graminicola</i>	H	<i>Triticum aestivum</i>
SUF15	Suffert et al. (2015)	<i>Mycosphaerella graminicola</i>	H	<i>Triticum aestivum</i>
TEN78	Teng and Close (1978)	<i>Puccinia hordei</i>	B	<i>Hordeum vulgare</i>
TIE92	Tiedemann (1992)	<i>Bipolaris sorokiniana</i> <i>Parastagonospora nodorum</i>	H H	<i>Triticum aestivum</i>
TOL85	Tollenaar (1985)	<i>Puccinia striiformis</i>	B	<i>Triticum aestivum</i>
TOM83	Tomerlin and Jones (1983)	<i>Spilocea pomi</i>	H	<i>Malus domestica</i>
TRA92	Trapero-Casas and Kaiser (1992)	<i>Ascochyta rabiei</i>	N	<i>Cicer arietinum</i>
VAN89	Vanniasingham and Gilligan (1989)	<i>Leptosphaeria maculans</i>	H	<i>Brassica napus</i>
VIL98	Viljanen-Rollinson et al. (1998)	<i>Erysiphe pisi</i>	B	<i>Pisum sativum</i>
VIL05	Viljanen-Rollinson et al. (2005)	<i>Mycosphaerella graminicola</i>	H	<i>Triticum aestivum</i>
WOL16	Wolfenbarger et al. (2016)	<i>Podosphaera macularis</i>	B	<i>Humulus lupulus</i>
XU999	Xu (1999)	<i>Sphaerotheca pannosa</i>	B	<i>Rosa</i> spp
XUR00	Xu and Robinson (2000)	<i>Podosphaera clandestina</i>	B	<i>Crataegus monogyna</i>
XUR01	Xu and Robinson (2001)	<i>Erysiphe polygoni</i>	B	<i>Clematis</i> spp
YAN06	Yan et al. (2006)	<i>Podosphaera pannosa</i>	B	<i>Rosa</i> sp
ZEA11	Zearfoss et al. (2011)	<i>Parastagonospora nodorum</i>	H	<i>Triticum aestivum</i>

Tableau 1: Continued from previous page.

Statistical methods

First look into the data

Data presentation in Figure 2 shows latent period data for each study on each pathogen species. Data presentation in Figure 3 shows average values calculated independently for each level of the three explanatory variables. Both figures display data standard deviations. Tukey's honest significant difference test has been performed to assess differences between levels of the three variables in Figure 3.

Statistical model

To investigate the putative effect of explanatory variables on the length of the latent period, we use the following generalized linear mixed model for latent period data:

$$Y_{i,j,k,l} = \mu + \alpha_i + \beta_j + \delta_k + \gamma_{i,j} + \gamma_{i,k} + \gamma_{j,k} + \mathcal{P}_s + \varepsilon_{i,j,k,l} \quad (1)$$

$$\text{with } \{\varepsilon_{i,j,k,l}\} \sim \mathcal{N}(0, \sigma_{i,j,k,l}^2)$$

where α is the main effect of trophic type, β the main effect of host level of resistance, δ the main effect of the environment of the study, γ the first order interaction terms between the three explanatory variables and ε the model residuals. Second order interactions could not be included in the model because of the biased factorial designed. Because our data are mean values calculated over different numbers of samples, the variance associated with each residual putative normal distribution was made dependant of the original sample size of the data. Finally, P represents the random effect of the study. For each data point, index i denotes the trophic type, j the host resistance level, k the environment of the study, s the study and l the repetitions.

A type III ANOVA was first performed using the previous model to test main effects and interactions significance (Table 2). Least squares means for trophic types, resistance levels, environmental conditions and their interactions were generated and represented in Figures 4 and 5 with standard errors.

To investigate the effect of trophic type and resistance level of the host on the length of the incubation period, a second statistical model was used. Because there was much less incubation data than latent period data available, the host resistance level categories “M” and “R” were grouped into a new “R” category. The effect of the environment was not tested on these data because the factorial design was too unbalanced. We use the following generalized linear mixed model for incubation period data:

$$Y_{i,j,l} = \alpha_i + \beta_j + \gamma_{i,j} + P_s + \varepsilon_{i,j,l} \quad (2)$$

$$\text{with } \{\varepsilon_{i,j,l}\} \sim \mathcal{N}(0, \sigma_{i,j,l}^2)$$

where α is the main effect of trophic type, β the main effect of host level of resistance and γ the interaction term between trophic type and resistance. P represents the random effect of the study. As for the latent period, the variance associated with each residual putative normal distribution was made dependant of the original sample size of the data. For each data point, index i denotes the trophic type, j the host resistance level, s the study and l the repetitions.

RESULTS

Data presentation

Figure 2 shows mean latent periods obtained from the 103 studies included in this meta-analysis. Latent period ranges from 45 ± 7.0 dd for the necrotrophic *Stemphylium botryosum* to 623 ± 65 dd for the hemibiotrophic *Cercospora coffeicola*. With the exception of the biotrophic *Erysiphe graminis*, all the pathogens with a mean latent period shorter than 100 dd are necrotrophs. The necrotroph with the longest latent period is *Ascochyta fabae* (134 ± 34 dd).

Among the 26 biotrophic fungi included in our study, 24 present a mean latent period comprised between 100 dd and 200 dd. Among them, seven out of eight pathogens with the shortest latent periods are mildews, whereas seven out of eight pathogens with the longest latent periods are rusts. Mildews from the order of the Erysiphales (genera *Erysiphe*, *Podosphaera* and *Sphaerotheca*) seem to have shorter latent periods than rusts (genera *Puccinia* and *Melampsora*). The biotroph with the longest latent period is the groundnut leaf rust *Puccinia arachidis* (322 ± 30 dd).

Among hemibiotrophic pathogens, only *Colletotrichum graminicola* has a mean latent period shorter than 150 dd (110 ± 39 dd). Most hemibiotrophs have a mean latent period longer than 200 dd. It even reaches more than 600 dd for *Cercospora coffeicola*. All but one of the rust fungi have quite similar latent periods, so do mildews and necrotrophs. By contrast, a strong heterogeneity can be seen among hemibiotrophs.



Figure 2: Mean latent periods (expressed in degree-days) for the 53 pathogen species included in the meta-analysis. The pathogen species have been ordered bottom-up according to increasing mean latent period. Bars represent standard errors. For pathogens present in several studies, data have been plotted separately for each study and are labelled with the study ID (see Table 1). Necrotrophs are in blue, biotrophs in green and hemibiotrophs in orange. Only data from susceptible cultivars have been plotted here.

Statistical analysis

The ANOVA analysis (Table 2) showed significant effects of all main explanatory variables: trophic type, resistance of the host cultivar and environment of the study. All interactions were significant. The statistical model confirms that the latent period of the necrotrophs is shorter than the latent period of the biotrophs, which is shorter than the one of the hemibiotrophs ($LP_N = 109.3 \pm 10.6$ dd, $LP_B = 172.1 \pm 12.3$ dd, $LP_H = 266.3 \pm 16.2$ dd, $p = 0.0016$ and $p < 0.0001$, Figure 3A). The statistical model also confirms the effect of resistance of the host cultivar on the latent period. It is shorter on susceptible cultivars, intermediate on moderately resistant cultivars and maximum on resistant cultivars ($LP_S = 147.4 \pm 6.4$ dd, $LP_M = 165.9 \pm 15.3$ dd, $LP_R = 208.3 \pm 12.0$ dd, $p < 0.0001$ for both differences, Figure 3B). Finally, estimated means show no significant differences between the different culture environments ($LP_D = 150.5 \pm 9.4$ dd, $LP_C = 174.5 \pm 15.3$ dd, $LP_G = 173.8 \pm 10.2$ dd, $LP_F = 192.0 \pm 19.6$ dd, Figure 3C). The least squared means estimates of each modality of the main effects are presented in Table 3.

Effects and interactions	χ^2	DF	P value
Trophic type	36.241	2	< 0.001
Environment	8.393	3	0.039
Resistance	8.696	2	0.013
Trophic type x Environment	42.452	6	< 0.001
Trophic type x Resistance	117.570	4	< 0.001
Environment x Resistance	46.318	6	< 0.001

Table 2: Statistical tests for the main effects and interactions of trophic type, culture environment, and level of resistance on latent period (in degree-days) and for contrasts involving these explanatory variables.

Figure 4 shows the interactions between trophic type, resistance of the host and environment of the study. For all environmental conditions, the latent period of necrotrophs is significantly lower than the one of hemibiotrophs. It is also less than biotrophs in the detached leaves and in the greenhouse conditions (Figure 4A). Biotrophs have a shorter latent period than hemibiotrophs in both controlled environment and in the greenhouse. The environment of the study does thus not change the effect of the trophic type on the latent period (Figure 4A).

Resistance impacts latent period in all trophic types (Figure 4B). Regarding biotrophs, latent period increases progressively from susceptible to resistant cultivars, whereas regarding

necrotrophs, latent period is the same on susceptible and moderately resistant cultivars, but is longer on resistant ones. Hemibiotrophs present a latent period increases with every level of resistance. Reciprocally, the differences in latent period between trophic types arise among all classes of partial resistance, except that resistant necrotrophs and resistant biotrophs tend to have similar latent periods (Figure 4B).

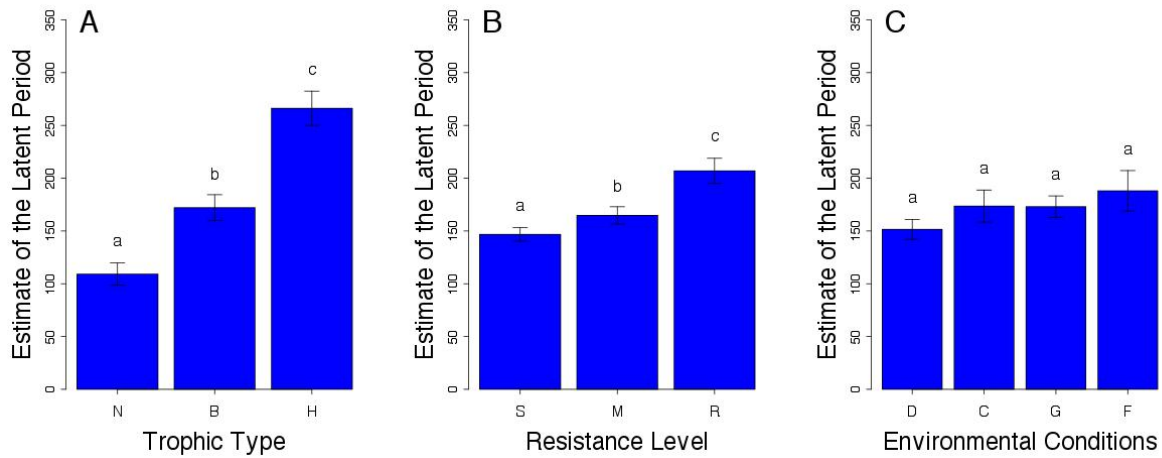


Figure 3: Least squares means latent periods and standard errors obtained using the statistical model for each mode of the three explanatory variables. Main effects of: A: trophic type (N: necrotrophs; B: biotrophs; H: hemibiotrophs; contrasts: N-B, $p = 0.0016$; B-H, $p < 0.0001$; N-H, $p < 0.0001$); B: Resistance level of the host (S: susceptible; M: moderately resistant; R: resistant; contrasts: S-M, M-R and S-R, $p < 0.0001$); C: Environment of the study (D: detached leaves or leaf disks; C: controlled environment cabinet; G: greenhouse; F: field; contrasts: C-D, $p = 0.4179$; C-F, $p = 0.8739$; C-G, $p = 1.000$; D-G, $p = 0.1464$; D-F, $p = 0.2715$; F-G, $p = 0.6675$). Within the same graph, different letters indicate significant contrasts. Latent periods are in degree-days.

Effects and modes	Least Square Means	Standard Error	Sample Size	Statistical Contrasts
Trophic Type :: N	109.3	10.6	593	a
Trophic Type :: B	172.1	12.3	838	b
Trophic Type :: H	266.3	16.2	1111	c
Environment :: D	150.5	9.4	762	a
Environment :: C	174.5	15.3	634	a
Environment :: G	173.8	10.2	755	a
Environment :: F	192.0	19.6	391	a
Resistance :: S	147.4	6.4	1704	a
Resistance :: M	165.9	8.2	586	b
Resistance :: R	208.3	12.0	252	c

Table 3: Least squares mean latent periods and standard errors estimated by the LP statistical model for each mode of the three explanatory variables. Main effects of: Trophic Type (N: necrotrophs; B: biotrophs; H: hemibiotrophs); Resistance level of the host (S: susceptible; M: moderately resistant; R: resistant) and Environment of the study (D: detached leaves or leaf disks; C: controlled environment cabinet; G: greenhouse; F: field). Latent periods estimates are in degree-days.

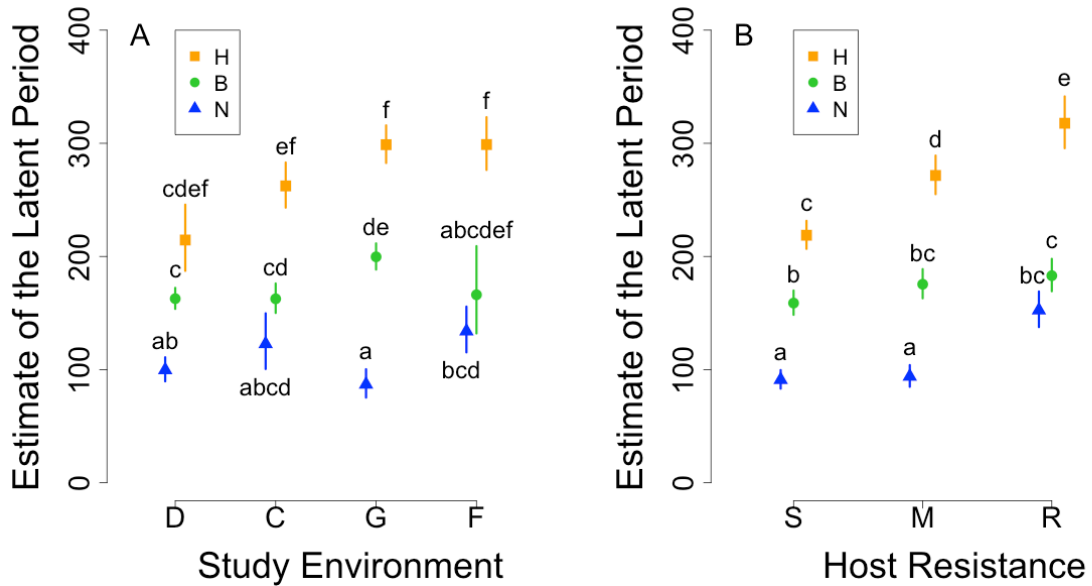


Figure 4: Least squares means latent periods and standard errors obtained using the statistical model for each mode of the three explanatory variables. A: Interactions between trophic type and environment of the study. Colors indicate the trophic type (necrotrophs in blue; biotrophs in green and hemibiotrophs in orange). B: Interactions between trophic type and resistance level of the host. Colors indicate the trophic type as in A. Trophic type: N = necrotrophs; B = biotrophs; H = hemibiotrophs; Resistance level of the host: S = susceptible; M = moderately resistant; R = resistant); Environment of the study: D = detached leaves or leaf disks; C = controlled environment cabinet; G = greenhouse; F = field). Latent periods are in degree-days.

Incubation versus latent period

As for latent period data, all biotrophs except *Puccinia arachidis* display a rather homogeneous incubation period of about 100 dd and all necrotrophs except *Ascochyta fabae* have an incubation period less than 100 dd (Figure 5). The incubation period of necrotrophic pathogens continuously ranges from 7.9 ± 1.8 dd for *Botrytis fabae* to 125.4 ± 35.0 dd for *Ascochyta fabae* while it ranges from 77.6 ± 8.9 dd for *Melampsora ciliata* to 253.0 ± 37.6 dd for *Puccinia arachidis*. Incubation period is less homogeneous among hemibiotrophs. It ranges from 100.2 ± 7.6 dd for *Ascochyta pinodes* to 430.9 ± 44.0 dd for *Cercospora coffeicola* (Figure 5). The example of *Parastagonospora nodorum* alone illustrates that heterogeneity well since its incubation period obtained from six studies varies between 50 and 300 dd.

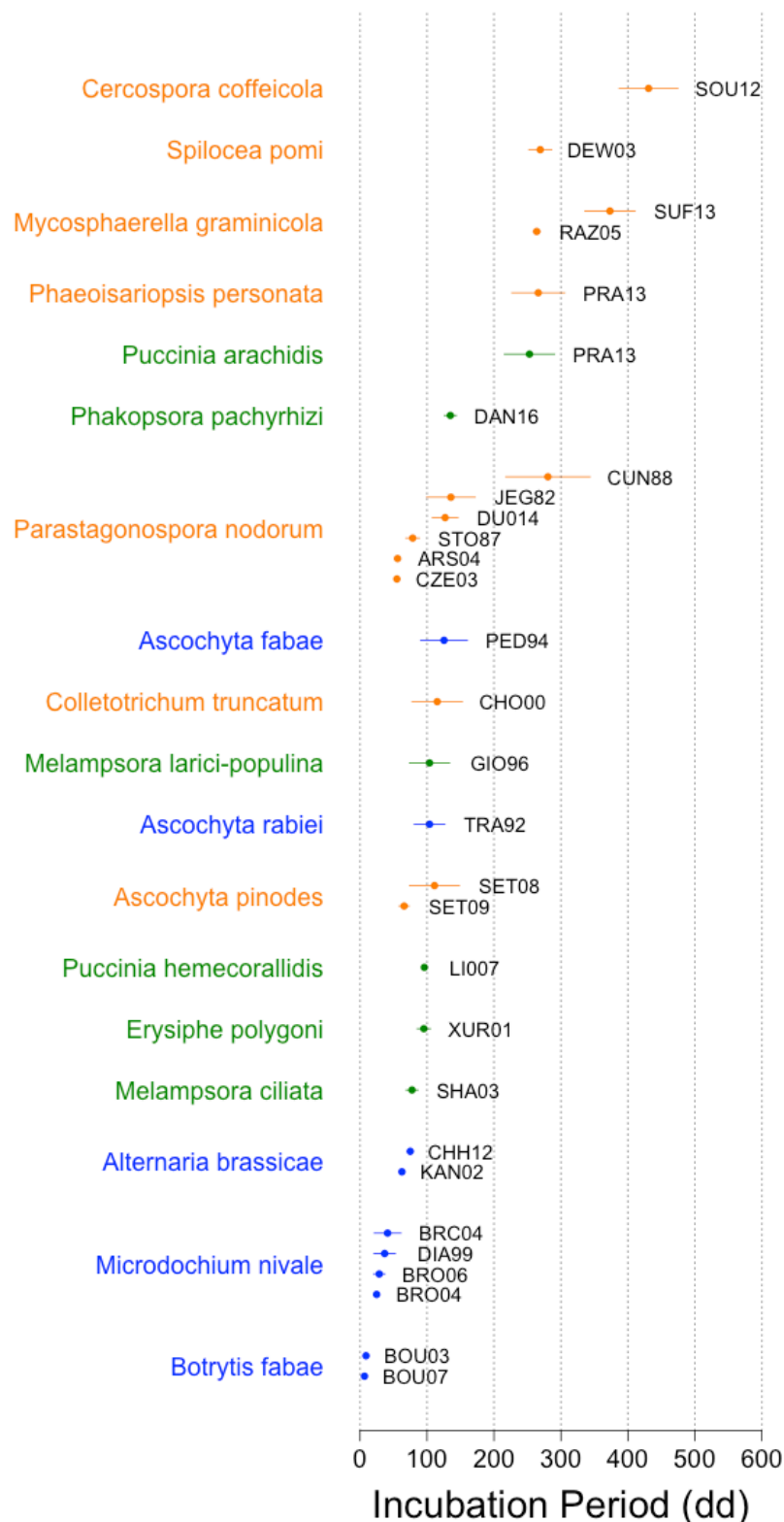


Figure 5: Mean incubation periods (expressed in degree-days) for 18 pathogen species included in the meta-analysis for which both latent period and incubation period data were available in the literature. The pathogen species have been ordered bottom-up according to increasing mean incubation period. Bars represent standard errors. For pathogens present in several studies, data have been plotted separately for each study and are labelled with the study ID (see Table 1). Necrotrophs are in blue, biotrophs in green and hemibiotrophs in orange. Only data from susceptible cultivars have been plotted here.

Figure 6A shows data from the 29 studies reporting both the latent and incubation periods. The latent period data of this subset have the same relation to trophic type and resistance of the host than the whole data set. Figure 6A shows that necrotrophs have a shorter incubation period than biotrophs ($IP_N = 40.9 \pm 1.9$ dd, $IP_B = 104.4 \pm 5.4$ dd, $p = 0.0031$) and hemibiotrophs ($IP_H = 208.8 \pm 5.8$ dd, $p = 0.0003$), but interestingly there is no significant difference between the incubation period of biotrophs and hemibiotrophs ($p = 0.2496$). Partial host resistance delays incubation period ($IP_S = 117.0 \pm 4.6$ dd, $IP_R = 128.5 \pm 7.0$ dd, $p < 0.0001$, Figure 6B). Least square means and statistical contrasts are presented in Table 4.

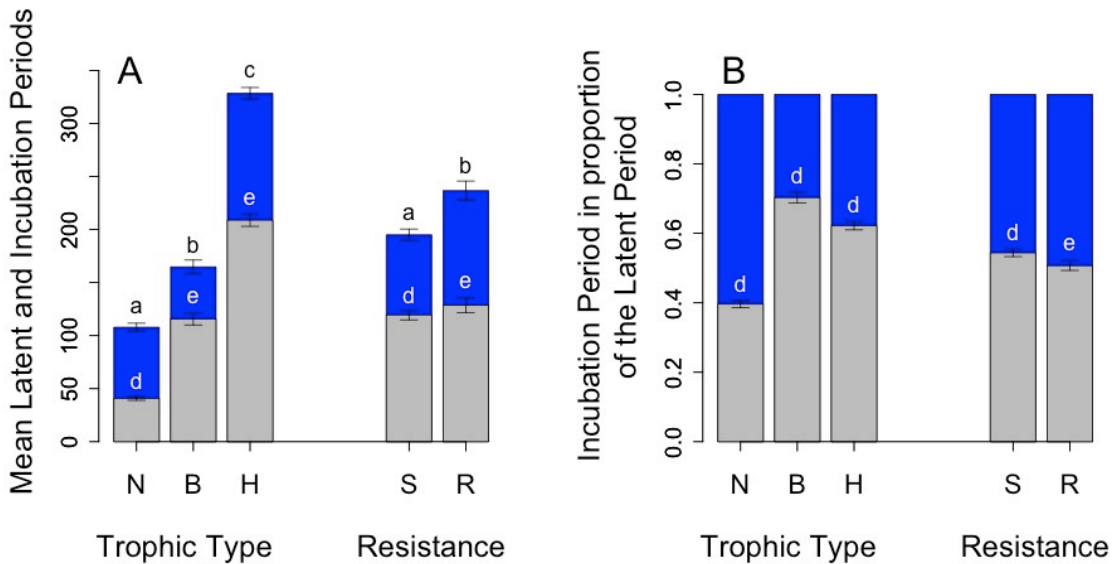


Figure 6: A: Mean latent (blue bars) and incubation periods (grey bars) and standard errors for each mode of the explanatory variables. Main effects of trophic type (N: necrotrophs; B: biotrophs; H: hemibiotrophs; contrasts from the IP statistical model: N-B, $p = 0.0031$; B-H, $p = 0.2496$; N-H, $p = 0.0003$) and Resistance level of the host (S: susceptible; R: resistant together with moderately resistant; contrast: S-R, $p < 0.0001$). Both periods are in degree-days. **B:** Proportion of the latent period corresponding to the incubation period for each mode of the explanatory variables. Letters *a*, *b* and *c* indicate significant contrasts between latent periods among trophic types and among resistance levels. Letters *d* and *e* indicate significant contrasts between incubation periods (A) or relative importance of the incubation period (B) among trophic types and among resistance levels. Data presented here come only from studies specifying both incubation and latent periods.

Figure 6B shows the proportion of the latent period corresponding to the incubation period. Although the incubation period of necrotrophs looks relatively shorter than the one of biotrophs and hemibiotrophs (N: $48.0 \pm 1.1\%$; B: $61.4 \pm 1.5\%$; H: $56.2 \pm 1.2\%$), there is no significant effect of the trophic type on that proportion (N-H: $p = 0.6975$; N-B: $p = 0.4332$; H-B: $p = 0.6115$). The proportion of the latent period corresponding to the incubation period is

however less on resistant plants than on susceptible ones (S: $54.4 \pm 1.1\%$; R: $50.7 \pm 1.4\%$; $p = 0.0103$; Figure 6B).

Effects and modes	Least Square Means	Standard Error	Sample Size	Statistical Contrasts
Trophic Type :: N	38.8	10.4	350	d
Trophic Type :: B	118.1	25.1	102	e
Trophic Type :: H	147.0	28.1	343	e
Resistance :: S	79.4	11.8	488	d
Resistance :: R	96.8	14.5	307	e

Table 4: Least squares mean incubation periods and standard errors estimated by the IP statistical model for each mode of the three explanatory variables. Main effects of: Trophic Type (N: necrotrophs; B: biotrophs; H: hemibiotrophs) and Resistance level of the host (S: susceptible; R: moderately resistant and resistant). Incubation periods estimates are in degree-days.

The data show a huge diversity among pathogens in the relation between incubation and latent period: the incubation period represents less than 10% of the latent period of *Botrytis fabae* (Figure 7C and D) while it represents 80 to 90% of the latent period of *Ascochyta fabae* (Figure 7J). In the case of the hemibiotroph *Parastagonospora nodorum*, we find a large variability of both the incubation period (as for the latent period, 56 ± 2.8 , 78.6 ± 10.2 , 127.1 ± 19.3 , 135.7 ± 36.2 and 280.5 ± 63.0 dd in five different studies), and of its relation to the latent period (18.5%, 29.8%, 41.9%, 60.1% and 86.6% of the latent period respectively, see Figure 7M-Q). In that particular case, the longer the latent period on more resistant plants, the more the proportion of the incubation period.

The impact of the host resistance level on the relation between incubation and latent period is variable and depends on the pathogen trophic type. For necrotrophs and hemibiotrophs, if the latent period of the pathogen increases on resistant hosts, it is either because the duration of symptom development increases with no increase in the incubation period (Figures 7B-F), or because both the incubation period and the duration of symptom development are longer on resistant plants (Figures 7A and G). For hemibiotrophs, the latter case does not exist: the latent period of the pathogen is longer on resistant plants either because incubation period increases (Figures 7K ,M ,O ,Q and R), or because the duration of symptom development increases (Figures 7J, L, N and P). There is no clear intermediate case. Moreover, the percentage of the latent period that the incubation period represents only slightly changes between susceptible and resistant plants in necrotrophs (Figures 7A-F) while this change is strong for hemibiotrophs (Figures 7K, L, N, O, Q and R).

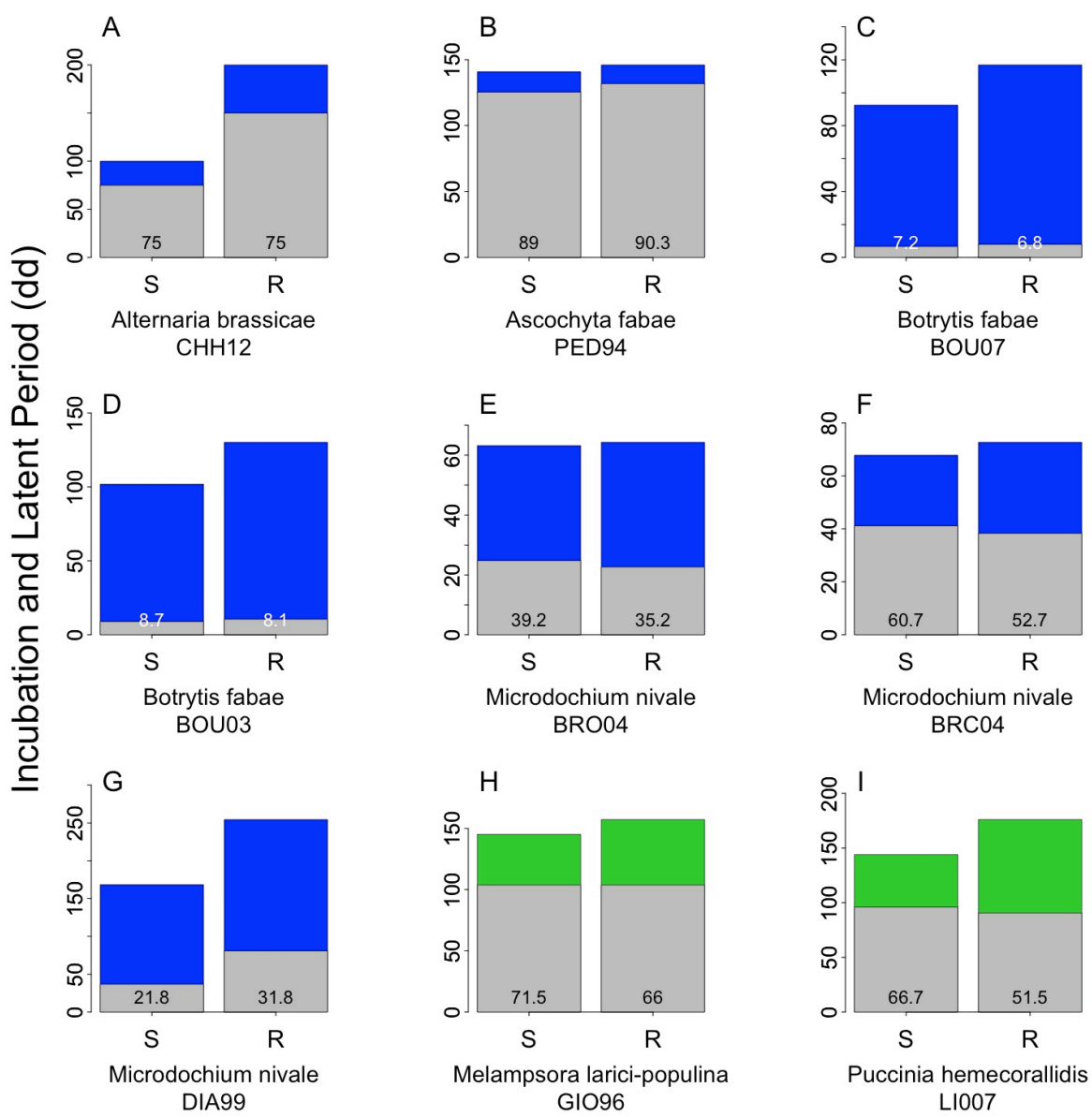


Figure 7: Relation between incubation and latent period for necrotrophic (blue) and biotrophic (green) pathogens inoculated on susceptible (S) or resistant (R) plants. Colored bars are latent periods, grey bars are incubation periods. Data relative to different pathogens from different studies have been represented in separate graphs. Numbers on bars indicate the percentage of the latent period that the incubation represents. Study IDs refer to Table 1.

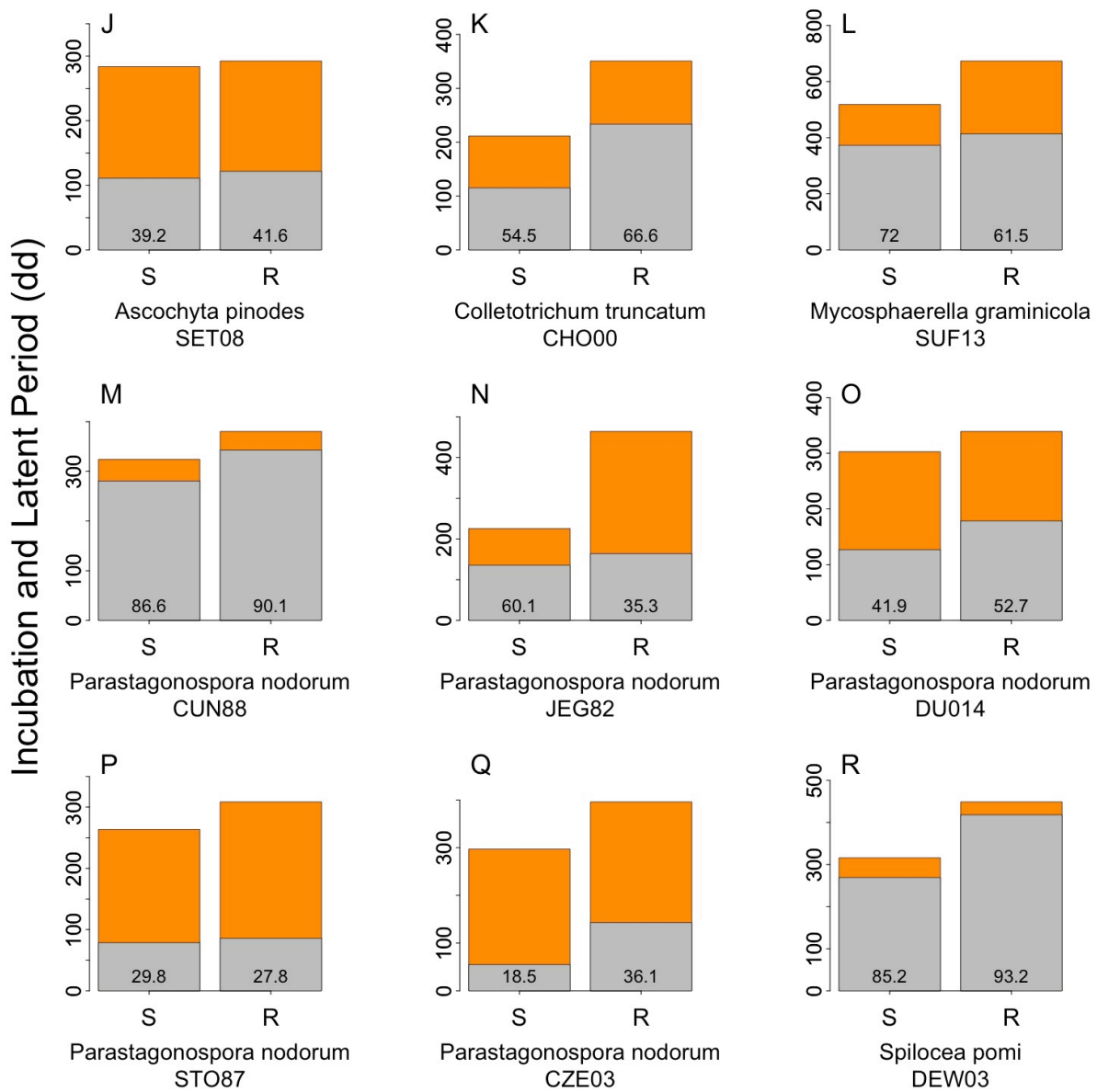


Figure 7: Continued from previous page. Relation between incubation and latent period for hemibiotrophic (orange) pathogens inoculated on susceptible (S) or resistant (R) plants. Colored bars are latent periods, grey bars are incubation periods. Data relative to different pathogens from different studies have been represented in separate graphs. Numbers on bars indicate the percentage of the latent period that the incubation represents. Study IDs refer to Table 1.

DISCUSSION

We performed a meta-analysis to investigate a putative correlation between pathogen trophic type and latent period. Here, the latent period is defined as the elapsed time between tissue infection and appearance of the first asexual reproductive structures. We gathered latent period data from 103 studies dealing with 53 pathogen species: 26 biotrophs, 15 hemibiotrophs and 12 necrotrophs representing 2542 mean latent periods. Our main result is that the three trophic types display significantly different latent periods (Figure 3). Necrotrophs have the smallest latent periods (109.7 dd on average), biotrophs have intermediate latent periods (165.2 dd on average) while hemibiotrophs have the longest (280.9 dd on average).

Our dataset also shows that host resistance delayed the latent period for the three kinds of pathogens, but with a stronger quantitative effect on the hemibiotrophic pathogens (Figure 4B). Regarding interaction with the experimental conditions, it is interesting to note that hemibiotrophs and biotrophs seem to be more responsive to environmental conditions than necrotrophic pathogens (Figure 4A).

Our data set shows that also the incubation period depends on the trophic type of the pathogens (Figure 5). As for the latent period, necrotrophs have a shorter incubation period than biotrophs and hemibiotrophs (Figure 6A), but we found no significant difference between the latters.

We also found that variability of both incubation and latent periods were quite moderate within biotrophs and necrotrophs. Variability is much larger among hemibiotrophs (Figure 2 and 5).

Defining the latent periods

Two main definitions of the latent period can be found in the literature. Some authors consider the latent period to be the minimal possible duration for an infection cycle. This corresponds to a latent period measured as the time interval from inoculation to first detection of functional reproductive structures (Shearer and Zadok 1972, Zadoks 1973, Parlevliet

1979). Others consider the latent period to be the average duration of an infection cycle. This corresponds to a latent period measured as the time required for 50% of the lesions to begin sporulation, calculated *a posteriori* from pustule appearance time series (Johnson 1980, Shaw 1986, 1990). We refer to these two definitions as the “minimal” and “average” definitions of the latent period.

Because, we have found no article measuring the “average” latent period of necrotrophic pathogens, we did not include “average” latent periods in our analysis in order to avoid having an unbalanced dataset. Broers (1997) showed that “minimal” and “average” latent periods were highly correlated in the (wind-dispersed) biotroph *Puccinia striiformis*. Similarly, Lovell et al. (2004) and Zearfoss et al. (2011), who measured both latent periods, showed similar responses of both latent periods to temperature and lesion development for the (splash-dispersed) hemibiotrophs *Zymoseptoria tritici* and *Parastagonospora nodorum*. Such similarities suggest that we could have found a similar relation between trophic type and latent period with “average” latent periods, at least for biotrophic and hemibiotrophic fungi, but this needs to be verified.

For a number of reasons, both definitions are probably biased descriptor of the role of the latent period in the infection cycle and the consequent epidemical dynamics. First, the date of the earliest sporulation event may not be related to the asymptotic intrinsic growth rate of the pathogen population (Shaw, 1990) whereas the “average” latent period is analogous to the average generation time. The latter is a conventional demographic measure that determines the asymptotic growth rate of a population, which makes the comparison with organisms other than fungi easier (Shaw, 1990). Second, both definitions, unless complemented by a range of variation, fail to describe the variability of the latent period within a population, which may have profound consequences on the development of epidemics (Zearfoss et al., 2011).

The “minimal” and “average” latent periods may each be relevant for different aspects of the epidemiological dynamics. This is illustrated by the following observation. In dispersal-limited diseases such as rust and septoria on wheat, there is a race between the growth of wheat and its disease progress (Lovell et al., 1997, 2004; Robert et al., 2008; Zearfoss et al., 2011; Suffert et al., 2013; Précigout et al., 2017; Robert et al., 2017). Once a given leaf has been infected, new and still healthy leaves emerge above it. If the pathogen is not able to

colonize these newly emerged leaves in time, the plant may be able to escape the disease since the currently occupied leaves have a limited lifespan. If the latent period of the pathogen does not allow it to reach its target leaves in time, plant growth may outrun disease progress. Primary colonization of new leaves in the canopy depends on the earliest emissions of spores within the crop canopy. The first lesions to sporulate are thus critical for the course of the epidemics (Robert et al., 2008; Frézal et al., 2009; Garin et al., 2014). The “minimal” latent period may therefore be especially relevant for the canopy colonisation process.

Thus, the onset of the sporulation period; and therefore the “minimal” latent period is of great importance in the course of epidemics. In any case, as pointed out by Shaw (1990), a study on a pathogen’s latent period should describe “both the temporal scale on which sporulating structures appear following infection at a single time, and the temporal pattern of that appearance” (p256) and both must be determined to ensure a good knowledge of each pathosystem.

Incubation and latent periods

In this chapter we use the common separation of the latent period into two phases: during the first phase the leaf is still green (the incubation period); during the second phase, non-sporulating symptoms appear and develop (the chlorotic period).

In the data presented in this chapter, there is a huge variability in the proportion of the latent period represented by the incubation period, from less than 10% in *Botrytis fabae* to almost 90% in *Ascochyta fabae*. In the latter case the incubation period is almost equal to the latent period with a very short duration of the chlorotic period. This proportion can also vary a lot between different studies on the same pathogen, since it ranges from 18% to 90% for the hemibiotrophic pathogen *Parastagonospora nodorum*. In necrotrophs, the incubation period likely corresponds to the time required for the pathogen to overcome immunity-triggered host cell necrosis and to set its arsenal of lytic enzymes and toxins in motion (Kabbage et al., 2015). The variability of the incubation period in necrotrophs may thus be attributed to twists and turns in the biochemical arms race for control of cell death pathways between the host and the pathogen.

For biotrophs and hemibiotrophs, the completion of the incubation period often means the appearance of yellowing area around the infection site. It is now believed that during the incubation period the hemibiotrophic pathogen *Z. tritici* remains in the apoplasm hidden from the plant's immune system (Sánchez-Vallet et al., 2015; Steinberg 2015). Following the incubation period, the appearance of chlorosis on leaves infected by *Z. tritici* corresponds to a phase of exponential mycelium growth that is followed by the onset of necrosis (Palma-Guerrero et al., 2016). This somehow quiescent incubation period is unlike the one of necrotrophs and resembles more an endophytic period or the quiescent stage of the so-called “latent pathogens” (Verhoeff 1974; Carroll 1988; Slippers et al., 2007). This may even be a new phase preceding a short “classical” incubation period, making *Z. tritici* look like a stealthy necrotroph (Sánchez-Vallet et al., 2015). In any case, it appears that the incubation period, as the latent period, is an important epidemiological and evolutionary trait of the leaf fungal pathogens infection cycle. But the quantitative relation between these two traits remains unclear.

As for the latent period, we found that the incubation period of necrotrophs was shorter than the incubation period of both biotrophs and hemibiotrophs, but unlike the latent period, we found no significant difference between the incubation period of biotrophs and hemibiotrophs (Figure 6A). It seems logical that necrotrophs, which have a short latent period, also have a short incubation period. More surprisingly, the incubation period of hemibiotrophs is no significantly longer than the one of biotrophs in our analysis. This would indicate that the chlorotic period is longer in hemibiotrophs. The absence of a difference between the proportional incubation periods in the three trophic types (Figure 6B) and the variability of that proportion among necrotrophs and among hemibiotrophs (Figure 7) rather suggests that the incubation period of the biotrophs is in fact intermediate between those of necrotrophs and hemibiotrophs, but the size of our dataset maybe does not allow us to capture it statistically.

Our results show that quantitative host resistance influences both the pathogen incubation period and its latent period. Disentangling the interplay between these two traits and host resistance could help understanding the relation between the two pathogen traits. Both are used to quantify the level of aggressiveness of a given pathogen strain (Andrade-Piedra et al., 2005; Miller et al., 1998; Pariaud et al., 2009; Setti et al 2008; Suffert et al., 2013). We show that both incubation and latent periods increase on resistant plants, but

Figure 6B also shows that the proportion of the latent period representing the incubation period is smaller on resistant than on susceptible plants. This implies that in our dataset quantitative resistance increases the latent period more than the incubation period. This is in line with a recent review, where French et al. (2016) list as mechanisms playing part in quantitative resistance: (i) polymorphic genes of the plant immune system (NBS-LRR R genes, wall associated kinases (WAKs), pattern recognition receptors (PRRs)), (ii) organ-, tissue- or developmental stage-specific gene expression and (iii) enzymatic activity in the host's secondary metabolism. All of these likely participate to slowing down mycelium growth once the pathogen develops inside the host.

Adaptation or constraints ?

Our data show that differences in pathogen trophic types translate into differences in latent periods. Our results suggest that there exist two opposed host exploitation strategies: on the one hand necrotrophs, causing a quick and virulent attack on the host tissue, and on the other hand biotrophs and hemibiotrophs, carefully avoiding or delaying the virulent phase of infection. Necrotrophs, by completing rapidly their infection cycle, access all the resources of the necrotic tissue. By avoiding or delaying necrosis, biotrophic and hemibiotrophic pathogens establish a longer-lasting interaction with the host. We argue that this main result can be explained by two different hypotheses. The length of the latent period is either set by constraints set by the trophic types, such as physiological limits or genetic programmes required for different trophic strategies, or it is the result of adaptation to contrasting conditions experienced by pathogens of different trophic type. In other words, is the latent period of hemibiotrophs long because it cannot be reduced for physiological reasons (constraints hypothesis) or because a long period is optimal (adaptation hypothesis).

Considering the constraint hypothesis, compared to necrotrophs, biotrophs and hemibiotrophs may need more time to develop longer-lasting interaction structures such as haustoria and interfacial extracellular matrices (Perfect and Green, 2001, Yi and Valent, 2013, Garnica et al., 2014). Also, it has been proposed that the long latent period of the hemibiotrophs is necessary for them to undergo the profound transcriptomic rearrangements underlying the switch between biotrophy and necrotrophy (Oh et al., 2008; O'Connell et al., 2012). Moreover,

Considering the adaptation hypothesis, we argue that these contrasted host exploitation strategies appear to be analogous to the so-called “milker” and “killer” strategies that have either a prudent or an aggressive exploitation strategy (Van Baalen and Sabelis, 1995). The advantage of the milker strategy is the expected benefit of continued host growth. The advantage of the killer strategy is immediate (and hence exclusive) access to the current host resource. Van Baalen and Sabelis (1995) show that the evolutionary success of milkers and killers depends on the spatial population structure and, more generally, on the likelihood of sharing resources with competitors. A high risk of competition for resources (i.e., through co-infection) is predicted to select for virulent strategies such as, in our case, necrotrophs. A low risk is predicted to select for more prudent strategies, such as hemibiotrophs. This idea is consistent with the work of van den Berg et al. (2013) that have shown that short latent periods are likely to be selected under conditions of autoinfection compared to alloinfection equally due to a higher risk of competition. From our results thus emerges an ecological hypothesis for the distribution of latent periods and trophic types that could be tested by careful analysis of the phylogeny and ecological history of different pathogen species.

REFERENCES

1. Agrios, G. (2004). Plant pathology: Fifth edition. pp 102-103.
2. Andrade-Piedra, J.L., Hijmans, R.J., Juárez, H.S., Forbes, G. a, Shtienberg, D., and Fry, W.E. (2005). Simulation of Potato Late Blight in the Andes. II: Validation of the LATEBLIGHT Model. *Phytopathology* 95, 1200–1208.
3. Andrivon, D., Montarry, J., Corbière, R., Pasco, C., Glais, I., Marquer, B., Clément, J.A.J., Castel, M., and Hamelin, F.M. (2013). The hard life of Phytophthora infestans: When trade-offs shape evolution in a biotrophic plant pathogen. *Plant Pathology* 62, 28–35.
4. Antonovics, J., and Alexander, H.M. (1989). The concept of fitness in plant-fungal pathogen systems. *Plant Disease Epidemiology* 2, 185–214.
5. Armour, T., Chng, S., Butler, R.C., Jamieson, P.D., and Zyskowski, R.F. (2004). Examining the Latent Period of Septoria Tritici Blotch in a Field Trial of Winter Wheat. *New Zealand Plant Protection* 57, 116–120.
6. Arseniuk, E., Czembor, P.C., Czaplicki, A., Song, Q., Cregan, P.B., Hoffman, D.L., and Ueng, P.P. (2004). QTL controlling partial resistance to Stagonospora nodorum leaf blotch in winter wheat cultivar Alba. *Euphytica* 137, 225–231.
7. Asalf, B., Health, P., and Division, P.P. (2016). Effects of Development of Ontogenic Resistance in Strawberry Leaves Upon Pre- and Postgermination Growth and Sporulation of Podosphaera aphanis. 100, 72–78.
8. Asher, M.J.C., and Thomas, C.E. (1987). The inheritance of mechanisms of partial resistance to Erysiphe graminis in spring barley. *Plant Pathology* 36, 66–72.
9. Austin, C.N., and Wilcox, W.F. (2012). Effects of Sunlight Exposure on Grapevine Powdery Mildew Development. *Phytopathology* 102, 857–866.
10. Baayen, R.P., and van der Plas, C.H. (1992). Localization ability, latent period and wilting rate in eleven carnation cultivars with partial resistance to Fusarium wilt. *Euphytica* 59, 165–174.
11. Bashi, E., and Rotem, J. (1975). Sporulation of Stemphylium botryosum f. sp. lycopersici in tomatoes and of Alternaria porri f. sp. solani in Potatoes Under Alternating Wet-Dry Regimes. *Phytopathology* 65, 532–535.
12. Behr, M., Humbeck, K., Hause, G., Deising, H.B., and Wirsel, S.G.R. (2010). The hemibiotroph Colletotrichum graminicola locally induces photosynthetically active green islands but globally accelerates senescence on aging maize leaves. *Molecular Plant-Microbe Interactions : MPMI* 23, 879–892.
13. Beresford, R.M., and Royle, D.J. (1988). Relationships between leaf emergence and latent period for leaf rust (*Puccinia hordei*) on spring barley, and their significance for disease monitoring. *Zeitschrift fur Pflanzenkrankheiten und Pflanzenschutz* 95, 361–71.
14. van den Berg, F., Gaucel, S., Lannou, C., Gilligan, C.A., and van den Bosch, F. (2013). High levels of auto-infection in plant pathogens favour short latent periods: A theoretical approach. *Evolutionary Ecology* 27, 409–428.
15. Bernard, F., Sache, I., Suffert, F., and Chelle, M. (2013). The development of a foliar fungal pathogen does react to leaf temperature! *New Phytologist* 198, 232–240.

16. Boiteux, L.S., Reifschneider, F.J.B., and Pessoa, H.B.S.V. (1995). Phenotypic expression of quantitative and qualitative components of partial resistance to powdery mildew (*Sphaerotheca fuliginea* race 1) in melon (*Cucumis melo*) germplasm. *Plant Breeding* 114, 185–187.
17. Bouhassan, A., Sadiki, M., Tivoli, B., and El Khiati, N. (2003). Analysis by detached leaf assay of components of partial resistance of faba bean (*Vicia faba* L.) to chocolate spot caused by *Botrytis fabae* Sard. *Phytopathologia Mediterranea* 42, 183–190.
18. Bouhassan, A., Sadiki, M., Tivoli, B., and Porta-Puglia, A. (2004). Influence of growth stage and leaf age on expression of the components of partial resistance of faba bean to *Botrytis fabae* Sard. *Phytopathologia Mediterranea* 43, 318–324.
19. Bouhassan, A., Sadiki, M., and Tivoli, B. (2007). Effets de la température et de la dose de l'inoculum sur les composantes de la résistance partielle de la fève au *Botrytis fabae* Sard. *Acta Botanica Gallica* 154, 53–62.
20. Brandon Matheny, P., Wang, Z., Binder, M., Curtis, J.M., Lim, Y.W., Henrik Nilsson, R., Hughes, K.W., Hofstetter, V., Ammirati, J.F., Schoch, C.L., et al. (2007). Contributions of *rpb2* and *tef1* to the phylogeny of mushrooms and allies (Basidiomycota, Fungi). *Molecular Phylogenetics and Evolution* 43, 430–451.
21. Broers, L.H.M. (1997). Components of quantitative resistance to yellow rust in ten spring bread wheat cultivars and their relations with field assessments. *Euphytica* 96, 215–223.
22. Browne, R.A., and Cooke, B.M. (2004). Development and evaluation of an in vitro detached leaf assay for pre-screening resistance to Fusarium head blight in wheat. *European Journal of Plant Pathology* 110, 91–102.
23. Browne, R.A., Murphy, J.P., Devaney, D., Walsh, E.J., Griffey, C.A., Hancock, J.A., Harrison, S.A., Hart, P., Kolb, F.L., McKendry, A.L., et al. (2004). Evaluation of Components of Fusarium Head Blight Resistance in Soft Red Winter Wheat Germ Plasm Using a Detached Leaf Assay. *Plant Disease* 89, 404–411.
24. Browne, R.A., Mascher, F., Golebiowska, G., and Hofgaard, I.S. (2006). Components of partial disease resistance in wheat detected in a detached leaf assay inoculated with *Microdochium majus* using first, second and third expanding seedling leaves. *Journal of Phytopathology* 154, 204–208.
25. Carroll, G. (1988). Fungal Endophytes in Stems and Leaves: From Latent Pathogen to Mutualistic Symbiont. *Ecology* 69(1), 2–9.
26. Carson, M.L., Van Dyke, C.G. (1994). Effect of light and temperature on expression of partial resistance of maize to *Exserohilum turcicum*. *Plant Disease* 78, 519–522.
27. Casela, C.R., Frederiksen, R.A., and Ferreira, A.S. (1993). Evidence for dilatory resistance to anthracnose in sorghum. *Plant Disease* 77, 908–911.
28. Chhikara, S., Chaudhury, D., Dhankher, O.P., and Jaiwal, P.K. (2012). Combined expression of a barley class II chitinase and type I ribosome inactivating protein in transgenic *Brassica juncea* provides protection against *Alternaria brassicaceae*. *Plant Cell, Tissue and Organ Culture* 108, 83–89.
29. Chongo, G., and Bernier, C.C. (2000). Effects of Host, Inoculum Concentration, Wetness Duration, Growth Stage, and Temperature on Anthracnose of Lentil. *Plant Disease* 84, 544–548.
30. Choudhury, R.A., McRoberts, N., and Gubler, W.D. (2014). Effects of punctuated heat stress on the grapevine powdery mildew pathogen, *Erysiphe necator*. *Phytopathologia Mediterranea* 53, 148–158.
31. Clulow, S.A., Lewis, B.G., Parker, M.L., and Matthews, P. (1991). Infection of pea epicotyls by *Mycosphaerella pinodes*. *Mycological Research* 95, 817–820.

32. Cooke, R. C., and Whipps, J. M. (1980). The evolution of modes of nutrition in fungi parasitic on terrestrial plants. *Biological Reviews* 55, 341–362.
33. Cromey, M.G. (1992). Adult plant resistance to stripe rust (*Puccinia striiformis*) in some New Zealand wheat cultivars. *New Zealand Journal of Crop and Horticultural Science* 20, 413–419.
34. Crous, P.W., Schoch, C.L., Hyde, K.D., Wood, A.R., Gueidan, C., de Hoog, G.S., and Groenewald, J.Z. (2009). Phylogenetic lineages in the Capnodiales. *Studies in Mycology* 64, 17–47.
35. Cunfer, B.M., Stooksbury, D.E., and Johnson, J.W. (1988). Components of partial resistance to *Leptosphaeria nodorum* among seven soft red winter wheats. *Euphytica* 37, 129–140.
36. Czembor, P.C., Arseniuk, E., Czaplicki, A., Song, Q., Cregan, P.B., and Ueng, P.P. (2003). QTL mapping of partial resistance in winter wheat to *Stagonospora nodorum* blotch. *Genome* 46, 546–554.
37. Danelli, A.L.D., and Reis, E.M. (2016). Quantification of incubation , latent and infection periods of *Phakopsora pachyrhizi* in soybean , according to chronological time and degree-days. 11–17.
38. De Vleesschauwer, D., Xu, J., and Höfte, M. (2014). Making sense of hormone-mediated defense networking: from rice to *Arabidopsis*. *Frontiers in Plant Science* 5.
39. Dehghani, H., and Moghaddam, M. (2004). Genetic analysis of the latent period of stripe rust in wheat seedlings. *Journal of Phytopathology* 152, 325–330.
40. Dehghani, H., Moghaddam, M., Ghannadha, M.R., Valizadeh, M., and Torabi, M. (2002). Inheritance of the latent period of stripe rust in wheat. *Journal of Genetics and Breeding* 56, 155–163.
41. Delaye, L., García-Guzmán, G., and Heil, M. (2013). Endophytes versus biotrophic and necrotrophic pathogens—are fungal lifestyles evolutionarily stable traits? *Fungal Diversity* 60, 125–135.
42. Dewdney, M., Charest, J., Paulitz, T., and Carisse, O. (2003). Multivariate analysis of apple cultivar susceptibility to *Venturia inaequalis* under greenhouse conditions. *Canadian Journal of Plant Pathology* 25, 387–400.
43. Diamond, H., and Cooke, B.M. (1999). Towards the development of a novel in vitro strategy for early screening of *Fusarium* ear blight resistance in adult winter wheat plants. *European Journal of Plant Pathology* 105, 363–372.
44. Diaz-Lago, J.E., Stuthman, D.D., and Leonard, K.J. (2003). Evaluation of Components of Partial Resistance to Oat Crown Rust Using Digital Image Analysis. *Plant Disease* 87, 667–674.
45. Divon, H.H., and Fluhr, R. (2007). Nutrition acquisition strategies during fungal infection of plants. *FEMS Microbiology Letters* 266, 65–74.
46. Dowkiw, A., Husson, C., Frey, P., Pinon, J., and Bastien, C. (2003). Partial resistance to *Melampsora larici-populina* leaf rust in hybrid poplars: Genetic variability in inoculated excised leaf disk bioassay and relationship with complete resistance. *Phytopathology* 93, 421–427.
47. Du, C.G., Nelson, L.R., and McDaniel, M.E. (1999). Diallel analysis of gene effects conditioning resistance to *Stagonospora nodorum* (Berk.) in wheat. *Crop Science* 39, 686–690.
48. Eaton, D.L., McVey, D.V., and Busch, R.H. (1984). Quantification of Infection Levels in Wheat Genotypes Varying in Stem Rust Resistance1. *Crop Science* 24, 122.
49. Engels, A.J.G., and de Waard, M. a. (1996). Fitness of isolates of *Erysiphe graminis* f.sp. *tritici* with reduced sensitivity to fenpropimorph. *Crop Protection* 15, 771–777.
50. Eversmeyer, M.G., Kramer, C.L., and Browder, L.E. (1980). Effect of Temperature and Host:Parasite Combination on the latent period of *Puccinia recondita* in seedling wheat plants. *Phytopathology* 70, 938–941.

51. Figueroa, L., Fitt, B.D.L., Shaw, M.W., McCartney, H.A., and Welham, S.J. (1995a). Effects of temperature on the development of light leaf spot *Pyrenopeziza brassicae* on oilseed rape *Brassica napus*. *Plant Pathology* 44, 51–62.
52. Figueroa, L., Fitt, B.D.L., Welham, S.J., Shaw, M.W., and McCartney, H.A. (1995b). Early Development of Light Leaf-Spot (*Pyrenopeziza-Brassicae*) on Winter Oilseed Rape (*Brassica-Napus*) in Relation to Temperature and Leaf Wetness. *Plant Pathology* 44, 641–654.
53. Fisher, A.J., Woods, D.M., Smith, L., and Bruckart, W.L. (2008). Latent period and viability of *Puccinia jaceae* var. *solstitialis* urediniospores: Implications for biological control of yellow starthistle. *Biological Control* 45, 146–153.
54. Flier, W.G., and Turkensteen, L.J. (1999). Foliar aggressiveness of *Phytophthora infestans* in three potato growing regions in the Netherlands. *European Journal of Plant Pathology* 105, 381–388.
55. French, E., Kim, B.S., and Iyer-Pascuzzi, A.S. (2016). Mechanisms of quantitative disease resistance in plants. *Seminars in Cell and Developmental Biology* 56, 201–208.
56. Frenkel, O., Brewer, M.T., and Milgroom, M.G. (2010). Variation in pathogenicity and aggressiveness of *Erysiphe necator* from different *Vitis* spp. and geographic origins in the eastern United States. *Phytopathology* 100, 1185–1193.
57. Frezal, L., Robert, C., Bancal, M.-O., and Lannou, C. (2009). Local dispersal of *Puccinia triticina* and wheat canopy structure. *Phytopathology* 99, 1216–1224.
58. Galea, V.J., and Price, T.V. (1988). Resistance of lettuce and related species to anthracnose (*Micromochium panattonianum*) in Australia. *Plant Pathology* 37, 363–372.
59. Garin, G., Fournier, C., Andrieu, B., Houlès, V., Robert, C., and Pradal, C. (2014). A modelling framework to simulate foliar fungal epidemics using functional-structural plant models. *Annals of Botany* 114, 795–812.
60. Garnica, D.P., Nemri, A., Upadhyaya, N.M., Rathjen, J.P., and Dodds, P.N. (2014). The Ins and Outs of Rust Haustoria. *PLoS Pathogens* 10.
61. Ghannadha, M., Nayyeri, F., Anseri, O. and Zali, A. (2005). Inheritance of the latent period of stripe rust in wheat. *International Journal of Agriculture and Biology* 7, 381–384.
62. Gilles, T., Fitt, B.D.L., Kennedy, R., Welham, S.J., and Jeger, M.J. (2000). Effects of temperature and wetness duration on conidial infection, latent period and asexual sporulation of *Pyrenopeziza brassicae* on leaves of oilseed rape. *Plant Pathology* 49, 498–508.
63. Gingera, G.R., Davis, D.W., and Groth, J.V. (1995). Identification and inheritance of delayed first pustule appearance to common leaf rust in sweet corn. *Journal of the American Society for Horticultural Science* 120, 667–672.
64. Giorcelli, a, Vietto, L., Anselmi, N., and Gennaro, M. (1996). Influence of clonal susceptibility, leaf age and inoculum density on infections by *Melampsora larici-populina* races E1 and E3. *European Journal of Forest Pathology* 26, 323–331.
65. Giri, P., Taj, G., and Kumar, A. (2013). Comparison of artificial inoculation methods for studying pathogenesis of *Alternaria brassicae* (Berk.) Sacc on *Brassica juncea* (L.) Czern. (Indian mustard). *African Journal of Biotechnology* 12, 2422–2426.
66. Graichen, F.A.S., Martinelli, J.A., de Lima Wesp, C., Federizzi, L.C., and Chaves, M.S. (2011). Epidemiological and histological components of crown rust resistance in oat genotypes. *European Journal of Plant Pathology* 131, 497–510.

67. Habtu, A., and Zadoks, J.C. (1995). Components of partial resistance in phaseolus beans against an Ethiopian isolate of bean rust. *Euphytica* 83, 95–102.
68. Hamelin, R.C., Shain, L., and Thielges, B.A. (1992). Adaptation of poplar leaf rust to Eastern cottonwood. *Euphytica* 62, 69–75.
69. Hamelin, R.C., Ferriss, R.S., and Shain, L. (1994). Prediction of poplar leaf rust epidemics from a leaf-disk assay. *Canadian Journal of Forest Research* 24, 2085-2088.
70. Hazra, S. (1998). Pathogenic variability in Sorghum anthracnose incited by *Colletotrichum graminicola*. Doctoral Thesis.
71. Héraudet, V., Salvaudon, L., and Shykoff, J.A. (2008). Trade-off between latent period and transmission success of a plant pathogen revealed by phenotypic correlations. *Evolutionary Ecology Research* 10, 912–924.
72. Hernandez Nopsa, J.F., and Pfender, W. (2014). A latent period duration model for wheat stem rust. *Plant Disease* 98, 140425065917001.
73. Horbach, R., Navarro-Quesada, A.R., Knogge, W., and Deising, H.B. (2011). When and how to kill a plant cell: Infection strategies of plant pathogenic fungi. *Journal of Plant Physiology* 168, 51–62.
74. Jacobsen, B.J., Johnston, M., Zidack, N.K., Eckhoff, J., and Bergman, J. (2004). Effects of high temperatures on cercospora leaf spot infection and sporulation and effects of variety and number of fungicide sprays on yield. *Sugarbeet Research and Extension Reports* 35, 205–208.
75. Jeger, M.J., Gareth Jones, D., and Griffiths, E. (1983). Components of partial resistance of wheat seedlings to *Septoria nodorum*. *Euphytica* 32, 575–584.
76. Johnson, D. a. (1980). Effect of Low Temperature on the Latent Period of Slow and Fast Rusting Winter Wheat Genotypes. *Plant Disease* 64, 1006.
77. Jorge, V., Dowkiw, A., Faivre-Rampant, P., and Basrtien, C. (2005). Genetic architecture of qualitative and quantitative *Melampsora larici-populina* leaf rust resistance in hybrid poplar: Genetic mapping and QTL detection. *New Phytologist* 167, 113–127.
78. Kabbage, M., Yarden, O., and Dickman, M.B. (2015). Pathogenic attributes of *Sclerotinia sclerotiorum*: Switching from a biotrophic to necrotrophic lifestyle. *Plant Science* 233, 53–60.
79. Kanrar, S., Venkateswari, J.C., Kirti, P.B., and Chopra, V.L. (2002). Transgenic expression of hevein, the rubber tree lectin, in Indian mustard confers protection against *Alternaria brassicae*. *Plant Science* 162, 441-448.
80. Karaoglanidis, G.S., Luo, Y. and Michailides, T.J. (2010). Competitive Ability and Fitness of *Alternaria alternata* Isolates Resistant to Qol Fungicides. *Plant Disease* 95, 178-182.
81. Kari, A.G. and Griffiths, E. (1993). Components of partial resistance of barley to *Rhynchosporium secalis*: use of seedling tests to predict field resistance. *Annals of Applied Biology* 123, 545-561.
82. Karolewski, Z., Evans, N., Fitt, B.D.L., Todd, A.D., and Baierl, A. (2002). Sporulation of *Pyrenopeziza brassicae* (light leaf spot) on oilseed rape (*Brassica napus*) leaves inoculated with ascospores or conidia at different temperatures and wetness durations. *Plant Pathology* 51, 654–665.
83. Kemen, A.C., Agler, M.T., and Kemen, E. (2015). Host-microbe and microbe-microbe interactions in the evolution of obligate plant parasitism. *New Phytologist* 206, 1207–1228.
84. Kochman, J.K. and Brown, J.F. (1975). Host and environmental effects on post-penetration development pf *Puccinia graminis avenae* and *P. coronata avenae*. *Annals of Applied Biology* 81, 33-41.

85. Kogel, K.H., Franken, P., and Huckelhoven, R. (2006). Endophyte or parasite--what decides? *Curr Opin Plant Biol* 9, 358–363.
86. Kolnaar, R.W., and Van Den Bosch, F. (2001). Effect of temperature on epidemiological parameters of *Puccinia lagenophorae*. *Plant Pathology* 50, 363–370.
87. Lascoux, M., Ramstedt, M., Aström, B., and Gullberg, U. (1996). Components of resistance of leaf rust (*Melampsora laricis epitea* Kleb./*Melampsora ribesii-viminalis* Kleb.) in *Salix viminalis* L. *Theoretical and Applied Genetics* 93, 1310–1318.
88. Lecompte, F., Abro, M.A., and Nicot, P.C. (2010). Contrasted responses of *Botrytis cinerea* isolates developing on tomato plants grown under different nitrogen nutrition regimes. *Plant Pathology* 59, 891–899.
89. Lee, S.-J., and Rose, J.K.C. (2010). Mediation of the transition from biotrophy to necrotrophy in hemibiotrophic plant pathogens by secreted effector proteins. *Plant Signaling & Behavior* 5, 769–772.
90. Lehman, J., and Shaner, G. (1996). Genetic Variation in Latent Period Among Isolates of *Puccinia recondita* f. sp. *tritici* on Partially Resistant Wheat Cultivars. *Phytopathology* 86, 633–641.
91. Lehman, J.S., and Shaner, G. (1997). Selection of Populations of *Puccinia recondita* f. sp. *tritici* for Shortened Latent Period on a Partially Resistant Wheat Cultivar. *Phytopathology* 87, 170–176.
92. Lehman, J.S., Hanson, K.A., and Shaner, G. (2005). Relationship Among Genes Conferring Partial Resistance to Leaf Rust (*Puccinia triticina*) in Wheat Lines CI 13227 and L-574-1. *Phytopathology* 95, 198–205.
93. Le May, C., Guibert, M., Leclerc, A., Andrivon, D., and Tivoli, B. (2012). A single, plastic population of *Mycosphaerella pinodes* causes ascochyta blight on winter and spring peas (*Pisum sativum*) in France. *Applied and Environmental Microbiology* 78, 8431–8440.
94. Li, Y.H., Windham, M.T., Trigiano, R.N., Fare, D.C., Spiers, J.M., and Copes, W.E. (2006). Development of *Erysiphe pulchra*, the causal agent of powdery mildew, on leaf disks of susceptible and resistant flowering dogwood (*Cornus florida*). *Canadian Journal of Plant Pathology* 28, 71–76.
95. Li, Y., Windham, M., and Trigiano, R. (2007). Microscopic and macroscopic studies of the development of *Puccinia hemerocallidis* in resistant and susceptible daylily cultivars. *Plant Disease* 91, 664–668.
96. Li, Y., Windham, M., Trigiano, R., Reed, S., Rinehart, T., and Spiers, J. (2009). Assessment of resistance components of bigleaf hydrangeas (*Hydrangea macrophylla*) to *Erysiphe polygoni* in vitro. *Canadian Journal of Plant Pathology* 31, 348–355.
97. Lightfoot, D.J., and Able, A.J. (2010). Growth of *Pyrenophora teres* in planta during barley net blotch disease. *Australian Plant Pathology* 39(6), 499–507.
98. Lo Presti, L., Lanver, D., Schweizer, G., Tanaka, S., Liang, L., Tollot, M., Zuccaro, A., Reissmann, S., and Kahmann, R. (2015). Fungal Effectors and Plant Susceptibility. *Annual Review of Plant Biology* 66, 513–545.
99. Loughman, R., Wilson, R.E., and Thomas, G.J. (1996). Components of resistance to *Mycosphaerella graminicola* and *Phaeosphaeria nodorum* in spring wheats. *Euphytica* 89, 377–385.
100. Lovell, D.J., Parker, S.R., Hunter, T., Royle, D.J., and Coker, R.R. (1997). Influence of crop growth and structure on the risk of epidemics by *Mycosphaerella graminicola* (*Septoria tritici*) in winter wheat. *Plant Pathology* 46, 126–138.
101. Lovell, D.J., Hunter, T., Powers, S.J., Parker, S.R., and Van Den Bosch, F. (2004). Effect of temperature on latent period of septoria leaf blotch on winter wheat under outdoor conditions. *Plant Pathology* 53, 170–181.

102. Madden, L.V., and Boudreau, M. a (1997). Effect of Strawberry Density on the Spread of Anthracnose Caused by *Colletotrichum acutatum*. *Phytopathology* 87, 828–838.
103. Magnin-Robert, M., Le Bourse, D., Markham, J.E., Dorey, S., Clément, C., baillieul, fabienne, and Dhondt-Cordelier, S. (2015). Modifications of sphingolipid content affect tolerance to hemibiotrophic and necrotrophic pathogens by modulating plant defense responses in *Arabidopsis*. *Plant Physiology* pp.01126.2015.
104. Mendgen, K., and Hahn, M. (2002). Plant infection and the establishment of fungal biotrophy. *Trends in Plant Science* 7, 352–356.
105. Mersha, Z., Zhang, S., and Hau, B. (2014). Effects of temperature, wetness duration and leaf age on incubation and latent periods of black leaf mold (*Pseudocercospora fuligena*) on fresh market tomatoes. *European Journal of Plant Pathology* 138, 39–49.
106. Miedaner, T., Moldovan, M., and Ittu, M. (2003). Comparison of spray and point inoculation to assess resistance to fusarium head blight in a multienvironment wheat trial. *Phytopathology* 93, 1068–1072.
107. Mikkelsen, B.L., Jørgensen, R.B., and Lyngkjær, M.F. (2015). Complex interplay of future climate levels of CO₂, ozone and temperature on susceptibility to fungal diseases in barley. *Plant Pathology* 64, 319–327.
108. Miller, J.S., Johnson, D. a, and Hamm, P.B. (1998). Aggressiveness of Isolates of *Phytophthora infestans* from the Columbia Basin of Washington and Oregon. *Phytopathology* 88, 190–197.
109. Milus, E.A., Seyran, E., and McNew, R. (2006). Aggressiveness of *Puccinia striiformis* f.sp.*tritici* isolates in the South-Central United States. *Plant Disease* 90, 847–852.
110. Milus, E. a, Kristensen, K., and Hovmöller, M.S. (2009). Evidence for increased aggressiveness in a recent widespread strain of *Puccinia striiformis* f. sp. *tritici* causing stripe rust of wheat. *Phytopathology* 99, 89–94.
111. Montarry, J., Cartolaro, P., Delmotte, F., Jolivet, J., and Willocquet, L. (2008). Genetic structure and aggressiveness of *Erysiphe necator* populations during grapevine powdery mildew epidemics. *Applied and Environmental Microbiology* 74, 6327–6332.
112. Morais, D., Laval, V., Sache, I., and Suffert, F. (2015). Comparative pathogenicity of sexual and asexual spores of *Zymoseptoria tritici* (*Septoria tritici* blotch) on wheat leaves. *Plant Pathology* 64, 1429–1439.
113. Mwakutuya, E. (2006). Epidemiology of *Stemphylium* blight ol lentil (*Lens culinaris*) in Saskatchewan. PhD Thesis.
114. Newcombe, G. (1998). Association of *Mmd1*, a Major Gene for Resistance to *Melampsora medusae* f. sp. *deltoidae*, with Quantitative Traits in Poplar Rust. *Phytopathology* 88, 114–121.
115. O'Connell, R.J., Thon, M.R., Hacquard, S., Amyotte, S.G., Kleemann, J., Torres, M.F., Damm, U., Buiate, E. a, Epstein, L., Alkan, N., et al. (2012). Lifestyle transitions in plant pathogenic *Colletotrichum* fungi deciphered by genome and transcriptome analyses. *Nature Genetics* 44, 1060–1065.
116. Oh, Y., Donofrio, N., Pan, H., Coughlan, S., Brown, D.E., Meng, S., Mitchell, T., and Dean, R.A. (2008). Transcriptome analysis reveals new insight into appressorium formation and function in the rice blast fungus *Magnaporthe oryzae*. *Genome Biology* 9, R85.
117. Ohm, R.A., Feau, N., Henrissat, B., Schoch, C.L., Horwitz, B.A., Barry, K.W., Condon, B.J., Copeland, A.C., Dhillon, B., Glaser, F., et al. (2012). Diverse Lifestyles and Strategies of Plant Pathogenesis Encoded in the Genomes of Eighteen Dothideomycetes Fungi. *PLoS Pathogens* 8.

118. Oliver, R.P., and Ipcho, S.V.S. (2004). Arabidopsis pathology breathes new life into the necrotrophs-vs.-biotrophs classification of fungal pathogens. *Molecular Plant Pathology* 5, 347–352.
119. Oliveira-Garcia, E., and Valent, B. (2015). How eukaryotic filamentous pathogens evade plant recognition. *Current Opinion in Microbiology* 26, 92–101.
120. Palma-Guerrero, J., Torriani, S.F.F., Zala, M., Carter, D., Courbot, M., Rudd, J.J., McDonald, B.A., and Croll, D. (2016). Comparative transcriptomic analyses of *Zymoseptoria tritici* strains show complex lifestyle transitions and intraspecific variability in transcription profiles. *Molecular Plant Pathology* 17, 845–859.
121. Pariaud, B., Robert, C., Goyeau, H., and Lannou, C. (2009). Aggressiveness components and adaptation to a host cultivar in wheat leaf rust. *Phytopathology* 99, 869–878.
122. Pariaud, B., Goyeau, H., Halkett, F., Robert, C., and Lannou, C. (2012). Variation in aggressiveness is detected among *Puccinia triticina* isolates of the same pathotype and clonal lineage in the adult plant stage. *European Journal of Plant Pathology* 134, 733–743.
123. Pariaud, B., Van den Berg, F., Van den Bosch, F., Powers, S.J., Kaltz, O., and Lannou, C. (2013). Shared influence of pathogen and host genetics on a trade-off between latent period and spore production capacity in the wheat pathogen, *Puccinia triticina*. *Evolutionary Applications* 6, 303–312.
124. Park, R.F., and Rees, R.G. (1989). Expression of adult plant resistance and its effect on the development of *Puccinia striiformis* f.sp. *tritici* in some Australian wheat cultivars. *Plant Pathology* 38, 200–208.
125. Parlevliet, J.E. (1979). Components of Resistance that Reduce the Rate of Epidemic Development. *Annual Review of Phytopathology* 17, 203–222.
126. Pedersen, E.A., and Morrall, R.A.A. (1994). Effects of Cultivar, Leaf Wetness Duration, Temperature, and Growth Stage on Infection and Development of Ascochyta Blight of Lentil. *Phytopathology* 84, 1024–1030.
127. Peever, T.L., and Milgroom, M.G. (1994). Lack of correlation between fitness and resistance to sterol biosynthesis-inhibiting fungicides in *Pyrenophora teres*. *Phytopathology* 84, 515–519.
128. Perfect, S.E., and Green, J.R. (2001). Infection structures of biotrophic and hemibiotrophic fungal plant pathogens. *Molecular Plant Pathology* 2, 101–108.
129. Pétriacoq, P., Stassen, J.H.M., and Ton, J. (2016). Spore Density Determines Infection Strategy by the Plant Pathogenic Fungus *Plectosphaerella cucumerina*. *Plant Physiology* 170, 2325–2339.
130. Prakash, C.S., and Thielges, B.A. (1989). Somaclonal Variation in Eastern Cottonwood for Race-Specific Partial Resistance to Leaf Rust Disease. *Phytopathology* 79, 805–808.
131. Prasad, K., Bhatnagar-mathur, P., Waliyar, F., and Sharma, K.K. Overexpression of a chitinase gene in transgenic peanut confers enhanced resistance to major s. *Journal of Plant Biochemistry and Biotechnology* 1–23.
132. Précigout, P-A., Claessen, D., and Robert, C. (2017). Crop fertilisation impacts epidemics and optimal latent period of biotrophic fungal pathogens. 10.1094/PHYTO-01-17-0019-R
133. Pringle, A., and Taylor, J.W. (2002). The fitness of filamentous fungi. *Trends in Microbiology* 10, 474–481.
134. Razavi, M., and Hughes, G.R. The relationship between molecular and pathogenic variability in a Saskatchewan population of *Mycosphaerella graminicola*. 10–10.

135. Robert, C., Fournier, C., Andrieu, B., and Ney, B. (2008). Coupling a 3D virtual wheat (*Triticum aestivum*) plant model with a *Septoria tritici* epidemic model (Septo3D): a new approach to investigate plant-pathogen interactions linked to canopy architecture. *Functional Plant Biology* 35, 997–1013.
136. Roderick, H.W., and Clifford, B.C. (1995). Variation in adult plant resistance to powdery mildew in spring oats under field and laboratory conditions. *Plant Pathology* 44, 366–373.
137. Roger, C., Tivoli, B., and Huber, L. (1999). Effects of temperature and moisture on disease and fruit body development of *Mycosphaerella pinodes* on pea (*Pisum sativum*). *Plant Pathology* 48, 1–9.
138. Rossi, V., Pattori, E., Giosué, S., and Bugiani, R. (2005). Growth and sporulation of *Stemphylium vesicarium*, the causal agent of brown spot of pear, on herb plants of orchard lawns. *European Journal of Plant Pathology* 111, 361–370.
139. Rotem, J., and Bashi, E. (1969). Induction of sporulation of *Alternaria porri* f. sp. *Solani* by inhibition of its vegetative development. *Transactions of the British Mycological Society* 53, 433–439.
140. Sánchez-Vallet, A., McDonald, M.C., Solomon, P.S., and McDonald, B.A. (2015). Is *Zymoseptoria tritici* a hemibiotroph? *Fungal Genetics and Biology* 79, 29–32.
141. Schoch, C.L., Crous, P.W., Groenewald, J.Z., Boehm, E.W.A., Burgess, T.I., de Gruyter, J., de Hoog, G.S., Dixon, L.J., Grube, M., Gueidan, C., et al. (2009). A class-wide phylogenetic assessment of Dothideomycetes. *Studies in Mycology* 64, 1–15.
142. Schweizer P. (2014). Host and Nonhost Response to Attack by Fungal Pathogens. In: Kumlehn J., Stein N. (eds) Biotechnological Approaches to Barley Improvement. *Biotechnology in Agriculture and Forestry*, vol 69 p208. Springer, Berlin, Heidelberg.
143. Setti, B., Bencheikh, M., Henni, J., and Neema, C. (2008). Effect of pea cultivar, pathogen isolate, inoculum concentration and leaf wetness duration on *Ascochyta* blight caused by *Mycosphaerella pinodes*. *Phytopathologia Mediterranea* 47, 214–222.
144. Setti, B., Bencheikh, M., Henni, J., and Neema, C. (2009). Comparative aggressiveness of *Mycosphaerella pinodes* on peas from different regions in western Algeria. *Phytopathologia Mediterranea* 48, 195–204.
145. Sharma, S., and Sharma, R.C. (2003). Influence of host genotype and pathogen isolate in the development of poplar leaf rust. *Zeitschrift Fur Pflanzenkrankheiten Und Pflanzenschutz-Journal of Plant Diseases and Protection* 110, 359–365.
146. Shaw, M.W. (1986). Effects of temperature and leaf wetness on *Pyrenophora teres* growing on barley cv. Sonja. *Plant Pathology* 35, 294–309.
147. Shaw, M.W. (1990). Effects of temperature, leaf wetness and cultivar on the latent period of *Mycosphaerella graminicola* on winter wheat. *Plant Pathology* 39, 255–268.
148. Shearer, B.L., and Zadoks, J.C. (1973). The latent period of *Septoria nodorum* in wheat . 1 . The effect of temperature and moisture treatments under controlled conditions. 80, 48–60.
149. Silva, D.N., Duplessis, S., Talhinhas, P., Azinheira, H., Paulo, O.S., and Batista, D. (2015). Genomic patterns of positive selection at the origin of rust fungi. *PLoS ONE* 10.
150. Slippers, B., and Wingfield, M.J. (2007). Botryosphaeriaceae as endophytes and latent pathogens of woody plants: diversity, ecology and impact. *Fungal Biology Reviews* 21, 90–106.
151. Sombardier, A., Savary, S., Blancard, D., Jolivet, J., and Willocquet, L. (2009). Effects of leaf surface and temperature on monocyclic processes in *Podosphaera aphanis*, causing powdery mildew of strawberry. *Canadian Journal of Plant Pathology* 31, 10.

152. Sosa-Alvarez, M., Madden, L., and Ellis, M. (1995). Effects of Temperature and Wetness Duration on Sporulation of *Botrytis cinerea* on Strawberry Leaf Residues. *Plant Disease* 79, 609–615.
153. Sosnowski, M.R., Scott, E.S., and Ramsey, M.D. (2005). Temperature, wetness period and inoculum concentration influence infection of canola (*Brassica napus*) by pycnidiospores of *Leptosphaeria maculans*. *Australasian Plant Pathology* 34, 339–344.
154. Souza, A.G.C., Maffia, L.A., and Mizubuti, E.S.G. (2012). Cultural and Aggressiveness Variability of *Cercospora coffeicola*. *Journal of Phytopathology* 160, 540–546.
155. Spanu, P.D. (2012). The Genomics of Obligate (and Nonobligate) Biotrophs. *Annual Review of Phytopathology* 50, 91–109.
156. Steinberg, G. (2015). Cell biology of *Zymoseptoria tritici*: Pathogen cell organization and wheat infection. *Fungal Genetics and Biology* 79, 17–23.
157. Stooksbury, D.E., Johnson, J.W., and Cunfer, B.M. (1987). Incubation period and latent period of wheat for resistance to *Leptosphaeria nodorum*. *Plant Disease* 71, 1109–1112.
158. Suassuna, N.D., Maffia, L.A., and Mizubuti, E.S.G. (2004). Aggressiveness and host specificity of Brazilian isolates of *Phytophthora infestans*. *Plant Pathology* 53, 405–413.
159. Suffert, F., Sache, I., and Lannou, C. (2013). Assessment of quantitative traits of aggressiveness in *Mycosphaerella graminicola* on adult wheat plants. *Plant Pathology* 62, 1330–1341.
160. Suffert, F., Ravigné, V., and Sachec, I. (2015). Seasonal changes drive short-term selection for fitness traits in the wheat pathogen *Zymoseptoria tritici*. *Applied and Environmental Microbiology* 81, 6367–6379.
161. Taylor, P.W.J., and Ford, R. (2007). Diagnostics, genetic diversity and pathogenic variation of ascochyta blight of cool season food and feed legumes. *European Journal of Plant Pathology* 119(1), 127–133.
162. Teng, P.S., and Close, R.C. (1978). Effect of temperature and uredinium density on urediniospore production, latent period, and infectious period of *Puccinia hordei* Otth. *New Zealand Journal of Agricultural Research* 21, 287–296.
163. Tiedemann, A.V. (1992). Ozone Effects on Fungal Leaf Diseases of Wheat in Relation to Epidemiology. *Phytopathology* 186, 177–186.
164. Tollenaar, H. (1985). Uredospore Germination and Development of Some Cereal Rusts from South-central Chile at Constant Temperatures. *Journal of Phytopathology* 114, 118–125.
165. Tomerlin, J.R., and Jones, A. (1983). Effect of temperature and relative Humidity on the latent period of *Venturia inaequalis* in apple leaves. *Phytopathology* 73, 51–54.
166. Trail, F. (2009). For Blighted Waves of Grain: *Fusarium graminearum* in the Postgenomics Era. *Plant Pathology* 149(1), 103–110.
167. Trapero-Casas, A., and Kaiser, W.J. (1992). Influence of Temperature, Wetness Period, Plant Age, and Inoculum Concentration of Infection and Development of Ascochyta Blight of Chickpea. *Phytopathology* 5, 589–596.
168. de Vallavieille-Pope, C., Giosue, S., Munk, L., Newton, A.C., Niks, R.E., Østergård, H., Pons-Kühnemann, J., Rossi, V., and Sache, I. (2000). Assessment of epidemiological parameters and their use in epidemiological and forecasting models of cereal airborne diseases. *Agronomie* 20, 715–727.
169. van baalen, M., and Sabelis, M.W. (1995). The Milker Killer Dilemma in Spatially Structured Predator Prey Interactions. *Oikos* 74, 391–400.

170. Vanniasingham, V.M., and Gilligan, C.A. (1989). Effects of host, pathogen and environmental factors on latent period and production of pycnidia of *Leptosphaeria maculans* on oilseed rape leaves in controlled environments. *Mycological Research* 93, 167–174.
171. Vargas, W.A., Martin, J.M.S., Rech, G.E., Rivera, L.P., Benito, E.P., Diaz-Minguez, J.M., Thon, M.R., and Sukno, S.A. (2012). Plant Defense Mechanisms Are Activated during Biotrophic and Necrotrophic Development of *Colletotrichum graminicola* in Maize. *PLANT PHYSIOLOGY* 158, 1342–1358.
172. Verhoeff, K. (1974). Latent Infections by Fungi. *Annual Reviews in Phytopathology* 12, 99–110.
173. Viljanen-Rollinson, S.L.H., Gaunt, R.E., Frampton, C.M. a., Falloon, R.E., and McNeil, D.L. (1998). Components of quantitative resistance to powdery mildew (*Erysiphe pisi*) in pea (*Pisum sativum*). *Plant Pathology* 47, 137–147.
174. Viljanen-Rollinson, S.L., Marroni, M.V., Butler, R.C., Deng, Y., and Armour, T. (2005). Latent periods of *Septoria tritici* blotch on ten cultivars of wheat. *New Zealand Plant Protection* 58, 256–260.
175. Wang, Z., Binder, M., Schoch, C.L., Johnston, P.R., Spatafora, J.W., and Hibbett, D.S. (2006). Evolution of helotialean fungi (Leotiomycetes, Pezizomycotina): A nuclear rDNA phylogeny. *Molecular Phylogenetics and Evolution* 41, 295–312.
176. White, D., and Chen, W. (2007). Towards identifying pathogenic determinants of chickpea pathogen *Ascochyta rabiei*. *European Journal of Plant Pathology* 119(1), 3–12.
177. Wolfenbarger, S.N., Massie, S.T., Ocamb, C., Eck, E.B., Grove, G.G., Nelson, M.E., Probst, C., Twomey, M.C., and Gent, D.H. (2016). Distribution and Characterization of *Podosphaera macularis* Virulent on Hop Cultivars Possessing R6 -Based Resistance to Powdery Mildew. *Plant Disease* 100, 1212–1221.
178. Xu, X.M. (1999). Effects of temperature on the length of the incubation period of rose powdery mildew (*Sphaerotheca pannosa* var. *rosae*). *European Journal of Plant Pathology* 105, 13–21.
179. Xu, X.-M., and Robinson, J.D. (2000). Effects of temperature on the incubation and latent periods of hawthorn powdery mildew (*Podosphaera clandestina*). *Plant Pathology* 49, 791–797.
180. Xu, X., and Robinson, J. (2001). The effects of temperature on the incubation and latent periods of powdery mildew (*Erysiphe polygoni*) on clematis. *Journal of Phytopathology* 149, 565–568.
181. Yan, Z., Dolstra, O., Prins, T.W., Stam, P., and Visser, P.B. (2006). Assessment of partial resistance to powdery mildew (*Podosphaera pannosa*) in a tetraploid rose population using a spore-suspension inoculation method. *European Journal of Plant Pathology* 114, 301–308.
182. Yarullina, L.G., Troshina, N.B., Cherepanova, E. a., Zaikina, E. a., and Maksimov, I.V. (2011). Salicylic and Jasmonic acids in regulation of the proantioxidant state in wheat leaves infected by *Septoria nodorum* Berk. *Applied Biochemistry and Microbiology* 47, 549–555.
183. Yarullina, L.G., Veselova, S.V., Ibragimov, R.I., Shpirnaya, I.A., Kasimova, R.I., Akhatova, A.R., Tsvetkov, V.O., and Maksimov, I.V. (2014). Search for Molecular Markers of Wheat Resistance to Fungal Pathogens. *Agricultural Sciences* 5, 722–729.
184. Yi, M., and Valent, B. (2013). Communication Between Filamentous Pathogens and Plants at the Biotrophic Interface. *Annual Review of Phytopathology* 51, 587–611.
185. Zearfoss, a. D., Cowger, C., and Ojiambo, P.S. (2011). A Degree-Day Model for the Latent Period of *Stagonospora nodorum* Blotch in Winter Wheat. *Plant Disease* 95, 561–567.

Discussion

La discussion de thèse est organisée en quatre parties : (1) la discussion des questions et de l'approche de modélisation, (2) l'effet de la fertilisation sur les épidémies (sans évolution), (3) l'évolution des pathogènes et les effets de la fertilisation et (4) la possibilité d'utiliser la fertilisation pour réguler les épidémies.

Questions, démarche et originalités du travail de these

1) Une démarche pluridisciplinaire

L'un des principes fondamentaux de l'agroécologie est de valoriser les interactions entre les organismes de l'agrosystème pour atteindre des propriétés d'autorégulation de ce dernier. Les pratiques agricoles, en jouant sur l'environnement que vont rencontrer les organismes, peuvent influencer ces derniers et leurs interactions. C'est pourquoi ces pratiques pourraient représenter des leviers pour l'invention une agriculture plus durable, inspirée du fonctionnement des écosystèmes naturels. Mais « quoi copier ? » dans les écosystèmes naturels, et « comment l'appliquer ? » dans les agroécosystèmes, restent des questions encore largement débattues (Ford et McGuire, 2015).

Concernant la protection des cultures face aux maladies fongiques, les principales méthodes actuellement employées sont l'utilisation de fongicides et de résistances variétales. Pour mettre en place des solutions agroécologiques, nous avons besoin de nouvelles connaissances qui nous permettent de comprendre les liens écologiques entre l'hôte, son pathogène et leur environnement. Etudier l'effet de la fertilisation des cultures sur les dynamiques hôte-pathogènes s'inscrit dans cette démarche, la fertilisation impactant directement le développement de l'hôte et donc potentiellement son pathogène. On peut noter que beaucoup d'études sur les maladies concernent des échelles fines, celle de la lésion ou de la plante, alors que les épidémies et les possibilités de gestion agroécologique des maladies opèrent à des échelles plus larges comme le couvert ou le paysage (Meentemeyer et coll., 2012). De plus, même à ces échelles fines, capturer les effets dynamiques de colonisation intra-hôte et inter-hôte par exemple, s'avère ne pas être une tâche aisée. Et tout cela va sans

compter sur les remarquables capacités d'adaptation des pathogènes aux pratiques culturales, qui poussent à inclure les échelles de temps longues et l'évolution dans des études déjà largement multi-échelles (Zhan et coll., 2014). Peu d'études ont à ce jour combiné une approche dynamique et multi-échelle des pathosystèmes avec une dimension évolutive (Meentemeyer et coll., 2012 ; Cunniffe et coll., 2015).

Des approches de modélisation ont eu pour objectif de comprendre les effets de l'architecture des plantes sur les épidémies dans une optique de régulation des épidémies par certains traits des plantes. Ainsi, des modèles épidémiques ont été couplés avec des modèles FSPM (« Functional-Structural Plant Models », Godin et Sinoquet 2005, Vos et coll. 2009, Sievänen et coll. 2014). Ces modèles laissent la part belle aux effets dynamiques de croissance et de colonisation des plantes (Robert et coll. 2008, Calonnec et coll. 2008, Baccar et coll. 2011, Garin et coll. 2014, Robert et coll, 2017). Malheureusement, ils ne prennent pas (encore) en compte les rétroactions du pathogène sur la plante, couvert qui a pour le moment une architecture dynamique mais non fonctionnelle. De plus, les temps de calcul associés aux modèles FSPM laissent peu d'espoir quant aux possibilités de les utiliser à des échelles spatiales plus grandes.

A l'opposé, les modèles d'épidémiologie du paysage (Plantagenest et coll., 2007) ont permis de montrer l'importance de l'hétérogénéité spatiale et des processus de dispersion/colonisation dans le développement des maladies (Skelsey et coll., 2010 ; Mundt et coll., 2011 ; Filipe et coll., 2012 ; Papaïx et coll., 2014, 2015). En revanche, ils ne tiennent pas souvent compte les particularités biologiques des pathosystèmes aux échelles infra-parcelle et incluent rarement les effets écologiques de la culture (en tout cas autres que le niveau de résistance) sur le développement des pathogènes et les pratiques culturales.

L'une des particularités de notre travail réside dans le fait que nous avons développé une approche qui combine des aspects écologiques, écophysiologiques et épidémiologiques afin de modéliser l'agroécosystème en considérant la plante, le pathogène et leurs interactions et cela aux différentes échelles spatiales de l'agroécosystème. Notre objectif a été d'utiliser des méthodes et concepts venus de l'écologie théorique pour répondre à une question agronomique. L'étude va de l'échelle de la lésion à celle du couvert puis du paysage. Au cœur de cette démarche, notre vision est de considérer le pathosystème comme un système consommateur-ressource, qui est une des pierres angulaires de la théorie écologique et de l'écologie évolutive. Cela nous a donné accès aux compromis qui le contraignent et par là aux conséquences des interactions hôte-pathogène. Simuler la dynamique épidémique sur de

nombreuses saisons nous donne accès aux réponses évolutives du pathogène aux changements de fertilisation et nous permet ainsi d'envisager la durabilité de pratiques de fertilisation qui réduiraient les épidémies à l'échelle du paysage.

Une autre originalité de notre étude réside dans son objet. En effet, il y a à notre connaissance et à ce jour peu d'études de modélisation ayant pour objet la réponse des pathogènes à une diminution de la fertilisation des cultures (surtout sur des systèmes plante-puceron ; Cisneros et coll., 2001 ; Grechi et coll., 2010). Il y en a encore moins qui s'intéressent à l'adaptation des pathogènes aux niveaux de fertilisants. Ce travail pose donc la question, encore peu explorée, de la durabilité des effets des pratiques agricoles (en dehors des pesticides et des résistances qui sont peu durables) sur les pathogènes, question centrale pour l'aménagement de systèmes agroécologiques. De plus, la fertilisation vue comme un possible levier de régulation des pathogènes dans l'agroécosystème, nous apparaît comme une proposition originale.

2) Difficultés et choix

Etudier le comportement des systèmes complexes comme la réponse d'un pathosystème à la fertilisation pose l'épineuse question du degré de complexité nécessaire à une bonne modélisation du système. Prenons l'exemple de notre premier modèle qui couvre les échelles de la lésion au couvert (Chapitre 1). Pour bien refléter l'effet de la fertilisation sur le système, le modèle devait *a minima* intégrer ces deux échelles spatiales. Pour bien refléter l'histoire de vie de la plante comme du pathogène, le modèle se devait d'être structuré par âge. Il fallait implémenter une dynamique intra-saisonnière pour tenir compte des effets dynamiques, mais aussi un forçage saisonnier pour suivre le devenir des épidémies. Enfin, pour modéliser la dispersion des spores et la progression de la maladie au sein du couvert, un minimum de structure spatiale était nécessaire. Le modèle développé apparaît donc plus compliqué que des modèles épidémiologiques tels que les SEIR, mais nous pensons qu'il s'agit d'un des modèles les plus simples possibles intégrant tous les éléments dont nous avions besoin pour étudier les réponses épidémiologiques et évolutives des pathogènes fongiques foliaires à la fertilisation des cultures.

Paramétriser nos modèles n'a pas toujours été facile, en partie à cause d'un manque de connaissance aux différentes échelles sur, par exemple, (1) l'utilisation des ressources foliaires par les champignons (pour construire son mycélium et ses spores), (2) sur la survie des spores pendant l'interculture, et enfin (3) sur les flux de spores dans le paysage.

3) Principales simplifications et perspectives de modélisation

Dans un souci de simplicité (et de temps), nous avons opéré un certain nombre de simplifications. Dans ce paragraphe, nous souhaitons souligner trois aspects qui nous semblent importants. Parmi les simplifications réalisées dans ce travail, deux éléments, majeurs dans le développement des épidémies, n'ont pas ou peu été considérés. Il s'agit de l'effet du climat et de la défense des plantes. Enfin, une perspective importante de notre travail est suggérée par les résultats de la méta-analyse : l'existence d'une relation entre latence et type trophique des pathogènes.

Effet « climat x fertilisation »

Dans l'ensemble des simulations réalisées avec les deux modèles, nous prenons en compte le climat de façon simplifiée. Le temps est mesuré en degrés-jour. Les dynamiques épidémiques dépendent donc implicitement de la température. L'initialisation des épidémies dans le modèle (paramètres d'initialisation) reflète un climat favorable qui permet chaque année le démarrage des épidémies. Cependant, une fois l'épidémie lancée, nous ne considérons pas d'effet d'autres variables abiotiques sur son déroulement (par exemple des périodes de sécheresse qui limiteraient le développement des pathogènes). Une perspective intéressante serait de tester la robustesse de nos résultats en intégrant dans le modèle un effet stochastique du climat reflétant des conditions météorologiques variables. Pour ce faire, nous pourrions utiliser différents paramètres de nos modèles.

Le premier paramètre est la date de début de l'épidémie. Dans le nord-ouest de l'Europe, les épidémies de Rouille du blé se déclarent généralement entre fin avril et début mai, soit environ 1 000 degrés-jours post-semis, mais avec des variations possibles de

démarrage selon les années (El Jarroudi et al. 2014 ; Duvivier et al. 2016). Nous avons déjà un peu travaillé sur cet effet dans nos modèles (données non présentées). De plus, dans le sud de l'Europe où les hivers sont plus doux, les épidémies peuvent démarrer nettement plus tôt, ce qui peut potentiellement entraîner des variations d'architecture du blé et donc des effets plus importants des maladies sur la plante et de la fertilisation sur les maladies.

Un deuxième paramètre via lequel nous pourrions simuler un effet climatique dans le modèle EBT est l'efficacité d'infection β . La rouille répond par exemple aux conditions d'humidité (Sache, 2000). Une efficacité de dispersion plus forte pourrait correspondre à un climat plutôt favorable au pathogène (Coakley, 1979 ; Zadoks, 2008 ; Duvivier et al. 2016).

Enfin, un troisième paramètre dont la variation peut être le résultat d'un effet climatique est la quantité de spores survivant à l'interculture et au passage de la mauvaise saison. Il serait possible de prendre cet effet en compte en introduisant un effet stochastique de l'année sur ce paramètre (ω dans le modèle EBT, θ dans le modèle paysage). Au niveau paysage, il serait alors possible de faire disparaître la maladie dans certaines parcelles tandis qu'elle survivrait dans d'autres, mimant ainsi un scénario d'extinctions/recolonisations ajoutant un degré d'hétérogénéité, cette fois temporelle, au paysage.

Une perspective serait donc de réaliser un jeu de simulations sur les effets de la fertilisation dans nos modèles mais en incluant une variabilité climatique afin de voir si (et si oui comment) elle change nos résultats.

Effet « fertilisation x niveau de résistance de l'hôte »

Les interactions entre fertilisation et niveau de défense des plantes est un champ d'étude en pleine expansion comme en témoignent les revues de Masclaux-Daubresse et coll. (2010) et de Mur et coll. (2017). Comme le soulignent ces auteurs, l'azote joue un rôle primordial dans la défense des plantes. En dépit d'études plus anciennes qui établissaient une relation négative entre fertilisation et mise en place de défenses physiques comme biochimiques chez le blé (Kirkham 1954 ; Király 1964 ; Matsuyama et Diamond 1973 ; Matsuyama 1975), il semble maintenant établi que l'usage de fertilisant synthétiques sous forme de nitrates peut favoriser les défenses des plantes (Mur et coll., 2017 et références incluses). Cela signifie donc que si le pathogène bénéficie des ressources apportées à la plante par la fertilisation, il

pourrait également faire face à un système immunitaire plus efficace ! Mais de la même façon que le pathogène est contraint par des compromis dans l'allocation de ses ressources, la plante l'est également par un compromis entre croissance et défense. Ainsi, à production photosynthétique constante, ce que l'une utilise d'une part, l'autre ne peut pas l'utiliser autre part (Herms et Mattson, 1992 ; Massad et coll., 2012). Lors de la domestication des céréales, la sélection directionnelle a sans doute davantage penché en faveur de la production de biomasse plutôt que de la réponse immunitaire. Si tel est le cas, l'effet dominant pourrait être celui de la fertilisation comme ressource pour le pathogène, mais cela reste à une hypothèse.

L'ajout d'un tel compromis (entre croissance et défense à l'échelle de la lésion) dans le fonctionnement du patch dans le modèle EBT serait possible en implémentant une relation négative entre l'efficacité de conversion du pathogène (I_{max}) et le taux de fertilisation. Un pathogène faisant face à un système immunitaire boosté par la fertilisation parviendrait à dériver moins de ressources de son hôte. La plus grande différence de ressources « perdues » entre ce qui est prélevé par le pathogène et ce qu'il utilise réellement pourrait dans ce cas refléter le coût de la défense pour la plante. C'est une excitante perspective!

Latence, type trophique et fertilisation

La méta-analyse qui est présentée dans le chapitre 5 de la thèse, a permis de mettre en évidence une relation entre la durée de latence et le type trophique des eumycètes pathogènes des cultures. Les trois types trophiques présentent en effet des latences significativement différentes. La plupart des nécrotrophes ont des latences courtes, tandis que la plupart des hémibiotrophes ont des latences très longues. La latence des biotrophes apparaît intermédiaire entre celles des nécrotrophes et des hémibiotrophes.

L'ensemble du travail de modélisation réalisé dans la thèse porte sur des pathogènes biotrophes de type rouille. Ces pathogènes ne se développent que sur des tissus vivants. Ce n'est pas le cas des autres types trophiques, qui peuvent se développer sur des tissus morts à la condition que ce soit eux qui aient activement provoqué cette mort (Horbach et coll., 2011 ; Kabbage et coll., 2015). Dans le cas du nécrotrophe, l'ensemble du cycle se fait sur du tissu mort, alors que chez les hémibiotrophes, le champignon a d'abord une phase de croissance biotrophe avant de sporuler sur des tissus morts (Kabbage et coll., 2015 ; De Silva et coll.,

2016). L'accessibilité à la ressource est sans doute bien différente entre un pathogène biotrophe qui prélève des nutriments provenant du symplasme via des haustoria et un pathogène hémibiotrophe dérivant des ressources de l'apoplasmé puis du tissu nécrotique (échelle lésion, Perfect et Green, 2001, Divon et Fluhr, 2007). Ainsi, les différents types de pathogènes n'auront pas accès aux mêmes ressources foliaires (type de ressources et leur disponibilité). Il y a donc fort à parier que les effets de la fertilisation ne seront pas perçus de la même façon par les trois types de pathogènes.

Une des perspectives de notre travail est d'adapter nos modèles pour les deux autres types trophiques de champignons. Nos modèles sont en effet tout à fait adaptés pour modifier l'exploitation des ressources de l'hôte par les pathogènes. De plus, pour aller plus loin, il serait intéressant de prendre en compte des complexes parasitaires dans le modèle. En effet, plusieurs pathogènes peuvent coloniser les mêmes feuilles et donc entrer en compétition directe pour les ressources foliaires. Notre modèle devrait permettre de simuler cette compétition et de voir comment elle change avec le niveau de ressource.

La fertilisation des cultures impacte les épidémies foliaires fongiques

Dans notre modèle, une augmentation de la fertilisation entraîne une aggravation des épidémies fongiques foliaires, à la fois en terme de production de spores et d'AUDPC (« Area Under Disease Progress Curve »), et cela quelle que soit l'échelle considérée : la lésion (chapitre 2), la parcelle (chapitre 2) et le paysage (chapitre 4). Ces résultats sont cohérents avec la littérature concernant les épidémies de rouilles (Howard et coll. 1994 ; Ash et Brown, 1991 ; Danial et Parlevliet 1995 ; Devadas et coll. 2014) et d'autres pathogènes biotropes sur céréales (Smith et Blair, 1950 ; Last, 1953, 1962 ; Bainbridge, 1974 ; Shaner et Finney, 1977 ; Daamen et coll., 1989 ; Olesen et coll., 2003).

Dans le travail à l'échelle de la parcelle (chapitres 1 à 3), nous avons conservé de la littérature scientifique trois principaux effets de la fertilisation sur la plante, susceptibles d'avoir des conséquences sur les épidémies (cf. introduction, Figure 7). Il s'agit de (1) : la concentration en métabolites dans les feuilles, (2) : la durée de vie des feuilles et (3) : la taille du couvert (nombre et taille des feuilles). Dans la pratique, la réponse du blé à la fertilisation

est une résultante de ces trois processus en interaction. Il est donc difficile de déterminer la part de chacun dans l'effet de la fertilisation sur la maladie. Notre approche de modélisation permet, dans une certaine mesure, de découpler ces effets. Nos résultats montrent que les trois effets pris indépendamment ont un impact sur les épidémies, (chapitre 2, Figure 6).

Robert et coll. (2006) montrent une augmentation d'environ 33% du contenu en azote des feuilles avec la fertilisation (de $0.18 \text{ mg N.cm}^{-2}$ pour 2g de fertilisant à $0.24 \text{ mg N.cm}^{-2}$ pour 18g de fertilisant). Dans notre modèle, pour une latence $\lambda = 100 \text{ dd}$ (et en prenant comme référence les paramètres standards du modèle EBT, chapitre 1 Tableau 1), une augmentation de métabolites foliaires de 30% entraîne une augmentation de la production de spores de 36% et une augmentation d'AUDPC de 3.5%.

Concernant la taille du couvert, le passage d'une fertilisation modérée à forte porte le gLAI (« green Leaf Area Index ») du couvert de 4 à 8 environ (Hinzman et coll. 1986 ; Benbi 1994 ; Bedoussac et Justes 2010 ; Vári et Máriás 2013), soit un doublement de son maximum saisonnier. Dans notre modèle, ceci équivaut à une augmentation de 176% de la production de spores et de 14% de l'AUDPC.

Enfin, la durée de vie des feuilles du blé peut largement doubler avec la fertilisation (Robert et coll., 2017). Dans notre modèle, passer d'une durée de vie verte de 600 dd à 1200 dd équivaut à une augmentation de 553% de la production de spores et de 44% de l'AUDPC.

Ces résultats suggèrent que la réduction de la taille de couvert et de la durée de vie des feuilles pourraient être les deux réponses à la fertilisation susceptibles d'avoir le plus d'effet sur les épidémies de rouille. De plus, ces deux facteurs correspondent aux premières réponses du blé à une baisse du niveau d'intrants (Savary et coll., 1995 ; Robert et coll., 2004). Mais tandis que l'effet de la densité du couvert sur les épidémies est déjà bien documenté (Darwinkel, 1980 ; Daamen et coll., 1989 ; Danial et Parlevliet, 1995 ; Savary et coll., 1995 ; Jensen et Munk, 1997 ; Lovell et coll., 1997 ; Robert et coll., 2008 ; Garin et coll., 2014) celui sur la durée de vie des feuilles l'est beaucoup moins (Robert et coll., 2017). Une des perspectives de ce travail serait ainsi de combiner, dans le modèle EBT, les trois effets discutés ci-dessus pour tester des scénarios de fertilisation. Pour aller plus loin, une perspective plus ambitieuse encore serait d'inclure un compartiment racinaire dans notre modèle, qui pourra répondre directement à la fertilisation avec une modélisation des flux entre le sol, les racines, et les parties aériennes des plantes. Ces résultats pourront enrichir des travaux en protection intégrée des cultures pour mieux tenir compte des interactions entre

fertilisation des cultures, épidémies et autres pratiques, interactions clés pour la protection intégrée des cultures.

Le passage à l'échelle du paysage a permis d'étendre nos résultats en questionnant l'effet de l'hétérogénéité des pratiques de fertilisation sur les épidémies. En particulier nous avons voulu tester comment une diversification d'un paysage hautement fertilisé incluant désormais un certain nombre de parcelles plus faiblement fertilisées impacterait les épidémies. Nous montrons que, sous l'hypothèse qu'il existe de la maladaptation au sein du paysage hétérogène (i.e. que les pathogènes adaptés à un niveau élevé de fertilisation se développent moins bien dans les parcelles moins fertilisées), un paysage hétérogène en terme de fertilisation permet effectivement de réduire les épidémies et les pertes qui leurs sont associées.

L'efficacité de cette pratique dépend des propriétés d'agrégation et de la proportion des types de parcelles dans le paysage hétérogène. Dans des paysages fortement agrégés ou des paysages dominés par les parcelles faiblement fertilisées, l'hétérogénéité se traduit par une diminution de la quantité d'inoculum libéré dans le paysage ainsi que d'un ralentissement de la colonisation du paysage par le pathogène. En revanche, un paysage avec un faible niveau d'agrégation ou un paysage dominé par des parcelles fortement fertilisées se comporte comme un paysage homogène fortement fertilisé. Ces résultats sont cohérents avec ceux de Mundt et coll. (2011) qui proposent que pour la Rouille brune (*Puccinia recondita*), réduire la fréquence d'hôtes susceptibles dans le paysage mêlant variétés sensibles et résistantes de blé permettrait de réduire l'incidence de la maladie. Des résultats similaires sont rapportés par Skelsey et coll. (2010) sur le Mildiou de la pomme de terre (*Phytophthora infestans*). Ainsi, dans notre modèle, en l'absence d'adaptation, les parcelles faiblement fertilisées jouent un rôle assez analogue aux variétés résistantes de Mundt et coll. (2011).

Le cœur des agrégats de parcelles faiblement fertilisées est protégé, pour un temps en tout cas, par la faible conductivité de ces parcelles à la maladie. Ces parcelles jouent un rôle de barrière à la propagation du pathogène (chapitre 4, Figure 15). Seules les marges de ces agrégats, soumises à la forte production d'inoculum de leurs voisins, sont davantage touchées par la maladie. Cet effet de protection lié à la taille des parcelles est connu sous le nom d'effet de bordures (« edge effect », Murcia 1995 ; Rizzo et Garbelotto, 2003). A titre d'exemple, Dallot et coll. (2004) montrent que, dans le cas de vergers de pêchers soumis à la pression

d'un inoculum viral extérieur, l'effet de bordures protège les arbres à l'intérieur des grandes parcelles, alors que les petites parcelles sont fortement attaquées. Une étude expérimentale par Johnson et Haddad (2011) sur le pathogène anémophile du maïs *Cochliobolus heterostrophus* montre que cet effet de bordures permet à lui seul d'expliquer les patrons d'incidence de la maladie.

Ainsi, que ce soit à l'échelle de la parcelle ou à celle du paysage, la gestion de la fertilisation azotée semble être un possible pour réguler les épidémies. Mais, que nous disent les résultats sur l'évolution des pathogènes : de telles solutions peuvent-elles être durables ?

Evolution des pathogènes face à des changements de fertilisation des cultures

Dans cette partie, nous discuterons d'une part des notions de valeur sélective (« fitness ») et de latence optimale, et de compromis écologiques qui sont en jeux. Dans un second temps, nous discuterons plus précisément des résultats sur la direction de l'évolution des pathogènes face à la fertilisation azotée, en prenant en compte les différentes échelles spatiales de l'étude.

1) Fitness, latence optimale et compromis

Une des fondations de ce travail a été de considérer le système hôte-pathogène comme un système consommateur-ressource. La fertilisation détermine la quantité de ressources disponible pour le pathogène, lequel doit mettre en place une stratégie d'exploitation optimale de ces ressources. Cette stratégie optimale va probablement changer selon le niveau mais surtout selon la dynamique de cette ressource. Dans nos modèles, nous montrons que le pathogène adopte effectivement une stratégie optimale pour l'allocation de ses ressources, avec une « latence optimale » qui émerge. Le calcul de cette latence optimale a été fait d'une part pour maximiser des mesures de valeur sélective *ad hoc*, comme la production de spores et la colonisation du couvert et d'autre part via la fitness d'invasion (« invasion fitness »),

latences ESS). On trouve dans tous les cas qu'une latence intermédiaire maximise la valeur sélective du pathogène, mais les latences optimales sont différentes selon le critère de valeur sélective utilisé.

Dans nos conditions de simulations, on trouve en effet que la latence optimale estimée par la fitness d'invasion est pratiquement la moyenne des latences optimales qui maximisent la production de spores saisonnière (fitness 1) et la vitesse de colonisation du couvert (fitness 2). Nous en concluons que le pathogène est soumis à deux compromis : à l'échelle du tissu, il doit produire suffisamment de spores mais à l'échelle du couvert il doit également aller suffisamment vite (chapitre 1). Dans cette discussion, nous avons voulu tester cette hypothèse en recalculant les latences optimales après avoir modifié certains paramètres du modèle qui déséquilibrent les compromis entre latence, production de spores et vitesse de colonisation.

Nous avons tout d'abord augmenté la taille du cône de dispersion (Δ), c'est à dire, en l'augmentant, rendu la dispersion moins limitante. La Figure 1A présente le devenir de la latence ESS (à fertilisation constante) lorsque la distance de dispersion augmente (valeur par défaut $\Delta = 200$). On observe que dans ce cas, la latence ESS augmente et qu'elle se rapproche de la latence optimale qui maximise la production de spores (valeur sélective N°1). Ainsi, dans ces conditions de simulation, on a relâché la course avec le couvert et le compromis qui prend le dessus est celui de l'optimisation de la production de spores. En parallèle, nous avons également augmenté l'efficacité d'infection (β). La figure 1B montre que la latence ESS diminue cette fois avec l'efficacité d'infection et qu'elle se rapproche de la latence optimale qui maximise la colonisation du couvert (valeur sélective N°2). Dans ce cas, augmenter l'efficacité d'infection rend la production de spores moins limitante et c'est la course au couvert, qui prend le rôle de facteur limitant.

Ces simulations confirment l'hypothèse selon laquelle la latence ESS résulte des deux compromis expliqués ci-dessus. On remarque que le paramétrage du modèle dans les chapitres 1 à 3 nous a placés dans un scénario où production de spores et colonisation du couvert sont d'importance assez égale, bien que cela reste à vérifier empiriquement.

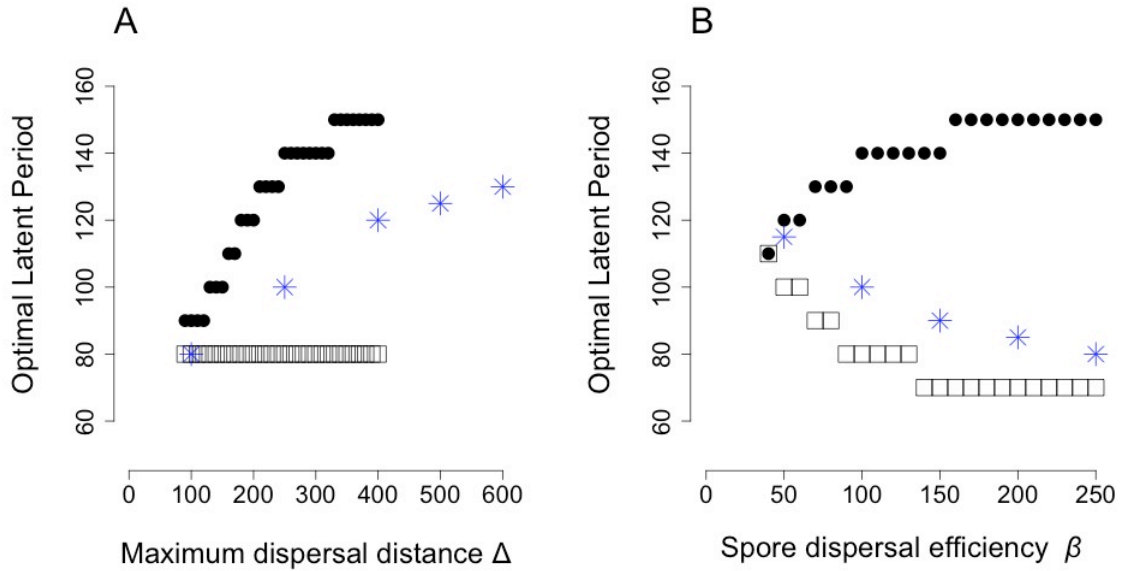


Figure 1 : Variation of optimal latent periods with **A** : the maximum dispersal distance Δ and **B** : the spore dispersal efficiency β in the reference fertilization parameters ($K = 1$, $\tau = 750$, $\rho = 1$; default values are $\beta = 100$ and $\Delta = 250$). Full circles are optimal latent periods corresponding to seasonal spore production as a fitness measure. Open squares are optimal latent periods corresponding to within-season exponential growth rate as a fitness measure of the pathogen. Blue stars correspond to the evolutionary singular strategies (ESS).

2) Fertilisation et évolution de la latence

2.1) Direction de l'évolution

Concernant la réponse évolutive de la latence à la fertilisation, nous considérons que les résultats donnés par le premier modèle (chapitres 1, 2 et 3) sont les plus pertinents que ceux donnés par le chapitre à l'échelle du paysage (chapitre 4). En effet, dans le chapitre 4, nous nous sommes davantage concentrés sur l'effet du changement d'échelle sur les dynamiques épidémiologiques et sur l'évolution, en ayant cette fois quasiment « forcé » le compromis entre fertilisation et production de spores (issue des résultats du chapitre 2).

Considérant ainsi uniquement le modèle EBT, l'un de nos résultats principaux est la comparaison entre latences optimales et fertilisation lorsqu'on utilise des mesures de valeur sélective « ad hoc » et la fitness d'invasion. On trouve que la latence optimale qui maximise

la production de spores saisonnière (valeur sélective N°1) augmente avec la fertilisation (et cela pour les 3 effets de la fertilisation sur le pathosystème), alors que celle qui maximise le taux de colonisation du couvert (valeur sélective N°2) diminue avec la fertilisation (et cela pour les 3 effets de la fertilisation). Les résultats sont bien différents pour la latence optimale estimée à partir de la fitness d'invasion (ESS). La latence optimale est alors comprise entre celles obtenues en utilisant les valeurs sélectives N°1 et 2. Enfin, nous trouvons que la latence optimale qui maximise la production de spores pendant la croissance du couvert (au début des épidémies, valeur sélective N°3) est très proche de celle estimée avec la fitness d'invasion. Cette comparaison des mesures de valeur sélective nous permet d'avancer dans la compréhension des contraints qui s'imposent sur le pathogène dans son adaptation. En particulier, nous pensons que le fait que le pathogène se développe dans un couvert en croissance impose une contrainte écologique qui a tendance à sélectionner des latences plus courtes que si le couvert était déjà en place au moment de l'inoculation initiale.

Dans la fin de ce paragraphe nous discutons plus précisément du comportement de la latence optimale ESS face aux différents effets de la fertilisation (chapitre 3). Les réponses évolutives de la latence à la fertilisation sont des stratégies stables (latences ESS) qui augmentent avec la durée de vie verte mais qui diminuent avec l'augmentation de la vitesse de croissance (et donc la taille) du couvert. Enfin, nous constatons que la latence ESS ne dépend pas du contenu en métabolites des feuilles. Ces relations semblent logiques car quand la durée de vie des feuilles augmente le pathogène n'a plus suffisamment de temps pour établir son mycélium, et car la course au couvert augmente lorsque la vitesse de croissance du couvert augmente. Dans ce dernier cas, si la taille du couvert diminue en réponse à la fertilisation, le pathogène peut se permettre de réduire sa latence tout en conservant l'avantage dans la course avec le couvert. Notons néanmoins que la gamme de variation de l'ESS relative à ces deux effets reste assez limitée (au plus 30 degrés-jours).

Il est ainsi intéressant de noter que, contrairement à l'impact sur les épidémies pour lequel les trois effets de la fertilisation donnaient des résultats similaires (tous les trois favorisant les épidémies), les trois effets étudiés ne livrent pas la même direction évolutive de la latence en réponse à une réduction de la fertilisation. Aux vues de ces résultats contrastés, il est même difficile de prédire la direction évolutive que prendra la latence pour des scénarios de fertilisation qui mobiliseront les trois effets. Décorrérer les effets de la fertilisation sur le

pathosystème permet donc de mettre en lumière le caractère contrasté de la réponse du pathosystème à ces différents effets.

2.2) Coexistence et maladaptation

Au niveau de la parcelle, les analyses d'invasion (les PIPs) montrent qu'il y a toujours une seule latence qui est évolutivement stable, soit une ESS globale (chapitre 3). De plus, les analyses d'invasion mutuelle (les TEPs) montrent que ces ESS sont caractérisées par une absence de coexistence. Au niveau du paysage, nous avons montré que l'évolution converge vers un point de branchement évolutif (en anglais : EBP, « evolutionary branching point ») (chapitre 4). L'émergence de la sélection disruptive, caractéristique des EBP, dans un paysage composé de deux types d'habitats n'est pas surprenante en soi (Ravigné et coll., 2009). Ce type d'équilibre est toujours associé avec la possibilité de coexistence de (au moins) deux souches (Geritz 1998). Ce que nous apprend l'étude de l'évolution au niveau du paysage (PIP et TEPs, chapitre 4), c'est donc que la coexistence devient tout à fait possible, même au sein des parcelles, grâce à l'effet de l'hétérogénéité spatiale. La coexistence au niveau du paysage est même présente dans toutes nos simulations de paysages hétérogènes. Notre étude montre que cette coexistence est la conséquence directe de la présence de deux types de parcelles, car les PIPs et les TEPs peuvent être construits en superposant les deux PIPs spécifiques pour chaque type de parcelle.

La convergence vers le point de branchement évolutif est aussi associée à de la maladaptation : une souche avec une latence correspondant à l'EBP est une souche plutôt généraliste, la « meilleure » souche pour exploiter l'ensemble du paysage, tandis qu'elle est relativement mal adaptée dans chacune des parcelles prises individuellement. Cependant cette souche maladaptée sera vite remplacée par d'autres souches qui apparaissent dans le paysage.

3) Prise en compte de la virulence dans le modèle

Dans notre modèle, la virulence du champignon passe principalement par une diminution de l'export des ressources depuis les patch infectés vers le pool de ressources commun (A, chapitre 1, Equation 1, 2, 19 and 26). Cela peut se traduire par une diminution de la croissance du couvert. En effet, ce réservoir est celui dans lequel puise la plante pour

produire de nouveaux patchs (chapitre 1, Equation 6, 10, 15 and 16). Cependant ce « grand réservoir commun » conduit avec le paramétrage actuel à une sous-estimation de la virulence et des effets possibles des épidémies sur la structure du couvert si les épidémies sont précoce.

De plus, nous n'avons pas implémenté d'effet direct de la sporulation sur la photosynthèse (Robert et al. 2004). Pourtant, cet effet, en diminuant les ressources effectivement disponibles pour le pathogène aurait potentiellement un impact sur l'allocation optimale de ressources. Des travaux préliminaires, encore en cours, montrent en particulier que la latence optimale pourrait dans ce cas être plus courte, mais que les résultats changeraient assez peu qualitativement (données non présentées). Tout cela reste à consolider.

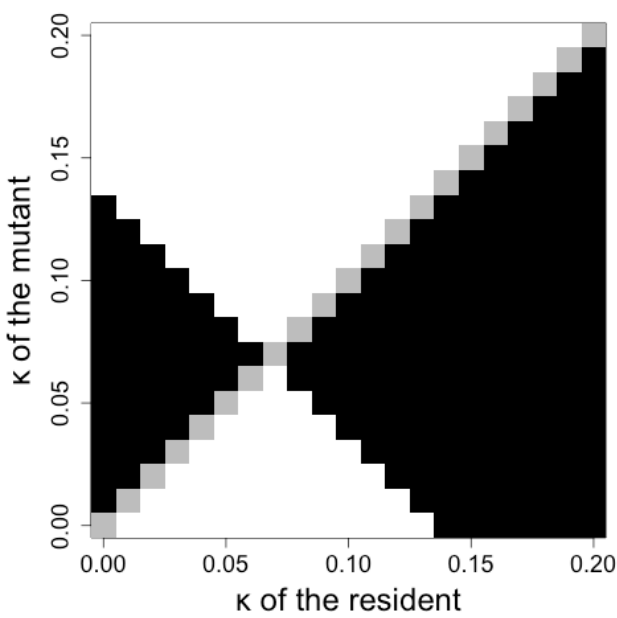


Figure 2 : PIP showing the ESS of pathogen resource allocation strategy for the reference fertilization parameters ($K = 1$, $\tau = 750$, $\rho = 1$, with $\lambda = 100$ and default parameter values)

colonisation du couvert.

4) La latence, seule adaptation des pathogènes à la fertilisation ?

Nous avons choisi la latence comme trait répondant à la fertilisation aussi bien au niveau de la parcelle que du paysage. Néanmoins, dans le modèle EBT, notre choix aurait pu se porter sur d'autres traits du cycle infectieux susceptibles d'évoluer en réponse à une changement de disponibilité des ressources. Parmi eux, le taux de consommation du pathogène est susceptible d'augmenter avec la quantité de ressources disponibles, et serait sans doute soumis à des compromis semblables à ceux liant la latence à la production de spores et à la

Un autre trait qu'il aurait été intéressant de creuser est la stratégie d'exploitation des ressources elle-même. Dans l'ensemble des chapitres 1 à 3, nous faisons l'hypothèse que le pathogène suit une stratégie de type bang-bang : allouant 100% de ses ressources à la croissance durant la latence, puis 100% à la reproduction ensuite. Il est très probable que relâcher cette hypothèse va avoir un impact sur les ESS. A titre d'exemple, si l'on autorise le champignon à continuer d'allouer une fraction κ de ses ressources à croissance en période de

reproduction, la stratégie ESS d'exploitation des ressources, pour une latence donnée, n'est pas la stratégie bang-bang, comme en témoigne la Figure 2 ci-dessus. Notons cependant que ceci n'est les cas que pour des latences courtes, c'est à dire pour des valeurs de $\lambda < \lambda_{ESS}$ dans le cas de $\kappa = 0$. Si on laissait coévoluer les deux traits (κ et λ) simultanément, la solution « optimale » serait bien une stratégie bang-bang.

D'autres traits, plus généraux, pourraient également requérir une attention particulière, comme le niveau de diversité génétique des populations de pathogènes, ou encore la présence/absence de phase sexuée (téléomorphe) dans le cycle de vie du pathogène. Ces traits ont été mis en avant par McDonald et Linde (2002) qui les utilisent pour proposer une hiérarchisation du risque d'adaptation des pathogènes aux pratiques culturelles. Selon eux, les pathogènes associant forte diversité génétique, présence d'une phase sexuée et capacités de dispersion importantes (ils nomment entre autres *Rhynchosporium secalis*, *Zymoseptoria tritici*, *Erysiphe graminis*, *Phytophthora infestans*, *Bremia lactucae*, *Puccinia graminis* et *Puccinia coronata*) sont les plus susceptibles de poser problème à l'avenir.

A l'échelle du paysage, les traits comme la distance moyenne de dispersion est également un trait potentiellement intéressant. Pour les épidémies polycycliques, le fort taux d'autoinfection lié à la répétition des cycles asexués assure l'augmentation en fréquence de tous les phénotypes dans le paysage (et promeut sans doute l'adaptation locale), tandis que l'alloinfection (plus ou moins assimilable à une migration dans un contexte de métapopulation), associée à la reproduction sexuée, permet l'arrivée de nouveaux phénotypes (van den Berg et coll., 2013). La complexité du cycle de vie du pathogène, et les traits qui lui sont associés, sont donc à prendre en compte à l'échelle du paysage. Dans plusieurs pays comme au Danemark (Zadoks, 2008) ou aux Etats-Unis (Peterson et coll., 2005) c'est l'utilisation conjointe de variétés résistantes et l'éradication de l'Epine vinette (*Berberis vulgaris*), hôte alternatif de la Rouille noire (*Puccinia graminis*) qui ont permis de réduire significativement l'incidence de cette maladie. Pour être fructueuses, les pratiques visant à limiter les maladie polycycliques ont du prendre en compte la reproduction sexuée.

Des pratiques de fertilisation comme levier pour limiter les épidémies ?

Ce travail montre que la fertilisation des cultures pourrait être utilisée pour réguler les épidémies de champignons pathogènes foliaires des cultures. En particulier, nous montrons que l'introduction de nouvelles pratiques de fertilisation dans le paysage va réduire les épidémies, du moins pendant un certain temps (tant qu'il existe suffisamment de maladaptation dans le paysage,). Cette technique est d'autant plus efficace que les nouvelles pratiques introduites dans le paysage sont majoritaires et agrégées. Notons que, bien que l'existence de l'adaptation locale (et donc de maladaptation) dans les agrosystèmes soit encore discutée (Strauss, 1997 ; Laine, 2005), plusieurs études montrent que le phénomène existe en contexte agricole et pour des populations sauvages de champignons pathogènes (Parker, 1985 ; Kaltz et coll., 1999 ; Zhan et coll., 2002 ; Suffert et coll., 2017). Il ne serait en tout cas pas limitant pour des pathogènes présentant des flux de gènes élevés à l'échelle du paysage (Gandon, 2002). Afin de s'en assurer, on pourrait par exemple comparer la latence de souches adaptées à des conditions de fortes (Europe occidentale) et de plus faibles fertilisations (Europe orientale) en allopatrie et en sympatrie.

Les études théoriques utilisant la dynamique adaptative pour prévoir l'évolution des pathogènes, par exemple dans le contexte de l'hétérogénéité spatiale, délivrent des conclusions sur le long terme car elles considèrent l'état du système à l'équilibre, i.e. dans la phase d'endémisme de la maladie (Lion et Gandon, 2016). Or, dans le contexte agricole, nous ne nous intéressons pas nécessairement à l'équilibre à long terme. En effet, les effets à court terme, dans les années mêmes qui suivent la mise en place des nouvelles pratiques, sont importants. De plus, un paysage agricole est sujet à une rotation temporelle des cultures qui affecte le développement des épidémies et peut éloigner le système d'un éventuel équilibre.

Dans un tel contexte, joindre à l'hétérogénéité spatiale une dimension d'hétérogénéité temporelle pourrait s'avérer précieux. Dans la nature, les maladies des plantes sont éphémères dans des populations isolées, très variables dans le temps et l'espace en fonction des phénomènes d'adaptation locale, d'extinction et de recolonisation (Burdon et Thrall, 2014). Imaginer des paysages agricoles correspondant à des mosaïques de fertilisation, de

déploiement de résistances variétales, de types de cultures et de mélanges de variétés et d'espèces, et qui soient également variables dans le temps, nous permettrait peut-être de nous rapprocher des conditions naturelles de limitation des épidémies.

Finalement ce travail démontre la nécessité de prendre en compte l'évolution des pathogènes pour estimer la durabilité de l'effet d'une pratique agricole sur les pathogènes, même si cet effet est « partiel ». Ce travail représente une brique importante dans la discussion actuelle sur la « possible plus grande durabilité » des pratiques de lutte « partielle » (en regard de méthodes de lutte visant la destruction du pathogène, comme l'application de fongicides par exemple). Il apparaît donc qu'un système de production durable doit prendre en compte les possibilités d'adaptation des pathogènes aux pratiques agricoles (Plantagenest et coll., 2007 ; Zhan et coll., 2014, 2015).

Conclusion

Cette thèse aura été pour moi captivante de bout en bout. D'une part parce qu'elle représente une belle expérience interdisciplinaire, mêlant écologie (ma spécialité d'origine), agronomie, épidémiologie et modélisation. D'autre part par la somme de connaissances qu'elle représente, que ce soit sur le fonctionnement des écosystèmes agricoles, sur l'agroécologie et les espoirs qu'elle porte, sur la biologie de ce groupe extraordinairement divers que sont les champignons pathogènes ou encore sur l'écologie et l'épidémiologie des paysages. Enfin par l'approche multi-échelle que nous avons adoptée, que je trouve élégante en ce qu'elle utilise comme base de l'échelle supérieure un concentré de résultats provenant de l'échelle inférieure. Une perspective très excitante de ce travail, et que j'aimerais mener à bien s'il me l'est permis, est d'intégrer au sein du même modèle les trois effets de la fertilisation en temps que niveau de ressources des chapitres 2 et 3 en une fertilisation plus réaliste, ainsi que des complexes parasitaires (de pathogènes appartenant à des types trophiques différents) au lieu d'une approche monospécifique.

References

1. Andrade-Piedra, J.L., Hijmans, R.J., Juárez, H.S., Forbes, G. a, Shtienberg, D., and Fry, W.E. (2005).

- Simulation of Potato Late Blight in the Andes. II: Validation of the LATEBLIGHT Model. *Phytopathology* 95, 1200–1208.
2. Ash, G.J., and Brown, J.F. (1991). Effect of nitrogen nutrition of the host on the epidemiology of *Puccinia striiformis* f.sp. *tritici* and crop yield in wheat. *Australasian Plant Pathology* 20, 108–114.
 3. Baccar, R., Fournier, C., Dornbusch, T., Andrieu, B., Gouache, D., and Robert, C. (2011). Modelling the effect of wheat canopy architecture as affected by sowing density on *Septoria tritici* epidemics using a coupled epidemic/virtual plant model. *Annals of Botany* 108, 1179–1194.
 4. Bainbridge, A. (1974). Effect of Nitrogen Nutrition of the Host on Barley Powdery Mildew. *Plant Pathology* 23, 160–161.
 5. Bedoussac, L., and Justes, E. (2010). Dynamic analysis of competition and complementarity for light and N use to understand the yield and the protein content of a durum wheat-winter pea intercrop. *Plant and Soil* 330, 37–54.
 6. Benbi, D.K. (1994). Prediction of leaf area indices and yields of wheat. *Journal of Agricultural Science* 122, 13–20.
 7. Broers, L. (1989). Influence of development stage and host genotype on three components of partial resistance to leaf rust in spring wheat. *Euphytica* 44, 187–195.
 8. Burdon, J.J., and Thrall, P.H. (2014). What have we learned from studies of wild plant-pathogen associations?—the dynamic interplay of time, space and life-history. *European Journal of Plant Pathology* 138, 417–429.
 9. Calonnec, A., Cartolaro, P., Naulin, J.M., Bailey, D., and Langlais, M. (2008). A host-pathogen simulation model: Powdery mildew of grapevine. *Plant Pathology* 57, 493–508.
 10. Carlisle, D.J., Cooke, L.R., Watson, S., and Brown, A.E. (2002). Foliar aggressiveness of Northern Ireland isolates of *Phytophthora infestans* on detached leaflets of three potato cultivars. *Plant Pathology* 51, 424–434.
 11. Cisneros, J.J., and Godfrey, L.D. (2001). Midseason Pest Status of the Cotton Aphid (Homoptera: Aphididae) in California Cotton - Is Nitrogen a Key Factor? *Environmental Entomology* 30, 501–510.
 12. Coakley, S.M. (1979). Climate variability in the Pacific Northwest and its effect on stripe rust disease of winter wheat. *Climatic Change* 2, 33–51.
 13. Corio-Costet, M.F., Dufour, M.C., Cigna, J., Abadie, P., and Chen, W.J. (2011). Diversity and fitness of *Plasmopara viticola* isolates resistant to QoI fungicides. *European Journal of Plant Pathology* 129, 315–329.
 14. Cunniffe, N.J., Koskella, B., E. Metcalf, C.J., Parnell, S., Gottwald, T.R., and Gilligan, C.A. (2015). Thirteen challenges in modelling plant diseases. *Epidemics* 10, 6–10.
 15. Daamen, R.A., Wijnands, F.G., and Vliet, G. vander (1989). Epidemics of Diseases and Pests of Winter Wheat at Different Levels of Agrochemical Input: A study on the possibilities for designing an integrated cropping system. *Journal of Phytopathology* 125, 305–319.
 16. Dallot, S., Gottwald, T., Labonne, G., and Quiot, J.-B. (2004). Factors Affecting the Spread of Plum pox virus Strain M in Peach Orchards Subjected to Roguing in France. *Phytopathology* 94, 1390–1398.
 17. Danial, D.L., and Parlevliet J.E. (1995). Effects of nitrogen fertilization on disease severity and infection type of yellow rust on wheat genotypes varying in quantitative resistance, *J. Phytopathology* 143 679–681.
 18. De Silva, N.I., Lumyong, S., Hyde, K.D., Bulgakov, T., Phillips, A.J.L., and Yan, J.Y. (2016). Mycosphere Essays 9: Defining biotrophs and hemibiotrophs. *Mycosphere* 7, 545–559.
 19. Devadas, R., Simpfendorfer, S., Backhouse, D., and Lamb, D.W. (2014). Effect of stripe rust on the

- yield response of wheat to nitrogen. *Crop Journal* 2, 201–206.
20. Develey-Rivière, M.P., and Galiana, E. (2007). Resistance to pathogens and host developmental stage: A multifaceted relationship within the plant kingdom. *New Phytologist* 175, 405–416.
 21. Divon, H.H., and Fluhr, R. (2007). Nutrition acquisition strategies during fungal infection of plants. *FEMS Microbiology Letters* 266, 65–74.
 22. Drecce, M. (2000). Dynamics of Vertical Leaf Nitrogen Distribution in a Vegetative Wheat Canopy. Impact on Canopy Photosynthesis. *Annals of Botany* 86, 821–831.
 23. Duvivier, M., Dedeurwaerder, G., Bataille, C., De Proft, M., and Legre've, A. 2016. Real-time PCR quantification and spatio-temporal distribution of airborne inoculum of *Puccinia triticina* in Belgium. *Eur. J. Plant Pathol.* 145:405-420.
 24. El Jarroudi, M., Kouadio, L., Delfosse, P., and Tychon, B. 2014. Brown rust disease control in winter wheat: I. Exploring an approach for disease progression based on night weather conditions. *Environ. Sci. Pollut. Res.* 21:4797-4808.
 25. Filipe, J.A.N., Cobb, R.C., Meentemeyer, R.K., Lee, C.A., Valachovic, Y.S., Cook, A.R., Rizzo, D.M., and Gilligan, C.A. (2012). Landscape epidemiology and control of pathogens with cryptic and long-distance dispersal: Sudden oak death in northern californian forests. *PLoS Computational Biology* 8.
 26. Flier, W.G., and Turkensteen, L.J. (1999). Foliar aggressiveness of *Phytophthora infestans* in three potato growing regions in the Netherlands. *European Journal of Plant Pathology* 105, 381–388.
 27. Ford Denison, R., and McGuire, A.M. (2015). What should agriculture copy from natural ecosystems? *Global Food Security* 4, 30–36.
 28. Gandon, S. (2002). Local adaptation and the geometry of host – parasite coevolution. *Ecology Letters* 5, 246–256.
 29. Garin G. 2015. Vers la compréhension des épidémies fongiques foliaires par modélisation multi-échelle dans les couverts architecturés. Thèse de Doctorat soutenue le 11 décembre 2015.
 30. Grechi, I., Hilgert, N., Sauphanor, B., Senoussi, R., and Lescourret, F. (2010). Modelling coupled peach tree-aphid population dynamics and their control by winter pruning and nitrogen fertilization. *Ecological Modelling* 221, 2363–2373.
 31. Godin, C., and Sinoquet, H. (2005). Functional-structural plant modelling. *New Phytologist* 166, 705–708.
 32. Herms, D.A., and Mattson, W.J. (1992). The Dilemma of Plants: To Grow or Defend. *The Quarterly Review of Biology* 67, 283–335.
 33. Hinzman, L.D., Bauer, M.E., and Daughtry, C.S.T. (1986). Effects of Nitrogen-Fertilization on Growth and Reflectance Characteristics of Winter-Wheat. *Remote Sensing of Environment* 19, 47–61.
 34. Horbach, R., Navarro-Quesada, A.R., Knogge, W., and Deising, H.B. (2011). When and how to kill a plant cell: Infection strategies of plant pathogenic fungi. *Journal of Plant Physiology* 168, 51–62.
 35. Howard, D., Chambers, A., and Logan, J. (1994). Nitrogen and Fungicide Effects on Yield Components and Disease Severity in Wheat. *Journal of Production Agriculture* 7, 448–454.
 36. Johnson, D. a. (1980). Effect of Low Temperature on the Latent Period of Slow and Fast Rusting Winter Wheat Genotypes. *Plant Disease* 64, 1006.
 37. Johnson, B.L., and Haddad, N.M. (2011). Edge effects, not connectivity, determine the incidence and development of a foliar fungal plant disease. *Ecology* 92, 1551–1558.

38. Kabbage, M., Yarden, O., and Dickman, M.B. (2015). Pathogenic attributes of *Sclerotinia sclerotiorum*: Switching from a biotrophic to necrotrophic lifestyle. *Plant Science* *233*, 53–60.
39. Kaltz, O., Gandon, S., Michalakis, Y., and Shykoff, J.A. (1999). Local Maladaptation in the Anther-Smut Fungus *Microbotryum violaceum* to Its Host Plant *Silene latifolia*: Evidence from a Cross-Inoculation Experiment. *Evolution* *53*, 395.
40. Király, Z. (1964). Effect of Nitrogen Fertilization on Phenol Metabolism and Stem Rust Susceptibility of Wheat. *Journal of Phytopathology* *51*, 252–261.
41. Kirkham, D.S. (1954). Significance of the ratio between the water-soluble aromatic and nitrogen constituents of apple and pear in the host-parasite relationships of *Venturia* species [16]. *Nature* *173*, 690–691.
42. Knott, E.A., and Mundt, C.C. (1991). Latent Period and Infection Efficiency of *Puccinia recondita* f. sp. *tritici* Populations Isolated from Different Cultivars. *Phytopathology* *81*, 435–439.
43. Laine, A.L. (2005). Spatial scale of local adaptation in a plant-pathogen metapopulation. *Journal of Evolutionary Biology* *18*, 930–938.
44. Last, F.T. (1953). Some Effects of Temperature and Nitrogen Supply on Wheat Powdery Mildew. *Annals of Applied Biology* *40*, 312–322.
45. Last, F.T. (1962). Effects of Nutrition on the Incidence of Barley Powdery Mildew. *Plant Pathology* *11*, 133–136.
46. Lion, S., and Gandon, S. (2016). Spatial evolutionary epidemiology of spreading epidemics. *Proceedings of the Royal Society B: Biological Sciences* *283*, 20161170.
47. Ma, H., and Singh, R.P. (1996). Expression of adult resistance to stripe rust at different growth stages of wheat. *Plant Disease* *375*–379.
48. Masclaux-Daubresse, C., Daniel-Vedele, F., Dechorganat, J., Chardon, F., Gaufichon, L., and Suzuki, A. (2010). Nitrogen uptake, assimilation and remobilization in plants: Challenges for sustainable and productive agriculture. *Annals of Botany* *105*, 1141–1157.
49. Massad, T.J., Dyer, L.A., and Vega C., G. (2012). Costs of Defense and a Test of the Carbon-Nutrient Balance and Growth-Differentiation Balance Hypotheses for Two Co-Occurring Classes of Plant Defense. *PLoS ONE* *7*.
50. Matsuyama, N., and Dimond, A.E. (1973). Effect of nitrogenous fertilizer on biochemical processes that could affect lesion size of rice blast. *Phytopathology* *63*, 1202–1203.
51. Matsuyama, N. (1975). The effect of ample nitrogen fertilizer on cell wall materials and its significance to rice blast disease. *Annual Phytopathological Society of Japan* *41*, 56–61.
52. McDonald, B.A., and Linde, C. (2002). Pathogen population genetics, evolutionary potential, and durable resistance. *Annual Review of Phytopathology* *40*, 349–379.
53. Meentemeyer, R.K., Haas, S.E., and Václavík, T. (2012). Landscape Epidemiology of Emerging Infectious Diseases in Natural and Human-Altered Ecosystems. *Annual Review of Phytopathology* *50*, 379–402.
54. Mundt, C.C., Sackett, K.E., and Wallace, L.D. (2011). Landscape heterogeneity and disease spread: Experimental approaches with a plant pathogen. *Ecological Applications* *21*, 321–328.
55. Mur, L.A.J., Simpson, C., Kumari, A., Gupta, A.K., and Gupta, K.J. (2017). Moving nitrogen to the centre of plant defence against pathogens. *Annals of Botany* *119*, 703–709.
56. Murcia, C. (1995). Edge effects in fragmented forests-implications for conservation. *Trends in Ecology & Evolution* *10*, 58–62.

57. Olesen, J.E., Mortensen, J.V., Jørgensen, L.N., and Andersen, M.N. (2000). Irrigation strategy, nitrogen application and fungicide control in winter wheat on a sandy soil. I. Yield, yield components and nitrogen uptake. *Journal of Agricultural Science* 134, 1–11.
58. Papaïx, J., Adamczyk-Chauvat, K., Bouvier, A., Kiêu, K., Touzeau, S., Lannou, C., and Monod, H. (2014). Pathogen population dynamics in agricultural landscapes: The Ddal modelling framework. *Infection, Genetics and Evolution* 27, 509–520.
59. Papaïx, J., Burdon, J.J., Zhan, J., and Thrall, P.H. (2015). Crop pathogen emergence and evolution in agro-ecological landscapes. *Evolutionary Applications* 8, 385–402.
60. Pariaud, B., Van den Berg, F., Van den Bosch, F., Powers, S.J., Kaltz, O., and Lannou, C. (2013). Shared influence of pathogen and host genetics on a trade-off between latent period and spore production capacity in the wheat pathogen, *Puccinia triticina*. *Evolutionary Applications* 6, 303–312.
61. Park, R.F., and Rees, R.G. (1989). Expression of adult plant resistance and its effect on the development of *Puccinia striiformis* f.sp. *tritici* in some Australian wheat cultivars. *Plant Pathology* 38, 200–208.
62. Parker, M.A. (1985). Local population differentiation for compatibility in an annual legume and its host-specific fungal pathogen. *Evolution* 39, 713–723.
63. Perfect, S.E., and Green, J.R. (2001). Infection structures of biotrophic and hemibiotrophic fungal plant pathogens. *Molecular Plant Pathology* 2, 101–108.
64. Peterson, P. D., Leonard, K. J., Miller, J. D., Laudon, R. J. & Sutton, T. B. 2005 Prevalence and distribution of common barberry, the alternate host of *Puccinia graminis*, in Minnesota. *Plant Dis.* 89, 159–163. (doi:10.1094/PD-89- 0159)
65. Plantegenest, M., Le May, C., and Fabre, F. (2007). Landscape epidemiology of plant diseases. *Journal of The Royal Society Interface* 4, 963–972.
66. Ravigné, V., U. Dieckmann, and I. Olivieri. (2009). Live where you thrive: joint evolution of habitat choice and local adaptation fa- cilitates specialization and promotes diversity. *American Naturalist* 174:E141–E169.
67. Rizzo, D., and Garbelotto, M. (2003). Sudden oak death: endangering California and Oregon forest ecosystems. *Frontiers in Ecology and the ...* 1, 197–204.
68. Robert, C., Bancal, M.O., Lannou, C., and Ney, B. (2006). Quantification of the effects of *Septoria tritici* blotch on wheat leaf gas exchange with respect to lesion age, leaf number, and leaf nitrogen status. In *Journal of Experimental Botany*, pp. 225–234.
69. Robert, C., Fournier, C., Andrieu, B., and Ney, B. (2008). Coupling a 3D virtual wheat (*Triticum aestivum*) plant model with a *Septoria tritici* epidemic model (Septo3D): A new approach to investigate plant-pathogen interactions linked to canopy architecture. *Functional Plant Biology* 35, 997–1013.
70. Robert C., Garin G., Pradal C., Fournier C. 2017. A plant-pathogen model reveals how plant architecture and foliar senescence impact the race between wheat growth and *Zymoseptoria tritici* epidemics. *Annals of Botany*. (In press).
71. Sache, I. (2000). Short-distance dispersal of wheat rust spores. *Agronomie* 20 (7),757-767.
72. Shaner, G., and Finney, R.E. (1977). The Effect of Nitrogen Fertilization on the Expression of Slow-Mildewing Resistance in Knox Wheat. *Phytopathology* 77, 1051–1056.
73. Shaw, M.W. (1990). Effects of temperature, leaf wetness and cultivar on the latent period of *Mycosphaerella graminicola* on winter wheat. *Plant Pathology* 39, 255–268.
74. Sievänen, R., Godin, C., De Jong, T.M., and Nikinmaa, E. (2014). Functional-structural plant models: A growing

- paradigm for plant studies. *Annals of Botany* 114, 599–603.
75. Smith, H.C., and Blair, I.D. (1950). Wheat Powdery Mildew Investigations. *Annals of Applied Biology* 37, 570–583.
 76. Strauss, S.Y. (1997). Lack of evidence for local adaptation to individual plant clones or site by a mobile specialist herbivore. *Oecologia* 110: 77–85.
 77. Suffert, F., Sache, I., and Lannou, C. (2013). Assessment of quantitative traits of aggressiveness in *Mycosphaerella graminicola* on adult wheat plants. *Plant Pathology* 62, 1330–1341.
 78. Suffert, F., Goyeau, H., Sache, I., Carpentier, F., Gélisse, S., Morais, D., and Delestre G. (2017). Trade-off between intra- and interannual scales in the evolution of aggressiveness in a local plant pathogen population. doi: <https://doi.org/10.1101/151068>
 79. Van Den Berg, F., Robert, C., Shaw, M.W., and Van Den Bosch, F. (2007). Apical leaf necrosis and leaf nitrogen dynamics in diseased leaves: A model study. *Plant Pathology* 56, 424–436.
 80. Van Den Berg, F., Van Den Bosch, F., Powers, S.J., and Shaw, M.W. (2008). Apical leaf necrosis as a defence mechanism against pathogen attack: Effects of high nutrient availability on onset and rate of necrosis. *Plant Pathology* 57, 1009–1016.
 81. Van den Berg, F., Gaucel, S., Lannou, C., Gilligan, C.A., and van den Bosch, F. (2013). High levels of auto-infection in plant pathogens favour short latent periods: A theoretical approach. *Evolutionary Ecology* 27, 409–428.
 82. Vári, E., and Máriás, K. (2013). The Impact of Crop Rotation and N Fertilization on the Leaf Area Index , Leaf Disease and Yield of Winter Wheat. *International Scholarly and Scientific Research & Innovation* 7, 1031–1034.
 83. Vos, J., Evers, J.B., Buck-Sorlin, G.H., Andrieu, B., Chelle, M., and De Visser, P.H.B. (2010). Functional-structural plant modelling: A new versatile tool in crop science. *Journal of Experimental Botany* 61.
 84. Wang, Z., Wang, J., Zhao, C., Zhao, M., Huang, W., and Wang, C. (2005). Vertical Distribution of Nitrogen in Different Layers of Leaf and Stem and Their Relationship with Grain Quality of Winter Wheat. *Journal of Plant Nutrition* 28, 73–91.
 85. Whalen, M.C. (2005). Host defence in a developmental context. *Molecular Plant Pathology* 6, 347–360.
 86. Zadoks, J.C. (2008). On the political economy of plant diseases epidemics – Capita selecta in historical epidemiology. Wageningen Academic Publishers. pp 39–119. ISBN 978-90-8686-086-9.
 87. Zhan, J., Mundt, C.C., Hoffer, M.E., and McDonald, B.A. (2002). Local adaptation and effect of host genotype on the rate of pathogen evolution: An experimental test in a plant pathosystem. *Journal of Evolutionary Biology* 15, 634–647.
 88. Zhan, J., Thrall, P.H., and Burdon, J.J. (2014). Achieving sustainable plant disease management through evolutionary principles. *Trends in Plant Science* 19, 570–575.
 89. Zhan, J., Thrall, P.H., Papaïx, J., Xie, L., and Burdon, J.J. (2015). Playing on a Pathogen's Weakness: Using Evolution to Guide Sustainable Plant Disease Control Strategies. *Annual Review of Phytopathology* 53, 19–43.

Annexes 1 : English version of section “Introduction”

Objectives and Methods

The objective of this work is to quantify the effect of fertilization on crop epidemics and the evolution of pathogens. A more applied objective is to determine whether it is theoretically possible to use fertilization as a lever to regulate crop epidemics. This work is based on the hypothesis that fertilization is a potentially interesting lever of action to control epidemics in agroecosystems through its effects on plant growth and development and on the interactions between plants and pathogenic fungi.

To attain these objectives our approach is to use mathematical models to simulate the impact of the various effects of fertilization on epidemics. We also investigate the evolutionary responses of pathogens to changes in fertilization regimes. To achieve a certain degree of biological realism, we take into account both the interactions between the pathogen and its host and the evolution of the pathogen in a changing (fertilization) environment. This allows us to test several fertilization practices and determine whether their (hopefully positive) effects on the pathosystem are "sustainable". Our idea is therefore to use fertilization to bring out the self-regulating properties of agroecosystems through interactions between organisms, more precisely through the study of the epidemiological and evolutionary responses of the pathosystem to changes in fertilization levels.

Our models were inspired by biological knowledge of the pathosystem of a wheat crop and a biotrophic fungal pathogen such as brown rust (*Puccinia triticina*), although we believe that the model is sufficiently generic to apply to other pathosystems as well; in particular, to other cereal-fungus pathosystems.

Many agronomic studies prior to this thesis have made it possible to determine which plants traits are influenced by fertilization. Several of these plant traits influence pathogen development, which in turn leads to feedbacks to the plant. These effects are dynamic and involve phenomena covering a range of spatial scales from fine spatial scales (exchange of nutrients at the scale of a lesion) to that of the wider crop canopy (whose size and density may

for instance affect the dispersal of the pathogen) and to that of the landscape in which the heterogeneity of practices could limit the extent of epidemics. They cover a range of time scales from from a single dispersal event, to the duration of an infectious cycle, to longer scales allowing for the evolution of pathogen populations (which requires several growing seasons).

Given the multiplicity of interactions we need to consider, we believe that mathematical modelling is a useful tool to better understand the effects of fertilization on epidemics and to simulate the response of the pathosystem at the above-mentioned spatial and temporal scales. It is therefore a modelling approach that was chosen for this work, with consideration of several spatial and temporal scales. **Two main models**, allowing us to study the link between fertilization, epidemics and pathogen evolution were developed during my thesis, the first one covering the spatial scales from a lesion to the canopy, the other from field to landscape. There is a strong link between these two models: in the landscape model, the implementation of the field-scale pathosystem dynamics corresponds to a metamodel based on the main results from the canopy model.

Among the great diversity of existing mathematical frameworks, four main types of models have inspired our work. (1) Functional-structural plant models (FSPMs) are models that seek to represent the three-dimensional spatial-temporal dynamics of plant development (Godin and Sinoquet 2005, Vos et al. 2009, Sievänen et al. 2014). They have been quite recently coupled with epidemic models to understand how the canopy architecture impacts the development of epidemics (Robert et al. 2008, Calonnec et al. 2008, Baccar et al. 2011, Garin et al. 2014, Robert et al. 2017). The results obtained in particular for wheat and fungal foliar diseases have enabled us to identify several key effects of wheat architecture on epidemics and select the corresponding mechanisms to be integrated into our own modelling work. This is particularly true for the rate at which the plant develops, which determines both the race between crop development and canopy colonization by the pathogen. It also determines the location and the dynamics of senescence of the leaves (Robert et al., 2017). Both effects influence the density of the crop canopy thereby affecting the dispersal of the pathogen within the canopy. From the FSPMs, we retain some biological realism and a functional dimension that allows us to model wheat as much more than just a static substrate to colonize. (2) Physiologically structured population models (PSPMs) from population ecology provide us with a powerful theoretical framework for describing the dynamics of biological populations with age, size or other physiological structure (De Roos et al. 1992, De Roos 1997, Claessen

et al. 2000). The use of such a theoretical framework allows us to model the plant tissue-age dependent developmental dynamics of the plant and the infection-age dependent pathogen life cycle and to describe quite rigorously the colonization of the canopy during the course of epidemics. By contrast with FSP models, they go into less biological details and are generally used to simulate population dynamics over many years. They inspired the architecture of the canopy model (Chapters 1, 2 and 3). (3) "Susceptible-exposed-infectious-removed" (SEIR) models are very common in epidemiology and are often used to describe temporal dynamics of diseases, predict their occurrence or model vaccine efficacy (Gilchrist et al. 2006, Li and Muldowney 1995, D' Onofrio 2002). Their simplicity and mathematical drivability, however, often operate at the expense of the biological realism of the host/pathogen interaction. From these compartmentalized models, we retain the description of the epidemic in host classes. We have produced a PSPM-like structured version of SEIR model that we use to describe epidemics at plot scale, and a spatial version of SEIR model to describe epidemics at landscape scale. (4) To simulate the eco-evolutionary dynamics of the pathosystem, we combine two different approaches. The first one is the classical optimisation principle from evolutionary ecology (Stearns, 1992; Roff, 2002). The second one is the theory of adaptive dynamics (Metz et al., 1992; Geritz et al., 1998). We use and compare both approaches at the different spatial scales in our models to predict how pathogens will adapt to changes in fertilization regimes. (5) Spatially explicit models of landscape epidemiology (yet still less commonly used) provide a framework for studying the effect of pathogen dispersal or spatial heterogeneity on epidemics (Park et al. 2001, Skelsey et al. 2010, Jones et al. 2011, Papaïx et al. 2014, 2015). They usually represent the landscape as a mosaic of fields with functioning as a pathogen meta-population. We have designed such a model to study the effect of fertilization on landscape scale epidemics.

One of the particularities of this thesis is its focus on the consumer-resource aspects of the pathosystem. This approach is necessary for us to make the link between ecological concepts and our agronomic question. Through its effects on the host, fertilization determines the quantity of resource that will be available for the pathogen. This quantity is of course not unlimited. In such context, life history theory predicts that the pathogen will face a resource allocation dilemma: it must optimally partition that finite amount of resource between its key biological functions, growth, defence, maintenance and reproduction (Stearns 1992, Roff 2002). It is clear that not all these functions can be maximized at the same time.

There will therefore be trade-offs between the traits underlying these biological functions, which will constrain the evolution of pathogens in response, for example, to variations in the accessibility of resources (lower fertilization, etc.). In our study, we focus on one such trait: the latent period. The latent period can be viewed alternatively as the duration of a somatic growth ("juvenile") period of the pathogen before reproduction (determining its size; thus related to growth), or as the minimum duration of an infection cycle (time between the establishment of new lesions on a leaf and the first emission of inoculum; thus related to reproduction), or as a measure of the efficacy of canopy colonization ("aggressiveness" in phytopathology). Assuming that the pathogen's sporulation rate is proportional to its body size (i.e. mycelium biomass determined by the latent period), the pathogen can either reproduce rapidly but less efficiently, or grow as much as possible before reproducing, at the risk of having depleted its resources when the time of reproduction finally comes. In life history theory, this is a classical question of the evolution of maturation (Cohen 1976, Stearns 1989, Kozlowski 1992, Engen and Saether 1994): since growth and reproduction cannot be optimized at the same time, the pathogen is likely to adopt an intermediate strategy, which we refer to as the "optimal latent period". The initial question on the link between fertilization, epidemic development and evolution now translates into the more practical question of the link between fertilization and latent period. In most chapters in this thesis, we aim at identifying optimal latent periods optimizing several life history traits of the pathogen.

Thesis outline

This thesis consists of five chapters and a general discussion of the results. The purpose of this section of the introduction is to briefly describe the objective of each chapter and to show the logic of the thesis development.

In Chapter 1, we present a model designed to study the epidemiological response of leaf fungal pathogen to fertilization at the canopy scale. The scales considered range from a single lesion to the canopy. The model is a combination of epidemiological and PSPM models. It corresponds to a SEIR model where all compartments benefit from double age-structure, in terms of age of the tissue and age of the infection. It allows us to study the interactions between the plant and pathogen and to identify optimal latent periods at the lesion

and canopy scales. The objective of this chapter is mostly to present the model that will be used in chapters 2 and 3 of the thesis.

Chapter 2 focuses on the effect of fertilization on epidemics and optimal latency at the field scale. It uses the model presented in Chapter 1 combined with several modelling scenarios corresponding to the main effects of fertilization on the pathosystem. We propose two empirical fitness measures for the pathogen and test how they respond to latent period in the different modelling scenarios in order to identify optimal latent periods. This chapter therefore deals with the effects of fertilization on epidemics and is a first step towards possible evolutionary responses.

Chapter 3 focuses on the evolution of pathogens in response to changes in crop fertilization. It compares the contrasting evolutionary responses obtained in Chapter 2 using "ad hoc" pathogen fitness measures with the ones, theoretically more rigorous, established using the tools of adaptive dynamics.

Chapter 4 presents the effect of fertilization on the disease at the landscape scale and in particular, the effect of spatial heterogeneity in terms of fertilization on epidemics and pathogen evolution. In this new model, the landscape is represented as a mosaic of fields with high or low fertilization. To implement the field-scale dynamics of the pathogen, the model directly uses the latency-sporulation trade-off established in the previous chapters of the thesis. In this chapter, we deal with larger spatial scales to study the responses of pathogens to fertilization at a scale better suited to implement disease-limiting cultural practices.

Chapter 5 presents, as an opening, a meta-analysis studying the relation between pathogen trophic types and latent period. If resource quantity/dynamics is indeed fundamental to optimizing the latent period, then trophic type should also influence the optimal latent period. This is what we test in this last chapter of the thesis.

The last part of the thesis is a general discussion of results and perspectives.

References

1. Baccar, R., Fournier, C., Dornbusch, T., Andrieu, B., Gouache, D., and Robert, C. (2011). Modelling the effect of wheat canopy architecture as affected by sowing density on *Septoria tritici* epidemics using a coupled epidemic/virtual plant model. *Annals of Botany* 108, 1179–1194.
2. Calonnec, A., Cartolaro, P., Naulin, J.M., Bailey, D., and Langlais, M. (2008). A host-pathogen simulation model: Powdery mildew of grapevine. *Plant Pathology* 57, 493–508.
3. Claessen, D., de Roos, A.M., and Persson, L. (2000). Dwarfs and Giants: Cannibalism and Competition in Size-Structured Populations. *The American Naturalist* 155, 219–237.
4. Cohen, D. (1976). On the Optimal Timing of Reproduction. *The American Naturalist*, 110(975), 801–807. <https://doi.org/10.1086/283495>
5. D’Onofrio, A. (2002). Stability properties of pulse vaccination strategy in SEIR epidemic model. *Mathematical Biosciences* 179, 57–72.
6. De Roos, A.M., Diekmann, O., and Metz, J.A.J. (1992). Studying the Dynamics of Structured Population Models: A Versatile Technique and Its Application to Daphnia. *The American Naturalist* 139, 123–147.
7. De Roos, A.M. A Gentle Introduction to Physiologically Structured Population Models. *Structured-Population Models in Marine, Terrestrial, and Freshwater Systems* 119-204 (1997).
8. Engen, S., and Saether, B. (1994). Optimal allocation of resources to growth and reproduction. *Theoretical Population Biology* 46, 232–248.
9. Garin G. 2015. Vers la compréhension des épidémies fongiques foliaires par modélisation multi-échelle dans les couverts architecturés. Thèse de Doctorat soutenue le 11 décembre 2015.
10. Geritz, S.A.H., Kisdi, É., Meszéna, G., and Metz, J.A.J. (1998). Evolutionarily singular strategies and the adaptive growth and branching of the evolutionary tree. *Evolutionary Ecology* 12, 35–57.
11. Gilchrist, M. A., Sulsky, D. L., and Pringle, A. 2006. Identifying fitness and optimal life-history strategies for an asexual filamentous fungus. *Evolution* 60:970-979.
12. Godin, C., and Sinoquet, H. (2005). Functional-structural plant modelling. *New Phytologist* 166, 705–708.
13. Kozłowski, J. (1992). Optimal allocation of resources to growth and reproduction: Implications for age and size at maturity. *Trends in Ecology & Evolution* 7, 15–19.
14. Li, M. Y., and Muldowney, J. S. 1995. Global stability for the SEIR model in epidemiology. *Math. Biosci.* 125:155-164.
15. Metz, J.a.J., Nisbet, R.M., and Geritz, S.a.H. (1992). How should we define 'fitness' for general ecological scenarios? *Trends in Ecology & Evolution* 7, 198-202.
16. Papaïx, J., Adamczyk-Chauvat, K., Bouvier, A., Kiêu, K., Touzeau, S., Lannou, C., and Monod, H. (2014). Pathogen population dynamics in agricultural landscapes: The Ddal modelling framework. *Infection, Genetics and Evolution* 27, 509–520.
17. Papaïx, J., Burdon, J.J., Zhan, J., and Thrall, P.H. (2015). Crop pathogen emergence and evolution in agro-ecological landscapes. *Evolutionary Applications* 8, 385–402.
18. Park, A., Gubbins, S., and Gilligan, C. (2001). Invasion and Persistence of Plant Parasites in a Spatially Structured Host Population. *Oikos* 94, 162–174.

19. Robert, C., Fournier, C., Andrieu, B., and Ney, B. (2008). Coupling a 3D virtual wheat (*Triticum aestivum*) plant model with a *Septoria tritici* epidemic model (Septo3D): A new approach to investigate plant-pathogen interactions linked to canopy architecture. *Functional Plant Biology* 35, 997–1013.
20. Robert C., Garin G., Pradal C., Fournier C. 2017. A plant-pathogen model reveals how plant architecture and foliar senescence impact the race between wheat growth and *Zymoseptoria tritici* epidemics. *Annals of Botany*. (In press).
21. Roff, D. A. 2002. Life history evolution. Sinauer Associates, Sunderland, Massachusetts.
22. Sievänen, R., Godin, C., De Jong, T.M., and Nikinmaa, E. (2014). Functional-structural plant models: A growing paradigm for plant studies. *Annals of Botany* 114, 599–603.
23. Skelsey, P., Rossing, W. a H., Kessel, G.J.T., and van der Werf, W. (2010). Invasion of *Phytophthora infestans* at the landscape level: how do spatial scale and weather modulate the consequences of spatial heterogeneity in host resistance? *Phytopathology* 100, 1146–1161.
24. Stearns, S.C. (1989). Trade-Offs in Life-History Evolution. *Functional Ecology* 3, 259.
25. Vos, J., Evers, J.B., Buck-Sorlin, G.H., Andrieu, B., Chelle, M., and De Visser, P.H.B. (2010). Functional-structural plant modelling: A new versatile tool in crop science. *Journal of Experimental Botany* 61.

Appendix 2: English version of section “Discussion”

Discussion

The discussion is divided into four subsections: (1) a discussion about our questions and modelling approaches, (2) the effect of fertilization on epidemics (without evolution), (3) the evolution of pathogens due to changes in fertilization, and (4) the possibility of using fertilization to regulate epidemics.

I) Scientific questions, modelling approaches and originality of our work

I.1) An interdisciplinary approach

One of the fundamental principles of agro-ecology is to use biotic interactions within the agroecosystem in order to promote ecosystem services and achieve some degree of self-regulation. By determining the environmental conditions within the agroecosystem, agricultural practices can influence the interactions between the organisms that live there. Hence, cultural practices may prove powerful levers for inventing a more sustainable agriculture, inspired by the functioning of natural ecosystems. To what extent agroecosystems must copy natural ecosystems, and what exactly they should copy is still widely debated (Ford and McGuire, 2015).

The main methods in crop protection against fungal pathogens are currently the use of fungicides and resistant varieties. To implement more sustainable agroecological solutions, we need to gain knowledge that allows us to understand how exactly the pathogen, its host and the environment interact. Since fertilization has a direct impact on the development of the host and thereby of the pathogen, studying the effect of crop fertilization on the pathosystem dynamics could help gaining such knowledge.

One of the peculiarities of our work is that we have developed an original approach, combining several ecological, ecophysiological and epidemiological aspects of plant/pathogen interaction. It allows us to model the plant, the pathogen and their interactions at the different spatial and temporal scales necessary for our study. It also allows us to use methods and concepts from theoretical ecology to answer an agronomic question. Our study covers spatial scales from that of the lesion to that of the canopy and that of the landscape. Considering the pathosystem as a consumer-resource system is the central idea in our work. Consumer-resource dynamics is one of the cornerstones of ecological theory and evolutionary ecology. Using it to model the relation between the pathogen and its host gives us access to the trade-offs that constrain the system and to the consequences of the interactions between the pathogen and its host. Simulating the epidemiological dynamics over many seasons gives us access to the evolutionary responses of the pathogen to changes in fertilization and allows us to discuss the sustainability of fertilization practices that would reduce epidemics at the landscape scale.

I.2) Scientific and technical difficulties and related choices

Which degree of complexity is required to adequately model the response of our pathosystem to changes in fertilization is far from being trivial. Let's take the example of our first model that covers the scales from a single lesion to the crop canopy (Chapter 1). To properly reflect the effect of fertilization on the system, the model had to integrate at least these two spatial scales. To properly reflect the life history of both the plant and the pathogen, the model had to be structured by age. Intra-seasonal dynamics had to be implemented to take into account dynamic effects (of canopy growth for example), but also seasonal forcing was needed to monitor epidemics in the long run. Finally, modelling spore dispersal and canopy colonization required at least some spatial structure.

Finding suitable parameter combinations was not an easy task either. This is partly due to a lack of knowledge about biological processes at different scales, for example about, (1) the use of foliar resources by fungi (to build up its mycelium and spores), (2) the survival of spores during overwintering, and (3) the flow of spores in the landscape.

Finally, for the sake of simplicity (and in order to save time), we allowed ourselves several simplifications. Among those, two major ones are discussed here: the effect of climate and of plant immunity.

In all the simulations and in both models, we use a rather crude description of climate. Using thermal time make the epidemiological dynamics implicitly depend on temperature scenarios. The onset of epidemics in the model (initialization parameter) reflects favourable weather conditions for germination and infection. However, we do not consider the effect of other abiotic variables on epidemics (e.g. periods of drought that would limit pathogen development). An interesting perspective would be to test the robustness of our results against climate variability.

The interactions between host fertilization and the level of pathogen defences is currently a hot topic (see reviews from Masclaux-Daubresse et al., 2010 and Mur et al. 2017). Nitrogen indeed plays an important role in plant protection. Despite early studies that established a negative relationship between fertilization and some levels of physical and biochemical defences in wheat (Kirkham 1954; Király 1964; Matsuyama and Diamond 1973; Matsuyama 1975), it now appears that the use of nitrates as synthetic fertilizers favours plant defences (Mur et al., 2017 and references within). This means that while the pathogen may benefit from the additional resources intended for the plant, it could also face a more efficient immune system! But just as pathogen adaptation is constrained by trade-offs in resource allocation, the plant is also constrained by a trade-off between growth and defence. Including this trade-off in the EBT model (of Chapters 1-3) would be possible by implementing a negative relation between the pathogen resource use efficiency and the fertilization rate.

I.3) Latent period, trophic type and fertilization

Our meta-analysis (Chapter 5) demonstrates the existence of a connection between latent period and trophic type of eumycete crop pathogens. Most necrotrophs have short latent periods while most hemibiotrophs display very long ones. The latent period of biotrophs appears to be intermediate between those of necrotrophs and hemibiotrophs.

All the simulations in Chapters 1 to 4 focus on rust-like biotrophic pathogens. The main feature of these pathogens is the necessity to develop on living plant tissues. By contrast, necrotrophs can develop exclusively on "dead" tissue, provided they are the one responsible

for the death of the tissue (Horbach et al., 2011; Kabbage et al., 2015). Hemibiotrophs also need to kill their host tissue to sporulate (Horbach et al., 2011; De Silva et al., 2016). Resource accessibility is probably quite different between biotrophic pathogens that derive nutrients from the symplast via haustoria and hemibiotrophic pathogens that derive nutrients from apoplastic resources of necrotic tissue (lesion scale, Perfect and Green, 2001, Divon and Fluhr, 2007). It is therefore likely that the effects of fertilization will not be perceived in the same way by these different types of pathogens.

An exciting perspective of this work would be to include necrotrophic and/or hemibiotrophic pathogens in our models. Our models are particularly well suited to test the effect of fertilization on different pathogens, or even on parasitic assemblages! Pathogens of different trophic types can indeed simultaneously colonize the same organs and are thus in competition for that resource. Since we can translate pathogen trophic types into characteristic latent periods (Chapter 5), our models should allow us to easily study the competition between two or more pathogen species.

II) Fertilization has an impact on fungal epidemics

In our model, increasing fertilization translates into worsening fungal epidemics, in terms of both spore production and AUDPC. This result stands whatever the spatial scale considered: from the lesion (Chapter 2), to the field (Chapter 2) to the landscape (Chapter 4). This result is also consistent with the literature on rust epidemics (Howard et al. 1994; Ash and Brown, 1991; Danial and Parlevliet, 1995; Devadas et al. 2014) and on other biotrophic pathogens of cereals (Smith and Blair, 1950; Last, 1953, 1962; Bainbridge, 1974; Shaner and Finney, 1977; Daamen et al., 1989; Olesen et al., 2003).

In the EBT model (Chapters 1-3), we retained from the scientific literature three main effects of fertilization on the plant that may also affect fungal epidemics (see Introduction, Figure 7). These are (1) the concentration of metabolites within leaves, (2) the leaf life span and (3) the size of the crop canopy (number and size of the leaves). In practice, the response of wheat to fertilization is a combination of these three processes. It is therefore difficult to determine the contribution of each fertilization effect independently. To some extent, our modelling approach allows us to disentangle these effects. Our results suggest that reducing canopy size and leaf life span have the greatest impacts on epidemics. Amazingly enough,

these two effects further correspond to the first response of wheat to a decrease in fertilization in the field (Savary et al., 1995; Robert et al., 2004). But while the effect of canopy density on epidemics is already well documented (Darwinkel, 1980; Daamen et al., 1989; Danial and Parlevliet, 1995; Savary et al., 1995; Jensen and Munk, 1997; Lovell et al., 1997; Robert et al., 2008; Garin et al., 2014) the effect of leaf lifespan has received much less attention (Robert et al., 2017). One of the perspectives of this work would be to combine the three above-mentioned effects of fertilization into a more realistic fertilization practices in the EBT model.

The transition from canopy to landscape scale was an opportunity to broaden our questioning to the effect of spatial heterogeneity of fertilization on epidemics. In particular, we wanted to test how diversifying a homogeneous landscape of high fertilization by including a number of low fertilization fields would impact the disease. We show that, under the hypothesis that pathogen maladaptation exists in the low fertilization fields in the heterogeneous landscape (i.e. that pathogens adapted to high fertilization levels develop poorly in low fertilization fields) then a heterogeneous fertilization landscape would effectively reduce epidemics and crop losses due to the pathogen.

The efficacy of such practices depends on the aggregation level and on the proportion of the field types in the landscape. In high aggregation landscapes or landscapes dominated by low fertilization fields, heterogeneity results in a decrease in the amount of inoculum released into the landscape and in a slowing down in the colonization of the landscape by the pathogen. On the other hand, a landscape with a low aggregation level or a landscape dominated by high fertilization fields behaves pretty much like a high fertilization homogeneous landscape. These results are consistent with those of Mundt et al. (2011) on brown rust (*Puccinia recondita*) who propose that reducing the frequency of susceptible hosts in a mixture of susceptible and resistant wheat varieties would reduce disease incidence. Similar results have been reported by Skelsey et al. (2010) on potato downy mildew (*Phytophthora infestans*). Thus, in our model, in the absence of adaptation, low fertilization fields play a role similar to the one of resistant crop varieties of Mundt et al. (2011).

The center of clusters of low fertilization fields is protected, even if temporarily, by the low conductivity of these plots to the disease. These clusters act as a barrier to the spread of the disease (Chapter 4, Figure 15). Only the edge of these clusters is more affected by the disease because fields at the edge of the clusters are subject to high levels of alloinfection by

their high fertilization inoculum-producing neighbours. Such effect of plot size is known as an “edge effect” (Murcia 1995; Rizzo and Garbelotto, 2003). For example, Dallot et al. (2004) show that in the case of peach orchards attacked by a virus, the boundary effect protects trees within large plots from external contamination, while small plots are heavily attacked. An experimental study by Johnson and Haddad (2011) on the wind-dispersed pathogen of maize *Cochliobolus heterostrophus* shows that the border effect alone makes it possible to understand the patterns of disease incidence.

Thus, whatever the scale considered (canopy, landscape), nitrogen fertilization seems to be a promising tool for regulating crop epidemics. But what do the results on pathogen adaptation to fertilization tell us about the sustainability of such practices?

III. Evolution of pathogens facing changing crop fertilization

In this section, we first discuss the notions of fitness, optimal latent period and ecological trade-offs. We then focus on the results relative to pathogen adaptation to fertilization at the different scales in our models.

III.1) Trade-offs, fitness and latent period

One of the bases of this work was to consider the pathosystem primarily as a consumer-resource system. Fertilization determines the quantity of (host) resource that will be available for the pathogen. The pathogen must therefore adopt a strategy for the optimal exploitation of this resource. That strategy will change according to the total amount of resource in the system and, more importantly, it will change over time according to resource dynamics. Our models show that the pathogen indeed adopts an optimal strategy of resource allocation, corresponding to an "optimal latent period". That optimal latent period is an emerging property of both models. The calculation of the optimal latent periods was performed by either maximizing *ad hoc* fitness measures such as spore production or canopy colonization or by using invasion fitness from adaptive dynamics (ESS latent period). In all cases, we find that an intermediate latent period maximizes fitness. Interestingly, these optimum values differ depending on which fitness measure we use.

In our simulations and with our set of default parameter values, we find that the optimal (ESS) latent period estimated by invasion fitness are practically the average values between the optimal latent periods obtained by maximizing the seasonal spore production (fitness 1) and the speed of canopy colonization (fitness 2). We therefore conclude that the pathogen faces two different trade-offs: (1) at the tissue scale it must produce enough spores, but at the canopy scale, it must be fast enough to colonize its host canopy (Chapter 1). In this section, we wanted to test this hypothesis by recalculating optimal latent periods with a new set of parameter values that will skew the trade-off towards either spore production or colonization rate.

We first broaden the dispersal kernel by increasing maximum dispersal distance Δ . As a consequence, spore dispersal becomes a far less limiting factor of epidemic development. Figure 1A shows the new ESS latent periods (for a given fertilization level) when Δ increases (default value $\Delta = 250$ dd). The ESS latent period increases with Δ and converges to the optimal latent period that maximizes the seasonal spore production (fitness 1). Under these conditions, we relax the race between the plant and the pathogen for canopy colonization. Thus, the trade-off linking latent period and spore production prevails.

We next increased pathogen infection efficiency β . Figure 1B shows that the ESS latent periods this time decrease with infection efficiency and converge to those that maximize canopy colonization. In this second case, increasing infection efficiency makes spore production less limiting. This time, the trade-off between latent period and canopy colonization prevails.

These simulations confirm our hypothesis that the ESS latent period emerges from the two trade-offs. Please note that the parameterization of the model in Chapters 1 to 3 has placed us in a scenario where spores production and canopy colonization are of similar importance, though this remains to be verified empirically.

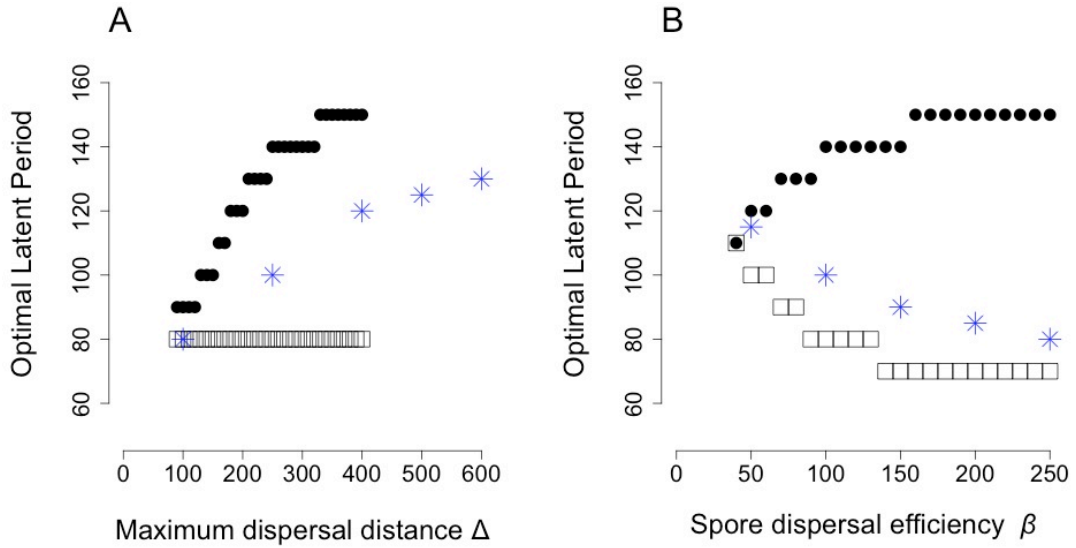


Figure 1: Variation of optimal latent periods with **A**: the maximum dispersal distance Δ and **B**: the spore dispersal efficiency β in the reference fertilization parameters ($K = 1$, $\tau = 750$, $\rho = 1$; default values are $\beta = 100$ and $\Delta = 250$). Full circles are optimal latent periods corresponding to seasonal spore production as a fitness measure. Open squares are optimal latent periods corresponding to within-season exponential growth rate as a fitness measure of the pathogen. Blue stars correspond to the evolutionary singular strategies (ESS).

III.2) Fertilization and latent period evolution

III.2.1 Evolutionary direction

Chapter 4 focuses on the consequences of the change of scale from field to landscape on the epidemiological and evolutionary dynamics of the pathogen. In Chapter 4, we rather "impose" the trade-off between fertilization and spore production than let it emerge from the model as in Chapters 1-3. As a consequence, we consider that the results given by the first model (Chapter 1,2 and 3) are the most relevant to assess the evolutionary direction in which pathogen latent period will change with fertilization.

One result of primary importance is the comparison between the optimal latent periods calculated using the "*ad hoc*" fitness measures and those obtained using invasion fitness. We find that the optimal latent period that maximizes seasonal spore production (fitness 1) increases with fertilization for the three effects of fertilization tested. By contrast, the optimal latent period that maximizes the rate of canopy colonization (fitness 2) decreases with

fertilization for the three fertilization effects tested. The optimal latent period estimated based on invasion fitness (ESS) gives yet another value that is intermediate between those from fitness 1 and 2. Finally, we find that the optimal latent period that maximizes spore production during canopy growth (at the beginning of epidemics, fitness 3) is very close to the one estimated based on invasion fitness. We argue that this comparison helps us gain understanding about the constraints imposed on the pathogen in its adaptation. In particular, we believe that the dynamic aspects of canopy growth impose an ecological constraint that tends to select for a shorter latent period than would be expected if the pathogen was spreading inside an already fully-grown crop canopy.

We will now further discuss the relation between the ESS latent period and the effects of fertilisation (Chapter 3). The evolutionary response of the latent period to fertilization corresponds to evolutionarily stable (ESS) latent periods that increase with leaf life span but decrease with increasing canopy growth rate (i.e., canopy size). These relations appear to be quite logical: in the first case, the longer the leaf lifespan, the more time for the pathogen to establish itself; in the other case the canopy race increases as the growth rate increases, which favours shorter latent periods that can still keep up with plant development. Nevertheless, the range of ESS variation in these cases remains rather limited (at most 30 degree-days). Furthermore, please note that the ESS latent periods do not respond to changes in leaf metabolite content.

By contrast with our previous results (fertilization worsened epidemics whatever the effect of fertilization tested), the three effects of fertilization lead to different responses of ESS latent periods to fertilization. Given these contrasting effects, predicting the evolutionary direction of the response of latent period to fertilization remains difficult, especially in a scenario that would combine the three fertilization effects. Thus, disentangling these effects allows identifying possible contrasting effects on fertilization on pathogen evolution.

III.2.2 Coexistence and maladaptation

At the canopy level, invasion analyses (PIPs) show that there is always a single latency that is evolutionarily stable, i. e. a global ESS (Chapter 3). In addition, analyses of mutual invasibility (TEPs) show that these ESSs are characterised by a lack of coexistence. At the landscape level, we have shown that evolution converges towards an evolutionary branching

point (EBP) (Chapter 4). The emergence of disruptive selection, characteristic of EBPs, in a landscape composed of two habitat types is not surprising in itself (Ravigné et al 2009). This type of point is always associated with the possibility of coexistence of (at least) two strains (Geritz 1998). What we learn from the study of evolution at the landscape level (PIPs and TEPs, Chapter 4) is that coexistence becomes possible, even within fields, thanks to the effect of spatial heterogeneity. The coexistence at landscape level is even present in all our simulations of heterogeneous landscapes. Our study shows that this coexistence is a direct consequence of the presence of two types of fields in the landscape, since the PIPs and TEPs can be constructed by superimposing the two type-specific PIPs.

Convergence towards the evolutionary branching point is also associated with maladaptation: a strain with a latent period corresponding to the EBP is a generalist, the "best" strain to exploit the whole landscape, but is relatively maladapted in each field. However, this strain will soon be replaced by other strains that appear in the landscape.

III.3) Additional perspectives

III.3.1) Taking into account pathogen virulence in the model

In our model, we did not consider the direct effect of sporulating lesions on photosynthesis (Robert et al. 2004). However, by reducing even more the quantity of resource available for the pathogen, such effect would potentially have an impact on the optimal resource allocation strategy of the pathogen. Preliminary work shows in particular that the optimal latent period would be shorter if we took this effect into account, but the qualitative results would not change much otherwise (data not shown). This matter requires further consideration.

III.3.2) Will pathogens adapt only through changes in their latent period?

In both canopy and landscape models, we study only the effect of fertilization on latent period. Nevertheless, other pathogen trait of the infection cycle could also respond to fertilization, especially in the canopy model. Among them, the uptake rate of the pathogen is likely to increase with the amount of resource available, and may also be embedded in trade-offs similar to those linking latent period to spore production and canopy colonization.

For example, if the pathogen is allowed to continue allocating a fraction κ of its resources to growth during the infectious period, the ESS resource exploitation strategy (for a

given latent period) is not the bang-bang strategy but to allocate 7% of energy to growth and the remaining 93% to reproduction (Figure 2). However, this is only true for short latent periods, i. e. for latent periods with $\lambda < \lambda_{ESS}$ when $\kappa = 0$. But when both traits (κ and λ) are allowed to coevolve, the "optimal" resource allocation strategy is the bang-bang strategy.

Other pathogen traits, though more qualitative, should also be paid more attention, such as the level of genetic diversity of pathogen populations, or the presence/absence of sexual reproduction cycles (teleomorphic stages). These traits have been emphasized by McDonald and Linde (2002) who use them to establish a hierarchy of life history traits that contribute the most to pathogen adaptability.

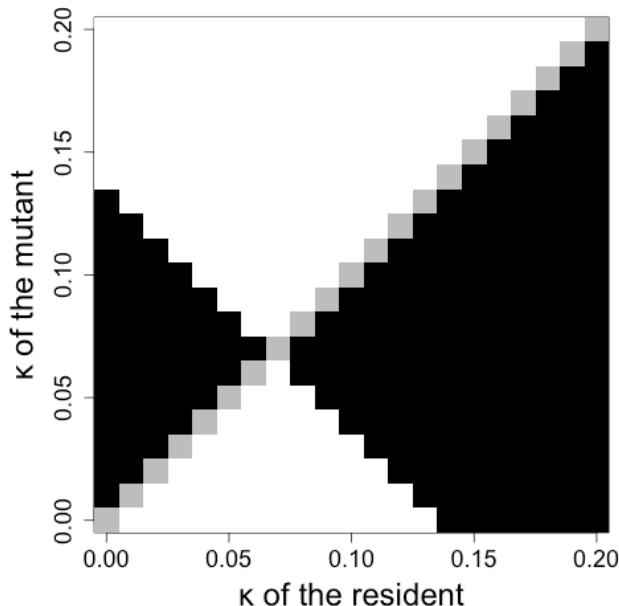


Figure 2: PIP showing the ESS of pathogen resource allocation strategy for the reference fertilization parameters ($K = 1$, $\tau = 750$, $\rho = 1$, with $\lambda = 100$ and default parameter values)

At the landscape scale, traits such as the average dispersal distance may prove particularly interesting. High rates of autoinfection associated with polycyclic diseases and asexual cycles ensure the increase in frequency of all phenotypes in the landscape (and probably promote local adaptation), while alioinfection (corresponding more or less to migration), combined with sexual reproduction, allows for the arrival of new phenotypes in the landscape (van den Berg et al., 2013).

IV. Fertilization as means to reduce epidemics?

Our results suggest that fertilization could be an interesting lever to regulate crop epidemics. In particular, we show that introducing new fertilization practices into the landscape will reduce epidemics, at least temporarily (as long as pathogen maladaptation exists in the landscape). Although the existence of local adaptation (and therefore maladaptation) in agroecosystems is still being discussed (Strauss, 1997; Laine, 2005), several studies show that the phenomenon exists in an agricultural context and in wild populations of pathogenic fungi outside agrosystems (Parker, 1985; Kaltz et al, 1999; Zhan et al., 2002; Suffert et al., 2017). Furthermore, it has been hypothesized that local adaptation would not be hindered if the gene flow within the pathogen metapopulation is significant (Gandon, 2002). To ascertain the existence of pathogen local adaptation to fertilization one could compare the latent periods of fungal strains adapted to high input levels (Western Europe) and those adapted to low fertilization levels (Eastern Europe) in allopatric and sympatric conditions.

Theoretical studies using adaptive dynamics to predict pathogen evolution, for example in the context of spatial heterogeneity, provide only long-term conclusions because they focus on systems that have reached their equilibrium (Lion and Gandon, 2016). In the agricultural context however, we are often rather interested in the transient or the short-term effects. In addition, an agricultural landscape is characterized by a temporal crop rotation that affects the development of epidemics and keeps the system out of equilibrium.

Hence, combining spatial and temporal heterogeneity of fertilization in the landscape could prove very valuable. In nature, plant diseases are ephemeral in isolated host populations. Disease incidence varies greatly in time and space depending on local adaptation and extinction and recolonization rates (Burdon and Thrall, 2014). Inventing agricultural landscapes corresponding to mosaics of fertilization, resistant crop varieties and mixtures of varieties and species, with the overall picture changing over time, may bring us closer to the natural conditions of epidemics limitation.

Finally, this thesis highlights the importance to take into account the evolution of pathogens in order to assess the sustainability of agricultural practices, even if in our case the effect of fertilization proves limited. It is an important contribution to the current discussion

about the possible greater sustainability of “partial” control methods (compared to methods seeking to completely eliminate the pathogens, such as fungicide application; Plantagenest et al., 2007; Zhan et al., 2014,2015).

V. Conclusion

This thesis was a fascinating work from the start. It first represents a wonderful interdisciplinary experience, mixing ecology (my original specialty), agronomy, epidemiology and modelling. It also offered me a lot of knowledge on both the functioning of agricultural ecosystems, agroecology and the hopes such a word can hold for our futures, the biology of this extraordinarily diverse group of plant pathogenic fungi, and on the ecological- and landscape epidemiology. Finally, I found the multi-scale approach of our models rather elegant in that it uses the product of the results from the lower scales as the basis to build up the higher ones. A very exciting perspective of this work, which I would enjoy taking part in, is to integrate the three resource effects of Chapters 2 and 3 into a more realistic fertilization model applied to the study of pathogen assemblages (dealing with pathogens with different trophic types).

VI. References

1. Andrade-Piedra, J.L., Hijmans, R.J., Juárez, H.S., Forbes, G. a, Shtienberg, D., and Fry, W.E. (2005). Simulation of Potato Late Blight in the Andes. II: Validation of the LATEBLIGHT Model. *Phytopathology* 95, 1200–1208.
2. Ash, G.J., and Brown, J.F. (1991). Effect of nitrogen nutrition of the host on the epidemiology of *Puccinia striiformis* f.sp. *tritici* and crop yield in wheat. *Australasian Plant Pathology* 20, 108–114.
3. Baccar, R., Fournier, C., Dornbusch, T., Andrieu, B., Gouache, D., and Robert, C. (2011). Modelling the effect of wheat canopy architecture as affected by sowing density on *Septoria tritici* epidemics using a coupled epidemic/virtual plant model. *Annals of Botany* 108, 1179–1194.
4. Bainbridge, A. (1974). Effect of Nitrogen Nutrition of the Host on Barley Powdery Mildew. *Plant Pathology* 23, 160–161.
5. Bedoussac, L., and Justes, E. (2010). Dynamic analysis of competition and complementarity for light and N use to understand the yield and the protein content of a durum wheat-winter pea intercrop. *Plant and Soil* 330, 37–54.
6. Benbi, D.K. (1994). Prediction of leaf area indices and yields of wheat. *Journal of Agricultural Science* 122, 13–20.

7. Broers, L. (1989). Influence of development stage and host genotype on three components of partial resistance to leaf rust in spring wheat. *Euphytica* 44, 187–195.
8. Burdon, J.J., and Thrall, P.H. (2014). What have we learned from studies of wild plant-pathogen associations?-the dynamic interplay of time, space and life-history. *European Journal of Plant Pathology* 138, 417–429.
9. Calonnec, A., Cartolaro, P., Naulin, J.M., Bailey, D., and Langlais, M. (2008). A host-pathogen simulation model: Powdery mildew of grapevine. *Plant Pathology* 57, 493–508.
10. Carlisle, D.J., Cooke, L.R., Watson, S., and Brown, A.E. (2002). Foliar aggressiveness of Northern Ireland isolates of *Phytophthora infestans* on detached leaflets of three potato cultivars. *Plant Pathology* 51, 424–434.
11. Cisneros, J.J., and Godfrey, L.D. (2001). Midseason Pest Status of the Cotton Aphid (Homoptera: Aphididae) in California Cotton - Is Nitrogen a Key Factor? *Environmental Entomology* 30, 501–510.
12. Coakley, S.M. (1979). Climate variability in the Pacific Northwest and its effect on stripe rust disease of winter wheat. *Climatic Change* 2, 33–51.
13. Corio-Costet, M.F., Dufour, M.C., Cigna, J., Abadie, P., and Chen, W.J. (2011). Diversity and fitness of *Plasmopara viticola* isolates resistant to QoI fungicides. *European Journal of Plant Pathology* 129, 315–329.
14. Cunniffe, N.J., Koskella, B., E. Metcalf, C.J., Parnell, S., Gottwald, T.R., and Gilligan, C.A. (2015). Thirteen challenges in modelling plant diseases. *Epidemics* 10, 6–10.
15. Daamen, R.A., Wijnands, F.G., and Vliet, G. vander (1989). Epidemics of Diseases and Pests of Winter Wheat at Different Levels of Agrochemical Input: A study on the possibilities for designing an integrated cropping system. *Journal of Phytopathology* 125, 305–319.
16. Dallot, S., Gottwald, T., Labonne, G., and Quiot, J.-B. (2004). Factors Affecting the Spread of Plum pox virus Strain M in Peach Orchards Subjected to Roguing in France. *Phytopathology* 94, 1390–1398.
17. Danial, D.L., and Parlevliet J.E. (1995). Effects of nitrogen fertilization on disease severity and infection type of yellow rust on wheat genotypes varying in quantitative resistance, *J. Phytopathology* 143 679–681.
18. De Silva, N.I., Lumyong, S., Hyde, K.D., Bulgakov, T., Phillips, A.J.L., and Yan, J.Y. (2016). Mycosphere Essays 9: Defining biotrophs and hemibiotrophs. *Mycosphere* 7, 545–559.
19. Devadas, R., Simpfendorfer, S., Backhouse, D., and Lamb, D.W. (2014). Effect of stripe rust on the yield response of wheat to nitrogen. *Crop Journal* 2, 201–206.
20. Develey-Rivière, M.P., and Galiana, E. (2007). Resistance to pathogens and host developmental stage: A multifaceted relationship within the plant kingdom. *New Phytologist* 175, 405–416.
21. Divon, H.H., and Fluhr, R. (2007). Nutrition acquisition strategies during fungal infection of plants. *FEMS Microbiology Letters* 266, 65–74.
22. Drecer, M. (2000). Dynamics of Vertical Leaf Nitrogen Distribution in a Vegetative Wheat Canopy. Impact on Canopy Photosynthesis. *Annals of Botany* 86, 821–831.
23. Duvivier, M., Dedeurwaerder, G., Bataille, C., De Proft, M., and Legre've, A. 2016. Real-time PCR quantification and spatio-temporal distribution of airborne inoculum of *Puccinia triticina* in Belgium. *Eur. J. Plant Pathol.* 145:405-420.
24. El Jarroudi, M., Kouadio, L., Delfosse, P., and Tychon, B. 2014. Brown rust disease control in winter wheat: I. Exploring an approach for disease progression based on night weather conditions. *Environ. Sci. Pollut. Res.* 21:4797-4808.
25. Filipe, J.A.N., Cobb, R.C., Meentemeyer, R.K., Lee, C.A., Valachovic, Y.S., Cook, A.R., Rizzo, D.M., and Gilligan, C.A. (2012). Landscape epidemiology and control of pathogens with cryptic and long-distance dispersal: Sudden oak death in northern californian forests. *PLoS Computational Biology* 8.

26. Flier, W.G., and Turkensteen, L.J. (1999). Foliar aggressiveness of *Phytophthora infestans* in three potato growing regions in the Netherlands. *European Journal of Plant Pathology* 105, 381–388.
27. Ford Denison, R., and McGuire, A.M. (2015). What should agriculture copy from natural ecosystems? *Global Food Security* 4, 30–36.
28. Gandon, S. (2002). Local adaptation and the geometry of host – parasite coevolution. *Ecology Letters* 5, 246–256.
29. Garin G. 2015. Vers la compréhension des épidémies fongiques foliaires par modélisation multi-échelle dans les couverts architecturés. Thèse de Doctorat soutenue le 11 décembre 2015.
30. Grechi, I., Hilgert, N., Sauphanor, B., Senoussi, R., and Lescourret, F. (2010). Modelling coupled peach tree-aphid population dynamics and their control by winter pruning and nitrogen fertilization. *Ecological Modelling* 221, 2363–2373.
31. Godin, C., and Sinoquet, H. (2005). Functional-structural plant modelling. *New Phytologist* 166, 705–708.
32. Herms, D.A., and Mattson, W.J. (1992). The Dilemma of Plants: To Grow or Defend. *The Quarterly Review of Biology* 67, 283–335.
33. Hinzman, L.D., Bauer, M.E., and Daughtry, C.S.T. (1986). Effects of Nitrogen-Fertilization on Growth and Reflectance Characteristics of Winter-Wheat. *Remote Sensing of Environment* 19, 47–61.
34. Horbach, R., Navarro-Quesada, A.R., Knogge, W., and Deising, H.B. (2011). When and how to kill a plant cell: Infection strategies of plant pathogenic fungi. *Journal of Plant Physiology* 168, 51–62.
35. Howard, D., Chambers, A., and Logan, J. (1994). Nitrogen and Fungicide Effects on Yield Components and Disease Severity in Wheat. *Journal of Production Agriculture* 7, 448–454.
36. Johnson, D. a. (1980). Effect of Low Temperature on the Latent Period of Slow and Fast Rusting Winter Wheat Genotypes. *Plant Disease* 64, 1006.
37. Johnson, B.L., and Haddad, N.M. (2011). Edge effects, not connectivity, determine the incidence and development of a foliar fungal plant disease. *Ecology* 92, 1551–1558.
38. Kabbage, M., Yarden, O., and Dickman, M.B. (2015). Pathogenic attributes of *Sclerotinia sclerotiorum*: Switching from a biotrophic to necrotrophic lifestyle. *Plant Science* 233, 53–60.
39. Kaltz, O., Gandon, S., Michalakis, Y., and Shykoff, J.A. (1999). Local Maladaptation in the Anther-Smut Fungus *Microbotryum violaceum* to Its Host Plant *Silene latifolia*: Evidence from a Cross-Inoculation Experiment. *Evolution* 53, 395.
40. Király, Z. (1964). Effect of Nitrogen Fertilization on Phenol Metabolism and Stem Rust Susceptibility of Wheat. *Journal of Phytopathology* 51, 252–261.
41. Kirkham, D.S. (1954). Significance of the ratio between the water-soluble aromatic and nitrogen constituents of apple and pear in the host-parasite relationships of *Venturia* species [16]. *Nature* 173, 690–691.
42. Knott, E.A., and Mundt, C.C. (1991). Latent Period and Infection Efficiency of *Puccinia recondita* f. sp. *tritici* Populations Isolated from Different Cultivars. *Phytopathology* 81, 435–439.
43. Laine, A.L. (2005). Spatial scale of local adaptation in a plant-pathogen metapopulation. *Journal of Evolutionary Biology* 18, 930–938.
44. Last, F.T. (1953). Some Effects of Temperature and Nitrogen Supply on Wheat Powdery Mildew. *Annals of Applied Biology* 40, 312–322.

45. Last, F.T. (1962). Effects of Nutrition on the Incidence of Barley Powdery Mildew. *Plant Pathology* 11, 133–136.
46. Lion, S., and Gandon, S. (2016). Spatial evolutionary epidemiology of spreading epidemics. *Proceedings of the Royal Society B: Biological Sciences* 283, 20161170.
47. Ma, H., and Singh, R.P. (1996). Expression of adult resistance to stripe rust at different growth stages of wheat. *Plant Disease* 375–379.
48. Masclaux-Daubresse, C., Daniel-Vedele, F., Dechorganat, J., Chardon, F., Gaufichon, L., and Suzuki, A. (2010). Nitrogen uptake, assimilation and remobilization in plants: Challenges for sustainable and productive agriculture. *Annals of Botany* 105, 1141–1157.
49. Massad, T.J., Dyer, L.A., and Vega C., G. (2012). Costs of Defense and a Test of the Carbon-Nutrient Balance and Growth-Differentiation Balance Hypotheses for Two Co-Occurring Classes of Plant Defense. *PLoS ONE* 7.
50. Matsuyama, N., and Dimond, A.E. (1973). Effect of nitrogenous fertilizer on biochemical processes that could affect lesion size of rice blast. *Phytopathology* 63, 1202–1203.
51. Matsuyama, N. (1975). The effect of ample nitrogen fertilizer on cell wall materials and its significance to rice blast disease. *Annual Phytopathological Society of Japan* 41, 56–61.
52. McDonald, B.A., and Linde, C. (2002). Pathogen population genetics, evolutionary potential, and durable resistance. *Annual Review of Phytopathology* 40, 349–379.
53. Meentemeyer, R.K., Haas, S.E., and Václavík, T. (2012). Landscape Epidemiology of Emerging Infectious Diseases in Natural and Human-Altered Ecosystems. *Annual Review of Phytopathology* 50, 379–402.
54. Mundt, C.C., Sackett, K.E., and Wallace, L.D. (2011). Landscape heterogeneity and disease spread: Experimental approaches with a plant pathogen. *Ecological Applications* 21, 321–328.
55. Mur, L.A.J., Simpson, C., Kumari, A., Gupta, A.K., and Gupta, K.J. (2017). Moving nitrogen to the centre of plant defence against pathogens. *Annals of Botany* 119, 703–709.
56. Murcia, C. (1995). Edge effects in fragmented forests-implications for conservation. *Trends in Ecology & Evolution* 10, 58–62.
57. Olesen, J.E., Mortensen, J.V., Jørgensen, L.N., and Andersen, M.N. (2000). Irrigation strategy, nitrogen application and fungicide control in winter wheat on a sandy soil. I. Yield, yield components and nitrogen uptake. *Journal of Agricultural Science* 134, 1–11.
58. Papaïx, J., Adamczyk-Chauvat, K., Bouvier, A., Kiêu, K., Touzeau, S., Lannou, C., and Monod, H. (2014). Pathogen population dynamics in agricultural landscapes: The Ddal modelling framework. *Infection, Genetics and Evolution* 27, 509–520.
59. Papaïx, J., Burdon, J.J., Zhan, J., and Thrall, P.H. (2015). Crop pathogen emergence and evolution in agro-ecological landscapes. *Evolutionary Applications* 8, 385–402.
60. Pariaud, B., Van den Berg, F., Van den Bosch, F., Powers, S.J., Kaltz, O., and Lannou, C. (2013). Shared influence of pathogen and host genetics on a trade-off between latent period and spore production capacity in the wheat pathogen, *Puccinia triticina*. *Evolutionary Applications* 6, 303–312.
61. Park, R.F., and Rees, R.G. (1989). Expression of adult plant resistance and its effect on the development of *Puccinia striiformis* f.sp. *tritici* in some Australian wheat cultivars. *Plant Pathology* 38, 200–208.

62. Parker, M.A. (1985). Local population differentiation for compatibility in an annual legume and its host-specific fungal pathogen. *Evolution* 39, 713–723.
63. Perfect, S.E., and Green, J.R. (2001). Infection structures of biotrophic and hemibiotrophic fungal plant pathogens. *Molecular Plant Pathology* 2, 101–108.
64. Peterson, P. D., Leonard, K. J., Miller, J. D., Laudon, R. J.& Sutton, T. B. 2005 Prevalence and distribution of common barberry, the alternate host of *Puccinia graminis*, in Minnesota. *Plant Dis.* 89, 159–163. (doi:10.1094/PD-89- 0159)
65. Plantegenest, M., Le May, C., and Fabre, F. (2007). Landscape epidemiology of plant diseases. *Journal of The Royal Society Interface* 4, 963–972.
66. Ravigné, V., U. Dieckmann, and I. Olivieri. (2009). Live where you thrive: joint evolution of habitat choice and local adaptation fa- cilitates specialization and promotes diversity. *American Naturalist* 174:E141–E169.
67. Rizzo, D., and Garbelotto, M. (2003). Sudden oak death: endangering California and Oregon forest ecosystems. *Frontiers in Ecology and the ...* 1, 197–204.
68. Robert, C., Bancal, M.O., Lannou, C., and Ney, B. (2006). Quantification of the effects of *Septoria tritici* blotch on wheat leaf gas exchange with respect to lesion age, leaf number, and leaf nitrogen status. In *Journal of Experimental Botany*, pp. 225–234.
69. Robert, C., Fournier, C., Andrieu, B., and Ney, B. (2008). Coupling a 3D virtual wheat (*Triticum aestivum*) plant model with a *Septoria tritici* epidemic model (Septo3D): A new approach to investigate plant-pathogen interactions linked to canopy architecture. *Functional Plant Biology* 35, 997–1013.
70. Robert C., Garin G., Pradal C., Fournier C. 2017. A plant-pathogen model reveals how plant architecture and foliar senescence impact the race between wheat growth and *Zymoseptoria tritici* epidemics. *Annals of Botany*. (In press).
71. Sache, I. (2000). Short-distance dispersal of wheat rust spores. *Agronomie* 20 (7),757-767.
72. Shaner, G., and Finney, R.E. (1977). The Effect of Nitrogen Fertilization on the Expression of Slow-Mildewing Resistance in Knox Wheat. *Phytopathology* 77, 1051–1056.
73. Shaw, M.W. (1990). Effects of temperature, leaf wetness and cultivar on the latent period of *Mycosphaerella graminicola* on winter wheat. *Plant Pathology* 39, 255–268.
74. Sievänen, R., Godin, C., De Jong, T.M., and Nikinmaa, E. (2014). Functional-structural plant models: A growing paradigm for plant studies. *Annals of Botany* 114, 599–603.
75. Smith, H.C., and Blair, I.D. (1950). Wheat Powdery Mildew Investigations. *Annals of Applied Biology* 37, 570–583.
76. Strauss, S.Y. (1997). Lack of evidence for local adaptation to individual plant clones or site by a mobile specialist herbivore. *Oecologia* 110: 77–85.
77. Suffert, F., Sache, I., and Lannou, C. (2013). Assessment of quantitative traits of aggressiveness in *Mycosphaerella graminicola* on adult wheat plants. *Plant Pathology* 62, 1330–1341.
78. Suffert, F., Goyeau, H, Sache, I., Carpentier, F., Gélisse, S., Morais, D., and Delestre G. (2017). Trade-off between intra- and interannual scales in the evolution of aggressiveness in a local plant pathogen population. doi: <https://doi.org/10.1101/151068>
79. Van Den Berg, F., Robert, C., Shaw, M.W., and Van Den Bosch, F. (2007). Apical leaf necrosis and leaf nitrogen dynamics in diseased leaves: A model study. *Plant Pathology* 56, 424–436.

80. Van Den Berg, F., Van Den Bosch, F., Powers, S.J., and Shaw, M.W. (2008). Apical leaf necrosis as a defence mechanism against pathogen attack: Effects of high nutrient availability on onset and rate of necrosis. *Plant Pathology* 57, 1009–1016.
81. Van den Berg, F., Gaucel, S., Lannou, C., Gilligan, C.A., and van den Bosch, F. (2013). High levels of auto-infection in plant pathogens favour short latent periods: A theoretical approach. *Evolutionary Ecology* 27, 409–428.
82. Vári, E., and Máriás, K. (2013). The Impact of Crop Rotation and N Fertilization on the Leaf Area Index , Leaf Disease and Yield of Winter Wheat. *International Scholarly and Scientific Research & Innovation* 7, 1031–1034.
83. Vos, J., Evers, J.B., Buck-Sorlin, G.H., Andrieu, B., Chelle, M., and De Visser, P.H.B. (2010). Functional-structural plant modelling: A new versatile tool in crop science. *Journal of Experimental Botany* 61.
84. Wang, Z., Wang, J., Zhao, C., Zhao, M., Huang, W., and Wang, C. (2005). Vertical Distribution of Nitrogen in Different Layers of Leaf and Stem and Their Relationship with Grain Quality of Winter Wheat. *Journal of Plant Nutrition* 28, 73–91.
85. Whalen, M.C. (2005). Host defence in a developmental context. *Molecular Plant Pathology* 6, 347–360.
86. Zadoks, J.C. (2008). On the political economy of plant diseases epidemics – Capita selecta in historical epidemiology. Wageningen Academic Publishers. pp 39-119. ISBN 978-90-8686-086-9.
87. Zhan, J., Mundt, C.C., Hoffer, M.E., and McDonald, B.A. (2002). Local adaptation and effect of host genotype on the rate of pathogen evolution: An experimental test in a plant pathosystem. *Journal of Evolutionary Biology* 15, 634–647.
88. Zhan, J., Thrall, P.H., and Burdon, J.J. (2014). Achieving sustainable plant disease management through evolutionary principles. *Trends in Plant Science* 19, 570–575.
89. Zhan, J., Thrall, P.H., Papaïx, J., Xie, L., and Burdon, J.J. (2015). Playing on a Pathogen's Weakness: Using Evolution to Guide Sustainable Plant Disease Control Strategies. *Annual Review of Phytopathology* 53, 19–43.